

Modeling Atmospheric Mercury Deposition to the Great Lakes

Final Report

for work conducted with FY2010 funding from the
Great Lakes Restoration Initiative

December 16, 2011

Mark Cohen, Roland Draxler, Richard Artz

NOAA Air Resources Laboratory

Silver Spring, MD, USA

Table of Contents.....	2
1. Introduction.....	8
1.1. Mercury in the Great Lakes Basin.....	8
1.2. What Do We Need to Know about Atmospheric Mercury Deposition to the Great Lakes?	9
1.3. Overview of Different Approaches Used to Estimate the Quantity of and Source Attribution for Atmospheric Mercury Deposition in the Great Lakes region	10
1.3.1. Sediment Cores.....	10
1.3.2. Atmospheric Measurements	10
1.3.3. Receptor-based and Trajectory Methods	12
1.3.4. Fate and Transport Modeling	15
1.3.5. Important Features of this Work	18
1.4. Goals of this 1st Phase of the Project	19
1.5. The Next Phases of the Project	19
2. Methodology	20
2.1. HYSPLIT-Hg Model.....	21
2.2. Meteorology	22
2.3. Emissions	24
2.3.1. Direct Anthropogenic Emissions in the United States	24
2.3.2. Direct Anthropogenic Emissions in Canada	26
2.3.3. Direct Anthropogenic Emissions in Mexico.....	28
2.3.4. Anthropogenic Emissions in the Rest of the World	29
2.3.5. Summary of Global Anthropogenic Emissions	31
2.3.6. Re-Emissions and Natural Emissions.....	33
2.3.7. Emissions Summary	38
2.4. Computational Methodology.....	41
2.4.1. Introduction.....	41
2.4.2. Standard Sources Used in the Analysis	42
2.4.3. Estimating Deposition at “Point” Monitoring Sites vs. Large Area Receptors	45
2.4.4. Configuration of the HYSPLIT-Hg Model used in this Study	47

3. Illustrative Results for Single Sources.....	49
4. An Initial Set of Results for Mercury Deposition to the Great Lakes	56
4.1. Overall mercury deposition to the Great Lakes.....	56
4.2. Country-Specific Source-Attribution Results for Great Lakes Mercury Deposition.....	59
4.3. Geographical Distributions of Source Attribution Results: Examples for Lake Erie	61
4.4. Atmospheric Mercury Contributions to the Great Lakes and Watershed as a Function of Distance	70
5. Model Evaluation.....	76
5.1. Comparison of Model Predicted Wet Deposition Fluxes with Measured Wet Deposition Fluxes in the Great Lakes Basin	76
5.2. Additional Considerations Regarding the Overall Mercury Mass Balance for the Great Lakes Basin	83
6. Conclusions.....	85
7. References	87
8. Appendices	101
Appendix 1. Atmospheric deposition contribution maps for each Great Lake for direct anthropogenic mercury emissions displayed on a 2x2 degree global grid.....	102
Appendix 2. Atmospheric deposition contribution maps for each Great Lake’s Watershed for direct anthropogenic mercury emissions displayed on a 2x2 degree global grid	108
Appendix 3. Atmospheric deposition contribution maps for each Great Lake for direct anthropogenic mercury emissions displayed on a 1x1 degree grid over a North American domain.....	114
Appendix 4. Atmospheric deposition contribution maps for each Great Lake’s Watershed for direct anthropogenic mercury emissions displayed on a 1x1 degree over a North American domain.....	120
Appendix 5. Atmospheric deposition contribution maps for each Great Lake for total atmospheric mercury emissions displayed on a 2x2 degree global grid	126
Appendix 6. Atmospheric deposition contribution maps for each Great Lake’s Watershed for total atmospheric mercury emissions displayed on a 2x2 degree global grid	132

Appendix 7. Atmospheric deposition contribution maps for each Great Lake for total atmospheric mercury emissions displayed on a 1x1 degree grid over a North American domain..... 138

Appendix 8. Atmospheric deposition contribution maps for each Great Lake’s Watershed for total atmospheric mercury emissions displayed on a 1x1 degree grid over a North American domain..... 144

Appendix 9. Atmospheric mercury emissions as a function of distance from each of the Great Lakes and their watersheds..... 150

Table of Figures

Figure 1. Great Lakes and their watersheds	8
Figure 2. Model-predicted deposition to the Great Lakes attributable to emissions from coal-fired power plants in the United States.....	16
Figure 3. The EDAS-40km Meteorological Model Data Grid (showing every 5 th grid point)	23
Figure 4. The NCEP/NCAR Reanalysis Model Data Grid (showing every 5th grid point)	23
Figure 5. Mercury Emissions from U.S. Point Sources estimated from the U.S. EPA 2005 National Emissions Inventory	25
Figure 6. Mercury Emissions from U.S. Area Sources estimated from the U.S. EPA 2002 National Emissions Inventory	26
Figure 7. Mercury Emissions from Canadian Point Sources estimated from Environment Canada's 2005 National Pollutant Release Inventory	27
Figure 8. Mercury Emissions from Canadian Area Sources used in this analysis	27
Figure 9. Mercury Emissions from Mexican Point Sources used in this analysis.....	28
Figure 10. Mercury Emissions from Mexican Area Sources used in this analysis.....	29
Figure 11. Mercury Emissions from Global Anthropogenic Sources	30
Figure 12. Anthropogenic Mercury Emissions	31
Figure 13. Atmospheric mercury emissions from direct anthropogenic sources displayed on a 1x1 degree grid over central North America	32
Figure 14. Natural mercury emissions displayed on a 2x2 degree global grid	33
Figure 15. Natural mercury emissions displayed on a 1x1 degree grid over a central North American domain	34
Figure 16. Atmospheric re-emissions of previously deposited mercury from anthropogenic sources displayed on a 2x2 degree global grid	36
Figure 17. Atmospheric re-emissions of previously deposited mercury from anthropogenic sources displayed on a 1x1 degree grid over a central North American domain.....	37
Figure 18. Atmospheric mercury emissions from all sources displayed on a 2x2 degree global grid.....	38
Figure 19. Atmospheric mercury emissions from all sources displayed on a 1x1 degree grid over central North America.....	39
Figure 20. Spatial Interpolation	41
Figure 21. Chemical Interpolation	42
Figure 22. Standard Points Outside of North America	44
Figure 23. Standard Points in North America	45
Figure 24. Conceptual Diagram of Sources, Monitoring Sites, and Receptors	46
Figure 25. Transfer Flux Coefficients For Pure Elemental Mercury Emissions at an Illustrative Subset of Standard Source Locations, for Deposition Flux Contributions to Lake Erie	50
Figure 26. Transfer Flux Coefficients For Pure Reactive Gaseous Mercury Emissions at an Illustrative Subset of Standard Source Locations, for Deposition Flux Contributions to Lake Erie	51
Figure 27. Standard Source Locations for which Illustrative Modeling Results Will be Shown.....	52
Figure 28. Transfer Flux Coefficients For Hg(0), Hg(II), and Hg(p) to Lake Erie (logarithmic scale).....	53

Figure 29. Transfer Flux Coefficients For Hg(0), Hg(II), and Hg(p) to Lake Erie (linear scale).....	53
Figure 30. Lake Erie Transfer Flux Coefficients for two kinds of Generic Coal-Fired Power Plants (logarithmic scale).....	55
Figure 31. Lake Erie Transfer Flux Coefficients for two kinds of Generic Coal-Fired Power Plants (linear scale).....	55
Figure 32. Overall model estimates of mercury deposition to the Great Lakes Basin	56
Figure 33. Model-estimated 2005 deposition fluxes (ug/m ² -year) to the Great Lakes and Great Lakes Watersheds.....	58
Figure 34. Model-estimated 2005 deposition amounts (kg/year) to the Great Lakes and Great Lakes Watersheds.....	59
Figure 35. Model-estimated 2005 deposition amount to the Great Lakes Basin from the ten countries with the highest modeled total contribution from direct and re-emitted anthropogenic sources	60
Figure 36. Model-estimated <i>per capita</i> 2005 deposition amount to the Great Lakes Basin from the countries with the highest modeled total contribution from direct and re-emitted anthropogenic sources.....	60
Figure 37. Global Geographical Distribution of Atmospheric Deposition Contributions to Lake Erie from Direct Anthropogenic Emissions.....	62
Figure 38. Geographical Distribution of Atmospheric Deposition Contributions to Lake Erie from Direct Anthropogenic Emissions in Central North America	63
Figure 39. Global Geographical Distribution of Atmospheric Deposition Contributions to Lake Erie from Re-emissions of Previously Deposited Anthropogenic Emissions	64
Figure 40. Geographical Distribution of Atmospheric Deposition Contributions to Lake Erie from Re- emissions of Previously Deposited Anthropogenic Emissions from Central North America.....	65
Figure 41. Global Geographical Distribution of Atmospheric Mercury Deposition Contributions to Lake Erie from Natural Emissions.....	66
Figure 42. Geographical Distribution of Atmospheric Mercury Deposition Contributions to Lake Erie from North American Natural Emissions.....	67
Figure 43. Global Geographical Distribution of Atmospheric Mercury Deposition Contributions to Lake Erie from All Modeled Sources	68
Figure 44. Geographical Distribution of Atmospheric Mercury Deposition Contributions to Lake Erie from All Modeled Sources, displayed on a Central North American domain	69
Figure 45. Atmospheric Emissions from Direct Anthropogenic, Re-emitted Anthropogenic and Natural Mercury Emissions as a Function of Distance from the Center of Lake Erie	70
Figure 46. Atmospheric Deposition Contributions to Lake Erie from Direct Anthropogenic, Re-emitted Anthropogenic and Natural Mercury Emissions as a Function of Distance from the Center of the Lake.....	71
Figure 47. Atmospheric Deposition Contributions to Lake Michigan from Direct Anthropogenic, Re- emitted Anthropogenic and Natural Mercury Emissions as a Function of Distance from the Center of the Lake.....	71

Figure 48. Atmospheric Deposition Contributions to Lake Superior from Direct Anthropogenic, Re-emitted Anthropogenic and Natural Mercury Emissions as a Function of Distance from the Center of the Lake.....	72
Figure 49. Atmospheric Deposition Contributions to Lake Huron from Direct Anthropogenic, Re-emitted Anthropogenic and Natural Mercury Emissions as a Function of Distance from the Center of the Lake.....	72
Figure 50. Atmospheric Deposition Contributions to Lake Ontario from Direct Anthropogenic, Re-emitted Anthropogenic and Natural Mercury Emissions as a Function of Distance from the Center of the Lake.....	73
Figure 51. Atmospheric Deposition Contributions to the Lake Erie Watershed from Direct Anthropogenic, Re-emitted Anthropogenic and Natural Mercury Emissions as a Function of Distance from the Center of the Watershed	73
Figure 52. Atmospheric Deposition Contributions to the Lake Michigan Watershed from Direct Anthropogenic, Re-emitted Anthropogenic and Natural Mercury Emissions as a Function of Distance from the Center of the Watershed	74
Figure 53. Atmospheric Deposition Contributions to the Lake Superior Watershed from Direct Anthropogenic, Re-emitted Anthropogenic and Natural Mercury Emissions as a Function of Distance from the Center of the Watershed	74
Figure 54. Atmospheric Deposition Contributions to the Lake Huron Watershed from Direct Anthropogenic, Re-emitted Anthropogenic and Natural Mercury Emissions as a Function of Distance from the Center of the Watershed	75
Figure 55. Atmospheric Deposition Contributions to the Lake Ontario Watershed from Direct Anthropogenic, Re-emitted Anthropogenic and Natural Mercury Emissions as a Function of Distance from the Center of the Watershed	75
Figure 56. Mercury Deposition Network Sites in the Great Lakes Region Considered in an Initial Model Evaluation Analysis	76
Figure 57. Comparison of Total 2005 Precipitation Measured at each of the Great-Lakes Region MDN Sites with the Precipitation in the Meteorological Datasets Used as Inputs to this Modeling Study	77
Figure 58. Comparison of 2005 precipitation total as measured at MDN sites in the Great Lakes region (circles) with precipitation totals assembled by the PRISM Climate Group, Oregon State University.....	78
Figure 59. Modeled vs. Measured Wet Deposition of Mercury at Sites in the Great Lakes Region	79
Figure 60. Modeled vs. Measured Wet Deposition of Mercury at Sites in the Great Lakes Region	80
Figure 61. Modeled vs. Measured Wet Deposition of Mercury at Sites in the Great Lakes Region	80
Figure 62. Standard source locations, MDN sites, and mercury emissions in the Great Lakes region	81
Figure 63. Gross deposition to the Great Lakes Basin in the base-case emissions scenario and a modified scenario.....	84

1. Introduction

1.1. Mercury in the Great Lakes Basin

Mercury contamination in the Great Lakes Basin remains an important public and wildlife health concern as well as an economic issue (Cain, Morgan and Brooks, 2011). The Great Lakes Basin is widely contaminated with mercury – with the current predominant loading pathway being atmospheric deposition – and the “scope and intensity of the impact of mercury on fish and wildlife in the Great Lakes region is much greater than previously thought” (Evers et al, 2011ab). For example, Evers et al (2011c) analyzed mercury measurements in the common loon and found seven “hotspots” of loon contamination in the Great Lakes region, as well as numerous additional areas with mercury levels in loons at or near levels with physiological consequences. State-wide mercury-related fish consumption advisories are present in each of the Great Lakes States, and mercury-related fish consumption advisories are also present for some Great Lakes fish. Bhavsar *et al.* (2011) found that while the majority of current fish advisories in the Great Lakes themselves were due to PCB’s and dioxins/furans, the level of mercury contamination is high enough in some cases to warrant its own advisory. In other words, mercury advisories would “replace” some of the existing PCB and/or dioxin/furan advisories if contamination of the latter were was brought below the advisory threshold.

This study involves a model-based analysis of atmospheric mercury deposition to each of the Great Lakes and each of the Great Lakes watersheds (Figure 1).

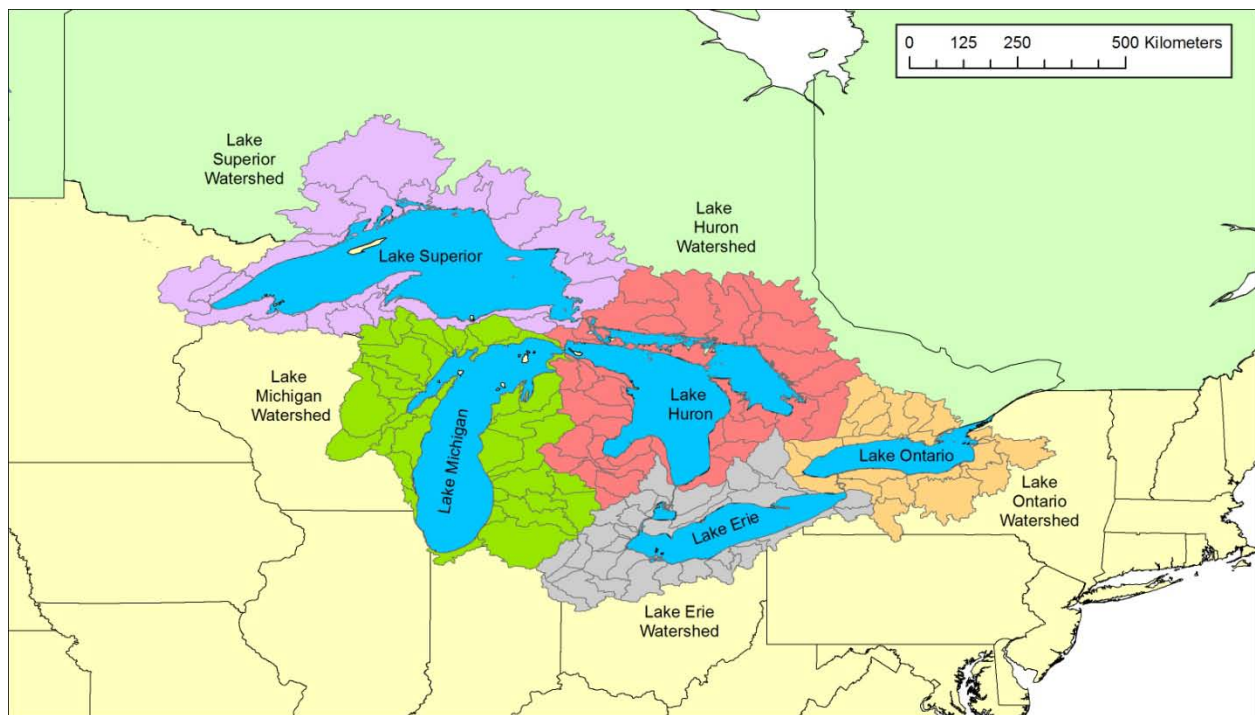


Figure 1. Great Lakes and their watersheds

1.2. What Do We Need to Know about Atmospheric Mercury Deposition to the Great Lakes?

Due to the importance of mercury contamination in the Great Lakes Basin, from a policy and scientific perspective it is important to have accurate estimates of:

- **The quantity of atmospheric deposition:** *How much of each form of mercury is deposited to each of the Great Lakes and their watersheds?* While atmospheric deposition is estimated to be a significant and even dominant loading pathway for mercury to the Great Lakes basin, an accurate estimate of the *quantity* of deposition is necessary to evaluate the relative importance of atmospheric deposition compared to other loading pathways (e.g., tributary, direct effluent discharge, runoff). In addition, an accurate estimate of the quantity of deposition is necessary to carry out a *mass balance* for each of the Great Lakes and their watersheds – a basic but scientifically challenging analysis. Also, an accurate estimate of the quantity of atmospheric deposition is needed as inputs to ecosystem models of the Great Lakes and their watersheds. Information about the deposition quantity is needed for the past (to account for historical loadings), for the present, and for alternative future scenarios.
- **Source attribution for atmospheric deposition:** *What is the relative importance of different source types and source regions contributing to the deposition to each of the Great Lakes and their watersheds?* Given the relative importance of the atmospheric deposition pathway, it is not enough to simply know the amount of deposition – it is critical to know the source of the mercury being deposited. This information is necessary to develop policies to reduce the atmospheric deposition loading. Moreover, it is important to have estimates of the impact on the Great Lakes Basin of different alternative future scenarios, for regional, national, and international mercury emissions.

In the next section, the major approaches that can be used to make estimates of the above two elements are summarized.

In this report we will refer to three “kinds” of atmospheric mercury: (i) elemental mercury, or Hg(0); (ii) reactive gaseous mercury (RGM), or Hg(II); and (iii) particulate mercury, or Hg(p). Except where noted, results presented in this report are for total mercury (the sum of the three different forms), for simplicity and brevity’s sake, even though the entire modeling analysis has been done with explicit treatment of the different mercury forms. In a few cases, the term “TGM” is used, referring to Total Gaseous Mercury, representing the sum of elemental and reactive gaseous mercury.

1.3. Overview of Different Approaches Used to Estimate the Quantity of and Source Attribution for Atmospheric Mercury Deposition in the Great Lakes region

There are different approaches to developing estimates for the quantity and source-attribution of atmospheric mercury deposition in the Great Lakes region – generally involving measurements and/or modeling -- and each has its inherent strengths and weaknesses. Blanchard (1999) has reviewed the variety of methodologies used in estimating source attribution for air pollutants.

1.3.1. Sediment Cores

One approach to estimating the quantity of overall net mercury loading to a given lake is to measure the mercury accumulation rate in sediments. It is challenging to estimate a whole-lake loading rate from sediments due to spatial variations and sediment focusing, i.e., the phenomenon in which suspended solids in the water column do not settle to the lake bottom evenly, in which there are areas where solids accumulate preferentially. Nevertheless, with “enough” sediment cores and proper attention to the focusing issue, overall estimates of deposition to the Great Lakes can be made from sediment core data. Of course, the overall loading rates so estimated represent the total net loading to the lake, from atmospheric deposition as well as tributary inputs, run-off, direct-discharges, and any other source of mercury to the lake. A strength of this method is that by determining the mercury accumulation rate at different depths in the sediment, the time-course of overall net loadings can be estimated. The temporal resolution of such estimates is generally somewhat coarse. For example, Rossman (2010) estimated the total net mercury load to Lake Michigan to be $21.4 \mu\text{g}/\text{m}^2\text{-yr}$ (1157 kg/yr), based on a core section that represented the time frame 1980-2002. So, this total net loading rate was the “average” net loading rate over that period. Rossman (2010) also estimated loadings for other time periods, including a preindustrial (≤ 1850) net flux of $3.09 \mu\text{g}/\text{m}^2\text{-yr}$ and a peak flux of $53.3 \mu\text{g}/\text{m}^2\text{-yr}$ in 1946.

1.3.2. Atmospheric Measurements

Another approach to yield information regarding the amount and source-attribution for mercury deposition to the Great Lakes is to make atmospheric measurements at specific sites. This has been done and continues to be done for atmospheric concentrations and wet deposition of mercury at many sites in the Great Lakes region.

These measurements are critically important because they give a relatively “exact” answer at a given location for the parameters measured, subject to measurement uncertainties, and they provide fundamental scientific data for input to and evaluation of atmospheric mercury models. However, since atmospheric deposition varies widely over space and time, and it is impossible to measure everywhere, continuously, measurements alone cannot generally be used to produce robust estimates of the quantity of atmospheric mercury deposition to the Great Lakes and their watersheds. Making a few measurements on the shore of one of the Great Lakes will not generally allow an accurate estimate of

the total deposition to that lake because of the high variability of deposition that may occur over the lake area. Further, while emerging isotope-based mercury measurement techniques are beginning to provide some limited, qualitative information on source-attribution (e.g., Sherman *et al.* (2011), Gratz *et al.* (2010)), it is currently impossible to make detailed mercury source-attribution estimates using measurements alone for even the measurement site itself, much less for large area receptor such as the Great Lakes. Finally, because measurements of mercury *dry deposition and surface exchange* are complex and relatively uncertain, there have been and continue to be relatively few such measurements in the Great Lakes region.

Examples of measurements of atmospheric mercury concentrations at sites in the Great Lakes region include the following studies: Keeler *et al.* (1995), Hoyer *et al.* (1995), Lamborg *et al.* (1995), Schroeder *et al.* (1995), Pirrone *et al.* (1996); Poissant, and Poissant *et al.* (1996, 1997, 1998, 2000, 2005), Ames *et al.* (1998), Blanchard *et al.* (2002), Landis *et al.* (2002), Lynam *et al.* (2002, 2005ab, 2006); Kellerhals *et al.* (2003), Liu *et al.* (2003), Han *et al.* (2004, 2005, 2007), Gildemeister *et al.* (2005); Yatavelli *et al.* (2006), Liu *et al.* (2007), Manolopoulos *et al.* (2007), Risch *et al.* (2007), Temme *et al.* (2007), Rutter *et al.* (2008), Gratz *et al.* (2010); Huang *et al.* (2010); Liu *et al.* (2010), Xu and Akhtar (2010), Cairns *et al.* (2011), and Wen *et al.* (2011). Common themes among these studies include finding higher concentrations in urban vs. rural locations and finding evidence of local, regional, and long-distance influences. Miller *et al.* (2005) synthesized measurements of total gaseous mercury in northeastern North America, including the Lake Ontario region, and discussed spatial patterns showing evidence for increasing atmospheric concentrations in proximity to sources and source-regions.

Numerous measurements of wet deposition have also been made at sites in the Great Lakes region, e.g., Glass *et al.* (1986, 1990, 1991), Sorensen *et al.* (1994), Hoyer *et al.* (1995), Lamborg *et al.* (1995), National Atmospheric Deposition Program (1996-2011), Landis and Keeler (1997), Poissant and Pilote (1998), Landis *et al.* (2002), Hall *et al.* (2005), Keeler *et al.* (2006), Yatavelli *et al.* (2006), Lai *et al.* (2007a), Choi *et al.* (2008b), White *et al.* (2009), and Gratz *et al.* (2010).

Studies of spatial and/or temporal trends of these and other wet deposition measurements in the Great Lakes region have been carried out, using a variety of statistical methodologies. Miller *et al.* (2005) synthesized rural wet deposition measurements in northeastern North America, including the Lake Ontario region, noting that deposition in and downwind of urban/industrial areas is likely to be much greater, and that "...the effects of urban and point-emissions sources are not well captured by the sparse, rural mercury observation network". Van Arsdale *et al.* (2005) discussed seasonal and spatial trends in the Great Lakes region (and Northeastern North America) and also noted the importance of relatively infrequent but "enhanced" wet deposition events to the annual totals at any given measurement site. Prestbo and Gay (2009) found no statistically significant temporal trend in wet deposition at Mercury Deposition Network (MDN) sites in the Great Lakes region over the period 1996-2005. Butler *et al.* (2008) found a statistically significant *decrease* in wet deposition at four sites in the Great Lakes region over the period from 1998-2005, but no statistically significant trends at other sites in the Great Lakes region that were examined. Risch *et al.* (2011) found statistically significant *decreases* in wet mercury deposition at four sites in the Great Lakes region, and statistically significant *increases* at three sites in the region over the period 2002-2008. The results of the above studies are not easily

comparable, as they utilized data from different subsets of available sites, over different time periods, and used different statistical methodologies.

In summary, atmospheric measurements of mercury in the Great Lakes region are important in and of themselves – e.g., for characterizing temporal trends at a given site and providing information about spatial differences across the region -- and are also critically important to provide data to ground-truth atmospheric models. However, given the sparse nature of such measurement sites, and the spatial variability in deposition, it is difficult to determine even the amount of deposition to large area receptors such as the Great Lakes and their watersheds using measurements alone. Moreover, while many of the measurement-based studies noted above have attempted some sort of receptor-based source-attribution assessment (as summarized in the next section), it is generally difficult to develop detailed quantitative source-attribution estimates using measurements alone. And, whatever source-attribution estimates that can be made from measurement data alone will generally apply only to the specific measurement location(s) being examined. Due to spatial variability in deposition, it is generally impossible to estimate source-attribution details for large area receptors such as the Great Lakes and their watersheds using measurement data alone.

1.3.3. Receptor-based and Trajectory Methods

In many cases, the measurements at a given site are analyzed with receptor-based and/or trajectory methods in order to provide information about source-attribution.

In “receptor-based” multivariate statistical modeling approaches, the data alone are used to develop estimates of source contributions (Henry et al., 1984; Gordon, 1988; Blanchard, 1999). Examples include chemical mass balance (CMB), positive matrix factorization (PMF), and principal components analysis (PCA). Using these approaches, one can generally obtain some qualitative and even semi-quantitative information about the relative importance of different source types to the measured pollutant levels at the site (but cannot typically distinguish among different source regions).

With trajectory-based analysis, there are both “back-trajectory” and “forward-trajectory” methodologies. In “back-trajectory” studies, back-trajectory information is combined with measurement data to estimate the relative importance of different source regions for contributing to the pollutant levels measured at the site. In essence, these methods attempt to distinguish between where the air parcels came from when the measurements were high – indicating a potentially important source region – and also when the measurements were low – indicating a potentially unimportant source region. At the end of such an analysis, a map of the geographical distribution of the relative likelihood of potential source regions can be created. These methods give qualitative and sometimes semi-quantitative information about the relative importance of different source regions contributing to measured pollutant levels at the site (but not generally distinguish among different source types). Examples of this type of methodology include Potential Source Contribution Function (PSCF), Residence Time Weighted Concentration (RTWC), and others (e.g., Zeng and Hopke, 1989; Blanchard, 1999).

The Hybrid-Receptor modeling approach is an example of a “forward-trajectory” methodology. In this approach, measured atmospheric concentrations are combined with forward trajectories (Keeler and Samson, 1989; Pirrone *et al.*, 1995b). Measured concentrations at sites upwind of a given receptor are projected forward in a Lagrangian simulation to estimate the impact at the receptor for air parcels originating at the measurement site. In this situation, the downwind impact at the receptor is equivalent to the impact of a hypothetical source at the sampling point. The hypothetical source emits pollution at a rate such that the concentration in the air in the vicinity of the source location would be the same as the measured atmospheric concentration. For measured concentrations downwind of the receptor of interest, an upwind virtual source is numerically constructed which can account for the measured concentrations. In these cases, the impact on the receptor is estimated by simulating the fate and transport of material emitted from the virtual source.

Receptor-based and trajectory approaches are particularly relevant to and/or rely heavily on the specific measurement sites used. It is challenging to make accurate estimates for surrounding regions with these methods, although this has been attempted for several of the Great Lakes. In these approaches, it is possible to get semi-quantitative information about source regions (using back-trajectories), source types (using principal components analysis and other statistical techniques), and even the total deposition to a given area receptor (using forward trajectories). Examples of these types of analyses applied to mercury in at one or more sites in the Great Lakes region are given in Table 1.

Virtually all of the trajectory-based studies cited in Table 1, for sites in the Great Lakes region, found evidence that measured mercury concentrations and wet deposition were significantly influenced by local and regional sources of mercury. In simplified terms, when the air masses tended to come from regions where there were known large sources of mercury, the measured concentration or deposition tended to be relatively high.

Table 1. Examples of Receptor-Based and Trajectory-Based Models applied to atmospheric mercury measurements at sites in the Great Lakes region

Studies	Form of Atmospheric Mercury	Methodological Approach (see text for definition of abbreviations)	Sites Location(s)
Landis and Keeler (2002)	TGM, Hg(p), Hg in precipitation	Deposition to Lake Michigan estimated using Interpolation	Lake Michigan: 4 sites around the lake
Landis <i>et al.</i> (2002)	TGM, Hg(p), Hg in precipitation	Trajectory cluster analysis	Lake Michigan: 5 sites in the region + over-water
Vette <i>et al.</i> (2002)	TGM	Air-water exchange of elemental mercury estimated for Lake Michigan using measurements of dissolved gaseous mercury and interpolated measurements of atmospheric Hg(0)	Lake Michigan: 4 sites around the lake + over-water
Manolopoulos <i>et al.</i> (2007a)	Hg(0), RGM, Hg(p)	Pollution roses; correlations among measured co-pollutants	IL: East St. Louis
Pirrone <i>et al.</i> (1995a)	Hg(p), TGM	Hybrid—Receptor method used to estimate dry deposition to Lake Huron, Lake Erie, and Lake St. Clair based on measurements at 2 sites in Detroit, coupled with forward trajectories	MI: Detroit (2 sites)
Gildemeister <i>et al.</i> (2005)	TGM, Hg(p)	Correlations / differences among different sites	MI: Dexter and 3 sites in the Detroit metropolitan area
Lynam & Keeler (2005b)	Hg(0), RGM, Hg(p)	Case studies with HYSPLIT back-trajectories	MI: Dexter, Detroit
Liu <i>et al.</i> (2010)	Hg(0), RGM, Hg(p)	Pollution roses; cluster analysis (HYSPLIT back trajectories); statistical analysis of urban/rural concentration differences	MI: Dexter, Detroit
Olmez <i>et al.</i> (1998)	Hg(p)	Back-trajectories (U. Mich trajectory model) & Factor Analysis	NY: Belleayre, Moss Lake, Perch River, Westfield, Willsboro
Liu <i>et al.</i> (2003)	TGM	Potential Source Contribution Function (PSCF (with HYSPLIT back-trajectories) and Positive Matrix Factorization (PMF)	NY: Stockton & Potsdam
Han <i>et al.</i> (2004)	TGM, RGM	Back-trajectories (HYSPLIT) and correlations among measured co-pollutants	NY: Stockton, Potsdam, and Sterling
Han <i>et al.</i> (2005)	RGM	Potential Source Contribution Function (PSCF) (with HYSPLIT back-trajectories and backward dispersion)	NY: Stockton, Potsdam, and Sterling
Han <i>et al.</i> (2007)	TGM	3 different trajectory-based methods: Potential Source Contribution Function (PSCF), Residence Time Weighted Concentration (RTWC), and Simplified Quantitative Transport Bias (SQTBA)	NY: Stockton, Potsdam, and Sterling
Lai <i>et al.</i> (2007a)	Hg in precipitation	Potential Source Contribution Function (PSCF) and Residence Time Weighted Concentration (RTWC) (both with HYSPLIT back-trajectories)	NY: Potsdam
Choi <i>et al.</i> (2008a)	Hg(0), RGM, Hg(p)	Potential Source Contribution Function (PSCF) (with HYSPLIT back-trajectories)	NY: Huntington Forest
Choi <i>et al.</i> (2008b)	Hg in precipitation and throughfall	back-trajectories (HYSPLIT)	NY: Huntington Forest
Huang <i>et al.</i> (2010)	Hg(0), RGM, Hg(p)	PCA, and case-studies based on wind direction before/after a local source closed	NY: Rochester
Wang <i>et al.</i> (2010)	Hg(0), RGM, Hg(p)	Correlations with co-pollutants; HYSPLIT back trajectories	NY: Huntington Forest
Keeler <i>et al.</i> (2006)	Hg in precipitation	Positive Matrix Factorization (PMF) and EPA's UNMIX multivariate statistical model	OH: Steubenville
Yatavelli <i>et al.</i> (2006)	Hg(0), RGM, Hg(p), Hg in precipitation	Pollution Roses	OH: Athens
White <i>et al.</i> (2009)	Hg in precipitation	Case studies using HYSPLIT back-trajectories	OH: Steubenville + 4 nearby sites

Studies	Form of Atmospheric Mercury	Methodological Approach (see text for definition of abbreviations)	Sites Location(s)
Blanchard et al. (2002)	TGM	Principal Components Analysis (PCA), Pollution Roses, Back-Trajectories (AES Trajectory Model)	ON: Egbert, Burnt Island, and Point Petre
Cheng et al. (2009)	Hg(0), RGM	Positive Matrix Factorization (PMF), Principal Components Analysis (PCA), back-trajectories (HYSPLIT), correlation with other pollutants	ON: Toronto
Xu and Akhtar (2010)	TGM	Potential Source Contribution Function (PSCF) (with HYSPLIT back-trajectories)	ON: Windsor
Wen <i>et al.</i> (2011)	TGM	STILT model (a statistical analysis of back-trajectories based on measured concentrations)	ON: Egbert, Burnt Island, and Point Petre
Poissant (1999)	TGM	Potential Source Contribution Function (PSCF) (with AES Trajectory Model trajectories)	PQ: St. Anicet, Mingan
Poissant et al. (2005)	Hg(0), RGM, Hg(p)	Wind direction sectors & case studies w. HYSPLIT back trajectories	PQ: St. Anicet
Lamborg et al. (1995)	TGM, Hg(p), Hg in precipitation	back-trajectories (HYSPLIT)	WI: Crab Lk & Max Lk
Manolopoulos et al. (2007b)	Hg(0), RGM, Hg(p)	Receptor-based comparison of measurements at urban and rural sites 65km apart	WI: Devil's Lake & Mt. Horeb
Kolker et al. (2010)	Hg(0), RGM, Hg(p)	Pollutant roses, case-study back-trajectories (HYSPLIT)	WI: 25, 50, and 100 km north of a large coal-fired power plant
Abbreviations: RGM = Reactive Gaseous Mercury; TGM = "Total Gaseous Mercury", the sum of elemental and reactive gaseous mercury (RGM)			

1.3.4. Fate and Transport Modeling

A fourth approach involves explicit modeling of the fate and transport modeling of mercury emitted from specific sources. These "forward dispersion" models can be divided into two categories – Lagrangian and Eulerian. In Lagrangian models, individual "puffs" or "points" of mercury emitted from sources are modeled as they are blown and dispersed downwind of the source. In Eulerian models, the fate and transport of emitted mercury is calculated as it moves among cells in a pre-set grid. A brief summary of Lagrangian and Eulerian atmospheric mercury models that have been applied in domains including portions of or the entire Great Lakes region is presented in Table 2.

There are general strengths and weaknesses inherent to the different kinds of modeling. Lagrangian forward dispersion models are particularly well suited to characterize fate and transport locally and regionally downwind from a given source, and to estimate detailed source-receptor relationships for any given source. In contrast, Eulerian models can more efficiently characterize fate and transport over global domains. But, it is more difficult to obtain detailed source-receptor relationships with Eulerian models, and it is more difficult to estimate near-field impacts of sources. Because of these differences, Lagrangian functionality is sometimes introduced into Eulerian models – e.g., the so-called "Plume-in-

Grid” capability (Vijayaraghavan *et al.*, 2008). In the work described in this report, we have essentially introduced an Eulerian computational approach into a Lagrangian model, in what could be called a “Grid-in-Plume” approach.

There are numerous uncertainties in atmospheric mercury modeling, as reviewed by Lin *et al.* (2006, 2007), Cohen *et al.* (2007), Pongprueksa *et al.*, (2008), and Subir *et al.* (2011, 2012). Atmospheric mercury model intercomparisons in a North American (Bullock *et al.*, 2008, 2009), European (Ryaboshapko *et al.*, 2007ab), and simple chemical droplet domain (Ryaboshapko *et al.*, 2002) have been carried out, including different subsets of the above models. The intercomparisons to date have generally showed significant differences in model predictions from one model to another, demonstrating the uncertainty in the scientific understanding of atmospheric mercury dynamics. A model comparison specifically for the Great Lakes was recently carried out comparing the model-predicted deposition to each lake from U.S. coal-fired power plants with the CMAQ-Hg model and the HYSPLIT-Hg model (Cohen *et al.*, 2007: Appendix A). Although the results were not strictly comparable – as they were based on two different years of meteorological data, and used different emissions inventories – this comparison showed that the two models gave reasonably similar results. Figure 2 shows the results for both models and it can be seen that the estimates for the most-impacted lake (Erie) are very similar. Differences between the two models are somewhat greater for the other lakes, with the largest proportional difference for Lake Superior. However, the magnitude of the deposition is smallest for Lake Superior, and so, the magnitude of the difference is not overly large. It is noted again that because the analyses were for two different meteorological years and used different emissions inventories, an exact match would not be expected even if the models were identical.

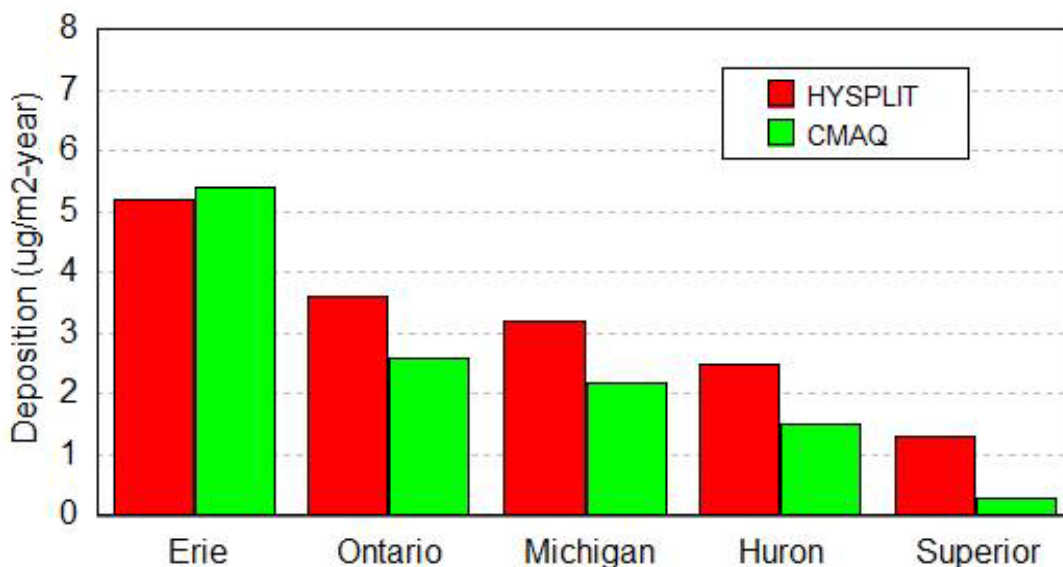


Figure 2. Model-predicted deposition to the Great Lakes attributable to emissions from coal-fired power plants in the United States

Table 2. Atmospheric Mercury Fate and Transport Models applied to domains including some or all of the Great Lakes region

Model	Model type	Notes	References
ASTRAP	Regional Lagrangian	Deposition estimates for the Great Lakes	Shannon and Voldner (1995)
RELMAP			Bullock <i>et al.</i> (1998); Bullock (2000)
HYSPLIT-Hg		Specific source-attribution results for the Great Lakes	Cohen <i>et al.</i> (2004, 2007)
CALPUFF		Primarily for the State of Maryland	Sherwell <i>et al.</i> (2006, 2010); summary in Gilmour <i>et al.</i> (2008)
TEAM	Regional Eulerian		Pai <i>et al.</i> (1997)
SAQM			Xu <i>et al.</i> (2000abc)
CMAQ-Hg			Bullock and Brehme (2002); Lin <i>et al.</i> (2003); Gbor <i>et al.</i> (2006, 2007); Vijayaraghavan <i>et al.</i> (2007); Sillman <i>et al.</i> (2007); Wen <i>et al.</i> (2011)
REMSAD			U.S. EPA (2008a); NESCAUM (2008)
CTM	Global Eulerian		Shia <i>et al.</i> (1999); Seigneur <i>et al.</i> (2006, 2008); Lohman <i>et al.</i> (2008)
CTM/TEAM		Specific source-attribution results for the Great Lakes** and five regional sites*	Seigneur <i>et al.</i> (2001, 2003, 2004ab*); Vijayaraghavan <i>et al.</i> (2004**)
MOGUNTIA			Bergan <i>et al.</i> (1999, 2001)
GRAHM			Dastoor and Larocque (2004)
MSCE-Hg-Hem		Hemispheric	Travnikov (2005)
GEOS-Chem			Selin <i>et al.</i> (2007, 2008); Strode <i>et al.</i> (2007, 2009); Selin and Jacob (2008); Holmes <i>et al.</i> (2010); Jacob <i>et al.</i> (2010); Corbitt <i>et al.</i> (2011)
HYSPLIT-Hg (with GEM)	Regional Lagrangian + Global Eulerian	Specific source-attribution results for the Great Lakes	This work

1.3.5. Important Features of this Work

There are several features of this work that make it particularly useful for providing information about atmospheric deposition of mercury to the Great Lakes. These are briefly summarized here.

- Contributions from sources at all distance scales -- local, regional, national, continental, and global – are included in the modeling analysis;
- Different numerical methodologies are used to estimate the deposition from distant sources vs. sources closer to the Great Lakes, improving the accuracy of contribution estimates over the use of a single “one-size-fits-all” approach;
- Deposition to each of the Great Lakes and their watersheds is explicitly tracked in the model. In essence, each of the lakes and their watersheds are considered a “grid square” (not actually square, but the actual shape of the lake or watershed) for the purpose estimating deposition. Most other models produce results for grid squares and the results for the Great Lakes have to be estimated based on apportioning the gridded output to one or more lakes or watersheds – a very approximate procedure, especially for Eulerian model with relatively coarse grids.
- Source-attribution information for each Great Lake and each watershed is estimated for each source in the emissions inventories used as input to the model. This level of source-attribution information is uniquely detailed, and goes far beyond the typical level of detail giving results for a handful of world regions (e.g., Asia, Europe, North America, etc.).
- This is the first time that the above features have been combined for analysis of atmospheric mercury deposition to the Great Lakes and their watersheds, and we believe that this study is providing the most comprehensive answers to date for the key questions summarized above (Section 1.2) – namely, the quantity of mercury deposited and where it comes from.

1.4. Goals of this 1st Phase of the Project

This report documents the activities carried out in the first of a multi-year project to estimate the amount and source-attribution for atmospheric mercury deposition to the Great Lakes. The goals of this first phase of this project were the following:

- Determine the study time period;
- Assemble and test required model inputs (e.g., meteorological data and emissions inventories);
- Conduct a wide variety of tests to guide selection of model physics options (e.g., time step, dispersion parameters);
- Select an initial set of standard source locations;
- Carry out an initial set of simulations for each of these standard sources locations, for each of the three primary forms of mercury emissions -- Hg(0), Hg(II), and Hg(p);
- Develop and test appropriate post-processing computer codes, e.g., programs that combine the emissions inventory data with the standard source location simulations using interpolation techniques;
- Using all of the above, create an initial set of “base case” results, that can serve as the basis for sensitivity analyses and further examination during the next phase of the project;
- Conduct an initial evaluation of the results by comparison of model predictions against ambient measurements in the Great Lakes region.

1.5. The Next Phases of the Project

This first phase of the project (above) can be thought of as setting up the computational framework for the analysis -- e.g., model inputs, model configuration, computational strategy, and post-processing programs -- and using this framework to create (and evaluate) an initial, baseline set of results. These activities were carried out successfully in this first phase and will be described in this report. The work planned for the 2nd phase of the project will build directly on this earlier work and will be briefly summarized here to provide context.

In the next phase, the computational framework constructed in the first phase will be utilized to carefully examine the sensitivity of the source-attribution and model-evaluation results to model inputs, assumptions, and parameters. This new analysis is expected to provide valuable quantitative information on the uncertainty in the results, and, will guide the selection of the optimum model configuration and computational strategy.

In carrying out this work, we plan to utilize a larger dataset of ambient measurements -- including, for example, concentrations of mercury in the atmosphere -- to the extent that they are available. Initially, we will attempt to identify and obtain these additional ambient data. As with work in the first phase, we will focus on data in the Great Lakes region. If time and resources allow, we will attempt to include data from outside the Great Lakes region.

Then, the modeling framework will be exercised numerous times using different -- but plausible -- inputs, assumption, and parameters, in each case producing a set of source-attribution and model-evaluation results. The results will characterize the sensitivity of the results to these computational variations. And, since the input variations will be proscribed to be within physically plausible ranges, the sensitivity will provide useful information about the uncertainty in the modeling analysis.

If funding is obtained for the 3rd phase of the project, the modeling framework developed in the 1st phase and honed in the 2nd phase will be used to examine numerous potential alternative emissions scenarios. A portion of the work in this 3rd phase will include working with stakeholders and others to obtain/assemble policy relevant scenarios.

If funding is obtained for the 4th phase of the project, the modeling analysis will be updated for a more recent year, e.g., 2008. The analysis will benefit from the vastly increased amount of ambient monitoring data that are available for more recent years, relative to the 2005 study year of the present analysis. As will be described immediately below, 2005 was chosen as the study year for the present analysis because it was the latest year for which emissions inventory information was available for the majority of emissions sources impacting the Great Lakes.

2. Methodology

In this section, the project methodology is described. The year 2005 was chosen for analysis as it represented the latest year for which U.S. and global mercury emissions inventory information was available. Accordingly, meteorological data for 2005 were utilized. The HYSPLIT-Hg model was used to simulate the fate and transport of mercury emitted from sources throughout the world. A “post-processing” methodology was used to estimate source-attribution for each source in the inventories utilized. Because the inventories and meteorological data were for the year 2005, a preliminary model evaluation was performed by comparing the model predictions against available 2005 ambient monitoring data. These components of the methodology are described below.

As noted earlier, in this report we will refer to three “kinds” of atmospheric mercury: (i) elemental mercury, or Hg(0); (ii) reactive gaseous mercury (RGM), or Hg(II); and (iii) particulate mercury, or Hg(p). Except where noted, results presented in this report are for total mercury (the sum of the three different forms), for simplicity and brevity’s sake, even though the modeling is done with explicit treatment of the different forms of atmospheric mercury.

2.1. HYSPLIT-Hg Model

The HYSPLIT model (Draxler and Hess, 1998) has been developed at the NOAA Air Resources Laboratory (ARL) and used for many applications. Examples include simulations of the atmospheric fate and transport of sulfur dioxide (Rolph *et al.*, 1992, 1993), ozone (Draxler, 2000; Stein *et al.*, 2000), smoke plumes (Draxler *et al.*, 1994; McQueen and Draxler, 1994), dioxin (Cohen *et al.*, 1995, 2002; Schaum *et al.* 2010), atrazine (Cohen *et al.*, 1997), emergency response (Draxler *et al.*, 1997), volcanic emissions (Hollingshead *et al.*, 2003) and eruptions (Stunder *et al.*, 2007), emissions from forest fires (Rolph *et al.*, 2009) and sand and dust storms (Wang *et al.*, 2011), and in verifying the Comprehensive Nuclear Test Ban Treaty (Becker *et al.*, 2007). The model was evaluated in each of the above applications and has also been evaluated in several field tests (e.g., Draxler, 1991, 2006; Draxler and Stunder, 1988; Draxler and Taylor, 1990).

A specially-configured research version of the NOAA HYSPLIT model, “HYSPLIT-Hg”, was utilized in this project. Initial HYSPLIT-Hg mercury modeling results for the Great Lakes have been published for 1996 (Cohen *et al.*, 2004), and for 1999 (Cohen *et al.*, 2007). In addition, the HYSPLIT-Hg model was recently used in a model Intercomparison study over a European domain (Ryaboshapko *et al.*, 2007ab).

The HYSPLIT-Hg model used in this analysis was based on a November 2010 release of HYSPLIT version 4.9. The additions to the base HYSPLIT model implemented to simulate atmospheric mercury include: (a) mercury phase-partitioning in the atmosphere; (b) mercury chemistry in the gas and aqueous (droplet) phases in the atmosphere; (c) wet and dry deposition algorithms modified to better simulate atmospheric mercury deposition; (d) additional source-receptor output to aid in source-attribution analyses. There are many differences between the HYSPLIT-Hg model utilized in this analysis compared to that used in the aforementioned Cohen *et al.* (2004, 2007) analyses. However, the principal difference is the inclusion of an integrated global Eulerian model (GEM) in the simulation. A stand-alone version of this GEM model (Draxler 2007) was incorporated into the base HYSPLIT model in ~2010, and the HYSPLIT-Hg model used here was based on this GEM-capable HYSPLIT version. Appropriate modifications to the base GEM algorithms were implemented to simulate mercury.

In HYSPLIT and HYSPLIT-Hg, the default simulation of emitted pollutants is carried out in a Lagrangian fashion. In essence, the pollutant is simulated in the plume – and only in the plume – as it is transported downwind of the source. In the GEM-capable versions of HYSPLIT and HYSPLIT-Hg, the user can transfer emitted pollutant mass older than a specified age from this Lagrangian framework into a global Eulerian grid. From that point on, the transferred pollutant is simulated on the Eulerian grid. The advantage of this approach is that fine-scale source-receptor details can be investigated in the local and regional areas around the source with a Lagrangian approach, but the larger scale simulation can be carried out with an Eulerian approach. The impetus for this methodology arose due to the fact that impractically large computational resources are required to accurately simulate large scale (e.g., global) dispersion solely with a Lagrangian approach. By switching to an Eulerian approach at a specified point downwind of the source, computation efficiency can be greatly improved with little or no loss of simulation accuracy.

Additional details regarding the configuration and types of simulations performed with the HYSPLIT-Hg model for this study are provided below, in Section 2.4.4 (page 47).

2.2. Meteorology

The HYSPLIT model utilizes three-dimensional, gridded meteorological data as an input. Two such datasets were used in this modeling analysis: the EDAS (Eta Data Assimilation System) and the NCEP/NCAR Global Reanalysis.

The EDAS data set (NOAA ARL, 2011a) is based on meteorological model output from the NOAA National Weather Service (NWS) National Centers for Environmental Prediction (NCEP). It is archived at NOAA ARL in a form readily usable by the HYSPLIT model. The EDAS data archived by ARL has a domain encompassing the continental United States, along with northern Mexico and southern Canada (see Figure 3), referred to in this report as “central North America”¹. The dataset is archived with a 3-hour temporal resolution, a horizontal spatial resolution of approximately 40 kilometers, and with 26 vertical levels up to a height of approximately 20,000 meters in the atmosphere.

To simulate the fate and transport of mercury outside of the EDAS domain, the global meteorological dataset “NCEP/NCAR Reanalysis” was used. The NCEP/NCAR Reanalysis Project is a joint project between the NOAA National Centers for Environmental Prediction (NCEP) and the National Center for Atmospheric Research (NCAR). As with EDAS, the data are archived at NOAA ARL in a form readily usable by the HYSPLIT model (NOAA ARL 2011b). The NCEP/NCAR Reanalysis dataset is archived with a 6-hour temporal resolution, a horizontal spatial resolution of approximately 250 kilometers (2.5 degrees), and with 17 vertical levels up to a height of approximately 30,000 meters in the atmosphere. The NCEP/NCAR model grid is shown below (Figure 4).

¹. A modeling domain referred to extensively in this study is the EDAS-40km meteorological modeling domain, comprising the Continental United States, Southern Canada, and Northern Mexico (see Figure 3). For notational efficiency, we will refer to this as a “central North American” domain in this report, as it does not contain the northern-most and southern-most portions of North America.

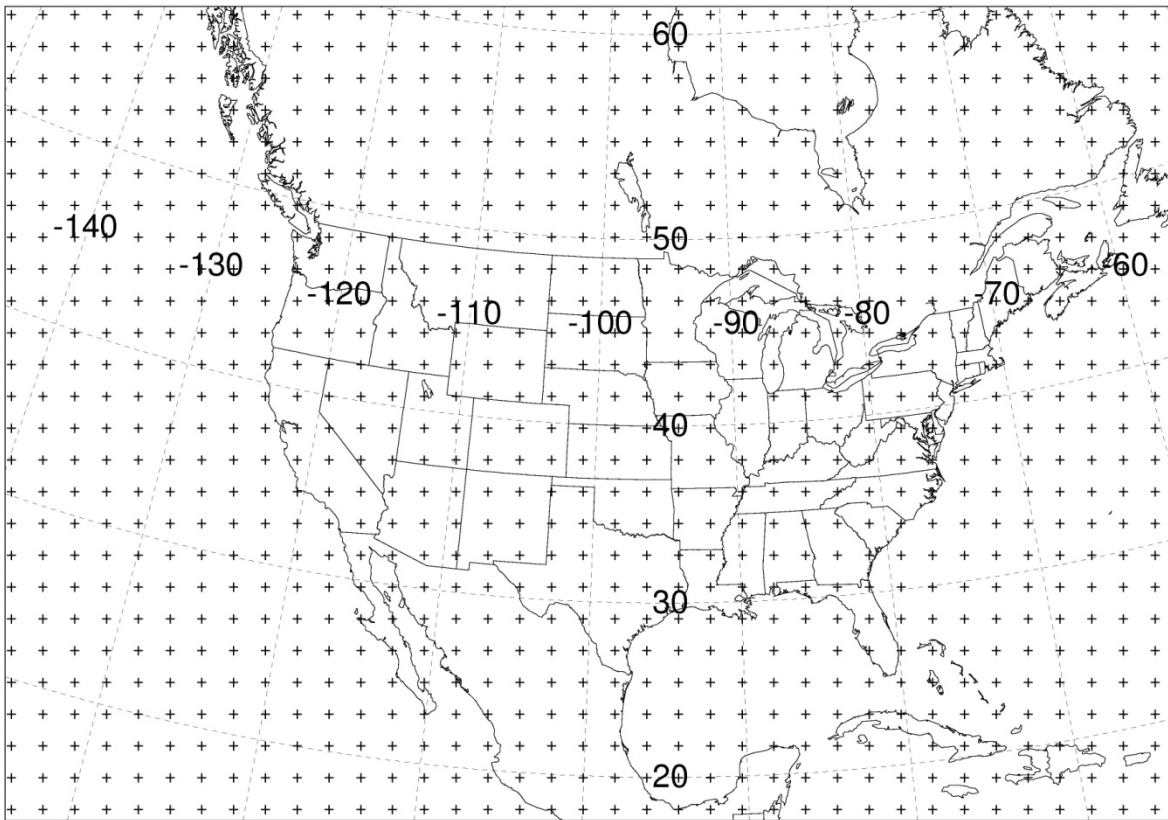


Figure 3. The EDAS-40km Meteorological Model Data Grid (showing every 5th grid point)

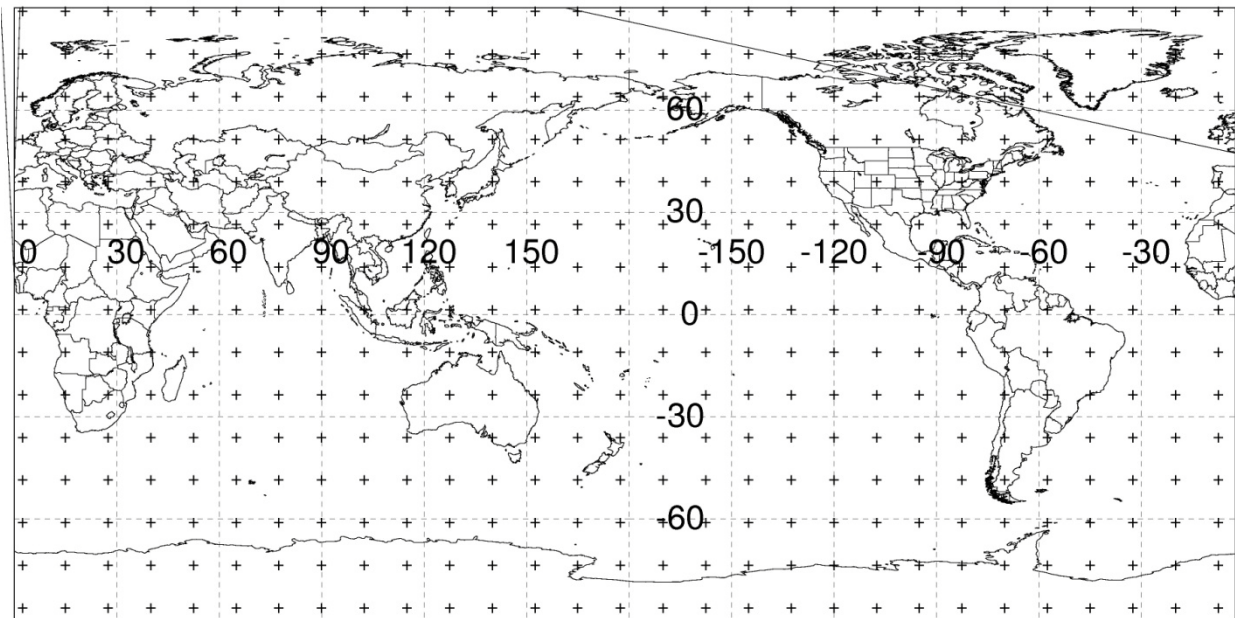


Figure 4. The NCEP/NCAR Reanalysis Model Data Grid (showing every 5th grid point)

2.3. Emissions

The following three types of emissions are considered in this study:

- **Direct Anthropogenic Emissions.** These are anthropogenic sources estimated to be “active” during 2005, including operating coal-fired power plants, metal smelters, waste incinerators, cement kilns, chlor-alkali plants, and other types of ongoing mercury emissions.
- **Re-Emitted Anthropogenic Emissions.** These are re-emissions of mercury previously deposited from the atmosphere as the result of previous direct anthropogenic emissions.
- **Natural Emissions.** These are emissions of mercury from natural processes such as volcanic activity and weathering of mercury-containing minerals. This category also includes re-emissions of deposited mercury originating from previous natural emissions. Natural emissions can be thought of as the emissions that would occur without any anthropogenic influence.

In order to carry out the atmospheric fate and transport modeling in this project, global, spatially-resolved inventories of the above types of sources are required. Since the modeling is done with explicit treatment of Hg(0), Hg(II), and Hg(p), the inventories must also be explicitly “speciated” into these three forms. The sources of data and the estimation methodology used to develop model-ready emissions inventories are described in the following sub-sections.

As noted above, the year 2005 was chosen for the “analysis” year of this study. This was done because 2005 was the most recent year for which emissions inventory data sets were generally available for the majority of source regions potentially impacting the Great Lakes. In the descriptions below, it can be seen that 2005 inventories were used for some, but not all, source types/regions. If emissions inventories were assembled with less time delay and with more frequency, it would have been possible to perform this analysis for a more recent year than 2005. Such an analysis would have been more policy relevant, and would have been able to benefit from the improved quality of meteorological data and larger quantity of mercury measurement data available in more recent years. To the extent that resources and suitable emissions inventories are available, this analysis will be updated to more recent years.

2.3.1. Direct Anthropogenic Emissions in the United States

For point-source mercury emissions in the United States, the U.S. EPA’s 2005 National Emissions Inventory (NEI) was utilized (U.S. EPA, 2008b). For sources whose emissions were not separated into elemental, reactive gaseous, and particulate forms, EPA-recommended “speciation” factors were utilized to appropriately partition the emissions. The emissions records were aggregated at the facility level for convenience in mapping and to enhance computational modeling efficiency. A total of 19353 emissions records are contained in this inventory, representing total mercury emissions of 95 Mg/yr. A

summary of the U.S. point source mercury emissions used in this work is presented in Figure 5. We note that total mercury emissions from U.S. coal-fired power plants used in this analysis is very consistent with a just-released 2005 power-plant inventory for North America (CEC, 2011).

Some sources are so small and widespread (e.g., mobile sources) they are classified as “area sources” and are only defined on an areal basis, e.g., on the county-level in the U.S. For these so-called area sources in the United States, the U.S. EPA’s 2002 National Emissions Inventory (NEI) was utilized (U.S. EPA: 2006, 2007). The overall emissions from this inventory are relatively small, on the order of 7% of direct U.S. anthropogenic emissions. Moreover, the 2002 area source inventory formed the predominant basis for the 2005 NEI area source inventory and so there are not expected to be significant differences between the two inventories. Whatever differences exist would be much less than 7% (and most likely much less than 1%) of the U.S. direct anthropogenic emissions. Thus, given that resources available for this project were tightly constrained, the use of the 2002 inventory -- which had been already processed for model use in a previous project -- was considered a reasonable time-saving measure. As with point sources, EPA-recommended “speciation” factors were utilized to appropriately partition the emissions. A total of 44848 emissions records are contained in this inventory, representing total mercury emissions of 7.4 Mg/yr. A summary of the U.S. area source mercury emissions used in this work is presented in Figure 6.

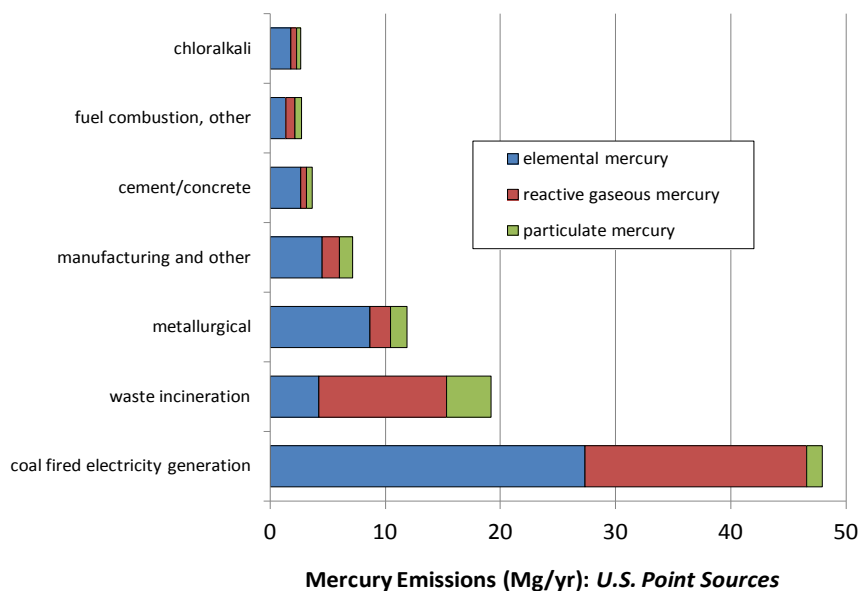


Figure 5. Mercury Emissions from U.S. Point Sources estimated from the U.S. EPA 2005 National Emissions Inventory

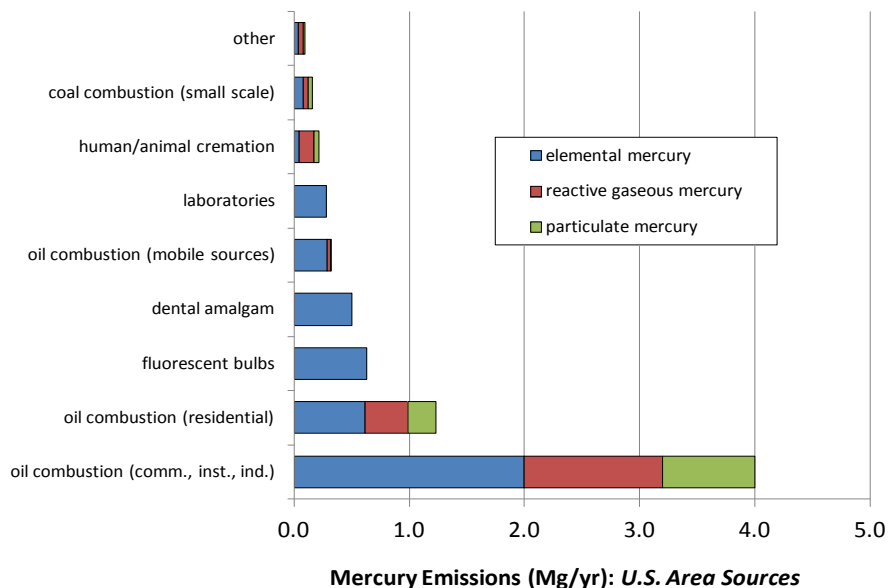


Figure 6. Mercury Emissions from U.S. Area Sources estimated from the U.S. EPA 2002 National Emissions Inventory

2.3.2. Direct Anthropogenic Emissions in Canada

For point-source mercury emissions in Canada, the 2005 Environment Canada’s 2005 National Pollutant Release Inventory (NPRI) was utilized (Environment Canada, 2011). Since mercury emissions in this inventory are not separated into elemental, reactive gaseous, and particulate forms, EPA-recommended “speciation” factors were utilized to appropriately partition the emissions. A total of 166 emissions records are contained in this inventory, representing total mercury emissions of 5.1 Mg/yr. A summary of the Canadian point source mercury emissions used in this work is presented in Figure 7. The total mercury emissions from Canadian coal-fired power plants used in this analysis is very consistent with a just-released 2005 power plant inventory for North America (CEC, 2011).

As with the U.S. inventory above -- and as is the common practice in the development of emissions inventories -- some small, widespread Canadian sources are classified as “area sources” and are only defined on an areal basis. For these so-called area sources in Canada, 2000 data from Environment Canada were utilized, defined on a 100-km grid (Environment Canada, 2008). Since the overall emissions from this inventory are relatively small, the use of the 2000 inventory was considered reasonable. As with the point sources, EPA-recommended “speciation” factors were utilized to appropriately partition the emissions. A total of 12372 emissions records are contained in this inventory, representing total mercury emissions of 2.4 Mg/yr. A summary of the Canadian area source mercury emissions used in this work is presented in Figure 8. It is noted that this Canadian area source inventory does contain emissions for a few moderately large point sources of mercury (not contained in the publically available NPRI database), due to Canadian policy regarding disclosure of emissions data.

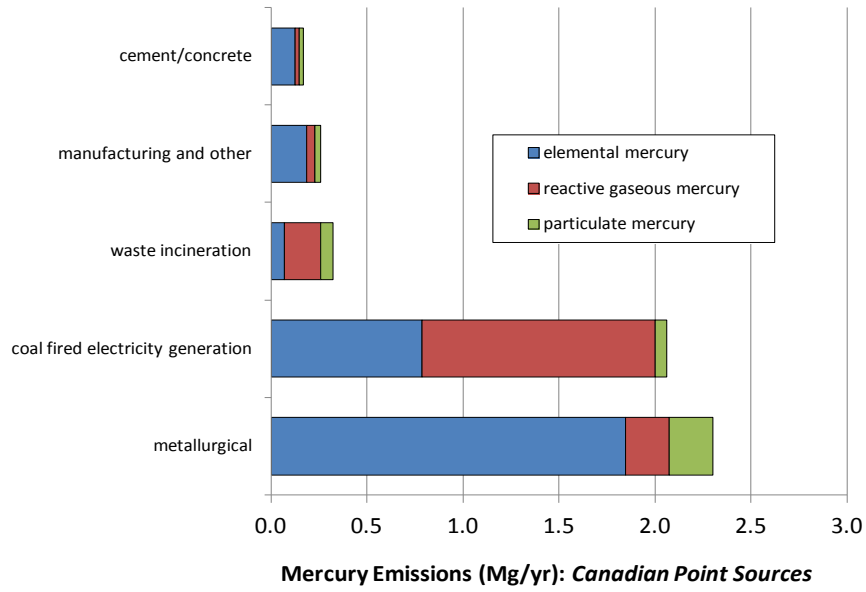


Figure 7. Mercury Emissions from Canadian Point Sources estimated from Environment Canada's 2005 National Pollutant Release Inventory

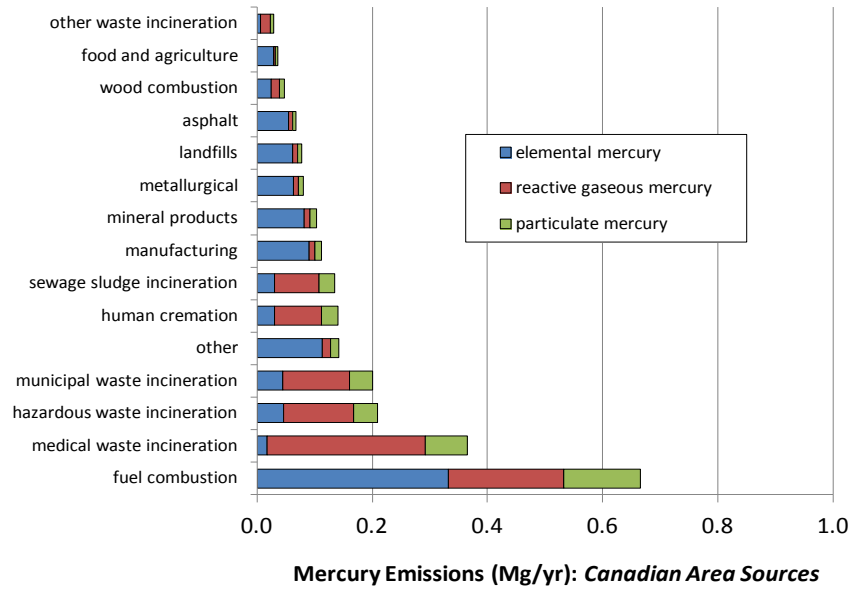


Figure 8. Mercury Emissions from Canadian Area Sources used in this analysis

2.3.3. Direct Anthropogenic Emissions in Mexico

For point source mercury emissions in Mexico, the latest detailed inventory that was available for use in this project was a 1999 inventory prepared for the Commission for Environmental Cooperation (CEC) by Acosta and Associates (Acosta-Ruiz and Powers, 2001). Since mercury emissions in this inventory are not separated into elemental, reactive gaseous, and particulate forms, EPA-recommended “speciation” factors were utilized to appropriately partition the emissions. A total of 268 emissions records are contained in this inventory, representing total mercury emissions of 29.3 Mg/yr. A summary of the Mexican point source mercury emissions used in this work is presented in Figure 9. The metallurgical category in this figure is made up of the following components: gold mining/refining - 11.3 Mg/yr, mercury mining/refining - 9.7 Mg/yr, copper smelters – 1.5 Mg/yr, primary lead and zinc smelters – 0.2 Mg/yr, and ferrous smelters – 0.09 Mg/yr. The total mercury emissions from Mexican coal-fired power plants used in this analysis is very consistent with a just-released 2005 power plant inventory for North America (CEC, 2011).

The Acosta-Ruiz and Powers (2001) inventory also contains estimates for five area source categories, for the entire nation, as summarized in Figure 10, totaling 1.9 Mg/yr. For the purposes of this project, these area-source emissions were geographically apportioned to each of the 32 Mexican states based on year-2000 population. The area sources for each Mexican state were assigned to the centroid of the state. This is a reasonable simplification for this project: the location “errors” introduced are only a very small fraction of the distance from the sources to the Great Lakes (~2000 – 3000 km).

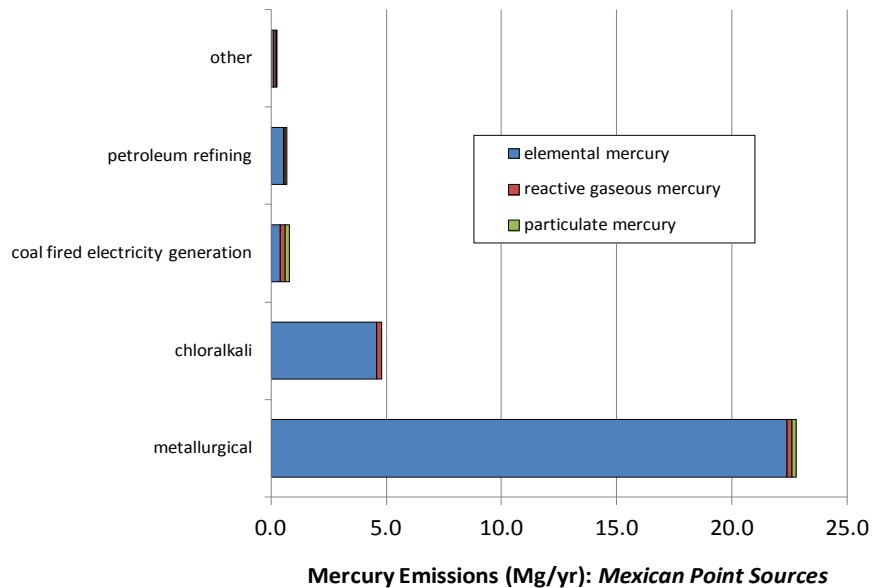


Figure 9. Mercury Emissions from Mexican Point Sources used in this analysis

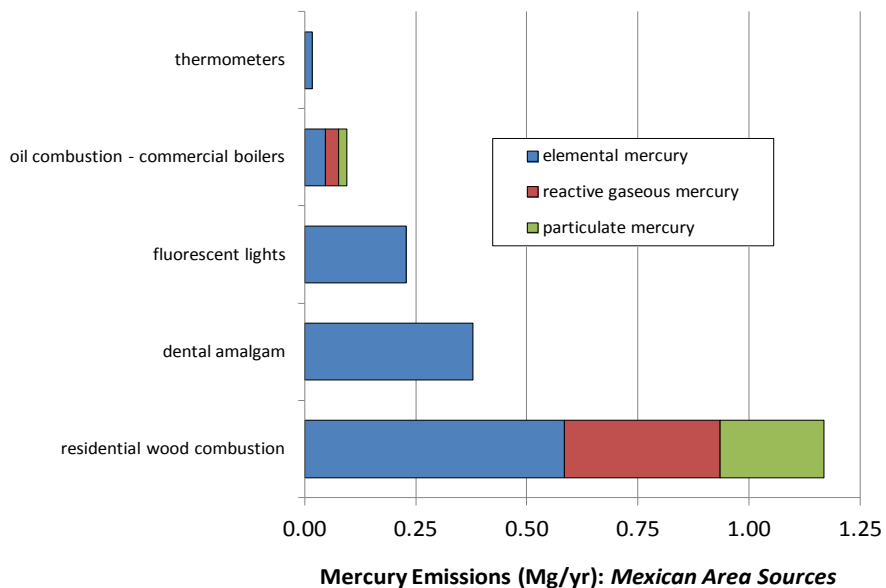


Figure 10. Mercury Emissions from Mexican Area Sources used in this analysis

2.3.4. Anthropogenic Emissions in the Rest of the World

For anthropogenic mercury emissions in the remainder of the world -- i.e., aside from the United States, Canada, and Mexico -- the global inventory of Jozef Pacyna and colleagues was used (Pacyna et al., 2010, Wilson et al., 2010). This inventory is specified on a 0.5 x 0.5 degree grid (approximately 50 km x 50 km), with total emissions of elemental, reactive gaseous, and particulate mercury for each grid cell. The contributions of different emissions sectors -- e.g., coal-fired electricity generation, waste incineration, etc. -- are not provided on a grid-cell by grid-cell basis. Emissions from grid points in North America were removed from the Pacyna inventory, and country-specific inventories were used, as described above. However, since the sector-specific estimates for individual grid cells are not given in the Pacyna inventory, it is not possible to show the sector breakdown for the resultant "global minus North America" inventory. Therefore, the "total" global emissions in the Pacyna inventory are shown in Figure 11, including values in that inventory for North America.

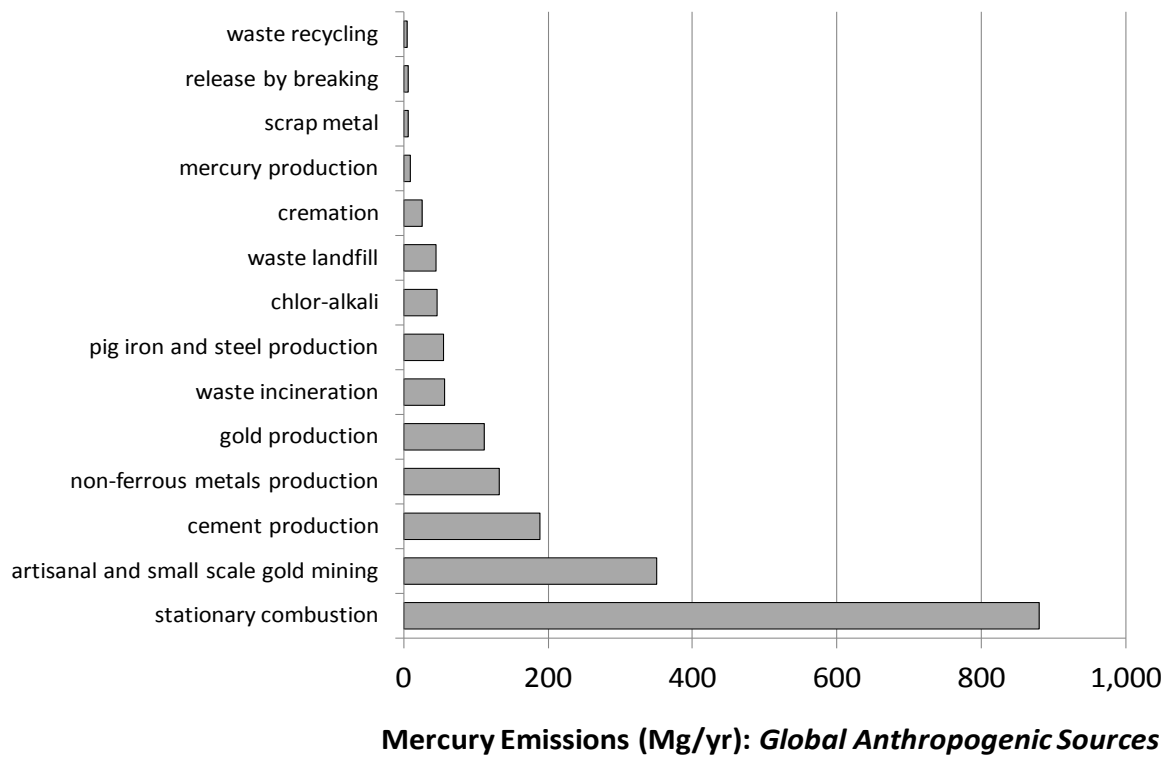


Figure 11. Mercury Emissions from Global Anthropogenic Sources

2.3.5. Summary of Global Anthropogenic Emissions

A summary of the global direct anthropogenic emissions inventories used in this analysis is shown below in Figure 12. To produce this map, the individual sources in the inventories were allocated to a 2x2 degree grid (approximately 200 km x 200km). The actual spatial resolution of the sources, especially the “point” sources in each of the North American inventories, is of course known to a much higher degree of spatial resolution. For the purposes of the modeling carried out, we have used the exact spatial coordinates of each source, to the extent that it is known. In Figure 12, we have simply summed up the sources over a 2x2 degree grid for display purposes.

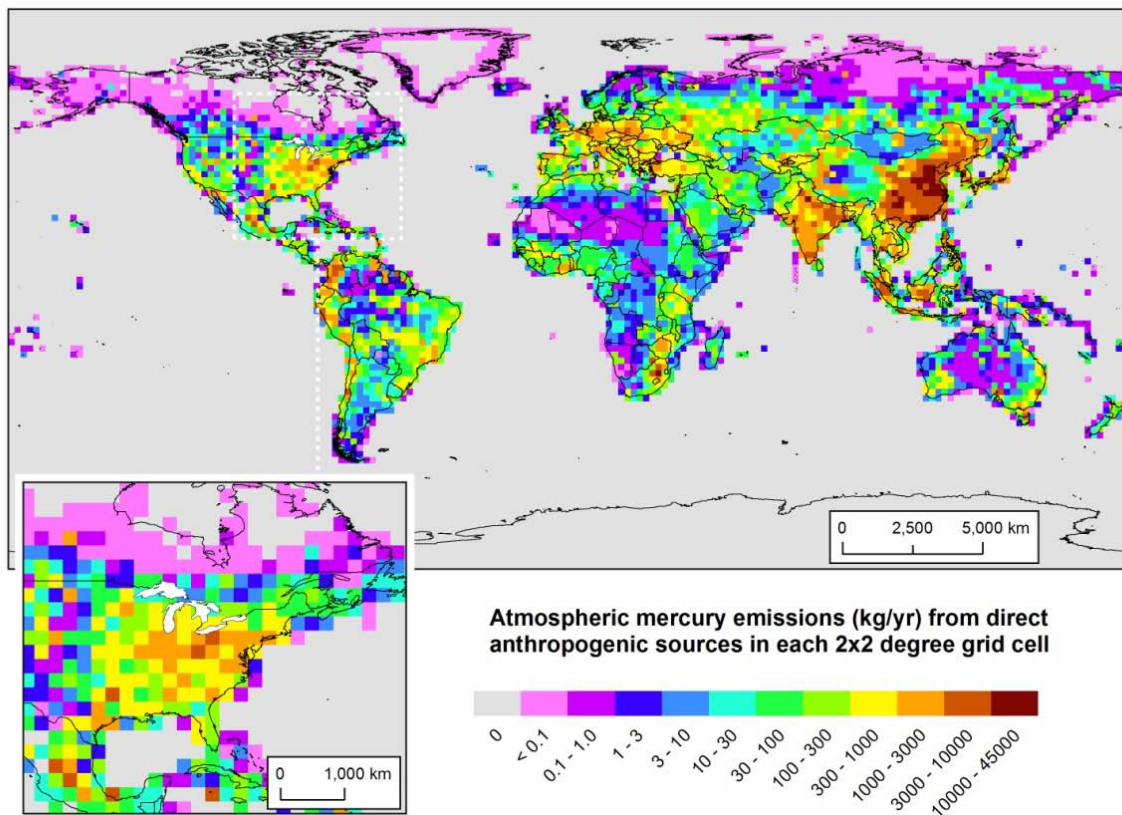


Figure 12. Anthropogenic Mercury Emissions

A summary of the same dataset of direct anthropogenic emissions sources is shown in higher resolution in Figure 13. In this map, the individual sources in the inventories were allocated to a 1x1 degree grid (approximately 100 km x 100km). As noted above, the actual spatial resolution of the sources is generally known to a higher resolution, but the sources have been aggregated onto a 1x1 degree grid for display purposes. Throughout this document, the similar display conventions will be used, i.e., a given dataset will be aggregated onto a 2x2 degree grid for global displays and will be aggregated onto a 1x1

degree grid for a central North American display. The comparatively sparse nature of the coverage in Mexico – with several grid cells showing emissions of “0” -- is likely due to two factors: (i) there are relatively few point sources in the Mexican inventory (only 268 for the entire country are included in the inventory) suggesting that this inventory may be incomplete; and (ii) the area sources have been aggregated at the state level and assigned to the center of each given state. As discussed above, this spatial allocation simplification for these sources is not expected to introduce any biases into the simulations.

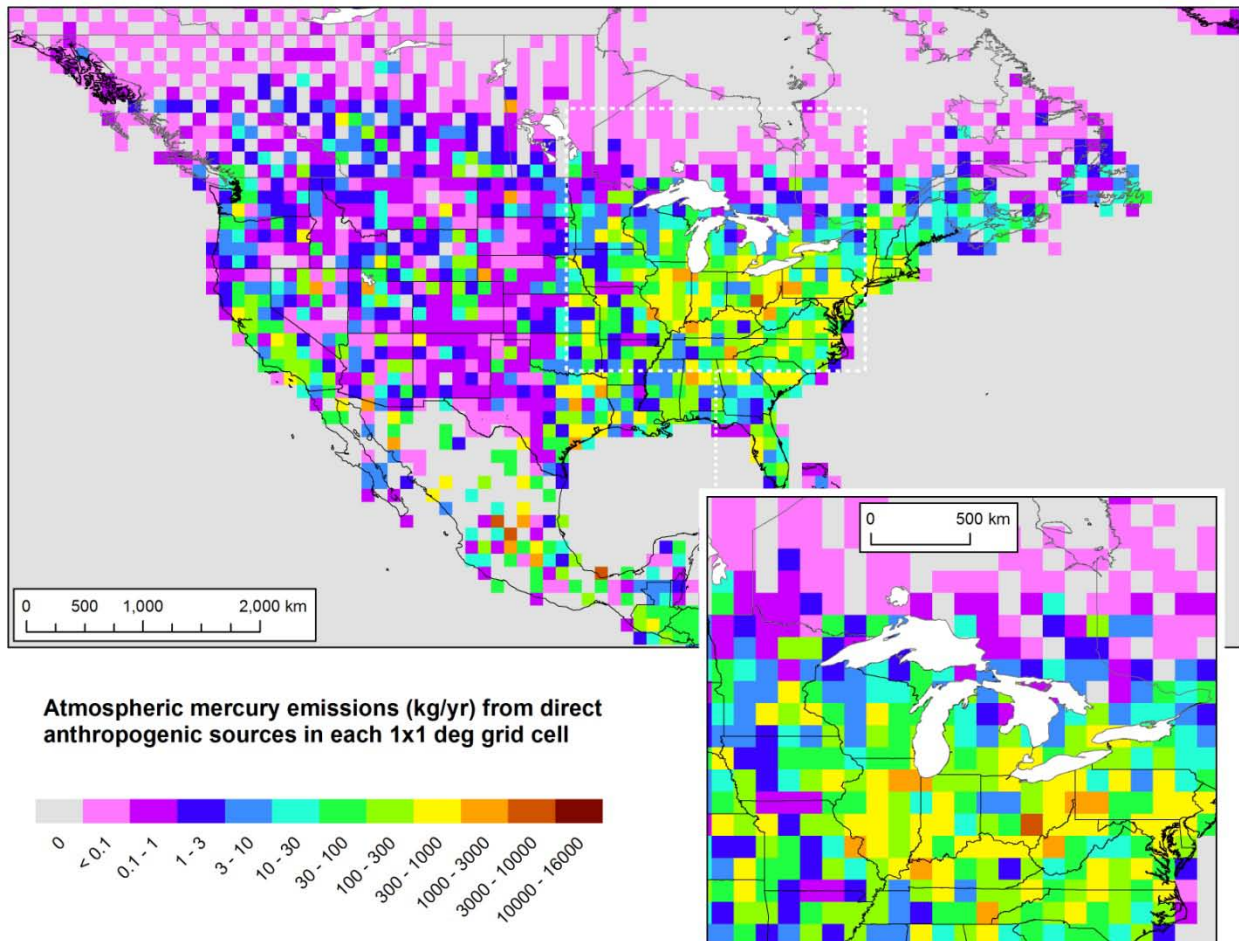


Figure 13. Atmospheric mercury emissions from direct anthropogenic sources displayed on a 1x1 degree grid over central North America

2.3.6. Re-Emissions and Natural Emissions

Natural emissions are those that arise from volcanic activity, from mercury-containing rocks and soils, and from other environmental processes. Once anthropogenic or natural mercury is deposited it can be re-emitted to the atmosphere. Re-emissions are generally considered to occur in the form of elemental mercury, as the volatility of Hg(II) (aka RGM) and Hg(p) forms are very low. Global estimates of the total amount of natural mercury emissions and mercury re-emissions are highly uncertain and vary widely (e.g., see review by Selin et al., 2007).

We have used provisional estimates for these processes in the present work with the intention of revisiting these estimates – and examining the sensitivity of the results to them -- in the next phase of this work. The total (and spatial distribution of) global natural emissions used provisionally in the present analysis is 1800 Mg/yr, following Ryaboshapko et al. (2007a). These emissions are shown on a global domain in Figure 14 and a central North American domain in Figure 15. As a provisional estimate, total re-emissions from land (and freshwater) surfaces are taken as 750 Mg/yr, and total re-emissions from the oceans are taken as 1250 Mg/yr. Land re-emissions are spatially distributed proportional to total anthropogenic emissions, and ocean re-emissions are spatially distributed proportional to natural ocean emissions from Ryaboshapko et al. (2007). Global and North American views of these inventories are shown in Figure 16 and Figure 17.

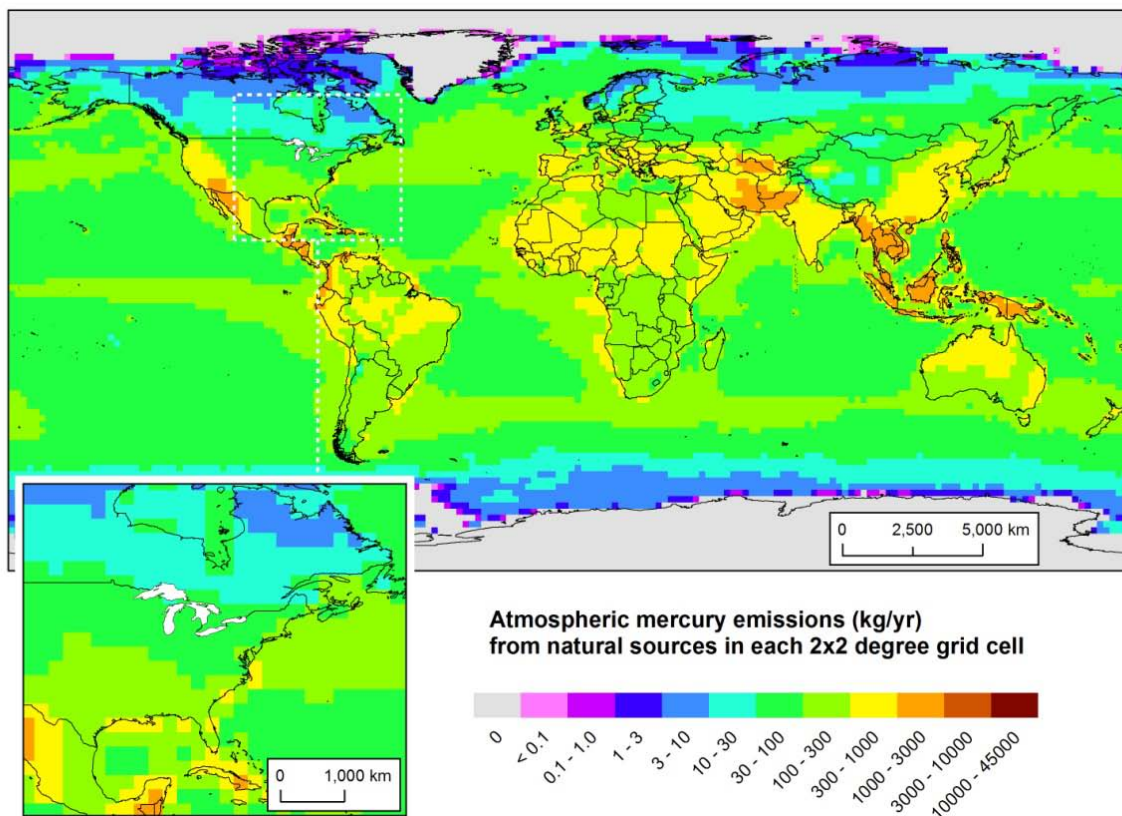


Figure 14. Natural mercury emissions displayed on a 2x2 degree global grid

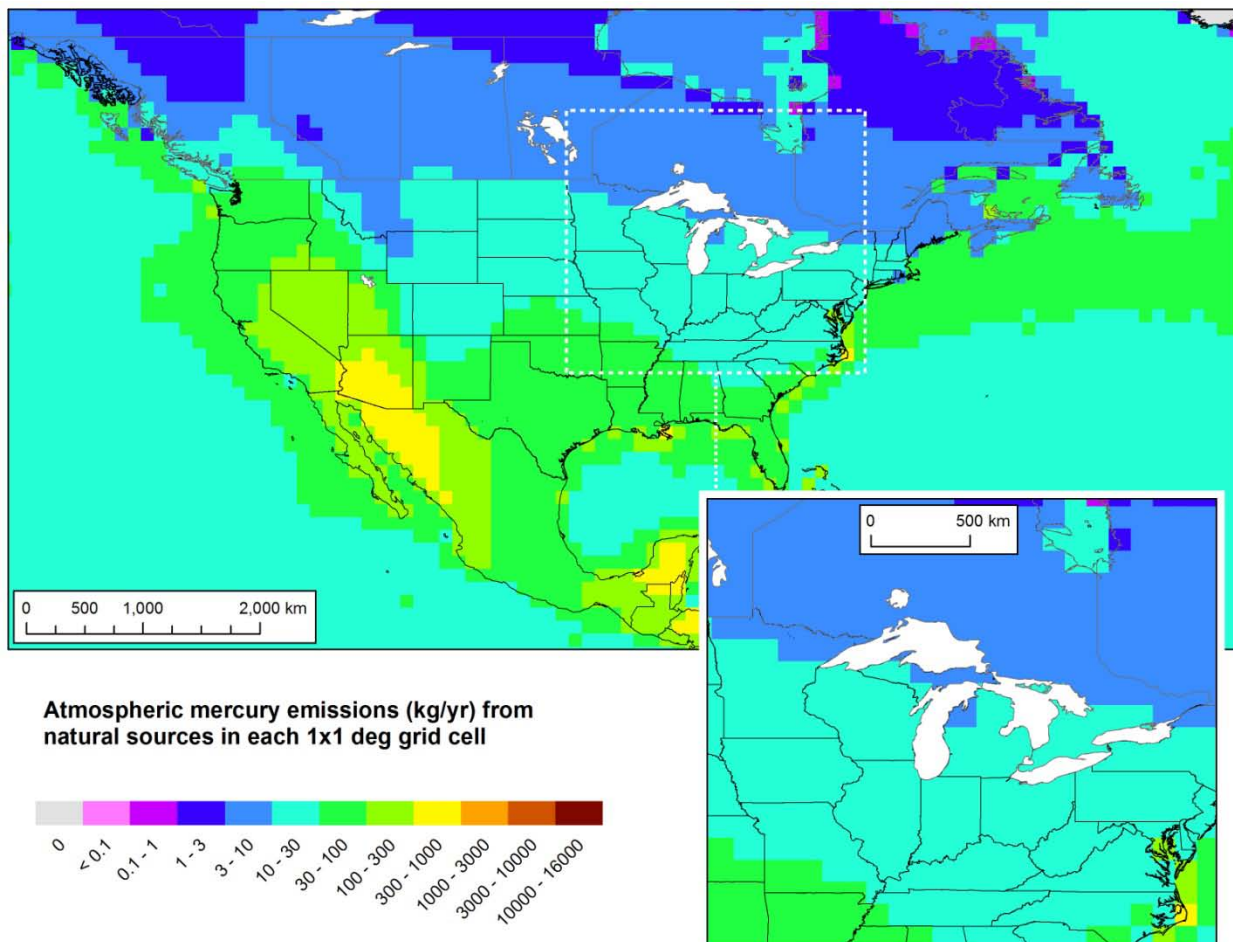


Figure 15. Natural mercury emissions displayed on a 1x1 degree grid over a central North American domain

It should be noted that by estimating the current re-emissions from land as being proportional to current emissions, we have likely underestimated the contribution from source regions – like the United States – which have had historically high emissions but which have recently reduced overall mercury emissions. This is because the amount of deposition in the past due to these source regions would have been much higher than in the present day, and so the re-emissions from these regions would likely be higher than that estimated using “current” emissions rates for those regions. For example, emissions in 2005 from the U.S. are significantly below historical U.S. emissions rates (e.g., Streets *et al.*, 2011; Pirrone *et al.*, 1998; Cohen *et al.*, 2007). So, the re-emissions from the U.S. from previously deposited U.S.-based anthropogenic emissions have probably been underestimated by this methodology.

In the present analysis, we have separated out the upward and downward portions of the net flux of elemental mercury at the earth’s surface. The emissions values being used for natural and re-emissions represent the “gross” or “one-way” volatilization flux that would occur if the concentration of elemental mercury in the atmosphere were zero, i.e., if there was no “back-pressure” of elemental mercury to

slow volatilization. Concurrently, elemental mercury deposition has been modeled as a comparable “gross” or “one-way” downward flux, estimated as if the concentration of elemental mercury in the surface layer was zero. Computational separation of the upward and downward components of elemental mercury’s surface exchange flux is commonly done and can be shown to be mathematically and physically equivalent to other types of computational methodologies. However, the approach used here is relatively simple in terms of the spatial and temporal variations in flux that occur in the real world. In future work, we will attempt to investigate the sensitivity of the results to different methodologies for estimating Hg(0) surface exchange.

As discussed above, in reality there is a continuous, dynamic two-way exchange of elemental mercury at the surface of the earth. It is not generally possible to separate out the different components of emission and deposition from one another. In reality, all that can generally be done is to estimate (or measure) the total net surface exchange, whether it be upwards (net emissions) or downwards (net deposition). From the provisional values used in this analysis, the global total net elemental mercury surface exchange flux, equal to the total natural and re-emitted mercury emissions minus the total elemental deposition from all sources – is a net volatilization of ~3100 Mg/year. It is noted that this net elemental mercury surface exchange flux is comparable to those used in recent modeling analyses carried out with the Geos-Chem model (Corbitt et al., 2011, in press; Selin et al., 2008). In these analyses, the total net elemental surface exchange fluxes were volatilizations of 3800 and 3400 Mg/year, respectively.

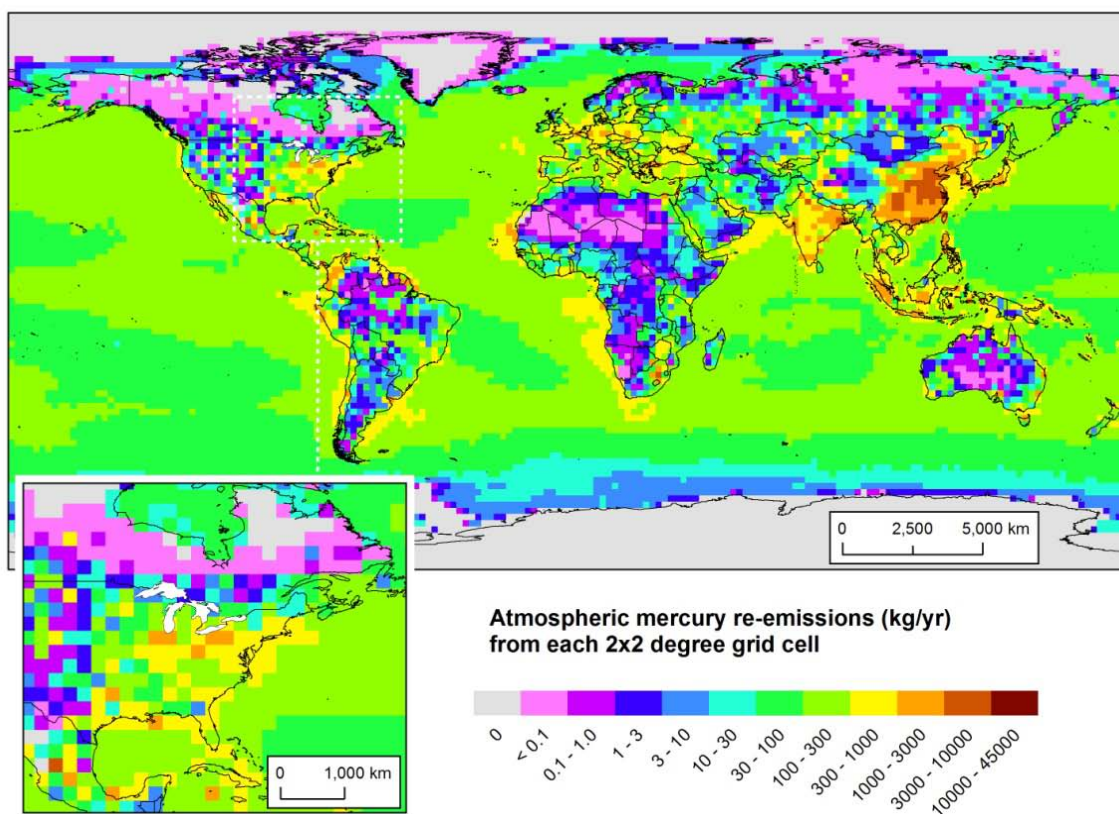


Figure 16. Atmospheric re-emissions of previously deposited mercury from anthropogenic sources displayed on a 2x2 degree global grid

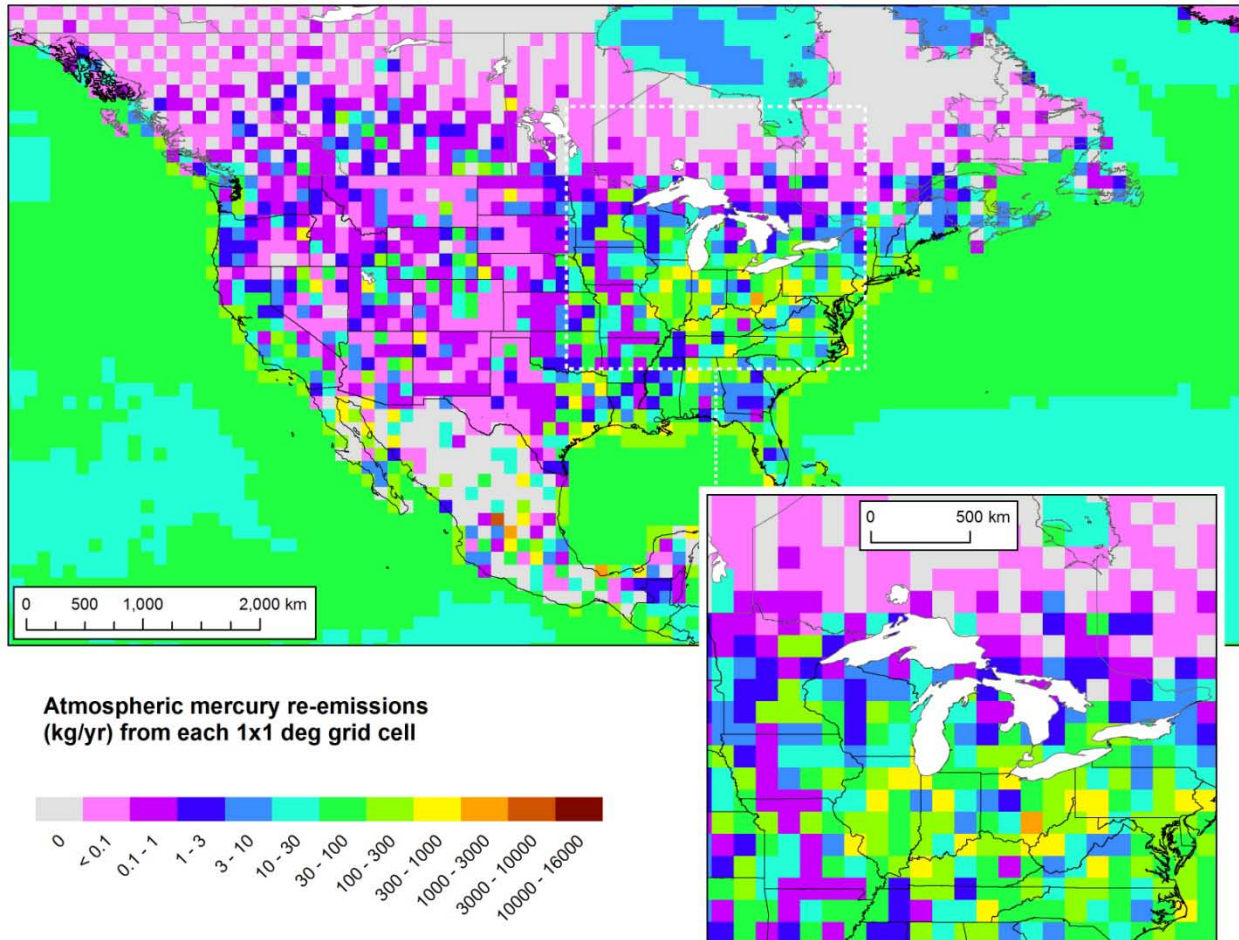


Figure 17. Atmospheric re-emissions of previously deposited mercury from anthropogenic sources displayed on a 1x1 degree grid over a central North American domain

2.3.7. Emissions Summary

Global and central North American maps of total mercury emissions – equal to direct anthropogenic, re-emitted anthropogenic, and natural sources – are shown in Figure 18 and Figure 19 . A summary of the emissions inventories used in this analysis is presented in Table 3. The total mercury emissions -- summed over all of the inventories -- is ~5700 Mg/year.

The primary reason why the year 2005 was chosen for this analysis is that at the time the project was begun, this was the most recent year for which emissions inventory data sets were generally available for all critical source regions potentially impacting the Great Lakes. Ideally, emissions inventories would be prepared with less time delay and with more frequency. If this were done, it would be possible to perform analyses such as this for more “recent” years. More contemporaneous analyses would be more policy relevant, and would be able to benefit from the generally improving quality of meteorological and mercury measurement data available in more recent years.

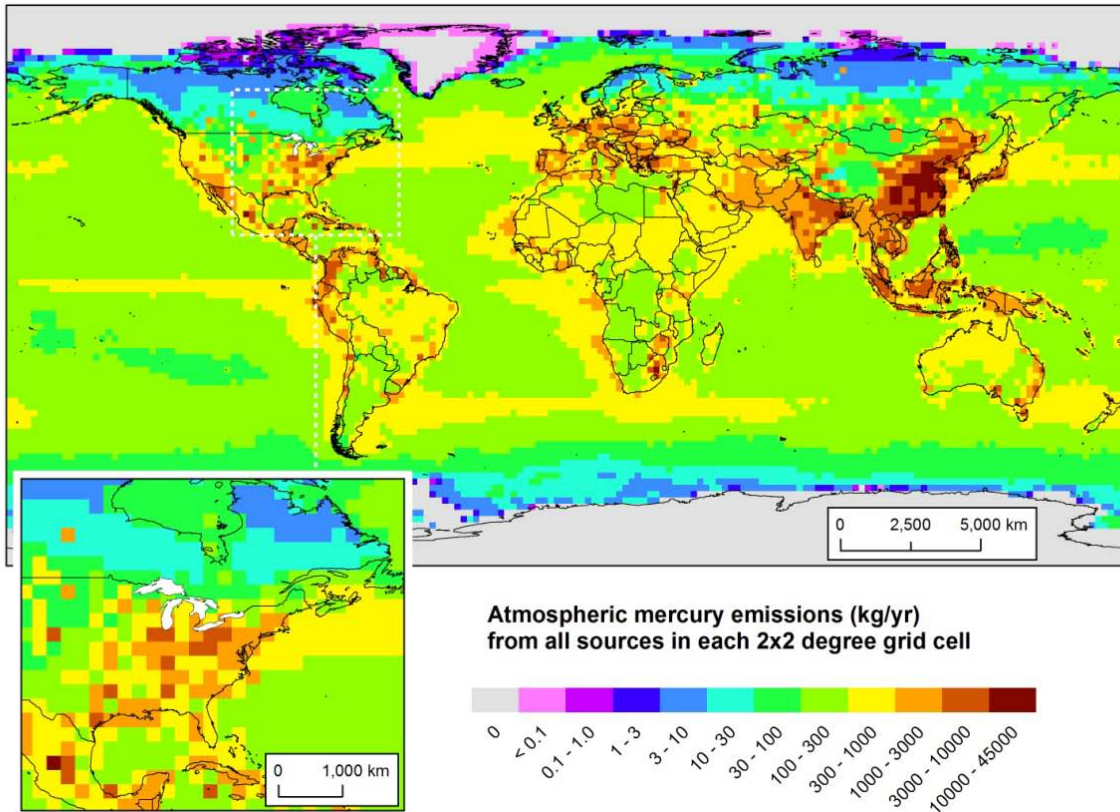


Figure 18. Atmospheric mercury emissions from all sources displayed on a 2x2 degree global grid

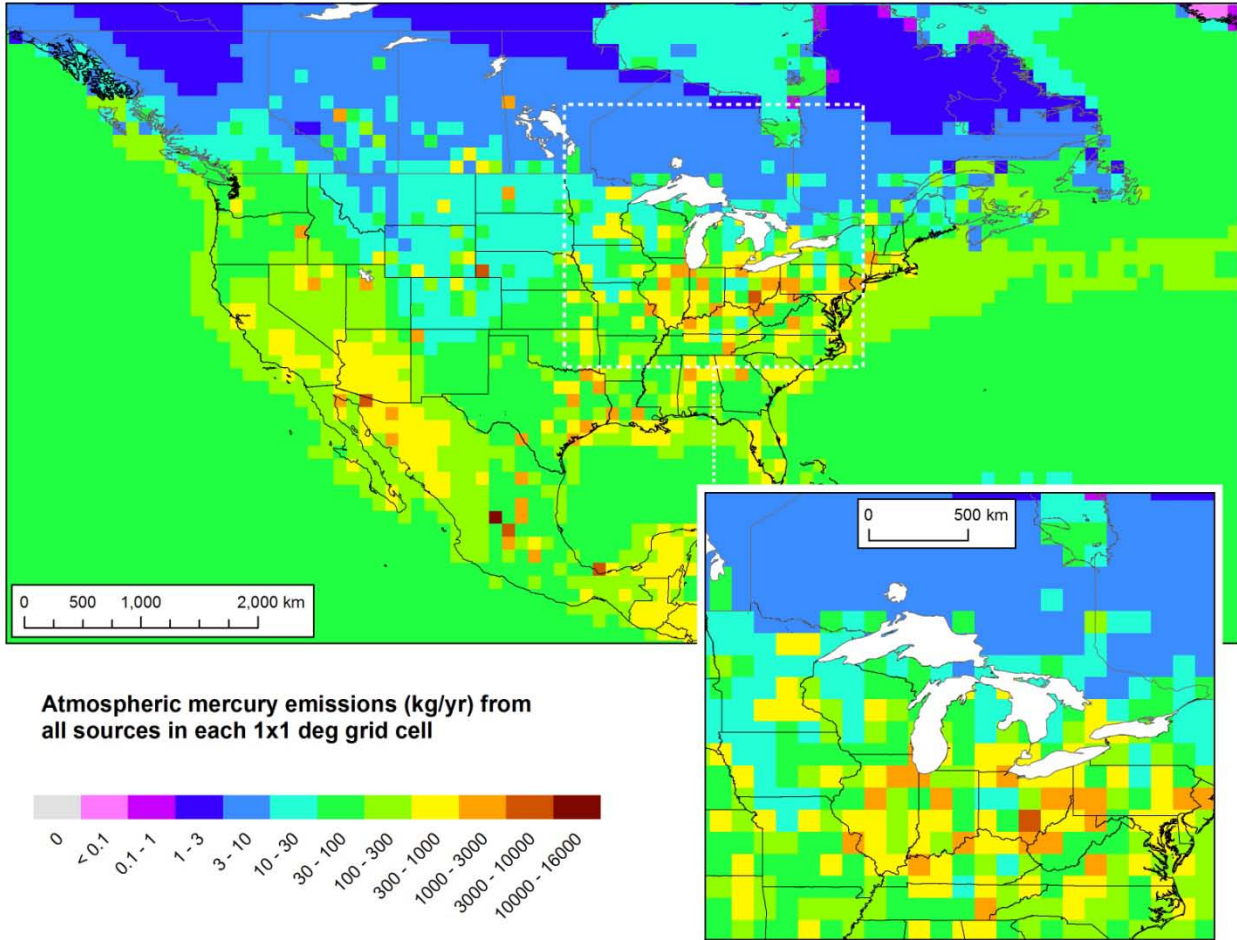


Figure 19. Atmospheric mercury emissions from all sources displayed on a 1x1 degree grid over central North America

Table 3. Summary of Mercury Emissions Inventories Used in this Analysis

Inventory	domain	Number of records	Hg(0) emissions (Mg/yr)	RGM emissions (Mg/yr)	Hg(p) emissions (Mg/yr)	Total mercury emissions (Mg/yr)
U.S. Point Sources	United States	19,353	50.6	35.5	9.1	95
U.S. Area Sources	United States	44,848	4.5	1.8	1.1	7.4
Canadian Point Sources	Canada	166	3.0	1.7	0.4	5.1
Canadian Area Sources	Canada	12,372	1.0	0.96	0.42	2.4
Mexican Point Sources	Mexico	268	28	0.81	0.46	29
Mexican Area Sources	Mexico	160	1.25	0.38	0.25	1.9
Global Anthropogenic Sources not in U.S., Canada, or Mexico	Global, except for the U.S., Canada, and Mexico	52,173	1,239	434	113	1,786
Global Re-emissions from Land	Global land (and freshwater) surfaces	129,180	750	0	0	750
Global Re-emissions from the Ocean	Global oceans	43,324	1,250	0	0	1,250
Global Natural Sources	Global	64,800	1,800	0	0	1,800
Total		366,804	5,127	475	125	5,728

2.4. Computational Methodology

2.4.1. Introduction

Conceptually, the overall modeling procedure involves modeling the emissions of mercury from each source in the inventory. However, because there are hundreds of thousands of sources in the combined U.S., Canadian, Mexican, and global emissions inventories, it is not feasible to explicitly model each individual source with its own simulation. A procedure has been developed that allows the individual impacts of *each* source in the inventory to be estimated, based on a more limited set of simulations (Cohen et al., 2002, 2004). In this technique, an interpolation procedure is used to estimate detailed source-receptor relationships. To conduct the analysis, explicit HYSPLIT-Hg simulations of emissions were performed for a limited number of *standard source locations*. Then, the impact of any given source – at other locations – on the Great Lakes was estimated based on a weighted average of the impacts of the nearest explicitly modeled *standard source locations* nearest to that given source. This procedure is illustrated conceptually in Figure 20.

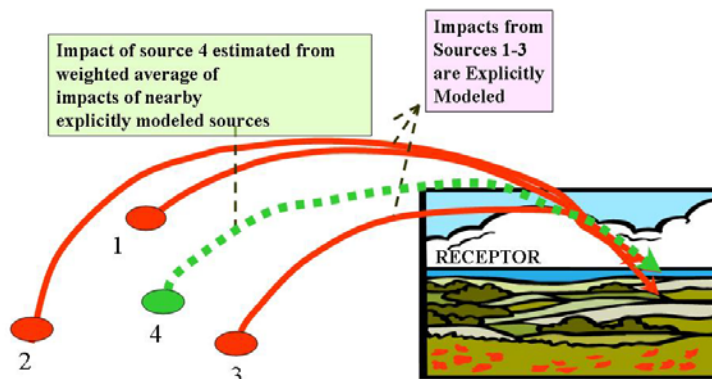


Figure 20. Spatial Interpolation

To account for the varying proportions of different mercury forms being emitted from different sources, separate unit-emission simulations of Hg(II) , Hg^0 , and Hg(p) emissions were made at each standard source location. The impact of a source emitting a mixture of Hg^0 , Hg(II) , and Hg(p) was estimated based on a linear combination of these pure-component unit emissions simulations. An example of this procedure is illustrated in Figure 21.

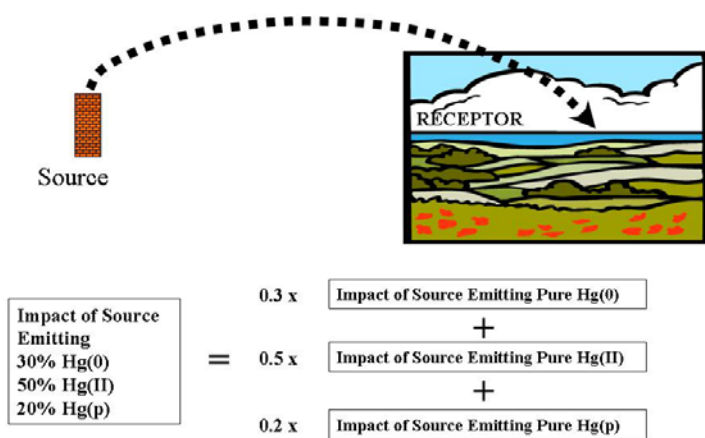


Figure 21. Chemical Interpolation

In sum, both spatial and chemical interpolation procedures were used to estimate the impact of each source in the inventory on each of the Great Lakes. This spatial and chemical interpolation methodology relies on the “assumption” that the atmospheric fate and transport of mercury from any given source is not influenced by the mercury emissions from any other source. This assumption is consistent with the current understanding of atmospheric mercury.

2.4.2. Standard Sources Used in the Analysis

The choice of the number and individual locations of “standard sources” is governed by the primary consideration that the interpolation procedures described above do not introduce unreasonable uncertainties into the analysis. The practical implications of this overarching dictum include the following:

- Standard sources should be located in regions with the highest emissions. These regions have the highest “priority” for ensuring interpolation accuracy.
- Conversely, few if any standard sources need to be located in regions with little or no emissions, as interpolation errors in those regions will not have much impact on the overall results.
- Very far from receptors of interest, the spacing between standard sources can be relatively large, as the “plume” from such distant source will be very diffuse by the time it eventually (if ever) reaches a receptor of interest. In essence, the plume will be so widespread that the precise location of the source will have little or no influence on its impact on the receptor. There can be exceptions to this guideline if there are significant meteorological or terrain gradients.

- Conversely, as the source region gets closer and closer to any receptor of interest, the density of standard source locations must generally increase, as the spatial gradients in impacts increase. For example, a source ~20 km away from a receptor in the prevailing “upwind” direction will have a dramatically different impact from an identical source ~20 km in the prevailing “downwind” direction, even though the sources are only ~40 km apart. Clearly one would want to have standard source locations in both upwind and downwind locations.
- A corollary to the above consideration is that the density of sources needs to be higher in the prevailing upwind directions than in the prevailing downwind directions away from a receptor of interest, as – all things being equal -- the greatest impacts will occur from sources generally upwind of the receptor. Or in other words, downwind of the receptor, it’s more acceptable to have larger interpolation errors because the overall impacts are relatively small.
- Due to computational resource constraints, it is important to not have more standard sources than are necessary to carry out the analysis at hand. With an optimum number of standard sources, more computational resources can be available for sensitivity and scenario analyses.

Fortunately it is possible to “check” the interpolation procedures by explicitly simulating source locations “in between” a base set of locations, and determining exactly the extent to which the interpolation procedure “worked”. These types of tests have been conducted exhaustively in previous studies (e.g., Cohen et al., 2002, 2004). It has been found that if the above guidelines are followed, uncertainties introduced by the interpolation procedure are generally trivial compared to uncertainties in essentially every other aspect of the fate and transport simulation (e.g., emissions, meteorological data, atmospheric chemistry, deposition processes).

With the above considerations in mind a total of 136 standard locations were selected and employed in the current analysis, as shown in Figure 22 and Figure 23. It can be seen from these figures that the above guidelines were generally followed. For example, given the large emissions from China, a relatively high density of standard sources were located there, even though the distance from China to the Great Lakes is very large. Conversely, few standard sources are located in regions of the earth with relatively small emissions. Also, the density of standard sources generally increases as one gets closer and closer to the Great Lakes basin. Overall, of the 136 standard source locations, ~75 are located in the U.S., southern Canada and northern Mexico (“central North America”), and ~61 are located outside of this region.

Note that in general, three simulations need to be carried out for each standard source location – one for unit emissions (1 g/hr) of pure Hg(0), one for unit emissions of pure Hg(II), and one for unit emissions of pure Hg(p). Each simulation was carried out starting in October 2004, which allowed 3 months of “spinup” simulation before the actual results for 2005 were obtained. Thus, each simulation was carried out for 15 months. A total of $136 \times 3 = 408$ simulations basic simulations were required. Depending on a number of simulation factors (e.g., time step chosen for a particular run), these individual runs took between 1 and 7 CPU-days each, with an average of about 3 CPU-days. Thus, the 408 simulations required a total of ~1200 CPU days, or more than 3 CPU-years. With the 16-processor workstation

utilized in this project, the calendar time alone required to carry out the runs was on the order of $1200 / 16 = 75$ days (about 2.5 months). While not discussed here, it is also noted that many hundreds of tests were done before the “production” runs were carried out, to ensure that the choices in simulation parameters were optimized.

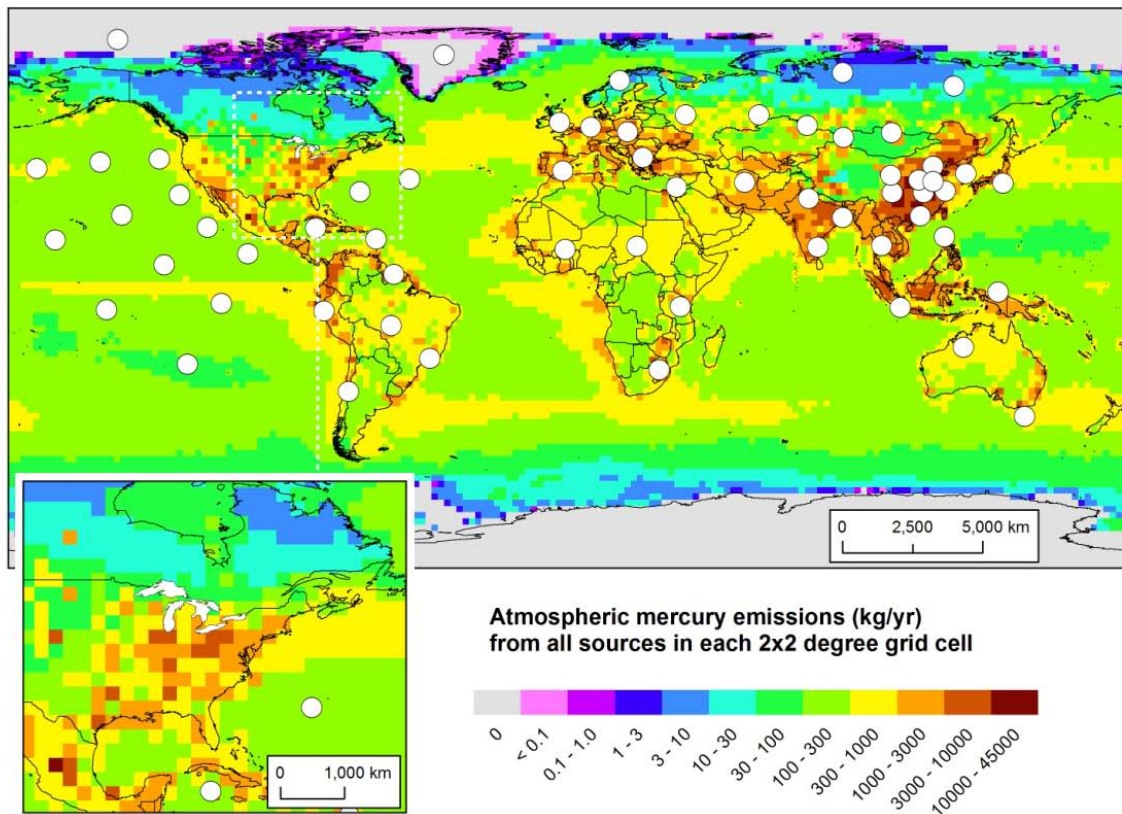


Figure 22. Standard Points Outside of North America

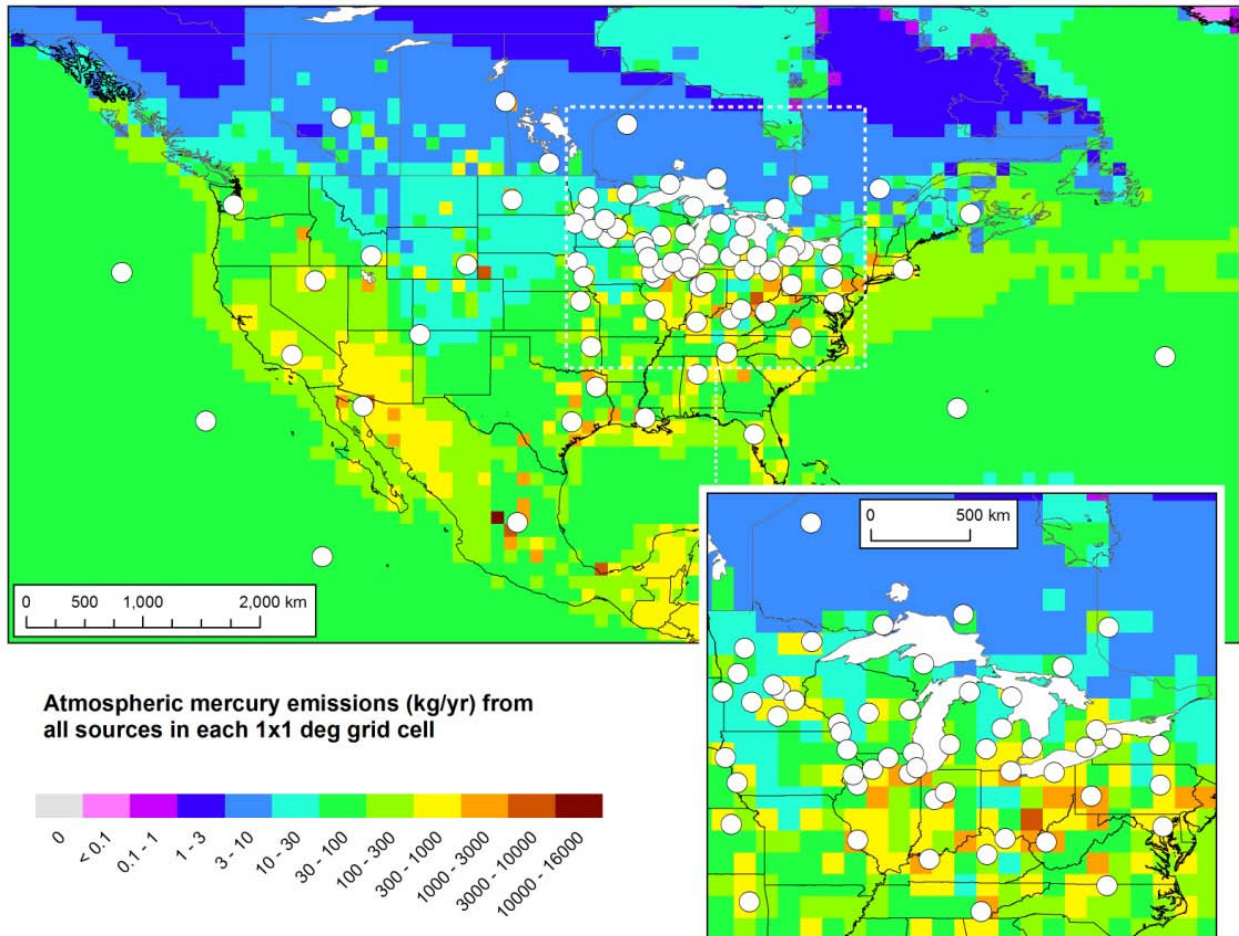


Figure 23. Standard Points in North America

2.4.3. Estimating Deposition at “Point” Monitoring Sites vs. Large Area Receptors

Typically, modeling analyses are evaluated by comparing their predictions with measurements at monitoring sites. We will present such an evaluation analysis in Section 5, below. However, the primary goal of this project is to create accurate estimates of the amount and source attribution for mercury deposition to the Great Lakes – *not* to produce deposition estimates at monitoring sites in the region.

As will be seen shortly, it is generally much more difficult – and computationally intensive – to accurately predict deposition at a single monitoring site (or a set of such sites) than it is to predict deposition for large area receptors such as the Great Lakes. Consider Figure 24, a conceptual diagram in which we show a *hypothetical* situation with a receptor of interest, a monitoring site, and several (8) mercury emissions sources in the vicinity of the monitoring site. For reference, a prevailing wind direction, distance scale, and map orientation are also shown. Since the winds do not always blow in the “prevailing” direction, all of the sources will have some impacts on the monitoring site. However, even if each of the sources were identical, they would likely have dramatically different impacts on the

monitoring site, given their different spatial orientation to the site. For example, given the prevailing wind direction, source #4 would be expected to have a relatively large impact on the site, but source #5 would be expected to have a relatively small impact on the monitoring site. The consequence is that to estimate the wet deposition of mercury at the monitoring site – arising simply from the sources in the vicinity of the site alone -- standard sources would most likely have to be located *at each of the eight sources shown*.

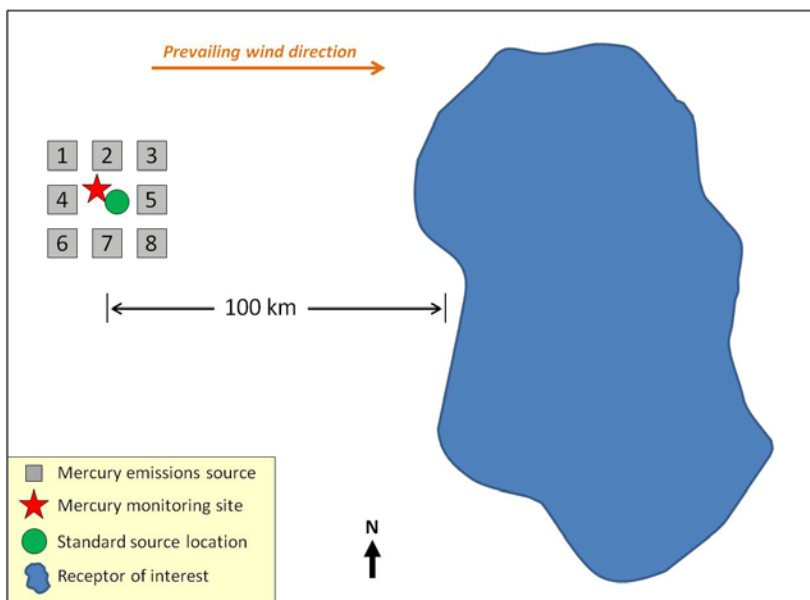


Figure 24. Conceptual Diagram of Sources, Monitoring Sites, and Receptors

However, to accurately estimate the impacts of the 8 sources on the receptor of interest, about 100 km away in this hypothetical example, a single standard source location located near the “center” of the source group would likely suffice. In other words, to estimate the concentration or deposition at the monitoring site in this simple, hypothetical example, 8 standard source locations would be needed – corresponding to 24 different computer simulations, one for each of the three forms of mercury emitted – whereas only 1 location (3 simulations) would be needed to estimate the deposition impact of the sources on the receptor of interest. Because of computational resource constraints, and given the overarching goals of this project, we have prioritized the estimation of deposition to the Great Lakes -- large area receptors – rather than focus on “point” monitoring sites in the region. Substantially more standard source locations than the 136 utilized would have had to have been used to generate the same accuracy for monitoring site estimates as were generated for the Great Lakes in this analysis. Notwithstanding all of the above, as will be shown in Section 5 below, this modeling analysis produced results at monitoring sites in the Great Lakes region that were encouragingly – and perhaps even surprisingly – close to the measurements made at these sites.

2.4.4. Configuration of the HYSPLIT-Hg Model used in this Study

In order to estimate source-receptor relationships during 2005, simulations were carried out starting in October 2004, and run through December 2005. Longer spin-up periods were tested but did not appreciably affect the results obtained. Spin-up periods shorter than 3 months were determined to be too short. Therefore, the use of a 3-month spin-up period (i.e., the period from Oct-Dec 2004) was determined to be optimal in this study, to balance the need for computational efficiency with computational accuracy. Only deposition in 2005 was considered in the analysis, but material emitted in the last 3 months of 2004 was allowed to deposit during 2005. It is recognized that the atmospheric life of atmospheric mercury is on the order of 6-12 months, i.e., longer than 3 months, but, it was found through testing that longer spin-up times did not significantly change the source-receptor results obtained in the modeling. In essence, the most significant “hits” at receptor from sources occurred within the first 3 months after emissions, and neglecting deposition of longer-lived mercury emitted before 2005 had did not matter in this analysis.

Based on testing, it was found that three different kinds of simulations could be used to carry out the modeling analysis, with each applied to specific aspects of the problem. The division of the simulations was done for reasons of computational efficiency and accuracy, and extensive testing was done to establish that the division did not adversely affect the results in any significant way. The three types of simulations were the following:

- 3-D Lagrangian puff simulations (“PUF”) (comparable to those described in Cohen et al. (2004)) over a central North American² domain to model the fate and transport of emissions of Hg(II) and Hg(p) from sources in central North America;
- Combined 3-D Lagrangian puff and global Eulerian model simulations (“COM”) over a global domain to model the fate and transport of emissions of Hg(0) from sources in central North America;
- Global Eulerian model simulations (“GEM”) over a global domain to model the fate and transport of emissions of Hg(0), Hg(II), and Hg(p) from sources outside of central North America.

For the “PUF” simulations, the use of Lagrangian puffs alone allowed a greater accuracy in the transport and dispersion simulation – and hence increased accuracy in the ultimate determine of source-receptor relationships – because the initially emitted pollution was not artificially dispersed over a preset computational grid (a limitation in Eulerian models, e.g., Pai *et al.*, 2000). A full global Eulerian model simulation was not needed for central North American Hg(II) and Hg(p) emissions, because it was found that the deposition contribution to the Great Lakes Basin resulting from atmospheric mercury once it initially left the North American domain was negligible. For example, if the mercury was allowed to

². As noted earlier, modeling domain referred to extensively in this study is the EDAS-40km meteorological modeling domain, comprising the Continental United States, Southern Canada, and Northern Mexico (see Figure 3). For notational efficiency, we will refer to this as a “central North American” domain in this report, as it does not contain the northern-most and southern-most portions of North America.

circumnavigate the globe and “hit” the Great Lakes Basin multiple times, there was no appreciable increase in deposition over the first “hit” from the source, during its initial transport within the North American domain. The time step in the “PUF” (and “COM”) simulations was nominally set at 60 minutes, but was reduced to as few as 10 minutes for source locations in the vicinity of receptors of interest (e.g., the Great Lakes, and monitoring sites in the Great Lakes region) so that there would be no danger of pollutant puffs “leap-frogging” the receptor. These “PUF” simulations were generally much faster than the “COM” or “GEM” simulations, because they did not include the global Eulerian model component of the simulation. Depending on the time step used in the simulation, the “PUF” simulations took between ~12 hours (with a 60 minute time step) and ~40 hours (with a 10 minute time step) on the Xeon E5540 1.596 MHz processors used in this study³.

“GEM” simulations were done for sources of mercury outside central North America, where there were no receptors of interest – relative to the specific Great Lakes focus of this study. So, the 3-D puff component of the simulation was not needed to provide transport/dispersion accuracy in the local/regional portion of the simulation. For these sources, the Great Lakes Basin was so distant, that there was no advantage to using 3-D Lagrangian pollutant puffs at the start of the simulation. By the time the emitted mercury was transported to the Great Lakes basin from these sources, it had been dispersed over large enough areas that the Eulerian grid provided adequate resolution. By using only the global Eulerian model component of the simulation for these sources, and not the additional 3-D puff component as well, computational resources were saved. A “GEM” simulation from a single source location took on the order of 3 days on the Xeon E5540 1.596 MHz processors used in this study.

To simulate the fate and transport of elemental mercury emitted from central North American sources, a combination of the above treatments was required. For these “COM” simulations, a 3-D puff simulation was carried out for the first three weeks (504 hours) of the transport, and then the mercury was transferred to the global Eulerian model for subsequent simulation. This approach uses the full Lagrangian-Eulerian integrated capability of the HYSPLIT model. For these sources, the 3-D puff simulation provided accurate source-receptor results for the local/regional “hits” at receptors of interest, and also allowed for the very long distance “hits” that occurred after, for example, the emitted mercury circumnavigated the globe one or more times. These “COM” simulations took the most time – approximately 4-5 days each on the processors used in this work -- as they used both components of the computation.

³. A 16-processor work-station was used for this study, but only one processor was used for any given simulation. In carrying out the work, 15 simulations were done at the same time (each on its own processor), leaving one processor free to manage various computer system function.

3. Illustrative Results for Single Sources

Using the methodology described above, simulations from each of the selected 136 standard source locations were carried out with the HYSPLIT-Hg model, with a 3-month “spin-up”, to estimate the fate and transport of atmospheric mercury during 2005. Before the overall results for the Great Lakes and their watersheds are presented in the next section, illustrative examples of results from the standard source locations will be shown. For clarity in mapping and graphing, results for only a subset (48) of the 136 standard source locations will be displayed.

In order to conveniently compare different model results, a “transfer flux coefficient” X will be used, defined as the following:

$$X = \frac{\text{deposition flux rate}}{\text{emissions rate}} = \frac{\frac{\text{grams Hg deposited per year}}{\text{km}^2 \text{ of receptor area}}}{\text{grams Hg emitted per year from the source}} [=] \frac{1}{\text{km}^2}$$

By expressing the modeling results for a given source and a given receptor in this “normalized way”, it is easier to compare and understand the different results that are found. As a concrete example, suppose that a particular modeled mercury emissions source had total mercury emissions of 200 kg/yr (equal to 200,000 g/yr). And suppose that the emissions from this source were modeled and it was estimated that the source contributed a total of 100 g/yr in total deposition to a particular receptor, say, Lake Erie. The surface area of Lake Erie is ~25,600 km², so, the total modeled mercury deposition flux is equal to 100 (g/yr) / 25600 (km²) = 0.00391 (g/km²-yr). In this situation – with this source and this receptor for these modeling results – the transfer flux coefficient is then calculated as:

$$X = 0.00391 \text{ (g/km}^2\text{-yr)} / 200,000 \text{ (g/yr)} = 1.96 \times 10^{-8} \text{ (1/km}^2\text{)}$$

The advantage of using the transfer flux coefficient is that it normalizes the results for the area of the receptor, and normalizes the results for the source emissions. If one is given the modeled transfer flux coefficient for a given source and a given receptor, then one can easily estimate the deposition flux contribution to the receptor arising from the source emissions:

$$\begin{aligned} \text{deposition flux rate} &= \frac{\text{grams Hg deposited per year}}{\text{km}^2 \text{ of receptor area}} \left(\frac{\text{g}}{\text{km}^2\text{yr}} \right) \\ &= \text{transfer flux coefficient} \left(\frac{1}{\text{km}^2} \right) * \text{source mercury emissions} \left(\frac{\text{g}}{\text{yr}} \right) \end{aligned}$$

In Figure 25, the Transfer Flux Coefficients calculated from the modeling results from a selected subset of standard source locations are shown for emissions of pure elemental mercury, contributing to total mercury deposition into Lake Erie, for the year 2005. As the spatial density of standard points increases dramatically as one gets closer and closer to the Great Lakes, it is not possible to display them clearly with one scale. So, the results are shown in three regions: a global domain, a central North American domain (lower left inset map), and a Great Lakes regional domain (lower right inset map). Each of the 48 standard source locations is shown on only one of the three maps. That is, 16 of the 48 illustrative points are shown on the global domain main map, 11 of the 48 illustrative points are shown on the central North American domain map (lower left inset map), and the remaining 21 of the 48 illustrative points are shown on the Great Lake regional domain map (lower right inset map). The same display protocol is used in Figure 26 and Figure 27, discussed below.

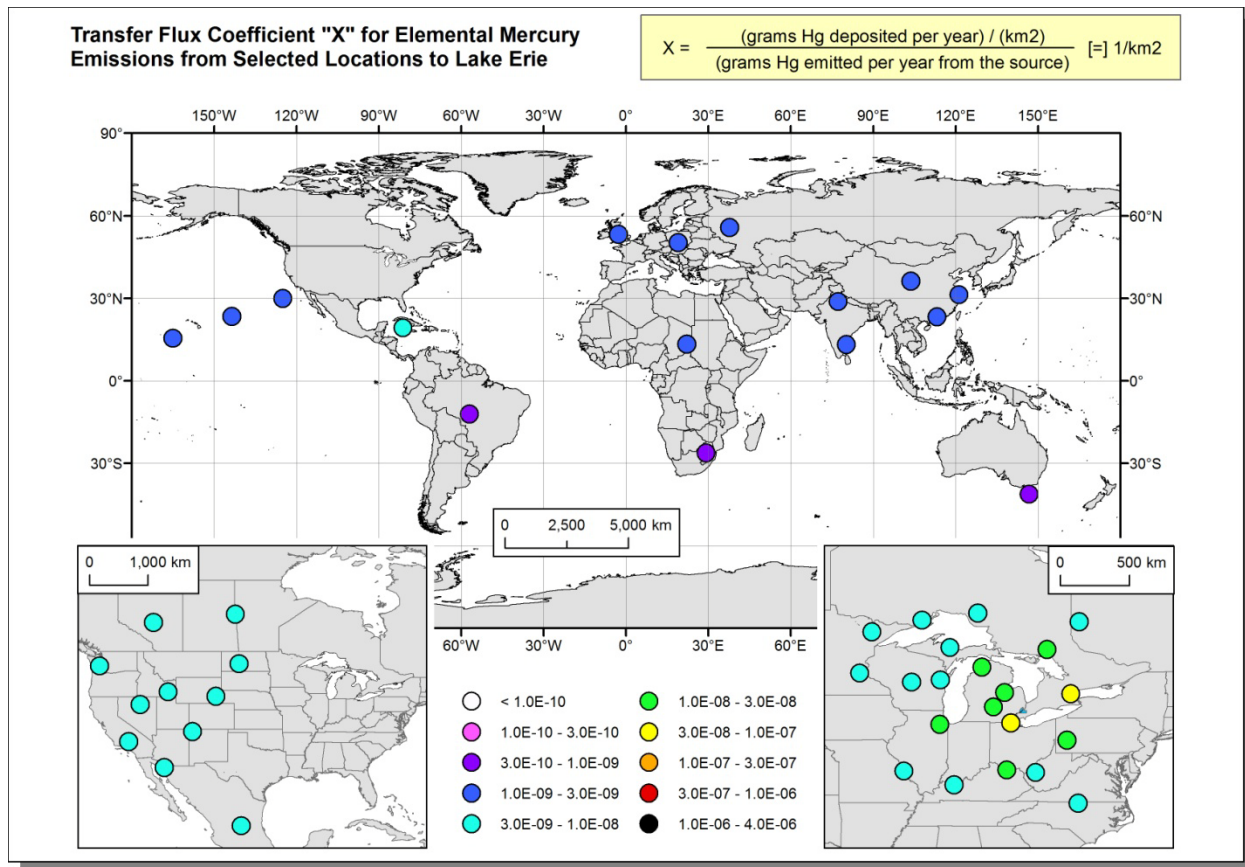


Figure 25. Transfer Flux Coefficients For Pure Elemental Mercury Emissions at an Illustrative Subset of Standard Source Locations, for Deposition Flux Contributions to Lake Erie

It can be seen that there are not dramatic differences, say, in the transfer flux coefficients for sources in Europe and Asia to Lake Erie. Thus, it appears that the density of standard sources in those regions likely does not need to be higher than that which was used, and perhaps could be lower. There were, for

example, actually 10 standard source locations in China, of which 3 are illustrated here (as shown in Figure 25 and related figures), and from the relative lack of spatial variation in the results, it likely would be possible to estimate source-receptor impacts from Chinese mercury sources with fewer than 10 standard sources. One of the activities that will be carried out in the next phase of the work will be to determine an “optimum”—but minimum -- set of standard source locations, for which the source-receptor calculations can be made with reasonable accuracy. With less redundancy, more computational resources will be able to be devoted to sensitivity and scenario analysis.

In Figure 26, comparable results are shown for emissions of pure reactive gaseous mercury. It can be seen that the difference in impacts between distant, regional, and “local” sources is relatively dramatic, spanning several orders of magnitude. This figure also clearly demonstrates the necessity of increasing the density of standard source locations near the receptors of interest: the gradient in impacts is quite dramatic over scales of 100’s of kilometers.

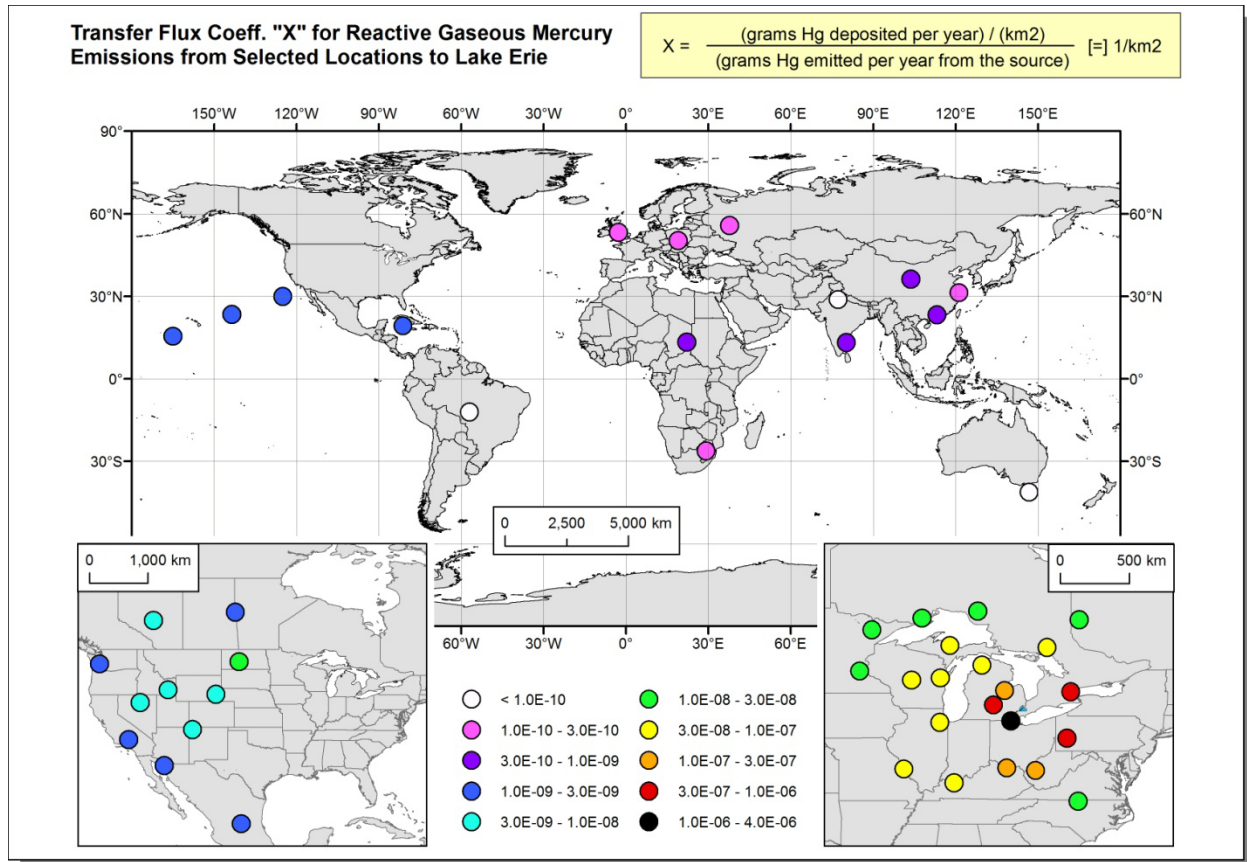


Figure 26. Transfer Flux Coefficients For Pure Reactive Gaseous Mercury Emissions at an Illustrative Subset of Standard Source Locations, for Deposition Flux Contributions to Lake Erie

To illustrate the standard source modeling results further, a series of bar graphs will be presented for the 48 standard source locations shown in the above figures. The actual “numbers” of the standard source locations – needed to interpret the following graphs – are shown in Figure 27.

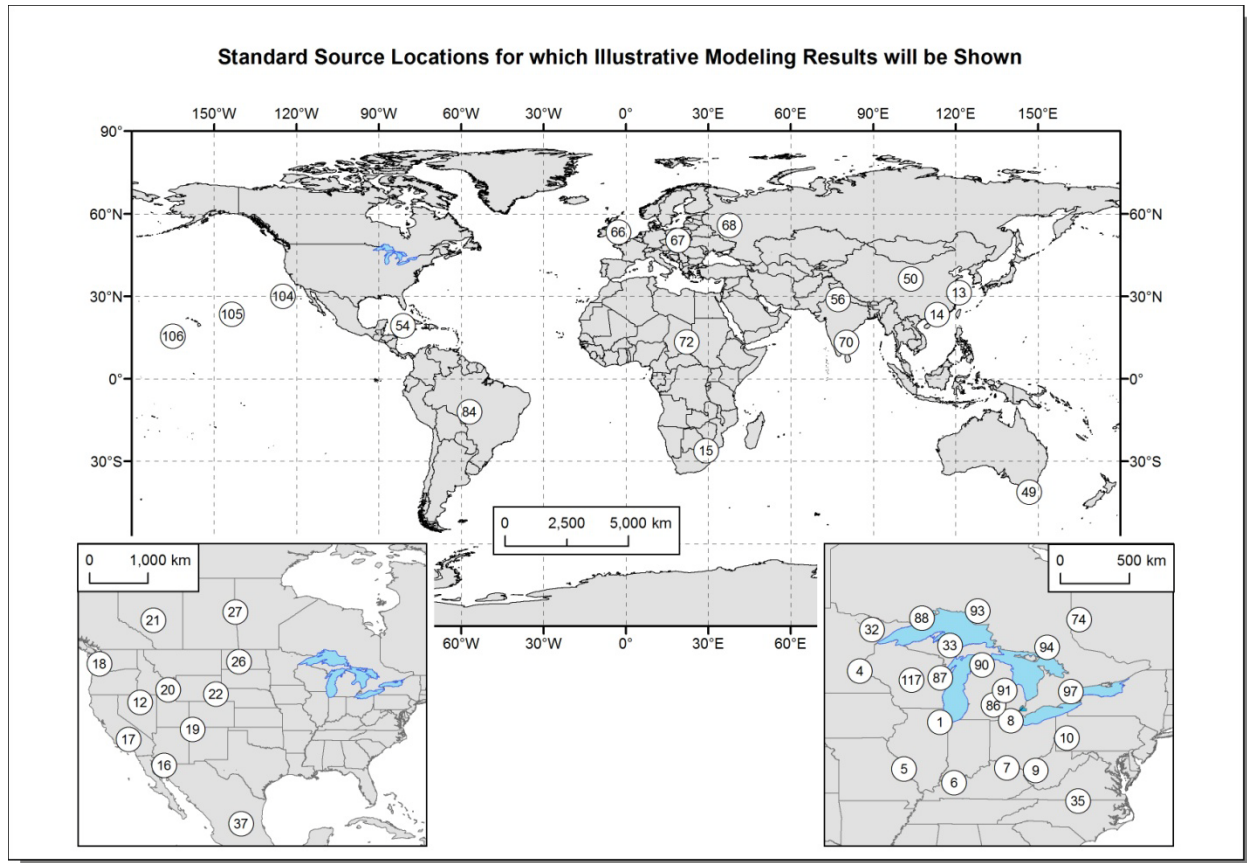


Figure 27. Standard Source Locations for which Illustrative Modeling Results Will be Shown

Figure 28 shows the transfer flux coefficients for contribution to Lake Erie for each of the 48 example standard source locations, for emissions of pure elemental mercury, pure reactive gaseous mercury, and pure particulate mercury. The elemental and reactive gaseous mercury data in this figure are the “same” as was mapped above. It can be seen that for sources in the Great Lakes region, on a “pound for pound basis”, emissions of Hg(II) have a greater impact than emissions of Hg(p), which in turn have a greater impact than emissions of Hg(0). However, for distant sources, the ordering of the relative contributions is reversed, due to the more rapid local and regional deposition of Hg(II), and to a lesser extent, Hg(p). In essence, for distant sources, emissions of elemental mercury have a greater impact than emission of Hg(II) or Hg(p) because these latter forms are wet and dry deposited out of the atmosphere to a greater extent as they are transported from the source to the receptor (in this example, Lake Erie). The range in contributions is fairly dramatic, with variations of many orders of magnitude among the different

example standard source locations. This dramatic difference can perhaps be seen more clearly in Figure 29, which shows the exact same data on a linear, rather than logarithmic scale.

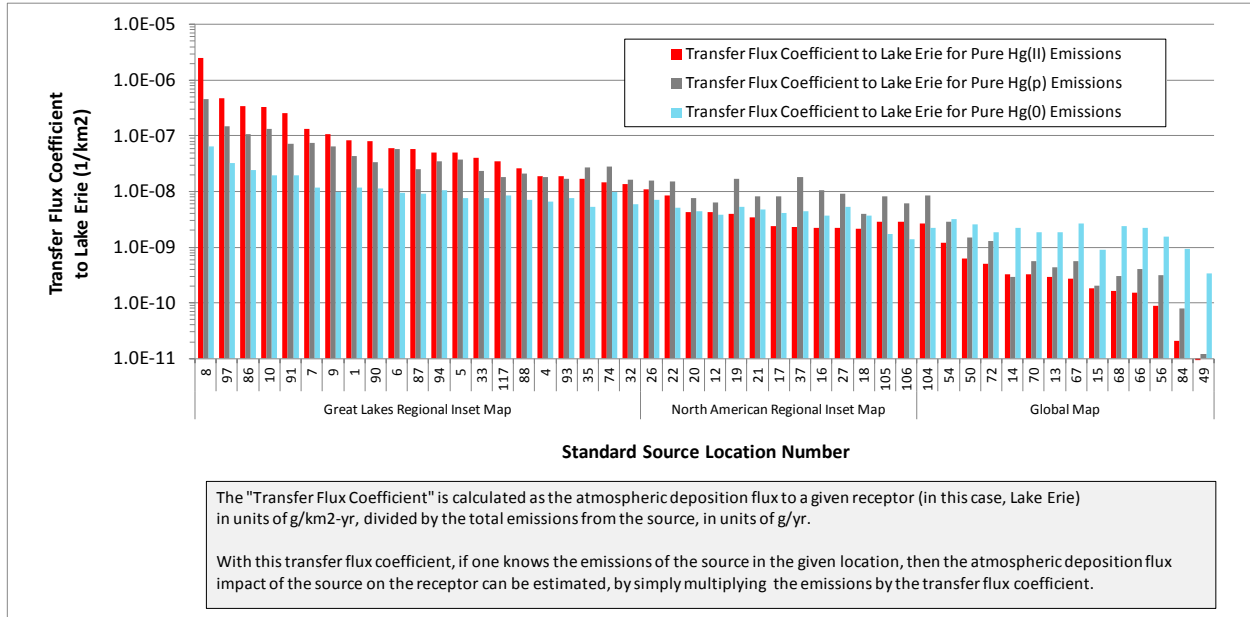


Figure 28. Transfer Flux Coefficients For Hg(0), Hg(II), and Hg(p) to Lake Erie (logarithmic scale)

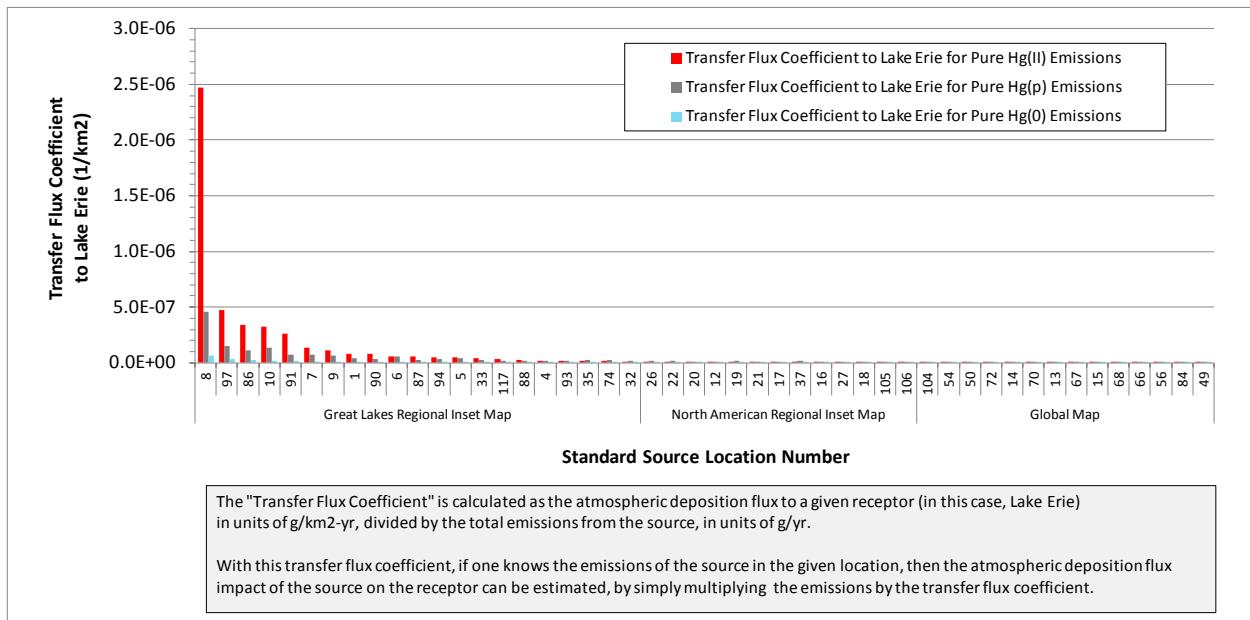


Figure 29. Transfer Flux Coefficients For Hg(0), Hg(II), and Hg(p) to Lake Erie (linear scale)

In the real world, most anthropogenic sources emit a mixture of Hg(0), Hg(II), and Hg(p), and the total impact of such a source is made up of the individual impacts of the different “pure components” of the emissions (see Section 2.4.1 above).

In Figure 30 (logarithmic) and Figure 31 (linear), model-derived Lake Erie Transfer Flux Coefficients are shown for two types of “generic” sources, with emissions fractions of:

- 57% Hg(0), 40% Hg(II), and 3% Hg(p)
- 22% Hg(0), 75% Hg(II), and 3% Hg(p).

The first profile is the average speciation profile for coal-fired power plants in the United States during 2005, based on the U.S. EPA 2005 National Emissions Inventory (see Section 2.3.1 above), and is described in the figure as a “typical” coal fired power plant. The 2nd profile is representative of a coal-fired power plant – or other source – with a somewhat higher proportion of Hg(II) emissions. In the 2005 U.S. mercury emissions inventory, a significant fraction of coal-fired power plants have profiles comparable to this 2nd profile. These higher-RGM-emissions fraction facilities are generally those without advanced pollution control devices like dry or wet scrubbers.

The dramatic difference in modeled impacts for “identical” sources in different parts of the world can be seen in these figures. *For example, a coal-fired power plant near Lake Erie – e.g., see standard source location number 8 – has approximately a 100-fold greater impact on Lake Erie than an identical facility in China – e.g., see results for standard points 13, 14, or 50.* This is not surprising given the relative proximity of the sources to the lake, but it is an important factor to keep in mind. Of course, the overall impacts depend on the number of such sources in any given region, and these overall impacts will be presented in the next section.

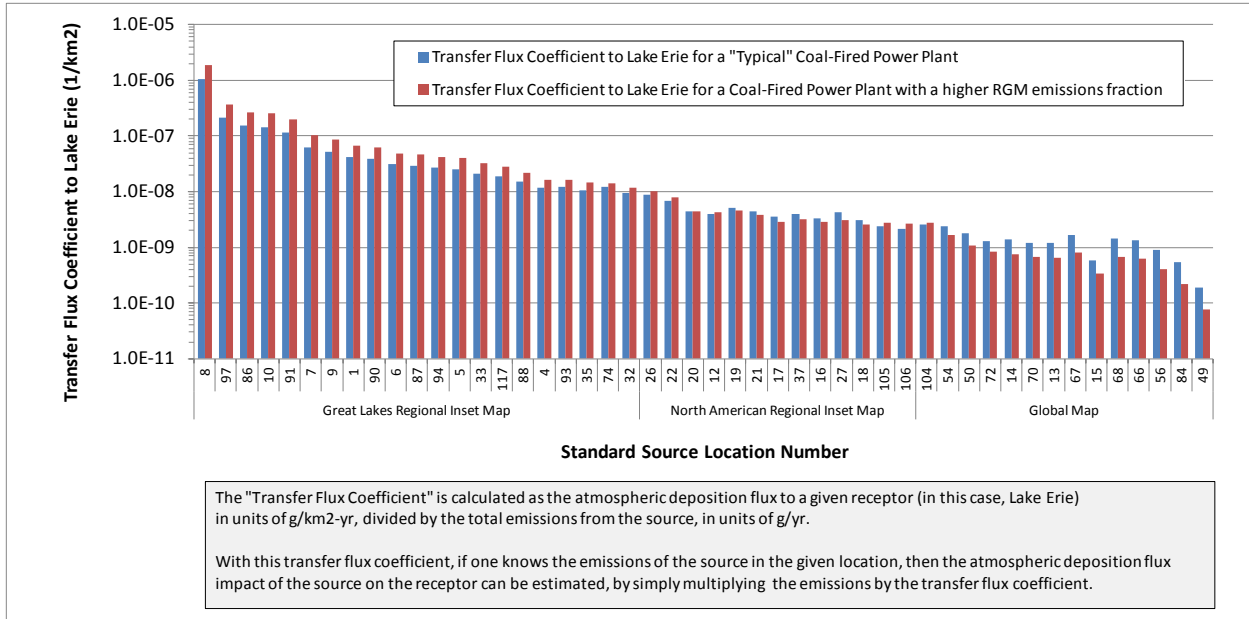


Figure 30. Lake Erie Transfer Flux Coefficients for two kinds of Generic Coal-Fired Power Plants (logarithmic scale)

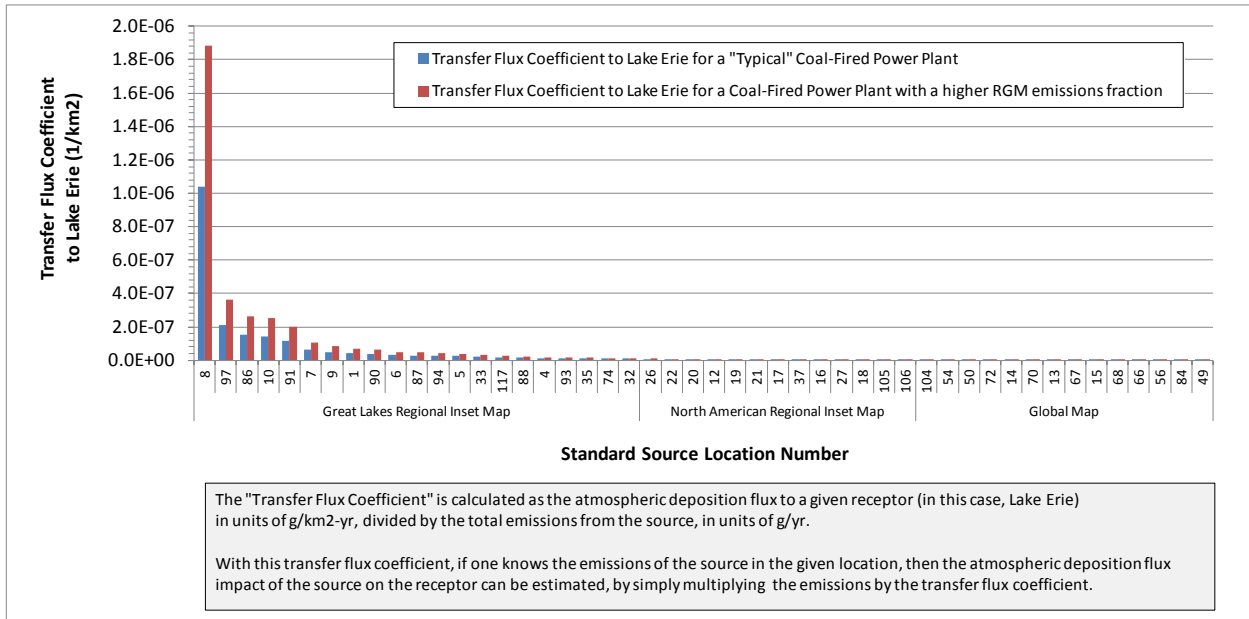


Figure 31. Lake Erie Transfer Flux Coefficients for two kinds of Generic Coal-Fired Power Plants (linear scale)

4. An Initial Set of Results for Mercury Deposition to the Great Lakes

Using the methodology described above, a basic set of results for the Great Lakes has been developed, and will be described in the section. It is important to note at the outset that these results should be regarded as an initial set of “base case” results that will be examined and refined in the next phase of the project.

4.1. Overall mercury deposition to the Great Lakes

Results were obtained for each of the Great Lakes and each Great Lake Watershed, and these will be presented below. However, an overall picture of mercury deposition can be obtained by adding up all of the individually tabulated deposition estimates to obtain a value for the entire Great Lakes Basin. Figure 32 shows the total model-estimated mercury deposition to the Great Lakes Basin from four broad source categories – direct anthropogenic emissions, re-emissions of previously deposited anthropogenic emissions from land and ocean surfaces, and natural emissions. Within these overall estimates, it can be seen that direct anthropogenic mercury emissions appear to have the greatest impact on deposition in these initial results.

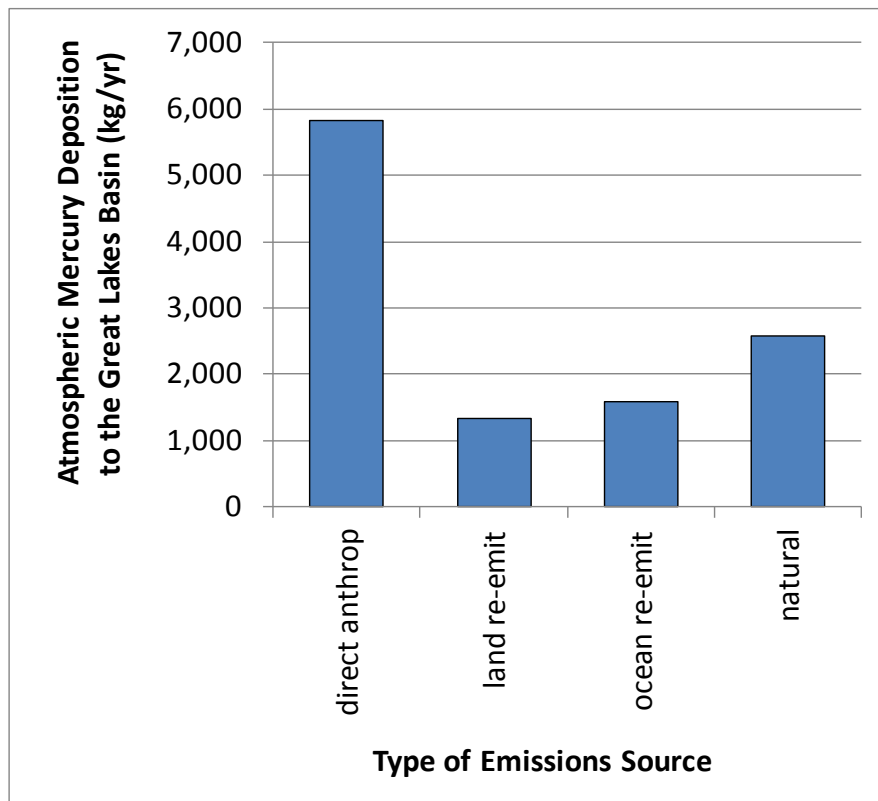


Figure 32. Overall model estimates of mercury deposition to the Great Lakes Basin

In Figure 33 and Figure 34, the overall modeled deposition fluxes and deposition amounts are shown for each Great Lake and each Great Lake watershed. It can be seen that modeled deposition fluxes are greater for Lake Erie and Lake Ontario than for the other Great Lakes. But, because these lakes and their watersheds are relatively small, the total deposition amounts to the different Great Lakes and watersheds are more similar.

It can also be seen from these figures that direct anthropogenic emissions from the United States contribute a significant fraction of the modeled atmospheric mercury deposition. For Lakes Erie, Ontario, and Michigan, these initial model results suggest that such sources in the United States are estimated to contribute more to the lakes and their watersheds than the sum total of all direct anthropogenic sources outside of North America.

As mentioned earlier, it is important to note that the deposition fluxes and amounts shown here are the model-estimated “one-way” or “gross” deposition values, estimated as the separate “downward” component of the two-way surface exchange flux of atmospheric mercury. To obtain the “net” deposition (or volatilization) amount, the upward flux of elemental mercury would have to be subtracted from the downward flux components estimated here.

Lai and Holsen *et al.* (2007b) have made detailed estimates of atmospheric deposition and net surface exchange flux over Lake Ontario. They estimated the total deposition of mercury to Lake Ontario for the 2002-2003 time frame to be on the order of ~560 kg/year, counterbalanced by emissions of elemental mercury of ~410 kg/year, for a net mercury loading of 150 kg/year.

Mason and Sullivan (1997) developed a mass balance for Lake Michigan for ~1995, estimating total atmospheric deposition of 960 kg/yr, counterbalanced by an evasion flux of elemental mercury of 520 kg/yr, for a net mercury loading of 440 kg/yr. Landis and Keeler (2002) created a mass balance for Lake Michigan for ~1994-1995, using interpolated measurement data from sites around the lake, estimating a total atmospheric deposition of 1170 kg/yr, counterbalanced by a net evasion flux of elemental mercury of 450 kg/yr, for a net mercury loading of 720 kg/yr.

Jeremiason *et al.* (2009) estimated the net evasion flux of elemental mercury to be on the order of 380-850 kg/year for Lake Michigan and on the order of 160-320 kg/year for Lake Superior, based on 2005-2006 measurements of mercury in the surface waters of the lakes and atmospheric elemental mercury measurements at the Burnt Island CAMNet atmospheric mercury monitoring site.

Rolfhus *et al.* (2003) estimated the total deposition to Lake Superior to be on the order of 740 kg/yr, counterbalanced by an elemental mercury evasion flux of 720 kg/yr, for a net atmospheric mercury loading of 20 kg/yr.

Denkenberger *et al.* (2011) have very recently estimated that the net elemental mercury evasion fluxes over the Great Lakes Basin are on the order of ~7.7 Mg/yr, and have estimated the geographical distribution of this net evasion flux over the entire Basin.

Additional aspects and details regarding the overall mass balance of atmospheric mercury in the Great Lakes Basin are discussed in Section 5.2. In the next phase of this project, these and other estimates of the net surface exchange of elemental mercury at the surface of the lakes – and their watersheds – will be carefully examined, and compared where possible with the estimates being developed in this work. A strict comparison is often not possible because studies have been done for different years, and, comparable terms are not always available, i.e., to compare net deposition vs. net deposition, or gross deposition vs. gross deposition. A goal will be to make an overall estimate of the mass-balance of mercury for each of the Great Lakes and their watersheds.

In the next subsection, more details regarding the geographic distribution of deposition contributions to the Great Lakes are presented.

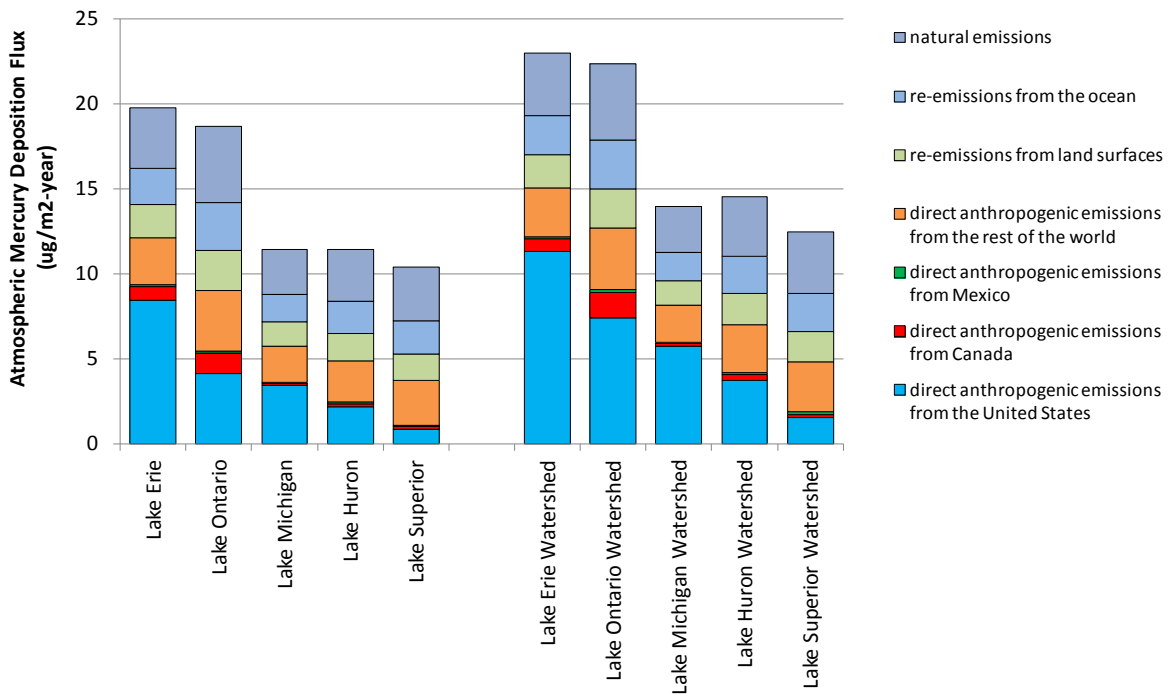


Figure 33. Model-estimated 2005 deposition fluxes (ug/m2-year) to the Great Lakes and Great Lakes Watersheds

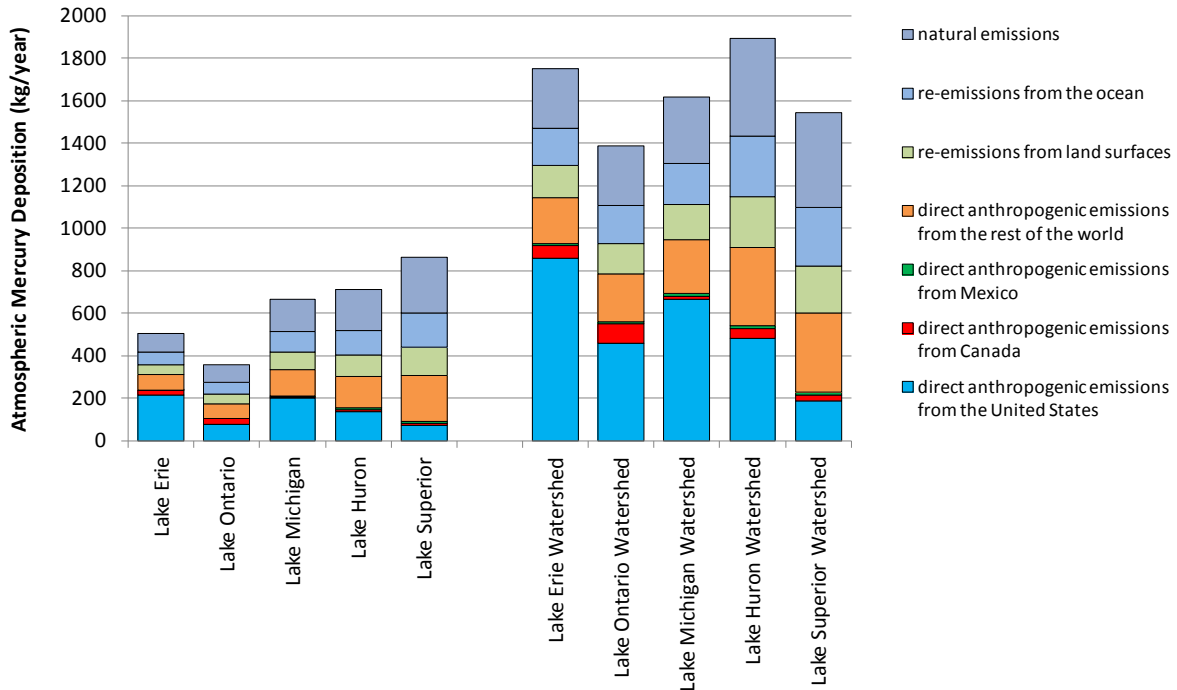


Figure 34. Model-estimated 2005 deposition amounts (kg/year) to the Great Lakes and Great Lakes Watersheds

4.2. Country-Specific Source-Attribution Results for Great Lakes Mercury Deposition

Using the procedures described in Section 2, estimates of the individual deposition contributions from each of the more than 360,000 emissions records to each of the Great Lakes and their watersheds were made. This is a uniquely detailed set of source-receptor modeling results. These estimates can be analyzed and displayed in numerous ways, and several examples will be shown here.

First, the direct and re-emitted anthropogenic emissions contributions were summed up for each of the world's countries, and the top-ten countries contributing to the Great Lakes Basin are shown in Figure 35. Based on this initial set of modeling results for 2005, in terms of direct and re-emitted anthropogenic sources, the United States appears to contribute more than any other country in the world to the Great Lakes basin. Not surprisingly, contributions from China are also very significant.

In Figure 36, the model-estimated contributions for these same 10 countries are expressed on a per capita basis. From this figure it is seen that the United States and Canada have the largest per capita rate among these largest contributors.

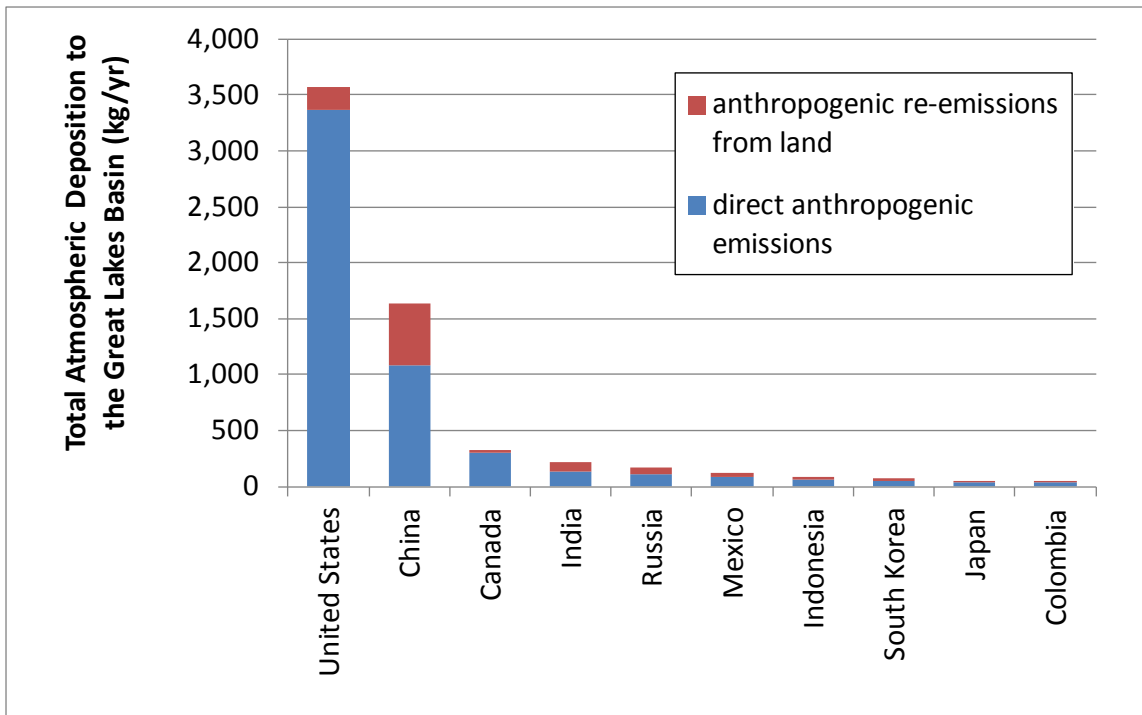


Figure 35. Model-estimated 2005 deposition amount to the Great Lakes Basin from the ten countries with the highest modeled total contribution from direct and re-emitted anthropogenic sources

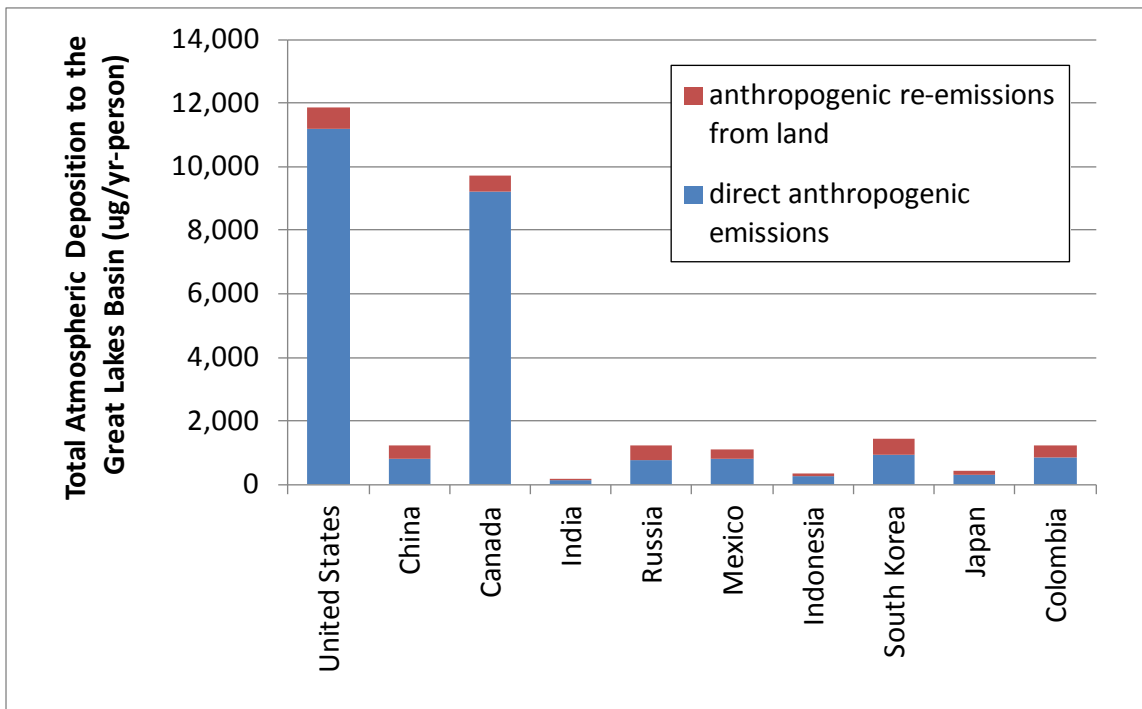


Figure 36. Model-estimated *per capita* 2005 deposition amount to the Great Lakes Basin from the countries with the highest modeled total contribution from direct and re-emitted anthropogenic sources

4.3. Geographical Distributions of Source Attribution Results: Examples for Lake Erie

The geographical distribution of contributions to Lake Erie from direct anthropogenic sources are shown in Figure 37 aggregated on a 2x2 degree global grid and in Figure 38, aggregated on a 1x1 degree grid over central North America. The relative importance of the modeled contributions from sources near the Lake can be seen clearly in these figures. A complete set of global-domain figures comparable to Figure 37 is provided in Appendix 1 for the Great Lakes and Appendix 2 for the Great Lakes Watersheds. In addition, a complete set of North-American-domain figures comparable to Figure 38 is provided in Appendix 3 for the Great Lakes and Appendix 4 for the Great Lakes Watersheds. In each of these maps, the importance of the local and regional sources can be seen. Comparable Lake Erie source-attribution maps for re-emitted anthropogenic mercury, natural mercury emissions and total emissions from all modeled sources are provided in the following pages. In Appendix 5 through Appendix 8, a full set of comparable maps for total emitted mercury are shown for each Great Lake and for each Watershed, over both global and North American domains.

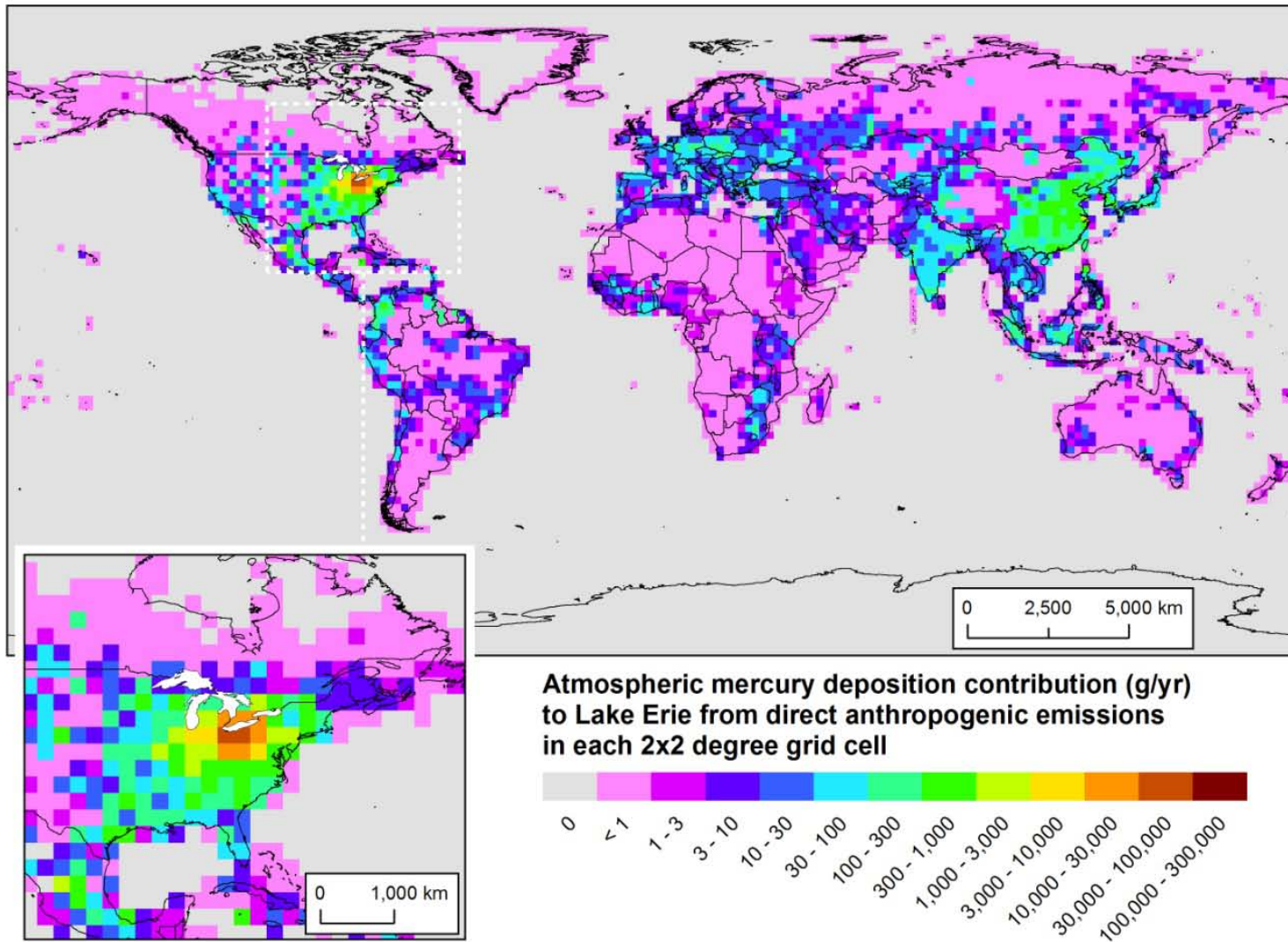


Figure 37. Global Geographical Distribution of Atmospheric Deposition Contributions to Lake Erie from Direct Anthropogenic Emissions

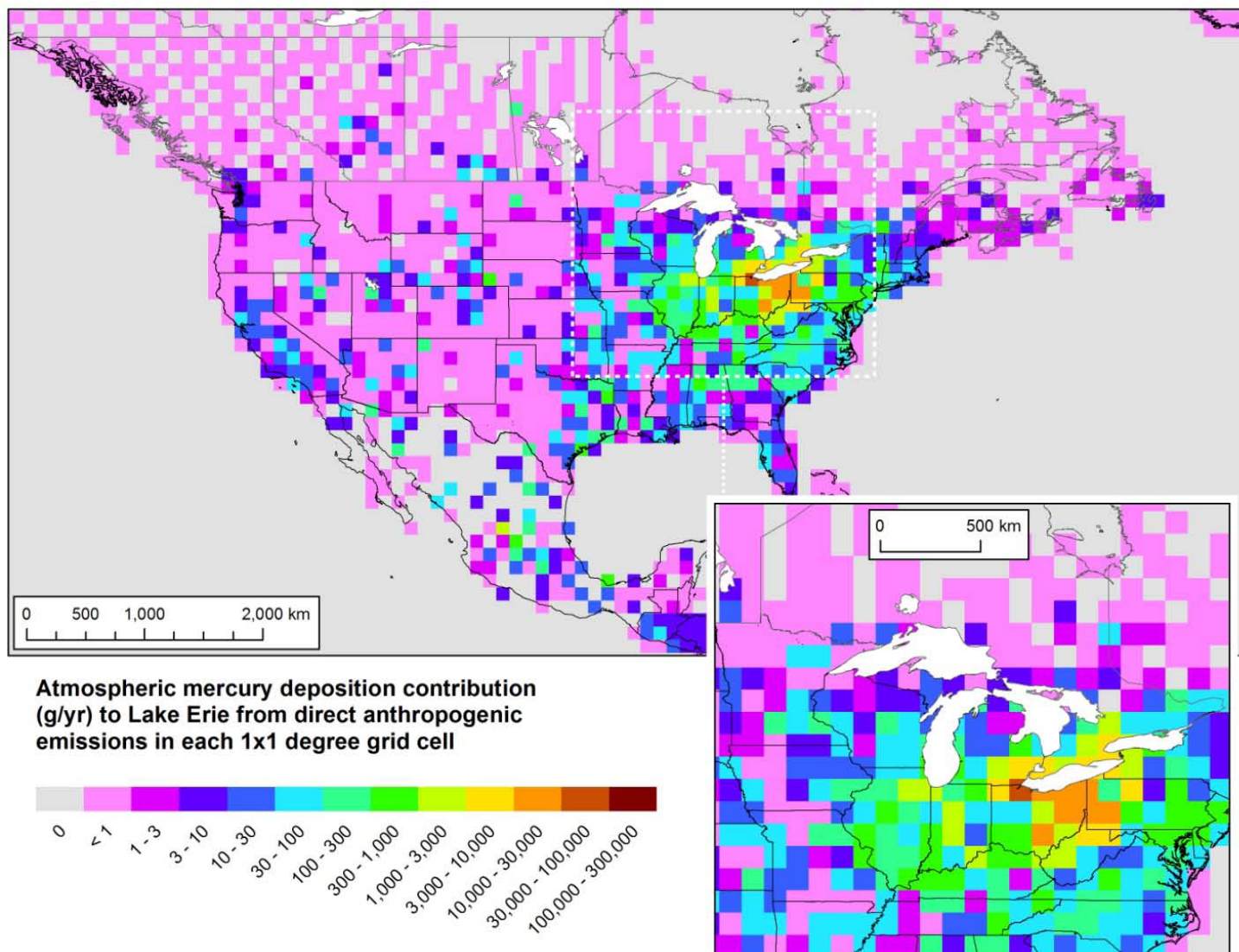


Figure 38. Geographical Distribution of Atmospheric Deposition Contributions to Lake Erie from Direct Anthropogenic Emissions in Central North America

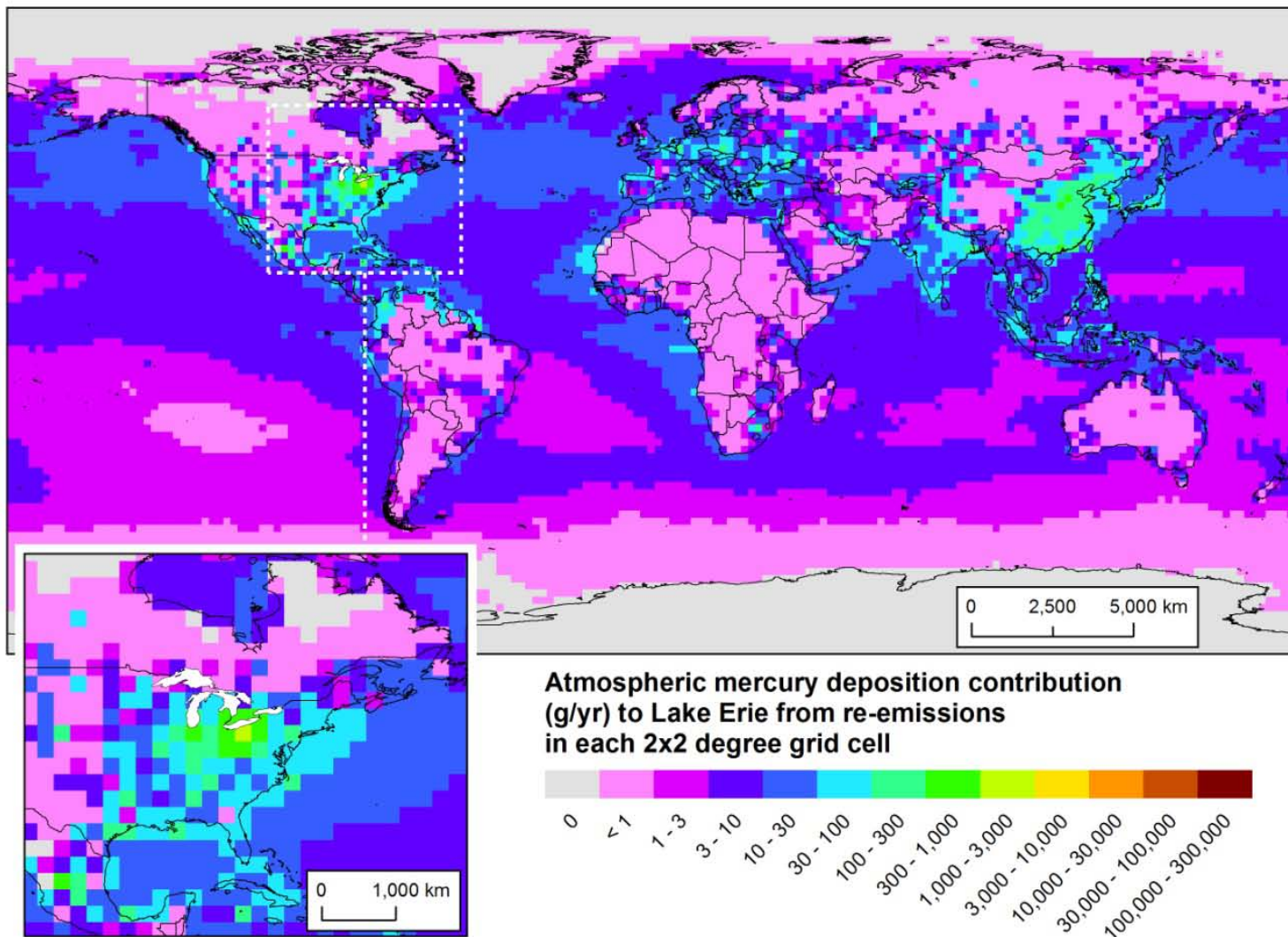


Figure 39. Global Geographical Distribution of Atmospheric Deposition Contributions to Lake Erie from Re-emissions of Previously Deposited Anthropogenic Emissions

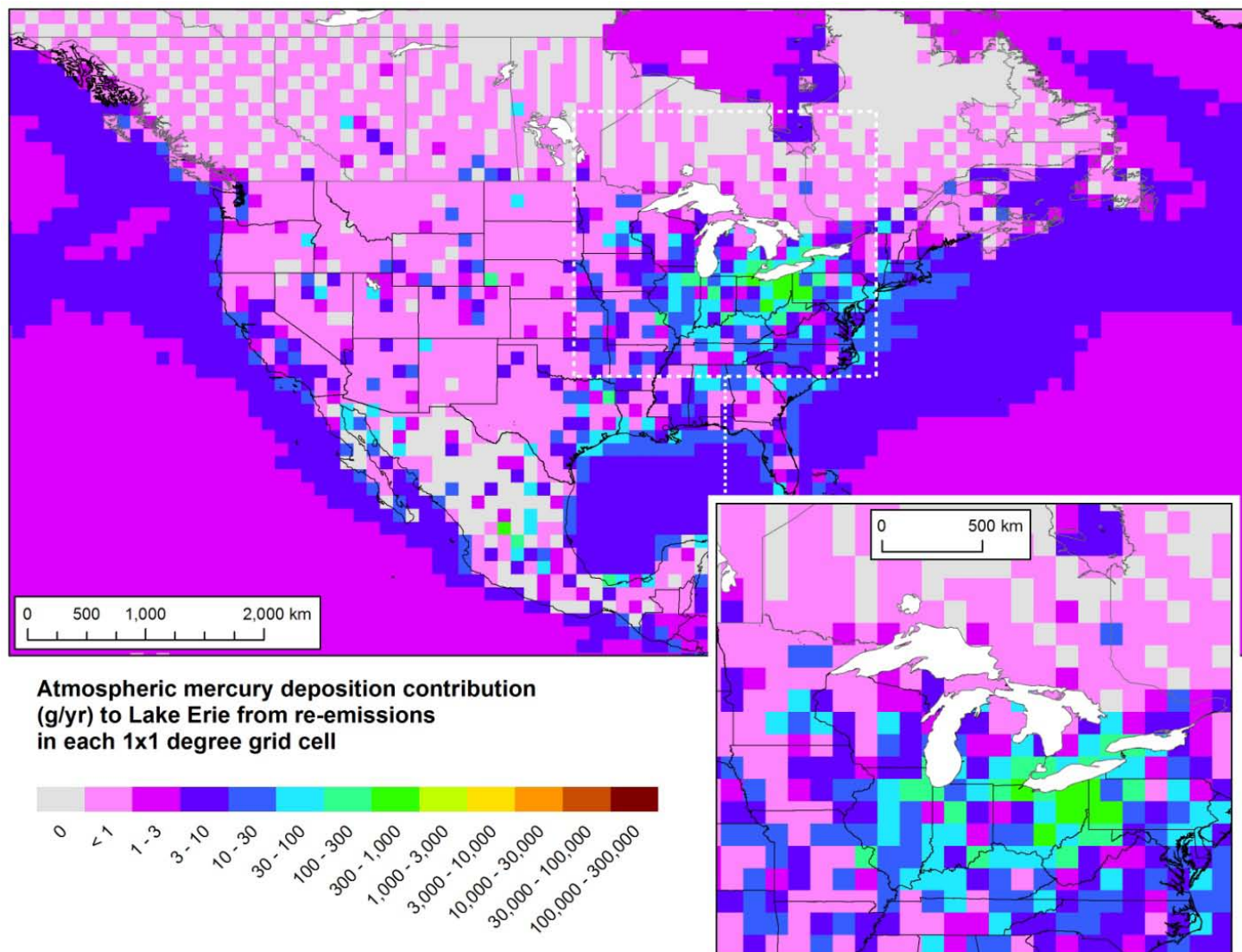


Figure 40. Geographical Distribution of Atmospheric Deposition Contributions to Lake Erie from Re-emissions of Previously Deposited Anthropogenic Emissions from Central North America

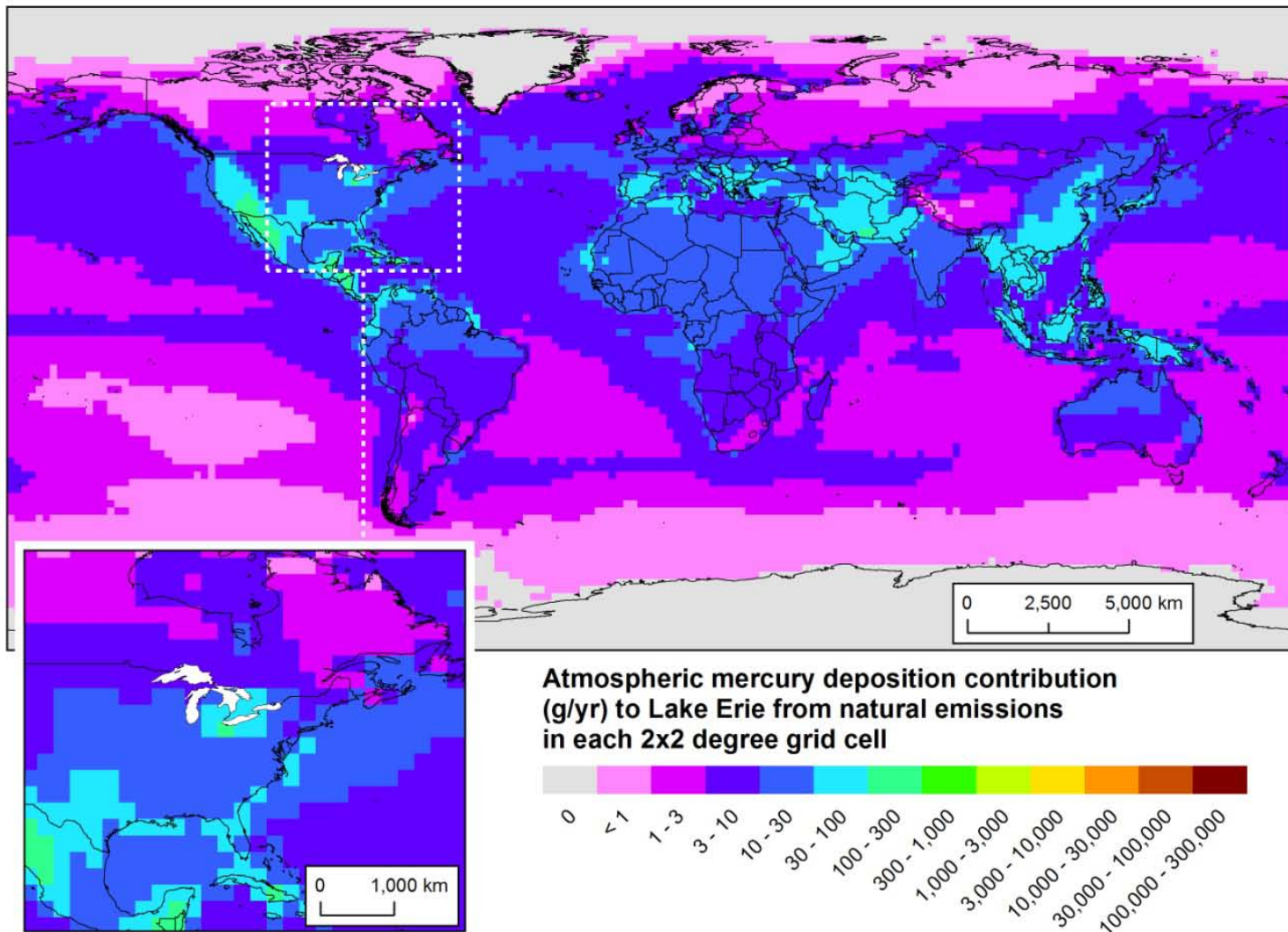


Figure 41. Global Geographical Distribution of Atmospheric Mercury Deposition Contributions to Lake Erie from Natural Emissions

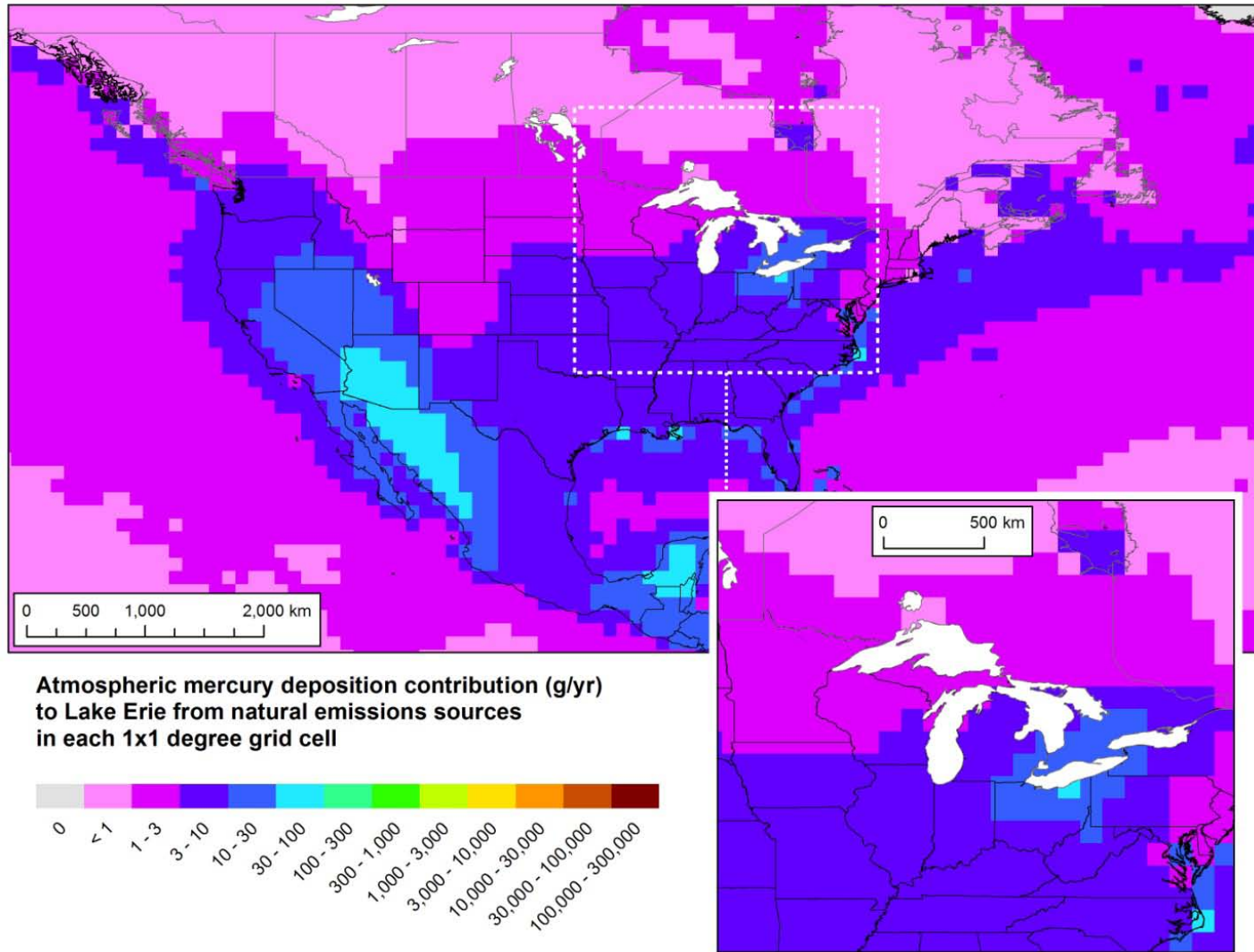


Figure 42. Geographical Distribution of Atmospheric Mercury Deposition Contributions to Lake Erie from North American Natural Emissions

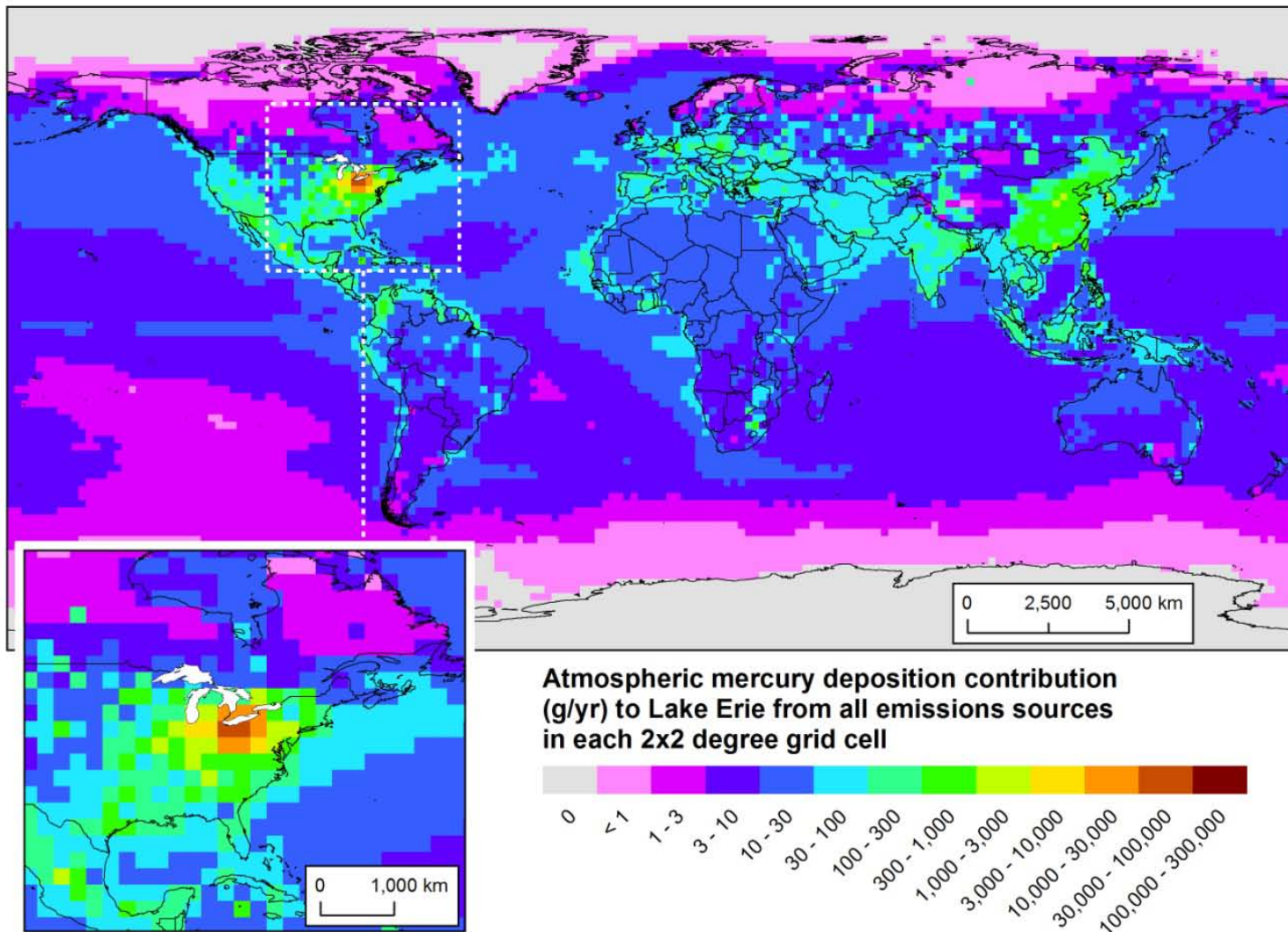


Figure 43. Global Geographical Distribution of Atmospheric Mercury Deposition Contributions to Lake Erie from All Modeled Sources

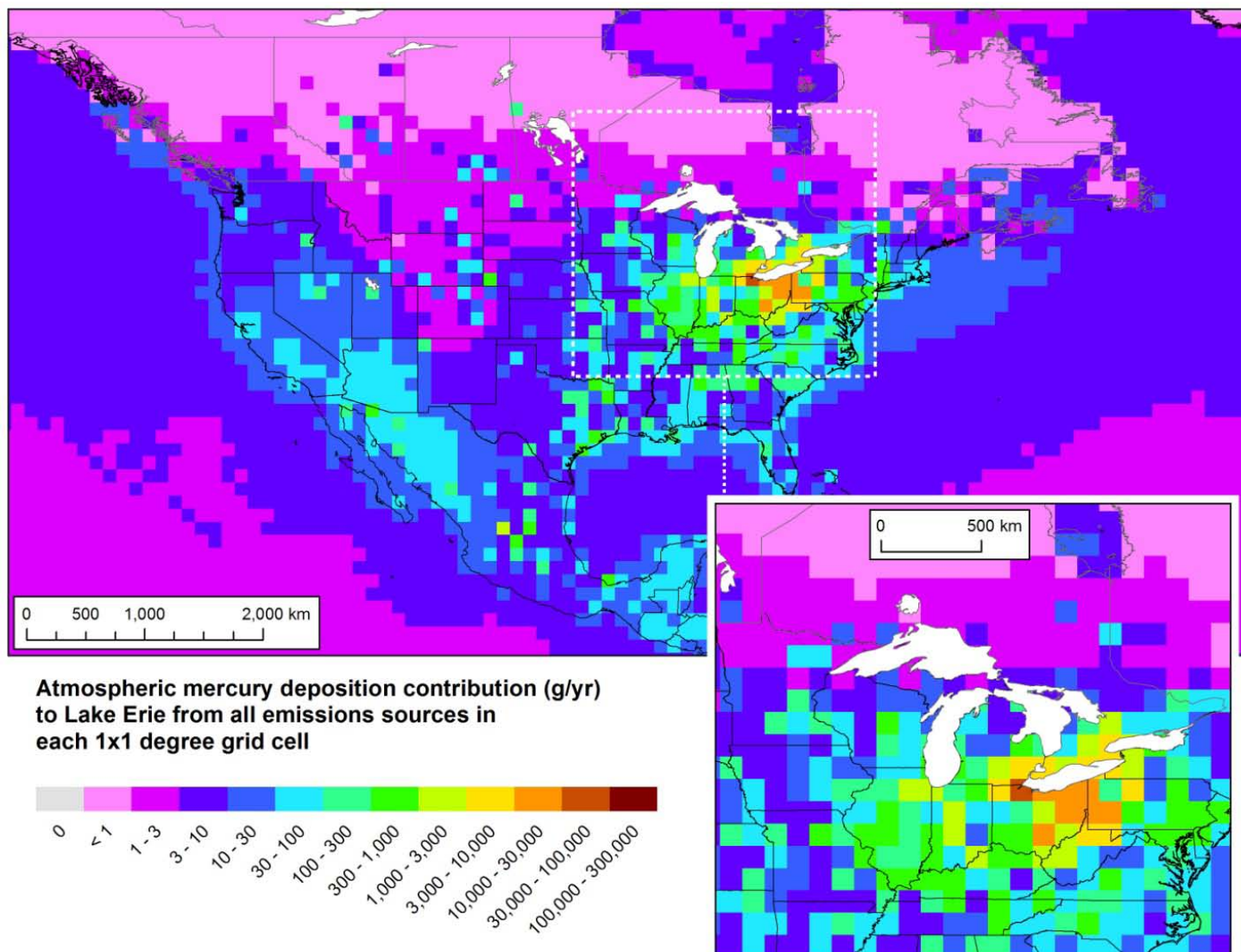


Figure 44. Geographical Distribution of Atmospheric Mercury Deposition Contributions to Lake Erie from All Modeled Sources, displayed on a Central North American domain

4.4. Atmospheric Mercury Contributions to the Great Lakes and Watershed as a Function of Distance

The distance of each of the more than 360,000 emissions records from the center of each Great Lake and watershed was calculated. Mercury emissions as a function of this distance were calculated, and an example of the results is given in Figure 45. It can be seen that the vast majority of emissions occur at large distances from Lake Erie, and the same is true for the other Great Lakes, and their watersheds (a complete set of comparable graphs is presented in Appendix 9).

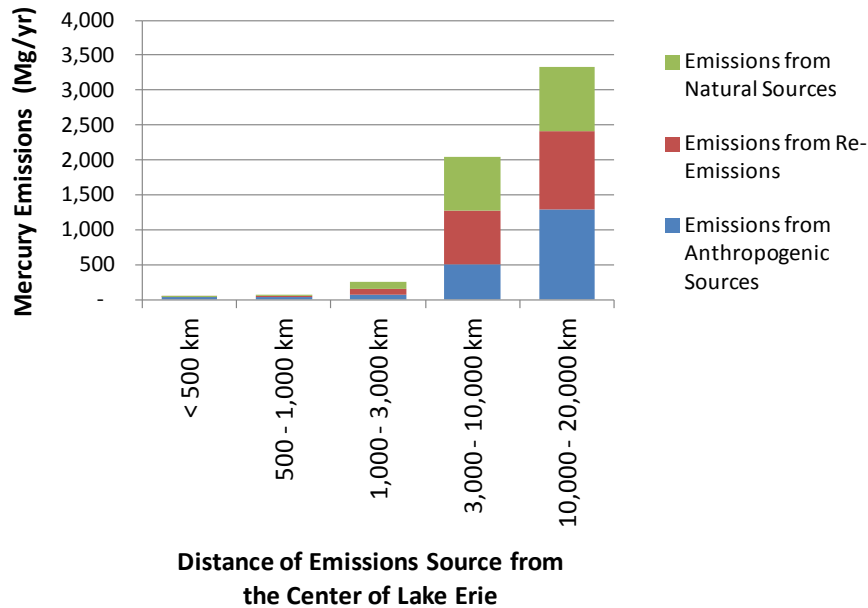


Figure 45. Atmospheric Emissions from Direct Anthropogenic, Re-emitted Anthropogenic and Natural Mercury Emissions as a Function of Distance from the Center of Lake Erie

The atmospheric mercury *deposition contributions* from direct anthropogenic, re-emitted anthropogenic and natural emissions were also determined as a function of this distance. A complete set of such graphs – for each Great Lake and watershed – are provided in Figure 46 through Figure 55, below.

Two patterns are readily apparent from examination of these figures:

- For Lakes Erie, Ontario, and Michigan, there is a significant contribution from regional sources, in addition to significant contributions from more distant sources.
- For Lakes Huron and Superior, distant sources are seen to generally be much more significant than regional sources. This finding is not unexpected given the relative lack of large mercury emissions sources upwind of these Lakes.

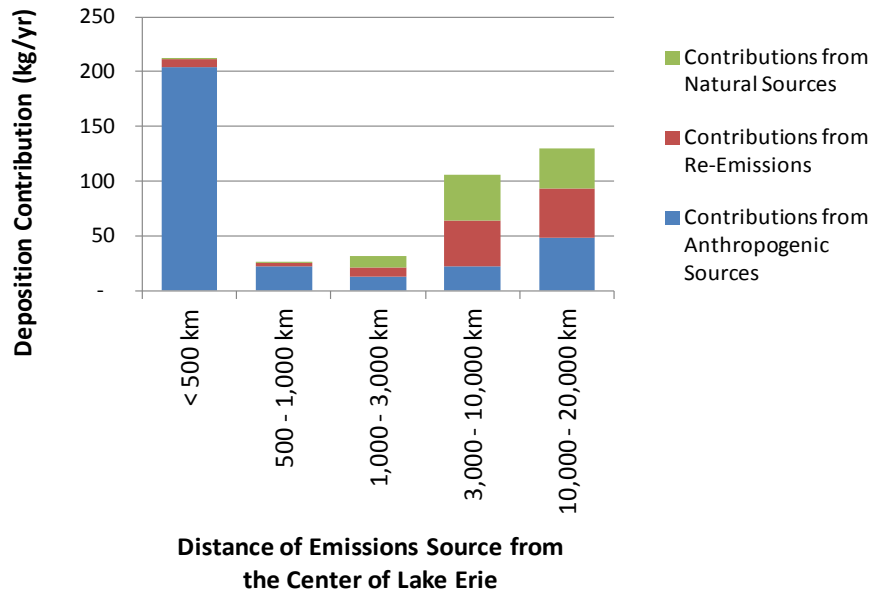


Figure 46. Atmospheric Deposition Contributions to Lake Erie from Direct Anthropogenic, Re-emitted Anthropogenic and Natural Mercury Emissions as a Function of Distance from the Center of the Lake

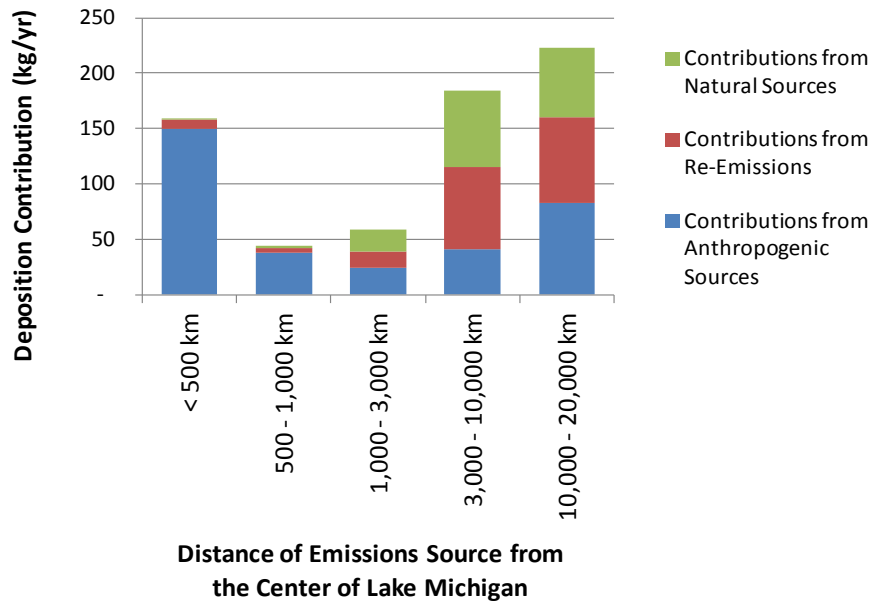


Figure 47. Atmospheric Deposition Contributions to Lake Michigan from Direct Anthropogenic, Re-emitted Anthropogenic and Natural Mercury Emissions as a Function of Distance from the Center of the Lake

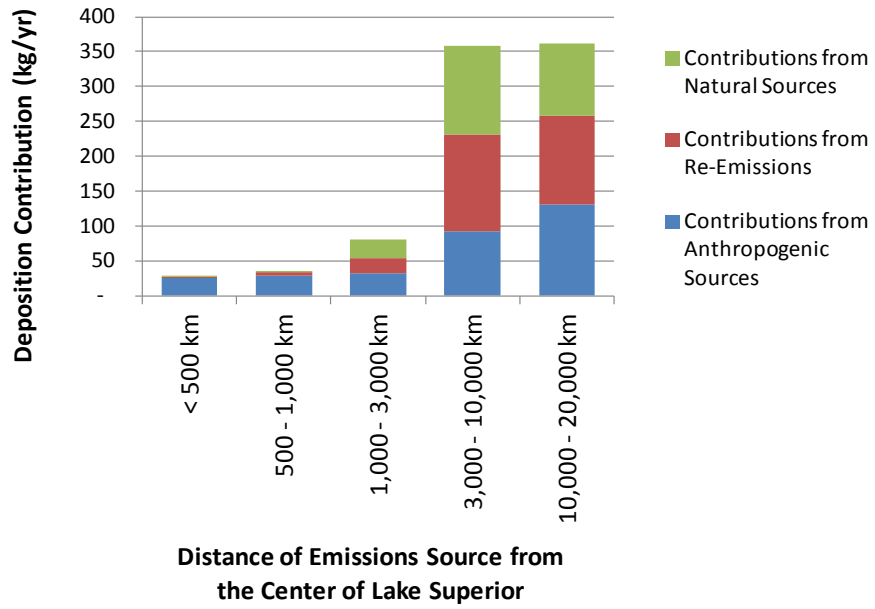


Figure 48. Atmospheric Deposition Contributions to Lake Superior from Direct Anthropogenic, Re-emitted Anthropogenic and Natural Mercury Emissions as a Function of Distance from the Center of the Lake

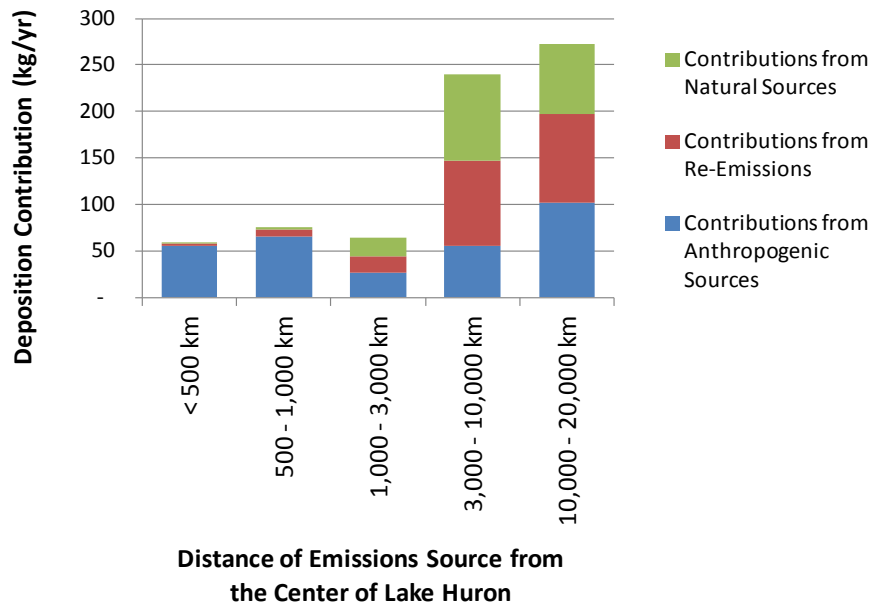


Figure 49. Atmospheric Deposition Contributions to Lake Huron from Direct Anthropogenic, Re-emitted Anthropogenic and Natural Mercury Emissions as a Function of Distance from the Center of the Lake

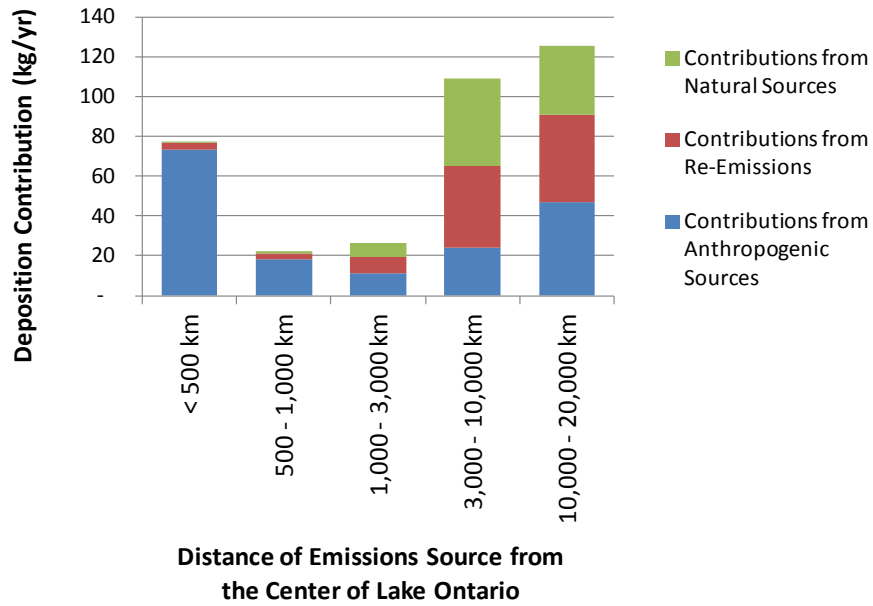


Figure 50. Atmospheric Deposition Contributions to Lake Ontario from Direct Anthropogenic, Re-emitted Anthropogenic and Natural Mercury Emissions as a Function of Distance from the Center of the Lake

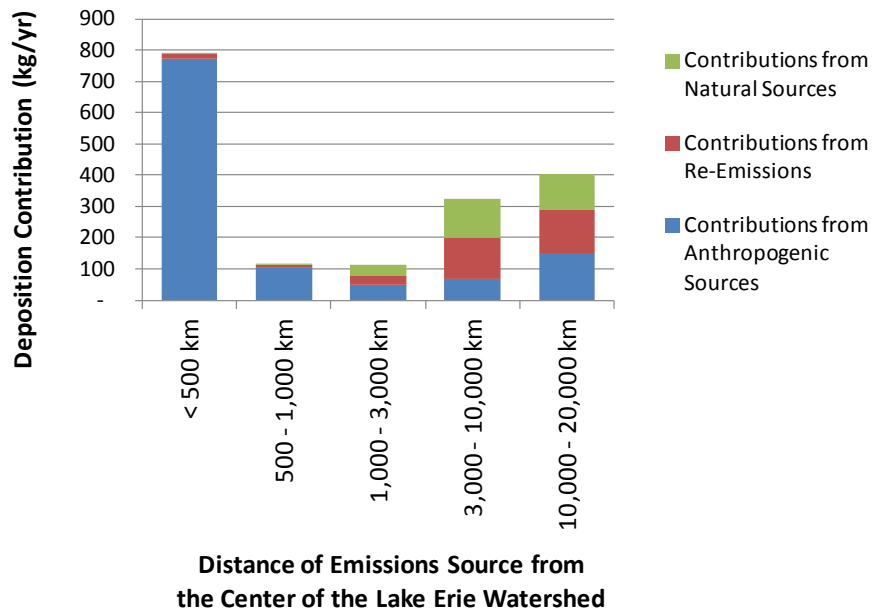


Figure 51. Atmospheric Deposition Contributions to the Lake Erie Watershed from Direct Anthropogenic, Re-emitted Anthropogenic and Natural Mercury Emissions as a Function of Distance from the Center of the Watershed

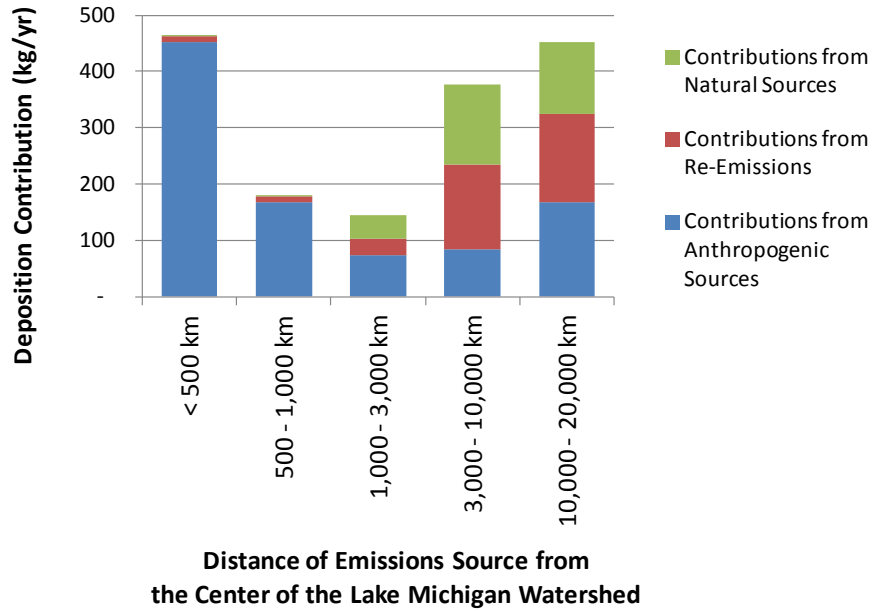


Figure 52. Atmospheric Deposition Contributions to the Lake Michigan Watershed from Direct Anthropogenic, Re-emitted Anthropogenic and Natural Mercury Emissions as a Function of Distance from the Center of the Watershed

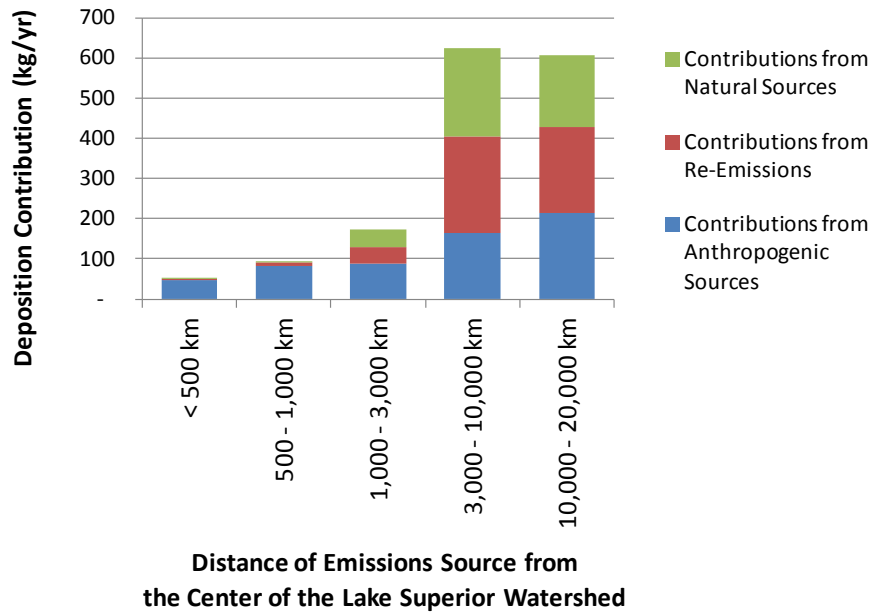


Figure 53. Atmospheric Deposition Contributions to the Lake Superior Watershed from Direct Anthropogenic, Re-emitted Anthropogenic and Natural Mercury Emissions as a Function of Distance from the Center of the Watershed

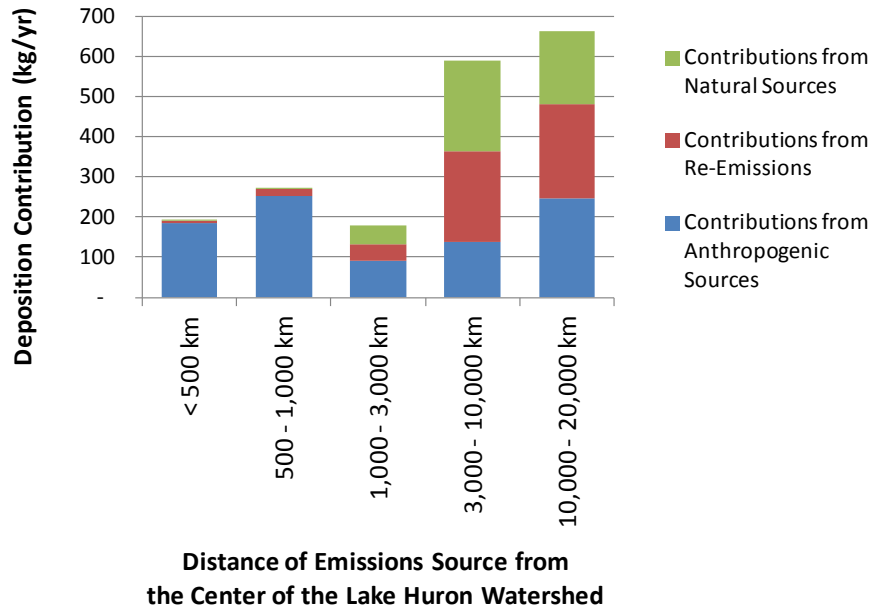


Figure 54. Atmospheric Deposition Contributions to the Lake Huron Watershed from Direct Anthropogenic, Re-emitted Anthropogenic and Natural Mercury Emissions as a Function of Distance from the Center of the Watershed

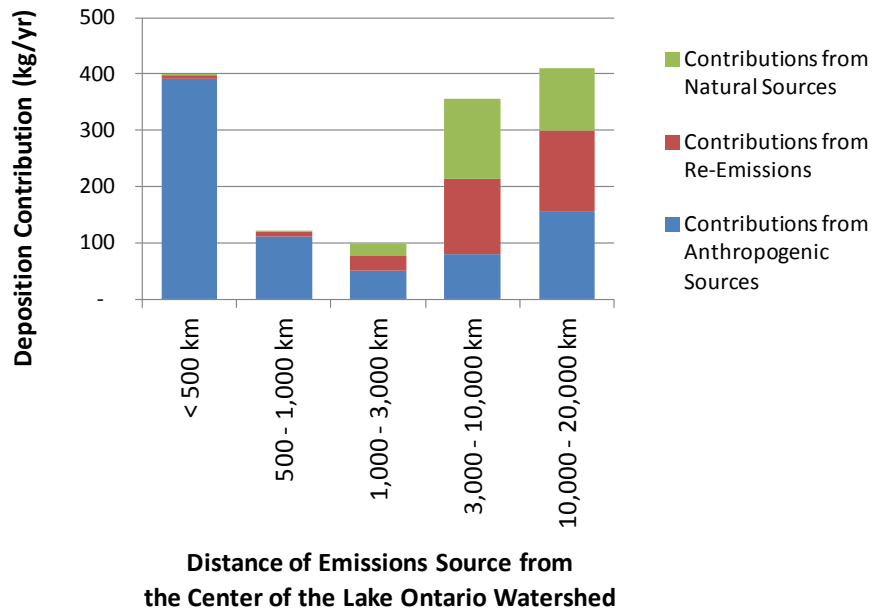


Figure 55. Atmospheric Deposition Contributions to the Lake Ontario Watershed from Direct Anthropogenic, Re-emitted Anthropogenic and Natural Mercury Emissions as a Function of Distance from the Center of the Watershed

5. Model Evaluation

5.1. Comparison of Model Predicted Wet Deposition Fluxes with Measured Wet Deposition Fluxes in the Great Lakes Basin

As discussed above in Section 2.4.3 (page 45), the primary goal of this project was to estimate deposition to the Great Lakes, as opposed to the much more computationally intensive exercise of estimating deposition at monitoring sites in the Great Lakes region. Nevertheless, an initial model evaluation exercise has been carried out in which model-predicted mercury wet deposition for 2005 has been compared against measured wet deposition in the Great Lakes region. Mercury Deposition Network sites with complete (or nearly complete) data records for 2005 were considered in this initial analysis and are shown in Figure 56.

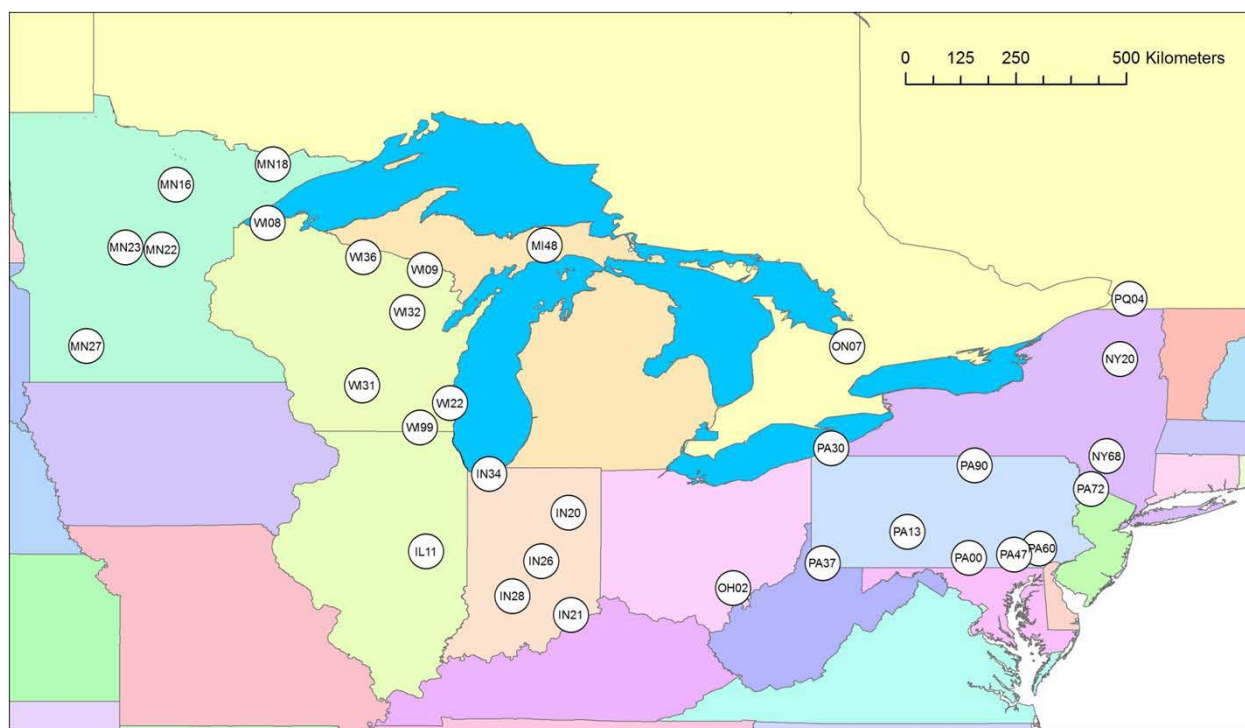


Figure 56. Mercury Deposition Network Sites in the Great Lakes Region Considered in an Initial Model Evaluation Analysis

As a first step in model evaluation, the precipitation data in the meteorological datasets used to drive the HYSPLIT-Hg model was compared with measured precipitation at each of these MDN sites. As described in described in Section 2.2 above, this initial model analysis utilized the NCEP/NCAR Global Reanalysis and the EDAS-40km gridded datasets. A comparison of the MDN-measured and met-data-set total precipitation for 2005 is shown in Figure 57. It can be seen that the global dataset (NCEP/NCAR

Reanalysis) is reasonably consistent with the measurements, with a moderate tendency towards overestimation. However, in a somewhat unexpected finding, there appears to be a significant, systematic underestimation of precipitation in the EDAS-40km dataset.

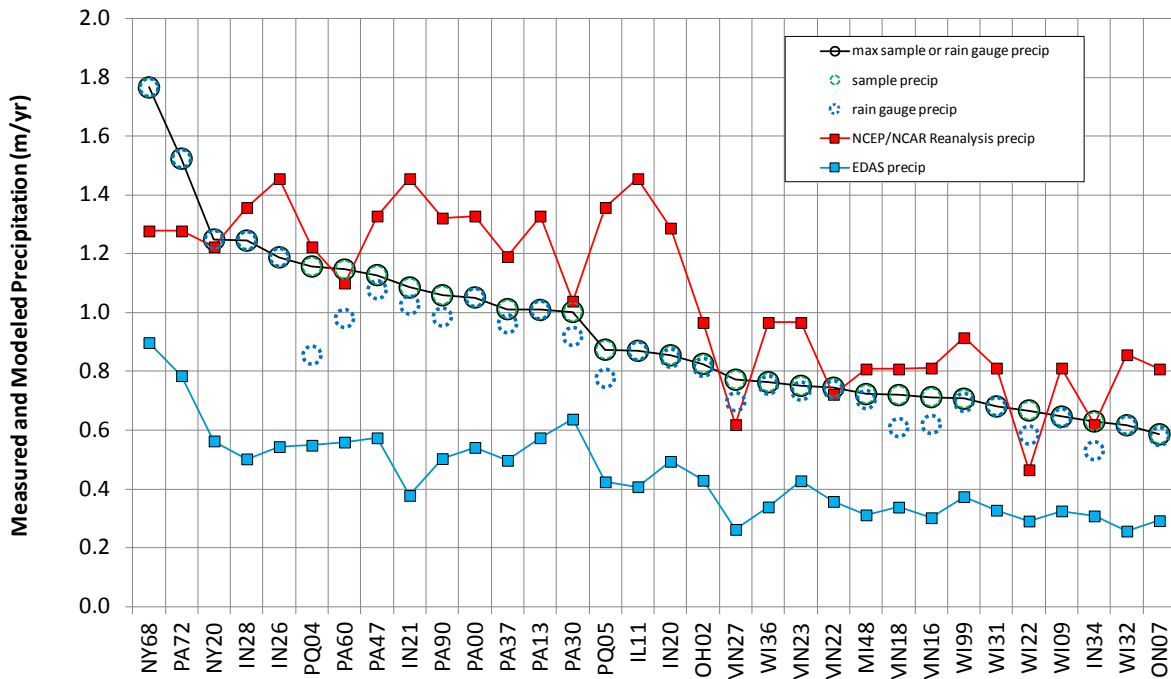


Figure 57. Comparison of Total 2005 Precipitation Measured at each of the Great-Lakes Region MDN Sites with the Precipitation in the Meteorological Datasets Used as Inputs to this Modeling Study

To investigate this further, the measured precipitation at the MDN sites was compared with a regional precipitation synthesis developed by the PRISM Climate Group at Oregon State University (<http://prism.oregonstate.edu>), and the results are shown in Figure 58. Note that there is no data shown in this Figure for the Great Lakes themselves, for the Atlantic Ocean, or for Canada. Nevertheless, in most cases, the precipitation measured at the MDN sites seems to be very consistent with the PRISM synthesis of other precipitation measurements in the vicinity of the sites. Thus, it appears that the inconsistency between the EDAS-40km dataset and the MDN precipitation measurements is indeed due to a systematic underestimation bias in that meteorological dataset. This issue was investigated further, and it was learned that the EDAS-40km dataset did tend to underestimate precipitation in 2005; this problem was “fixed” in 2006 and data for subsequent years are much more consistent with measurements (Rogers, 2011). In future work in this project, alternative meteorological datasets will be utilized, such as the North American Regional Reanalysis (NARR) dataset (<http://www.emc.ncep.noaa.gov/mmb/rrean/>).

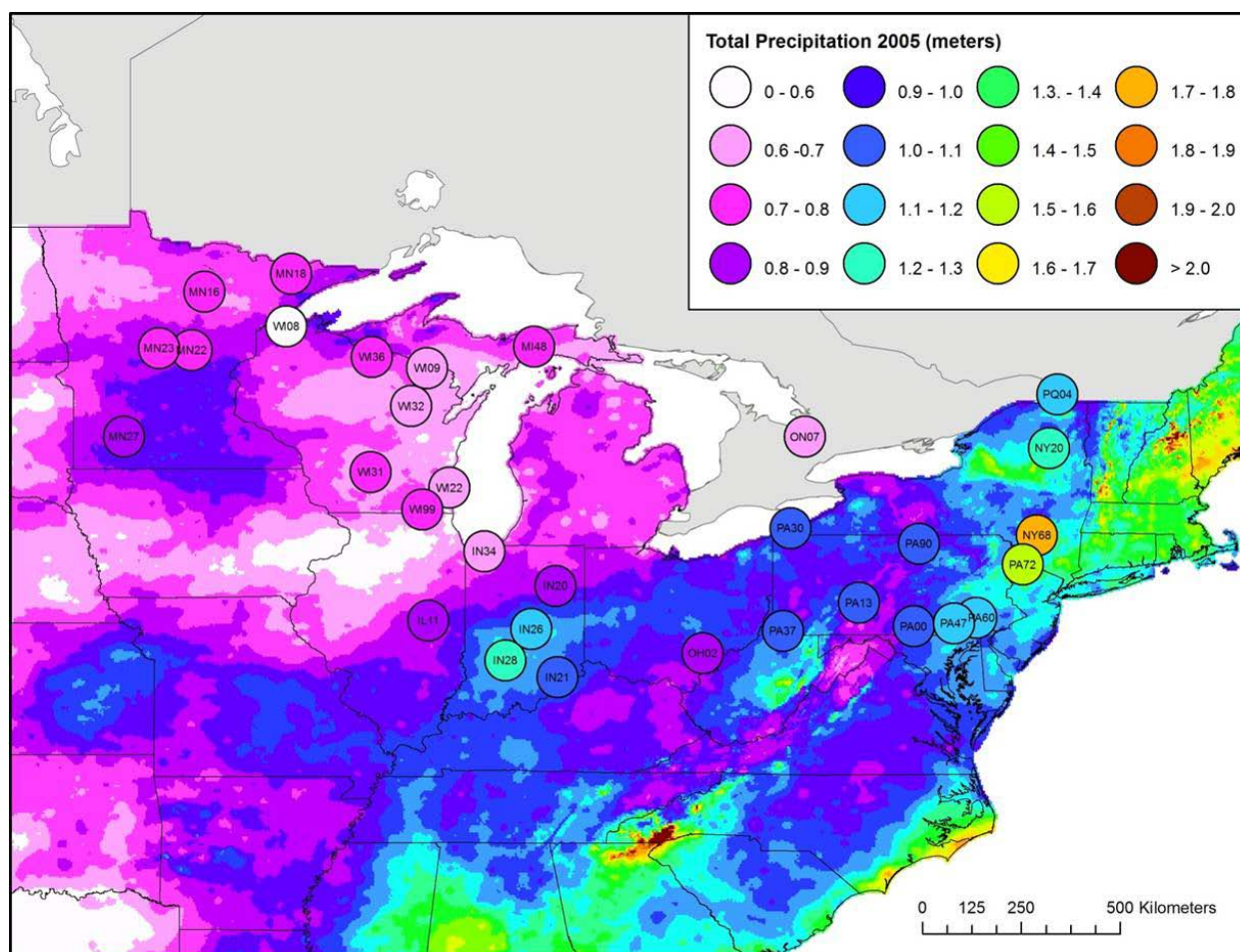


Figure 58. Comparison of 2005 precipitation total as measured at MDN sites in the Great Lakes region (circles) with precipitation totals assembled by the PRISM Climate Group, Oregon State University.

Recognizing the uncertainties discussed above, a comparison was nevertheless made between model predictions and MDN-measured mercury wet deposition. In carrying out this comparison, we have considered four different methods. In the first, no adjustment was made to any of the model-predicted wet deposition estimates. In the second, the portion of the wet deposition estimates at the MDN sites that was estimated using the EDAS-40km dataset was adjusted proportionally to balance out the precipitation “error” in the EDAS-40km data. In the third method, a comparable adjustment was made for the proportion of the wet mercury deposition at the MDN sites for which the NCEP/NCAR Global Reanalysis was utilized. In the fourth method, both of the adjustments in the previous two methods were made. It is recognized that the impact of the precipitation “errors” in the meteorological datasets will introduce complex, non-linear deviations in the simulations. For example, over- or under-estimates of precipitation along the transport path of an air parcel making its way from the emissions source to the MDN site will have an impact on the modeled wet deposition at the MDN site, even if the model-

input and measured precipitation matched perfectly at the site. So, the approaches described above involving the measured/model-input precipitation ratio at any given site are clearly oversimplifications. This simple methodology can be considered to provide an approximate estimate of the order of magnitude of the uncertainty introduced by the inherent precipitation biases in the input meteorological data. In future work on this project, extensive sensitivity analyses will be conducted that will allow more precise estimates of the influence of errors in the input data.

The initial results of this comparison are shown in Figure 59. In this figure the model estimates shown are the average of the values for the four methods described above, and the “error bars” indicate the range in wet deposition values over the four different methods. In spite of the issues with the underlying precipitation data used in this initial modeling – not to mention, uncertainties in emissions, atmospheric chemistry, and fate processes -- this figure shows that there is a reasonable consistency between the measured and modeled values.

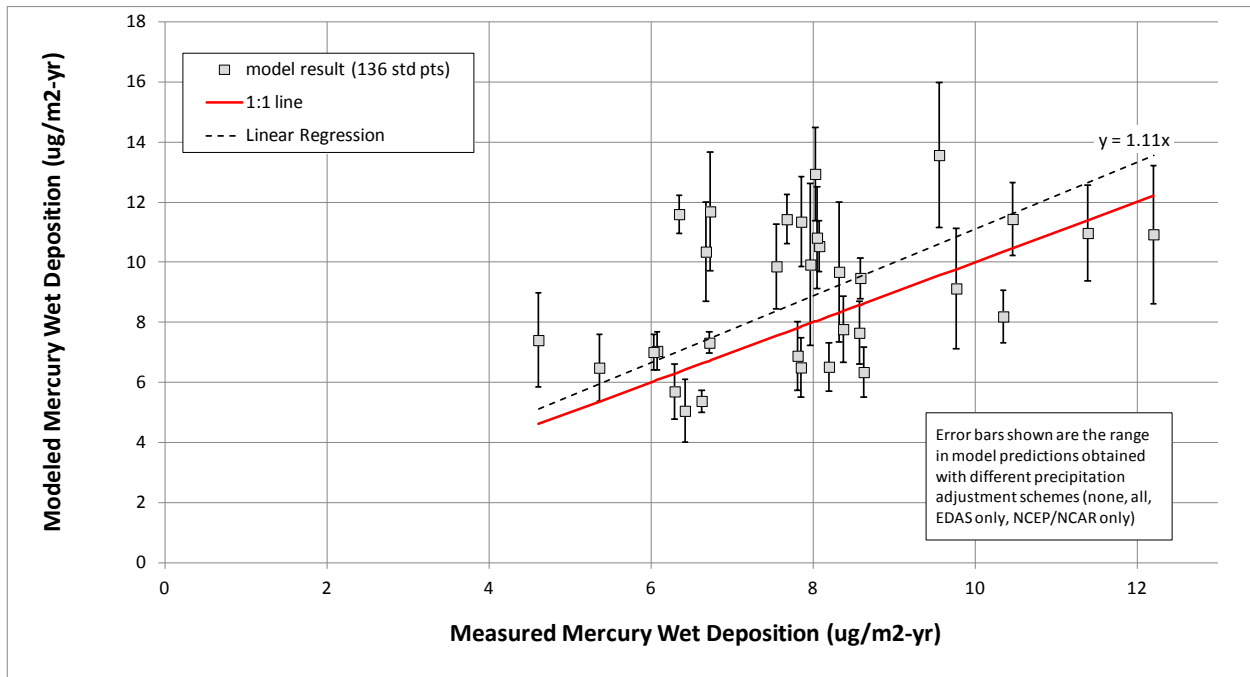


Figure 59. Modeled vs. Measured Wet Deposition of Mercury at Sites in the Great Lakes Region

Further examination of these results shows that the model tended to systematically over-predict mercury wet deposition at the 12 eastern-most MDN sites. This is demonstrated in Figure 60 and Figure 61, where the results for the 20 western-most sites and the 12 eastern-most sites are shown separately.

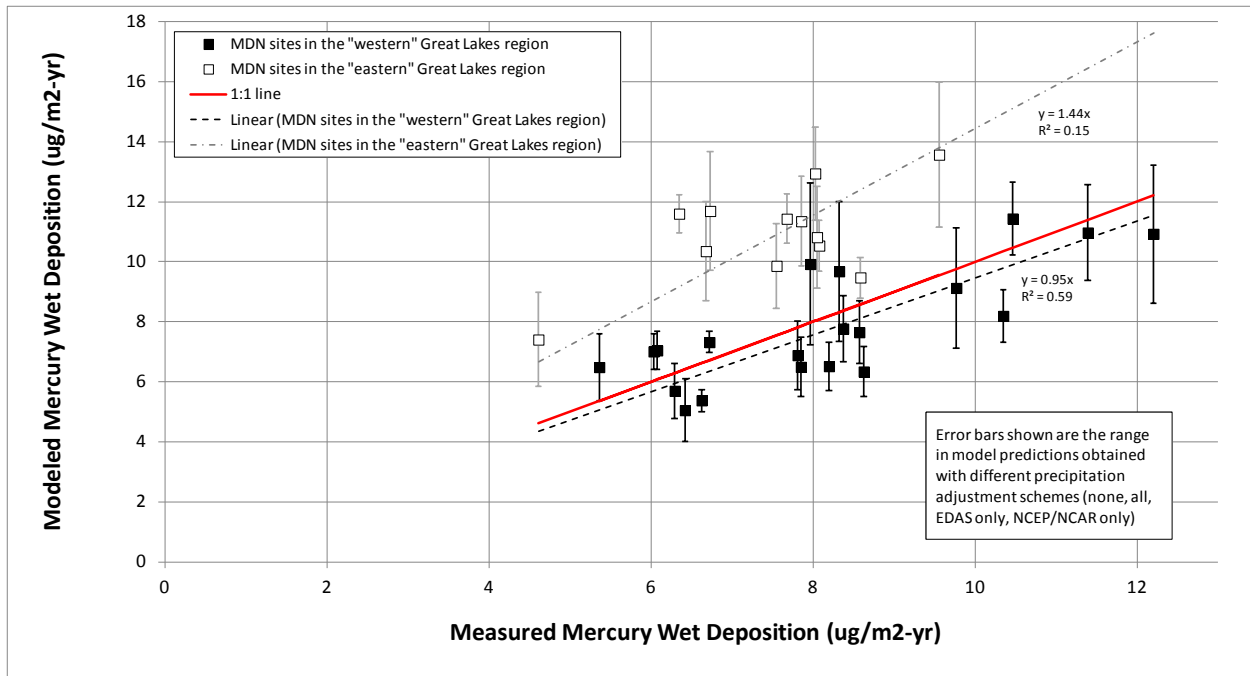


Figure 60. Modeled vs. Measured Wet Deposition of Mercury at Sites in the Great Lakes Region

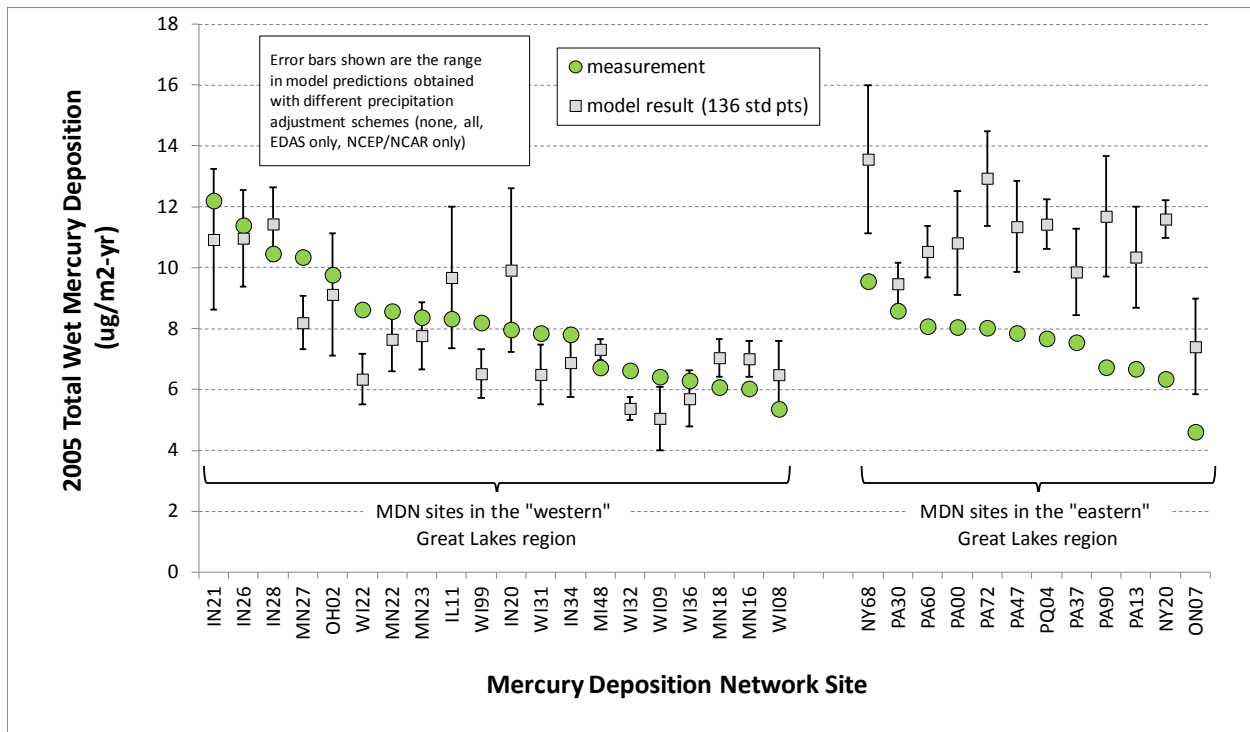


Figure 61. Modeled vs. Measured Wet Deposition of Mercury at Sites in the Great Lakes Region

As can be seen from these figures, while there is a moderate, systematic over-prediction at the 12 eastern-most sites, there is a much better overall agreement between the model predictions and the MDN measurements at the 20 western-most sites. Separate linear regression results are shown for the two groups in Figure 60. For the 20 western sites, the linear regression result reflect the relatively high degree of consistency (slope = 0.95; $R^2 = 0.69$), whereas for the eastern sites the regression results reflect the poorer agreement (slope = 1.44; $R^2 = 0.15$).

The reasons for the regional differences in model performance will be carefully examined in the next phase of the project, but an initial explanation may be apparent from an examination of Figure 62. In this figure, the emissions (gridded) and standard source locations used in the analysis are shown in relation to the MDN sites at which the comparisons are being made.

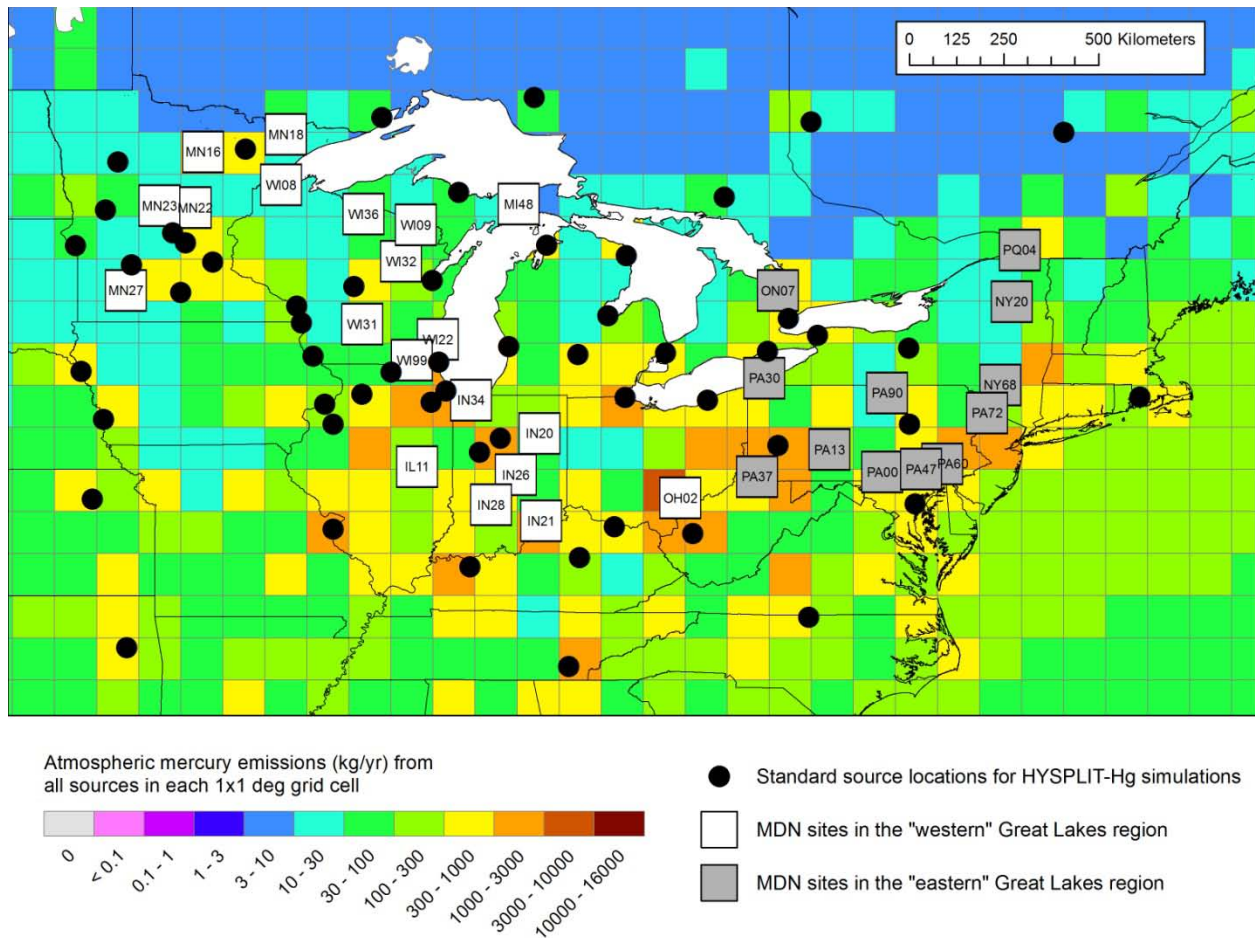


Figure 62. Standard source locations, MDN sites, and mercury emissions in the Great Lakes region

It is seen in Figure 62 that the density of standard source locations is generally lower in the region of the eastern-most MDN sites. The reason why more standard source locations were not utilized at the outset

was computational resource constraints. As discussed above in Section 2.4, the consequence of this sparseness is a higher likelihood that interpolation errors will affect the results. In particular, the general situation regarding the difference in estimating deposition at point monitoring sites vs. large area receptors – discussed above in Section 2.4.3, page 45 – seems to be especially relevant here. That is, the density of standard source locations required to estimate deposition to the Great Lakes is much less than that required for estimating deposition at a set of monitoring sites throughout the Great Lakes region. Or put another way, for the same set of standard source locations – or the same expenditure of computational resources -- the expected accuracy of deposition estimates for large area receptors – e.g., in this case, the Great Lakes and their watersheds – is much higher than the expected accuracy for deposition estimates at a set of monitoring sites throughout the region.

With additional standard source locations in the regions surrounding each of these eastern-most Great Lakes region MDN sites, the agreement between modeled and measured wet deposition will likely improve. At the same time, the addition of these new standard source locations will likely not change the results for the Great Lakes very much. We will test these hypotheses in the next phase of the work.

Returning to the issue of precipitation biases in the underlying meteorological data, note that that the approximate, simple “ratio-based adjustments” were considered only for the point estimates of wet deposition at the selected MDN sites. It is not possible to make comparable adjustments to the deposition to the large area receptors of this study (i.e., the Great Lakes and their watersheds), because the precipitation amounts over these large areas are only known at point measurements at various locations in the region. Due to spatial gradients in precipitation, the actual deposition to any large area receptor is therefore not known precisely. Perhaps more importantly, the effect of precipitation biases on the results is not a straightforward matter to quantify. For example, if wet deposition in the region is underestimated, increased dry deposition may at least partially make up for this deficiency. Moreover, as discussed above, the impact (on the eventual deposition to the Great Lakes) of precipitation biases along the transport pathway of any given parcel of emitted mercury would depend in detail on numerous aspects, including the detailed spatio-temporal pattern of meteorological parameters including (but not limited to) precipitation, and is not amenable to a simple adjustment.

Notwithstanding the above, the positive precipitation bias in the NCEP/NCAR Global Reanalysis -- i.e., the precipitation in the Great Lakes region appears to be overestimated – *may* have had the result of overestimating the deposition to the Great Lakes from sources outside of central North America whose impacts were estimated with these data. At the same time, the negative precipitation bias in the EDAS-40km dataset *may* have resulted in an underestimate in the Great Lakes deposition attributable to the central North American sources for which this EDAS-40km dataset was used. In other words, if the precipitation biases are treated simply, the analysis presented here may have overestimated the impacts of global sources and underestimated the impacts of central North American sources.

The next phase of the project will focus extensively on model evaluation, and on the sensitivity of model results – both for comparisons against ambient measurements and for source-attribution estimates – on model parameters, assumptions, algorithms, and model input data. In relation to the discussion above, we will plan to carefully examine the impact of precipitation data biases.

5.2. Additional Considerations Regarding the Overall Mercury Mass Balance for the Great Lakes Basin

In the next phase of this project, we will explore the overall mass balance in each of the Great Lakes and in the Great Lakes Basin as a whole in detail. However, a very brief discussion will be initiated here.

Denkenberger et al. (2011) have recently estimated total deposition of mercury to the Great Lakes Basin to be ~15.9 Mg/yr counterbalanced by a net evasion of elemental mercury of ~7.7 Mg/yr, resulting in the basin being an overall net mercury sink of ~8.2 Mg/yr. The authors acknowledge that these estimates contain significant uncertainties.

In the initial set of simulations performed here, a “gross” elemental mercury deposition of ~1.2 Mg/yr was estimated. A “gross” volatilization of ~9.0 Mg/yr would be required, counterbalanced by the 1.2 Mg/yr gross deposition, to be consistent with the Denkenberger et al. estimate of net Hg(0) surface exchange flux. Additionally, the initial results presented here represent a combined of Hg(II) + Hg(p) deposition of ~10 Mg/yr, somewhat less but comparable to the 15.9 Mg/yr estimated by Denkenberger and colleagues.

A brief sensitivity analysis was conducted in which a 2nd emissions scenario was utilized, in which the total re-emissions from land were 2000 Mg/yr (instead of 750 Mg/yr) and the total re-emissions from the ocean were 2000 Mg/yr (instead of 1250 Mg/yr). The land and ocean re-emissions were spatially distributed in the same way as in the base case. There are large uncertainties in the overall estimates of global re-emissions, and these higher estimates fall within the range of potential values.

The overall results for the Great Lakes Basin in the original and modified emissions scenario are shown in Figure 63 below. With the modified re-emissions scenario, a total “gross” elemental mercury deposition of 1.7 Mg/yr and a total combined Hg(II) + Hg(p) deposition of 12.7 Mg/yr was estimated. Analogously, a “gross” volatilization of ~9.5 Mg/yr would be required to match the 7.7 Mg/yr net volatilization flux estimated by Denkenberger et al. In this modified emissions scenario, the deposition of other forms of mercury of 12.7 Mg/yr is even more consistent with the 15.9 Mg/yr deposition estimate in that study.

In the next phase of this project, a series of sensitivity analyses will be conducted to examine the influence of simulation inputs, parameters, assumptions, and algorithms on the overall results, such as the overall mass balance considerations briefly touched upon here. In this next phase, we will review the above and other mass-balance estimates for mercury in the Great Lakes Basin and compare these alternative estimates with the model results produced.

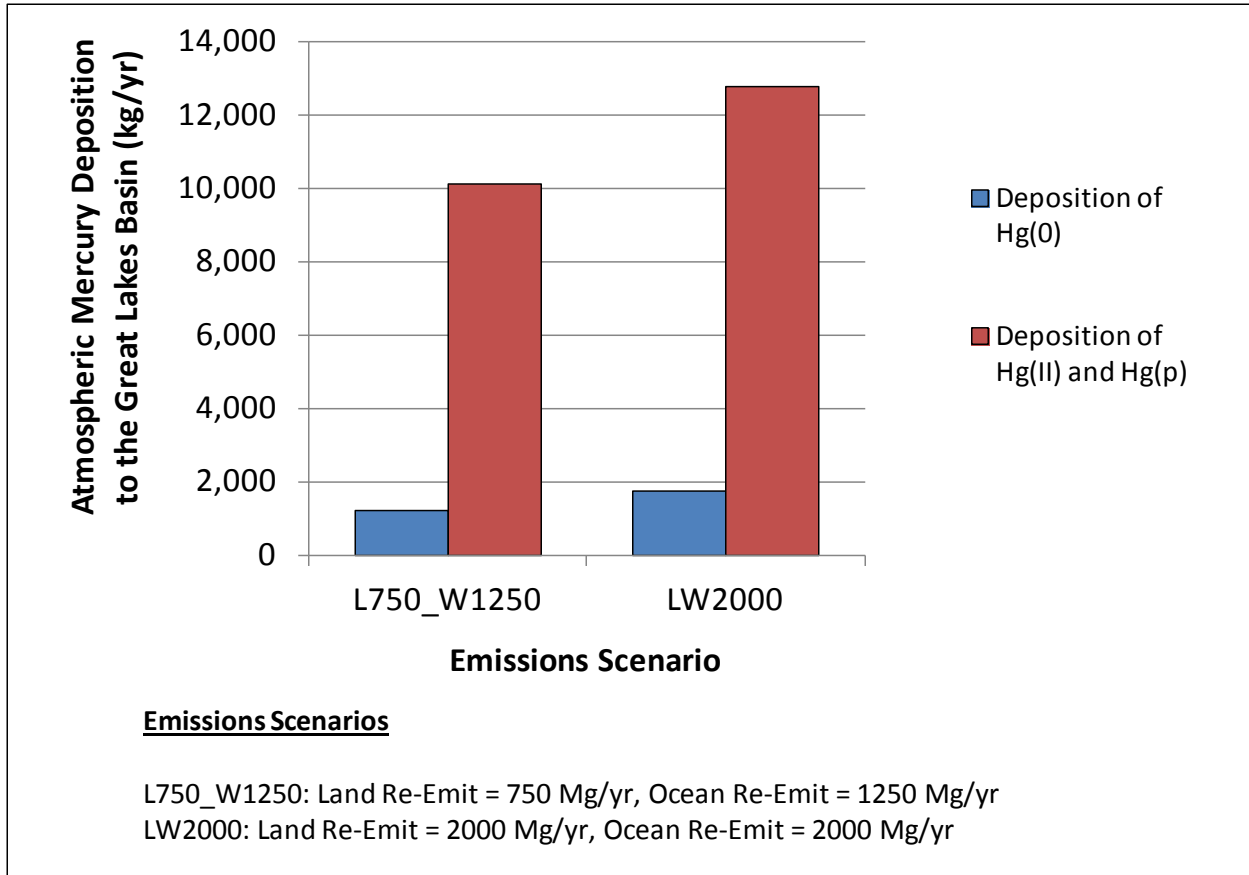


Figure 63. Gross deposition to the Great Lakes Basin in the base-case emissions scenario and a modified scenario

6. Conclusions

In this first phase of this project, the goals of the project (Section 1.4) were successfully carried out, as documented in this report:

- The time period for the analysis was selected (2005) (Section 2);
- Required model inputs were assembled and tested, e.g., meteorological data (Section 2.2) and emissions inventories (Section 2.3);
- A wide variety of tests were conducted to guide selection of model physics options (e.g., time step, dispersion parameters) (Section 2.4.4);
- An initial set of standard source locations were selected (Section 2.4.2);
- An initial set of simulations were carried out for each of these standard sources, for each of the three primary forms of mercury emissions (Hg(0), Hg(II), and Hg(p)) (Section 3);
- Post-processing computer codes were developed and tested, e.g., programs that combine the emissions inventory data with the standard source location simulations using the interpolation techniques outlined above (outlined in Section 2.4.1);
- Using all of the above, an initial set of “base case” results was created, that will serve as the basis for sensitivity analyses and further examination during the next phase of the project (Section 4);
- An initial evaluation of the results was conducted by comparison of model predictions against a limited set of ambient measurements in the Great Lakes region (Section 5).

The methodology utilized has a number of features that make it particularly relevant and useful for providing information about the quantity of and source-attribution for atmospheric mercury deposition to the Great Lakes. One such feature is that deposition was explicitly modeled to the actual area of the lakes and watersheds during the simulation, rather than the usual practice of ascribing portions of gridded deposition to these areas in a post-processing step. Another key feature is the unique combination of Lagrangian and Eulerian modeling frameworks that allow accurate and computationally efficient estimates of the fate and transport of atmospheric mercury over all relevant length scales – from “local” to global. A 3rd key feature of the work is the fact that tremendously detailed source-attribution information is created – the atmospheric deposition contribution to each of the Great Lakes and their watersheds from each source in the emissions inventories used is estimated individually. The level of source discrimination is only limited by the detail in the input inventories. So, for example, source-type breakdowns were not possible in this first phase of the work for global sources, because the available geographically resolved global emissions inventory did not have source-type breakdowns for each grid square.

As shown herein, the methodology utilized was able to successfully produce uniquely detailed source-attribution results, as well as produce results for “single sources” that illustrate important source-receptor relationships. A set of such illustrative results presented here demonstrate the often dramatic difference in Great Lakes impacts from sources in different locations in the world. For example, the model results show that a “typical” coal-fired power plant near Lake Erie may contribute on the order of 100x the mercury – for the same emissions – as a comparable facility in China.

One overall finding in this initial analysis for 2005 is that regional, national, and global mercury emissions are all important contributors to mercury deposition in the Great Lakes Basin, with varying relative source attribution patterns. For Lakes Erie and Ontario, the U.S. contribution is at its most significant, while for Lakes Huron and Superior, the U.S. contribution is less significant. Due to their relative proximity to the lakes, local and regional sources have disproportionately much greater atmospheric deposition contributions than their emissions, as a fraction of total global mercury emissions, would suggest.

Another key finding is that despite numerous uncertainties in model input data and other modeling aspects, the model results are reasonably consistent with measurements in the Great Lakes region. The comparison at sites in regions where significant computational resources were expended – corresponding to regions that were the most important for estimating deposition to the Great Lakes and their watersheds – showed very good consistency between model predictions and measured quantities. For a smaller subset of sites generally downwind of the Great Lakes (in regions not expected to contribute most significantly to Great Lakes atmospheric deposition), less computational resources were expended, and the comparison showed moderate, but understandable, discrepancies.

The modeling framework, methodology and this initial set of results will provide an excellent starting point for the next phase of this work. In this next phase, the modeling results will be evaluated more extensively against ambient monitoring data and, sensitivity analyses will be conducted to examine the influences of model uncertainties on the results.

7. References

- Acosta-Ruiz, G., and Powers, B. (2001). *Preliminary Atmospheric Emissions Inventory of Mercury in Mexico*. Prepared by Acosta and Associates, Agua Prieta, Sonora, Mexico, for the Commission for Environmental Cooperation. Report (14 pages) and database.
- Ames, M., G. Gullu and I. Olmez (1998). Atmospheric mercury in the vapor phase, and in fine and coarse particulate matter at Perch River, New York. *Atmospheric Environment* 32(5): 865-872.
- Becker, A., G. Wotawa, et al. (2007). Global backtracking of anthropogenic radionuclides by means of a receptor oriented ensemble dispersion modelling system in support of Nuclear-Test-Ban Treaty verification. *Atmospheric Environment* 41(21): 4520-4534.
- Bergan, T., L. Gallardo and H. Rodhe (1999). Mercury in the global troposphere: a three-dimensional model study. *Atmospheric Environment* 33(10): 1575-1585.
- Bergan, T. and H. Rodhe (2001). Oxidation of elemental mercury in the atmosphere; Constraints imposed by global scale modelling. *Journal of Atmospheric Chemistry* 40(2): 191-212.
- Blanchard, C. L. (1999). Methods for attributing ambient air pollutants to emission sources. *Annual Review of Energy and the Environment* 24: 329-365.
- Blanchard, P., F. A. Froude, J. B. Martin, H. Dryfhout-Clark and J. T. Woods (2002). Four years of continuous total gaseous mercury (TGM) measurements at sites in Ontario, Canada. *Atmospheric Environment* 36(23): 3735-3743.
- Bullock, O. R., K. A. Brehme, et al. (1998). Lagrangian modeling of mercury air emission, transport and deposition: An analysis of model sensitivity to emissions uncertainty. *Science of the Total Environment* 213(1-3): 1-12.
- Bullock, O. R. (2000). Modeling assessment of transport and deposition patterns of anthropogenic mercury air emissions in the United States and Canada. *Science of the Total Environment* 259(1-3): 145-157.
- Bullock, O. R. and K. A. Brehme (2002). Atmospheric mercury simulation using the CMAQ model: formulation description and analysis of wet deposition results. *Atmospheric Environment* 36(13): 2135-2146.
- Bullock, O. R., D. Atkinson, T. Braverman, K. Civerolo, A. Dastoor, D. Davignon, J. Y. Ku, K. Lohman, T. C. Myers, R. J. Park, C. Seigneur, N. E. Selin, G. Sistla and K. Vijayaraghavan (2008). The North American Mercury Model Intercomparison Study (NAMMIS): Study description and model-to-model comparisons. *Journal of Geophysical Research-Atmospheres* 113(D17).
- Bullock, O. R., D. Atkinson, T. Braverman, K. Civerolo, A. Dastoor, D. Davignon, J. Y. Ku, K. Lohman, T. C. Myers, R. J. Park, C. Seigneur, N. E. Selin, G. Sistla and K. Vijayaraghavan (2009). An analysis of simulated wet deposition of mercury from the North American Mercury Model Intercomparison Study. *Journal of Geophysical Research-Atmospheres* 114.

- Butler, T. J., M. D. Cohen, F. M. Vermeylen, G. E. Likens, D. Schmeltz and R. S. Artz (2008). Regional precipitation mercury trends in the eastern USA, 1998-2005: Declines in the Northeast and Midwest, no trend in the Southeast. *Atmospheric Environment* 42(7): 1582-1592.
- Cairns, E., K. Tharumakulasingam, M. Athar, M. Yousaf, I. Cheng, Y. Huang, J. L. Lu and D. Yap (2011). Source, concentration, and distribution of elemental mercury in the atmosphere in Toronto, Canada. *Environmental Pollution* 159(8-9): 2003-2008.
- CEC (2011). *North American Power Plant Air Emissions*. Commission for Environmental Cooperation, Montreal, Quebec, Canada. Available at: <http://www2.cec.org/site/PPE>
- Cheng, I., J. Lu and X. J. Song (2009). Studies of potential sources that contributed to atmospheric mercury in Toronto, Canada. *Atmospheric Environment* 43(39): 6145-6158.
- Choi, H. D., T. M. Holsen, et al. (2008a). Atmospheric mercury (Hg) in the Adirondacks: Concentrations and sources. *Environmental Science & Technology* 42(15): 5644-5653.
- Choi, H. D., T. J. Sharac and T. M. Holsen (2008b). Mercury deposition in the Adirondacks: A comparison between precipitation and throughfall. *Atmospheric Environment* 42(8): 1818-1827.
- Cohen, M., Commoner, B., Eisl, H., Bartlett, P., Dickar, A., Hill, C., Quigley, J., and Rosenthal, J. (1995). *Quantitative Estimation of the entry of dioxins, furans, and hexachlorobenzene into the Great Lakes from airborne and waterborne sources*. Flushing, NY, Center for the Biology of Natural Systems, Queens College.
- Cohen, M., Commoner, B., Bartlett, P., Cooney, P., Eisl, H. (1997). *Exposure to Endocrine Disruptors from Long Range Air Transport of Pesticides*. Flushing, NY, Center for the Biology of Natural Systems, Queens College.
- Cohen, M., Artz, R., Draxler, R. (2007). *NOAA Report to Congress: Mercury Contamination in the Great Lakes*. Silver Spring, MD, NOAA Air Resources Laboratory: 162 pages.
- Cohen, M., R. Artz, et al. (2004). Modeling the atmospheric transport and deposition of mercury to the Great Lakes. *Environmental Research* 95(3): 247-265.
- Cohen, M. D., R. R. Draxler, et al. (2002). Modeling the atmospheric transport and deposition of PCDD/F to the Great Lakes. *Environmental Science & Technology* 36(22): 4831-4845.
- Corbitt, E.S., Jacob, J.J., Holmes, C.D., Streets, D.G., and Sunderland, E.M. (2011). Global Source-Receptor Relationships for Mercury Deposition Under Present-Day and 2050 Emissions Scenarios. *Environmental Science & Technology* 45(24): 10477-10484.
- Dastoor, A. P. and Y. Larocque (2004). Global circulation of atmospheric mercury: a modelling study. *Atmospheric Environment* 38(1): 147-161.

- Denkenberger, J.S., Driscoll, C.T., Branfireun, B., Eckley, C.S., Cohen, M., and Selvendiran, P. (2011). A Synthesis of Rates and Controls on Elemental Mercury Evasion in the Great Lakes Basin. *Environmental Pollution*, accepted, in press.
- Draxler, R. R. (1991). The Accuracy of Trajectories During Anatex Calculated Using Dynamic-Model Analyses Versus Rawinsonde Observations. *Journal of Applied Meteorology* 30(10): 1446-1467.
- Draxler, R. R., Hess, G.D. (1998). An overview of the HYSPLIT_4 Modelling System for Trajectories, Dispersion and Deposition. *Australian Met. Mag.* 47: 295-308.
- Draxler, R. R. (2000). Meteorological factors of ozone predictability at Houston, Texas. *Journal of the Air & Waste Management Association* 50(2): 259-271.
- Draxler, R. R. (2006). The use of global and mesoscale meteorological model data to predict the transport and dispersion of tracer plumes over Washington, D. C. *Weather and Forecasting* 21(3): 383-394.
- Draxler, R. R. (2007). Demonstration of a global modeling methodology to determine the relative importance of local and long-distance sources. *Atmospheric Environment* 41(4): 776-789.
- Draxler, R. R., R. Dietz, et al. (1991). Across North-America Tracer Experiment (ANATEX) - Sampling and Analysis. *Atmospheric Environment Part a-General Topics* 25(12): 2815-2836.
- Draxler, R. R., M. Jean, et al. (1997). Emergency preparedness - Regional specialised meteorological centres at Washington and Montreal. *Radiation Protection Dosimetry* 73(1-4): 27-30.
- Draxler, R. R., J. T. McQueen, et al. (1994). An Evaluation of Air Pollutant Exposures due to the 1991 Kuwait Oil Fires Using a Lagrangian Model. *Atmospheric Environment* 28(13): 2197-2210.
- Draxler, R. R. and B. J. B. Stunder (1988). Modeling the Captex Vertical Tracer Concentration Profiles. *Journal of Applied Meteorology* 27(5): 617-625.
- Draxler, R. R. and A. D. Taylor (1990). An Advective-Interpolation Method for Estimating Pollutant Movement During ANATEX. *Atmospheric Environment Part a-General Topics* 24(2): 431-433.
- Environment Canada (2011). 2005 National Pollutant Release Inventory (NPRI) mercury emissions data downloaded from the NPRI website on Aug 4, 2011. <http://www.ec.gc.ca/inrp-npri>
- Environment Canada (2008). Personal Communication from Patricia Smith, GIS Analyst, Criteria Air Contaminant Section, Pollution Data Division, Science and Technology Branch, Environment Canada, Gatineau, Quebec. March 26, 2008.
- Evers, D., J. Wiener, et al. (2011a). Mercury in the Great Lakes region: bioaccumulation, spatiotemporal patterns, ecological risks, and policy. *Ecotoxicology* 20(7): 1487-1499.

- Evers, D.C., Wiener, J.G., Driscoll, C.T., Gay, D.A., Basu, N., Monson, B.A., Lambert, K.F., Morrison, H.A., Morgan, J.T., Williams, K.A., Soehl, A.G. (2011b). *Great Lakes Mercury Connections: The Extent and Effects of Mercury Pollution in the Great Lakes Region*. Biodiversity Research Institute. Gorham, Maine. Report BRI 2011-18. 44 pages. <http://www.briloon.org/mercuryconnections/greatlakes>
- Gbor, P. K., D. Y. Wen, F. Meng, F. Q. Yang, B. N. Zhang and J. J. Sloan (2006). Improved model for mercury emission, transport and deposition. *Atmospheric Environment* 40(5): 973-983.
- Gbor, P. K., D. Y. Wen, F. Meng, F. Q. Yang and J. J. Sloan (2007). Modeling of mercury emission, transport and deposition in North America. *Atmospheric Environment* 41(6): 1135-1149.
- Gildemeister, A. E., J. Graney and G. J. Keeler (2005). Source proximity reflected in spatial and temporal variability in particle and vapor phase Hg concentrations in Detroit, MI. *Atmospheric Environment* 39(2): 353-358.
- Gilmour, C., R. Mason, A. Heyes, and M. Castro (2008). *An Examination of the Factors that Control Methylmercury Production and Bioaccumulation in Maryland Reservoirs*. Resource Assessment Service, MONITORING AND NON-TIDAL ASSESSMENT DIVISION, MANTA- AD-08-1, Publication # 12-482008-298, Maryland Department of Natural Resources. 119 pages. http://dnr.maryland.gov/streams/pdfs/12-482008-298_hg.pdf
- Glass, G. E., E. N. Leonard, W. H. Chan and D. B. Orr (1986). Airborne Mercury in Precipitation in the Lake-Superior Region. *Journal of Great Lakes Research* 12(1): 37-51.
- Glass, G. E., J. A. Sorensen, K. W. Schmidt and G. R. Rapp (1990). New Source Identification of Mercury Contamination in the Great-Lakes. *Environmental Science & Technology* 24(7): 1059-1069.
- Glass, G. E., J. A. Sorensen, K. W. Schmidt, G. R. Rapp, D. Yap and D. Fraser (1991). Mercury Deposition and Sources for the Upper Great-Lakes Region. *Water Air and Soil Pollution* 56: 235-249.
- Gratz, L. E., G. J. Keeler, J. D. Blum and L. S. Sherman (2010). Isotopic Composition and Fractionation of Mercury in Great Lakes Precipitation and Ambient Air. *Environmental Science & Technology* 44(20): 7764-7770.
- Hall, B. D., H. Manolopoulos, J. P. Hurley, J. J. Schauer, V. L. St Louis, D. Kenski, J. Graydon, C. L. Babiarz, L. B. Cleckner and G. J. Keeler (2005). Methyl and total mercury in precipitation in the Great Lakes region. *Atmospheric Environment* 39(39): 7557-7569.
- Han, Y. J., T. M. Holsen, S. O. Lai, P. K. Hopke, S. M. Yi, W. Liu, J. Pagano, L. Falanga, M. Milligan and C. Andolina (2004). Atmospheric gaseous mercury concentrations in New York State: relationships with meteorological data and other pollutants. *Atmospheric Environment* 38(37): 6431-6446.
- Han, Y. J., T. M. Holsen, P. K. Hopke and S. M. Yi (2005). Comparison between back-trajectory based modeling and Lagrangian backward dispersion Modeling for locating sources of reactive gaseous mercury. *Environmental Science & Technology* 39(6): 1715-1723.

- Han, Y. J., T. M. Holsen and P. K. Hopke (2007). Estimation of source locations of total gaseous mercury measured in New York State using trajectory-based models. *Atmospheric Environment* 41(28): 6033-6047.
- Henry, R. C., C. W. Lewis, P. K. Hopke and H. J. Williamson (1984). Review of Receptor Model Fundamentals. *Atmospheric Environment* 18(8): 1507-1515.
- Holmes, C. D., D. J. Jacob, E. S. Corbitt, J. Mao, X. Yang, R. Talbot and F. Slemr (2010). Global atmospheric model for mercury including oxidation by bromine atoms. *Atmospheric Chemistry and Physics* 10(24): 12037-12057.
- Hoyer, M., J. Burke and G. Keeler (1995). Atmospheric Sources, Transport and Deposition of Mercury in Michigan - 2 Years of Event Precipitation. *Water Air and Soil Pollution* 80(1-4): 199-208.
- Hollingshead, A. T., S. Businger, et al. (2003). Dispersion Modelling of the Kilauea plume. *Boundary-Layer Meteorology* 108(1): 121-144.
- Huang, J. Y., H. D. Choi, P. K. Hopke and T. M. Holsen (2010). Ambient Mercury Sources in Rochester, NY: Results from Principle Components Analysis (PCA) of Mercury Monitoring Network Data. *Environmental Science & Technology* 44(22): 8441-8445.
- Jacob, D. J., C. D. Holmes, A. Soerensen, E. D. Sturges and E. M. Sunderland (2010). Global modeling of mercury with Br as atmospheric oxidant. *Geochimica Et Cosmochimica Acta* 74(12): A452-A452.
- Jeremiason, J.D., Kanne, L.A., Lacoé, T.A., Hulting, M., Simcik, M.F.(2009). A comparison of mercury cycling in Lakes Michigan and Superior. *Journal of Great Lakes Research* 35(3): 329-336.
- Keeler, G. J. and P. J. Samson (1989). Spatial Representativeness of Trace-Element Ratios. *Environmental Science & Technology* 23(11): 1358-1364.
- Keeler, G., G. Glinsorn and N. Pirrone (1995). Particulate Mercury in the Atmosphere - Its Significance, Transport, Transformation and Sources. *Water Air and Soil Pollution* 80(1-4): 159-168.
- Keeler, G. J., M. S. Landis, G. A. Norris, E. M. Christianson and J. T. Dvonch (2006). Sources of mercury wet deposition in Eastern Ohio, USA. *Environmental Science & Technology* 40(19): 5874-5881.
- Kellerhals, M., S. Beauchamp, W. Belzer, P. Blanchard, F. Froude, B. Harvey, K. McDonald, M. Pilote, L. Poissant, K. Puckett, B. Schroeder, A. Steffen and R. Tordon (2003). Temporal and spatial variability of total gaseous mercury in Canada: results from the Canadian Atmospheric Mercury Measurement Network (CAMNet). *Atmospheric Environment* 37(7): 1003-1011.
- Kolker, A., M. L. Olson, D. P. Krabbenhoft, M. T. Tate and M. A. Engle (2010). Patterns of mercury dispersion from local and regional emission sources, rural Central Wisconsin, USA. *Atmospheric Chemistry and Physics* 10(10): 4467-4476.
- Lai, S. O., T. M. Holsen, P. K. Hopke and P. Liu (2007a). Wet deposition of mercury at a New York state rural site: Concentrations, fluxes, and source areas. *Atmospheric Environment* 41(21): 4337-4348.

- Lai, S. O., T. M. Holsen, Y. J. Han, P. P. Hopke, S. M. Yi, P. Blanchard, J. J. Pagano and M. Milligan (2007b). Estimation of mercury loadings to Lake Ontario: Results from the Lake Ontario atmospheric deposition study (LOADS). *Atmospheric Environment* 41(37): 8205-8218.
- Lamborg, C. H., W. F. Fitzgerald, G. M. Vandal and K. R. Rolfhus (1995). Atmospheric Mercury in Northern Wisconsin - Sources and Species. *Water Air and Soil Pollution* 80(1-4): 189-198.
- Landis, M. S. and G. J. Keeler (1997). Critical evaluation of a modified automatic wet-only precipitation collector for mercury and trace element determinations. *Environmental Science & Technology* 31(9): 2610-2615.
- Landis, M. S. and G. J. Keeler (2002). Atmospheric mercury deposition to Lake Michigan during the Lake Michigan Mass Balance Study. *Environmental Science & Technology* 36(21): 4518-4524.
- Landis, M. S., A. F. Vette and G. J. Keeler (2002). Atmospheric mercury in the Lake Michigan basin: Influence of the Chicago/Gary urban area. *Environmental Science & Technology* 36(21): 4508-4517.
- Lin, X. and Y. Tao (2003). A numerical modelling study on regional mercury budget for eastern North America. *Atmospheric Chemistry and Physics* 3: 535-548.
- Lin, C. J., P. Pongprueksa, S. E. Lindberg, S. O. Pehkonen, D. Byun and C. Jang (2006). Scientific uncertainties in atmospheric mercury models I: Model science evaluation. *Atmospheric Environment* 40(16): 2911-2928.
- Lin, C. J., P. Pongprueks, O. Russell Bullock, S. E. Lindberg, S. O. Pehkonen, C. Jang, T. Braverman and T. C. Ho (2007). Scientific uncertainties in atmospheric mercury models II: Sensitivity analysis in the CONUS domain. *Atmospheric Environment* 41(31): 6544-6560.
- Liu, W., P. K. Hopke, Y. J. Han, S. M. Yi, T. M. Holsen, S. Cybart, K. Kozlowski and M. Milligan (2003). Application of receptor modeling to atmospheric constituents at Potsdam and Stockton, NY. *Atmospheric Environment* 37(36): 4997-5007.
- Liu, B., G. J. Keeler, J. T. Dvonch, J. A. Barres, M. M. Lynam, F. J. Marsik and J. T. Morgan (2007). Temporal variability of mercury speciation in urban air. *Atmospheric Environment* 41(9): 1911-1923.
- Liu, B., G. J. Keeler, J. T. Dvonch, J. A. Barres, M. M. Lynam, F. J. Marsik and J. T. Morgan (2010). Urban-rural differences in atmospheric mercury speciation. *Atmospheric Environment* 44(16): 2013-2023.
- Lohman, K., C. Seigneur, M. Gustin and S. Lindberg (2008). Sensitivity of the global atmospheric cycle of mercury to emissions. *Applied Geochemistry* 23(3): 454-466.
- Lynam, M. M. and G. J. Keeler (2002). Comparison of methods for particulate phase mercury analysis: sampling and analysis. *Analytical and Bioanalytical Chemistry* 374(6): 1009-1014.

- Lynam, M. M. and G. J. Keeler (2005a). Artifacts associated with the measurement of particulate mercury in an urban environment: The influence of elevated ozone concentrations. *Atmospheric Environment* 39(17): 3081-3088.
- Lynam, M. M. and G. J. Keeler (2005b). Automated speciated mercury measurements in Michigan. *Environmental Science & Technology* 39(23): 9253-9262.
- Lynam, M. M. and G. J. Keeler (2006). Source-receptor relationships for atmospheric mercury in urban Detroit, Michigan. *Atmospheric Environment* 40(17): 3144-3155.
- Manolopoulos, H., D. C. Snyder, J. J. Schauer, J. S. Hill, J. R. Turner, M. L. Olson and D. P. Krabbenhoft (2007a). Sources of speciated atmospheric mercury at a residential neighborhood impacted by industrial sources. *Environmental Science & Technology* 41(16): 5626-5633.
- Manolopoulos, H., J. J. Schauer, M. D. Purcell, T. M. Rudolph, M. L. Olson, B. Rodger and D. P. Krabbenhoft (2007b). Local and regional factors affecting atmospheric mercury speciation at a remote location. *Journal of Environmental Engineering and Science* 6(5): 491-501.
- Mason, R. P. and K. A. Sullivan (1997). Mercury in Lake Michigan. *Environmental Science & Technology* 31(3): 942-947.
- McQueen, J. T. and R. R. Draxler (1994). Evaluation of Model Back Trajectories of the Kuwait Oil Fires Smoke Plume Using Digital Satellite Data. *Atmospheric Environment* 28(13): 2159-2174.
- Miller, E. K., A. Vanarsdale, G. J. Keeler, A. Chalmers, L. Poissant, N. C. Kamman and R. Brulotte (2005). Estimation and mapping of wet and dry mercury deposition across northeastern North America. *Ecotoxicology* 14(1-2): 53-70.
- National Atmospheric Deposition Program (1996-2011). Mercury Deposition Network. NADP Program Office, Illinois State Water Survey, 2204 Griffith Dr., Champaign, IL 61820.
<http://nadp.sws.uiuc.edu/MDN/>
- NESCAUM (2008). *Sources of Mercury Deposition in the Northeast United States*. Northeast States for Coordinated Air Use Management. 75 pages. http://www.nescaum.org/documents/nescaum-sources-of-hg-depo-in-northeast_2008-final.pdf
- NOAA, Air Resources Laboratory (ARL) (2011a). Eta Data Assimilation System (EDAS40) Archive Information (<http://ready.arl.noaa.gov/edas40.php>). The archive can be accessed from: <http://ready.arl.noaa.gov/archives.php>
- NOAA, Air Resources Laboratory (ARL) (2011b). NCEP/NCAR Global Reanalysis Data Archive Information (http://ready.arl.noaa.gov/gbl_reanalysis.php). The archive can be accessed from: <http://ready.arl.noaa.gov/archives.php>
- Olmez, I., M. R. Ames and G. Gullu (1998). Canadian and US sources impacting the mercury levels in fine atmospheric particulate material across New York State. *Environmental Science & Technology* 32(20): 3048-3054.

- Pacyna, E. G., et al. (2010). Global emission of mercury to the atmosphere from anthropogenic sources in 2005 and projections to 2020. *Atmospheric Environment* 44(20): 2487-2499.
- Pai, P., P. Karamchandani and C. Seigneur (1997). Simulation of the regional atmospheric transport and fate of mercury using a comprehensive Eulerian model. *Atmospheric Environment* 31(17): 2717-2732.
- Pai, P., P. Karamchandani and C. Seigneur (2000). On artificial dilution of point source mercury emissions in a regional atmospheric model. *Science of the Total Environment* 259(1-3): 159-168.
- Pirrone, N., et al. (1998). Historical atmospheric mercury emissions and depositions in North America compared to mercury accumulations in sedimentary records. *Atmospheric Environment* 32(5): 929-940.
- Pirrone, N., G. Glinsorn and G. J. Keeler (1995a). Ambient Levels and Dry Deposition Fluxes of Mercury to Lakes Huron, Erie and St Clair. *Water Air and Soil Pollution* 80(1-4): 179-188.
- Pirrone, N., G. J. Keeler and T. M. Holsen (1995b). Dry Deposition of Trace-Elements to Lake-Michigan - a Hybrid-Receptor Deposition Modeling Approach. *Environmental Science & Technology* 29(8): 2112-2122.
- Pirrone, N., G. J. Keeler, J. O. Nriagu and P. O. Warner (1996). Historical trends of airborne trace metals in Detroit from 1971 to 1992. *Water Air and Soil Pollution* 88(1-2): 145-165.
- Poissant, L., B. Harvey and A. Casimir (1996). Application of a new telemetry and remote monitoring design for an automatic atmospheric vapour phase mercury analyser: Preliminary results. *Environmental Technology* 17(8): 891-896.
- Poissant, L. (1997). Field observations of total gaseous mercury behaviour: Interactions with ozone concentration and water vapour mixing ratio in air at a rural site. *Water Air and Soil Pollution* 97(3-4): 341-353.
- Poissant, L. and A. Casimir (1998). Water-air and soil-air exchange rate of total gaseous mercury measured at background sites. *Atmospheric Environment* 32(5): 883-893.
- Poissant, L. and M. Pilote (1998). Mercury concentrations in single event precipitation in southern Quebec. *Science of the Total Environment* 213(1-3): 65-72.
- Poissant, L. (1999). Potential sources of atmospheric total gaseous mercury in the St. Lawrence River valley. *Atmospheric Environment* 33(16): 2537-2547.
- Poissant, L. (2000). Total gaseous mercury in Quebec (Canada) in 1998. *Science of the Total Environment* 259(1-3): 191-201.
- Poissant, L., M. Pilote, C. Beauvais, P. Constant and H. H. Zhang (2005). A year of continuous measurements of three atmospheric mercury species (GEM, RGM and Hg-p) in southern Quebec, Canada. *Atmospheric Environment* 39(7): 1275-1287.

- Pongprueksa, P., C. J. Lin, S. E. Lindberg, C. Jang, T. Braverman, O. R. Bullock, T. C. Ho and H. W. Chu (2008). Scientific uncertainties in atmospheric mercury models III: Boundary and initial conditions, model grid resolution, and Hg(II) reduction mechanism. *Atmospheric Environment* 42(8): 1828-1845.
- Prestbo, E. M. and D. A. Gay (2009). Wet deposition of mercury in the US and Canada, 1996-2005: Results and analysis of the NADP mercury deposition network (MDN). *Atmospheric Environment* 43(27): 4223-4233.
- Risch, M.R., D.A. Gay, K.K. Fowler, G.J. Keeler, S.M. Backus, P. Blanchard, J.A. Barres, J.T. Dvonch (2011). Spatial Patterns and Temporal Trends in Mercury Concentrations, Precipitation Depths, and Mercury Wet Deposition in the North American Great Lakes Region, 2002-2008. *Environmental Pollution* (in press). doi:10.1016/j.envpol.2011.05.030
- Risch, M. R., E. M. Prestbo and L. Hawkins (2007). Measurement of atmospheric mercury species with manual sampling and analysis methods in a case study in Indiana. *Water Air and Soil Pollution* 184(1-4): 285-297.
- Rogers, E. (2011). Personal Communication. NOAA National Centers for Environmental Prediction (NCEP).
- Rolfhus, K. R., H. E. Sakamoto, L. B. Cleckner, R. W. Stoor, C. L. Babiarz, R. C. Back, H. Manolopoulos and J. P. Hurley (2003). Distribution and fluxes of total and methylmercury in Lake Superior. *Environmental Science & Technology* 37(5): 865-872.
- Rolph, G. D., R. R. Draxler, et al. (1992). Modeling Sulfur Concentrations and Depositions in the United-States During ANATEX. *Atmospheric Environment Part a-General Topics* 26(1): 73-93.
- Rolph, G. D., R. R. Draxler, et al. (1993). The Use of Model-Derived and Observed Precipitation in Long-Term Sulfur Concentration and Deposition Modeling. *Atmospheric Environment Part a-General Topics* 27(13): 2017-2037.
- Rolph, G. D., R. R. Draxler, et al. (2009). Description and Verification of the NOAA Smoke Forecasting System: The 2007 Fire Season. *Weather and Forecasting* 24(2): 361-378.
- Rossmann, R. (2010). Protocol to Reconstruct Historical Contaminant Loading to Large Lakes: The Lake Michigan Sediment Record of Mercury. *Environmental Science & Technology* 44(3): 935-940.
- Rutter, A. P., J. J. Schauer, G. C. Lough, D. C. Snyder, C. J. Kolb, S. Von Klooster, T. Rudolf, H. Manolopoulos and M. L. Olson (2008). A comparison of speciated atmospheric mercury at an urban center and an upwind rural location. *Journal of Environmental Monitoring* 10(1): 102-108.
- Ryaboshapko, A., R. Bullock, R. Ebinghaus, I. Ilyin, K. Lohman, J. Munthe, G. Petersen, C. Seigneur and I. Wangberg (2002). Comparison of mercury chemistry models. *Atmospheric Environment* 36(24): 3881-3898.

- Ryaboshapko, A., O. R. Bullock, et al. (2007a). Intercomparison study of atmospheric mercury models: 1. Comparison of models with short-term measurements. *Science of the Total Environment* 376(1-3): 228-240.
- Ryaboshapko, A., O. R. Bullock, et al. (2007b). Intercomparison study of atmospheric mercury models: 2. Modelling results vs. long-term observations and comparison of country deposition budgets. *Science of the Total Environment* 377(2-3): 319-333.
- Schaum, J., M. Cohen, et al. (2010). Screening Level Assessment of Risks Due to Dioxin Emissions from Burning Oil from the BP Deepwater Horizon Gulf of Mexico Spill. *Environmental Science & Technology* 44(24): 9383-9389.
- Schroeder, W. H., G. Keeler, H. Kock, P. Roussel, D. Schneeberger and F. Schaedlich (1995). International Field Intercomparison of Atmospheric Mercury Measurement Methods. *Water Air and Soil Pollution* 80(1-4): 611-620.
- Seigneur, C., P. Karamchandani, K. Lohman, K. Vijayaraghavan and R. L. Shia (2001). Multiscale modeling of the atmospheric fate and transport of mercury. *Journal of Geophysical Research-Atmospheres* 106(D21): 27795-27809.
- Seigneur, C., K. Lohman, K. Vijayaraghavan and R. L. Shia (2003). Contributions of global and regional sources to mercury deposition in New York State. *Environmental Pollution* 123(3): 365-373.
- Seigneur, C., K. Vijayaraghavan, K. Lohman, P. Karamchandani and C. Scott (2004a). Global source attribution for mercury deposition in the United States. *Environmental Science & Technology* 38(2): 555-569.
- Seigneur, C., K. Vijayaraghavan, K. Lohman, P. Karamchandani and C. Scott (2004b). Modeling the atmospheric fate and transport of mercury over North America: power plant emission scenarios. *Fuel Processing Technology* 85(6-7): 441-450.
- Seigneur, C., Vijayaraghavan, K., Lohman, K. (2006). Atmospheric mercury chemistry: Sensitivity of global model simulations to chemical reactions. *Journal of Geophysical Research* 111, D22306, doi:10.1029/2005JD006780.
- Seigneur, C. and K. Lohman (2008). Effect of bromine chemistry on the atmospheric mercury cycle. *Journal of Geophysical Research-Atmospheres* 113(D23).
- Selin, N., Jacob, D., Park, R., Yantosca, R., Strode, S., Jaegle, L., Jaffe, D. (2007). Chemical cycling and deposition of atmospheric mercury: Global constraints from observations. *Journal of Geophysical Research* 112, D02308, doi:10.1029/2006JD007450.

- Selin, N., Jacob, D., Park, R., Yantosca, R., Strode, S., Jaegle, L., and Sunderland, E. (2008). Global 3-D Land-Ocean-Atmosphere Model for Mercury: Present-Day versus Preindustrial Cycles and Anthropogenic Enrichment Factors. *Global Biogeochemical Cycles* 22: GB2011, doi: 10.1029/2007/GB003040.
- Selin, N. E. and D. J. Jacob (2008). Seasonal and spatial patterns of mercury wet deposition in the United States: Constraints on the contribution from North American anthropogenic sources. *Atmospheric Environment* 42(21): 5193-5204.
- Shannon, J.D. and E.C. Voldner (1995). Modeling atmospheric concentrations of mercury and deposition to the Great Lakes. *Atmospheric Environment* 29, 1649-1661.
- Sherman, L.S., J.D. Blum, G.J. Keeler, J.D. Demers, and J.T. Dvonch (2011). Investigation of local mercury deposition from a coal-fired power plant using mercury isotopes. *Environ. Sci. Technol.*, Just Accepted Manuscript, DOI: 10.1021/es202793c, Publication Date (Web): 21 Nov 2011.
- Sherwell, J., M. Garrison, A. Yegnan, A. Baines (2006). Application of the CALPUFF Modeling System for Mercury Assessments in Maryland. In *Proceedings 99th Annual Meeting of the Air and Waste Management Association*, Paper No. 429, Air and Waste Management Association, Pittsburgh, PA.
- Sherwell, J., T. Rule, and M. Garrison (2010). Linking Air Emissions and Water Quality: Mercury TMDLs in Maryland. Poster presented at *National Atmospheric Deposition Program (NADP) 2010: Networking the Networks*. Lake Tahoe, CA, October 19-21, 2010.
- Shia, R. L., C. Seigneur, P. Pai, M. Ko and N. D. Sze (1999). Global simulation of atmospheric mercury concentrations and deposition fluxes. *Journal of Geophysical Research-Atmospheres* 104(D19): 23747-23760.
- Sillman, S., F. J. Marsik, K. I. Al-Wali, G. J. Keeler and M. S. Landis (2007). Reactive mercury in the troposphere: Model formation and results for Florida, the northeastern United States, and the Atlantic Ocean. *Journal of Geophysical Research-Atmospheres* 112(D23).
- Smith-Downey, N., Sunderland, E., and Jacob, D. (2010). Anthropogenic impacts on global storage and emissions of mercury from terrestrial soils: Insights from a new global model. *Journal of Geophysical Research* 115: G03008, doi: 10.1029/2009JG001124
- Sorensen, J. A., G. E. Glass and K. W. Schmidt (1994). Regional Patterns of Wet Mercury Deposition. *Environmental Science & Technology* 28(12): 2025-2032.
- Stein, A. F., D. Lamb, et al. (2000). Incorporation of Detailed Chemistry into a Three-Dimensional Lagrangian-Eulerian Hybrid Model: Application to Regional Tropospheric Ozone. *Atmospheric Environment* 34(25): 4361-4372.

- Streets, D.G., Devane, M.K., Lu, Z., Bond, T.C., Sunderland, E.M., Jacob, D. (2011). All-Time Releases of Mercury to the Atmosphere from Human Activities. *Environmental Science and Technology* 45(24): 10485-10491.
- Strode, S. A., L. Jaegle, N. E. Selin, D. J. Jacob, R. J. Park, R. M. Yantosca, R. P. Mason and F. Slemr (2007). Air-sea exchange in the global mercury cycle. *Global Biogeochemical Cycles* 21(1).
- Strode, S., L. Jaegle and N. E. Selin (2009). Impact of mercury emissions from historic gold and silver mining: Global modeling. *Atmospheric Environment* 43(12): 2012-2017.
- Stunder, B. J. B., J. L. Heffter, et al. (2007). Airborne volcanic ash forecast area reliability. *Weather and Forecasting* 22(5): 1132-1139.
- Subir, M., P. A. Ariya and A. P. Dastoor (2011). A review of uncertainties in atmospheric modeling of mercury chemistry I. Uncertainties in existing kinetic parameters - Fundamental limitations and the importance of heterogeneous chemistry. *Atmospheric Environment* 45(32): 5664-5676.
- Subir, M., P. A. Ariya and A. P. Dastoor (2012). A review of the sources of uncertainties in atmospheric mercury modeling II. Mercury surface and heterogeneous chemistry -- A missing link. *Atmospheric Environment* 46: 1-10.
- Temme, C., P. Blanchard, A. Steffen, C. Banic, S. Beauchamp, L. Poissant, R. Tordon and B. Wiens (2007). Trend, seasonal and multivariate analysis study of total gaseous mercury data from the Canadian atmospheric mercury measurement network (CAMNet). *Atmospheric Environment* 41(26): 5423-5441.
- Travnikov, O. (2005). Contribution of the intercontinental atmospheric transport to mercury pollution in the Northern Hemisphere. *Atmospheric Environment* 39(39): 7541-7548.
- U.S. EPA (2006). Documentation for the Final 2002 Nonpoint Sector (Feb 06 Version) National Emission Inventory for Criteria and Hazardous Air Pollutants. Emissions Inventory and Analysis Group (C339-02), Air Quality Assessment Division, Office of Air Quality Planning and Standards, U.S. Environmental Protection Agency, Research Triangle Park, NC.
- U.S. EPA (2007). Documentation for the Final 2002 Mobile National Emissions Inventory, Version 3. Emissions Inventory Group (D205-01), Emissions, Monitoring and Analysis Division, Office of Air Quality Planning and Standards, U.S. Environmental Protection Agency, Research Triangle Park, NC.
- U.S. EPA (2008a). *Model-Based Analysis And Tracking Of Airborne Mercury Emissions To Assist in Watershed Planning*. Watershed Branch (4503-T), Office of Wetlands, Oceans, and Watersheds, Washington, DC. 350 pages. Available at: <http://www.epa.gov/owow/tmdl/techsupp.html>
- U.S. EPA (2008b). Documentation for the 2005 Point Source National Emissions Inventory. Emission Inventory and Analysis Group, Emissions, Monitoring and Analysis Division, Research Triangle Park, NC.

- Van Arsdale, A., J. Weiss, G. Keeler, E. Miller, G. Boulet, R. Brulotte and L. Poissant (2005). Patterns of mercury deposition and concentration in northeastern North America (1996-2002). *Ecotoxicology* 14(1-2): 37-52.
- Vette, A. F., M. S. Landis and G. J. Keeler (2002). Deposition and emission of gaseous mercury to and from Lake Michigan during the Lake Michigan Mass Balance Study (July, 1994 October, 1995). *Environmental Science & Technology* 36(21): 4525-4532.
- Vijayaraghavan, K., C. Seigneur, K. Lohman, S.Y. Chen, and P. Karamchandani (2004). *Modeling Deposition of Atmospheric Mercury in Michigan and the Great Lakes Region*. Atmospheric & Environmental Research, Inc., San Ramon, CA. Prepared for EPRI, Palo Alto, California. Document # CP184-04-02. 42 pages.
- Vijayaraghavan, K., C. Seigneur, P. Karamchandani and S. Y. Chen (2007). Development and application of a multipollutant model for atmospheric mercury deposition. *Journal of Applied Meteorology and Climatology* 46(9): 1341-1353.
- Vijayaraghavan, K., P. Karamchandani, C. Seigneur, R. Balmori and S. Y. Chen (2008). Plume-in-grid modeling of atmospheric mercury. *Journal of Geophysical Research-Atmospheres* **113**. Article D24305. DOI: 10.1029/2008JD010580.
- Wang, Y. G., J. Y. Huang, T. J. Zananski, P. K. Hopke and T. M. Holsen (2010). Impacts of the Canadian Forest Fires on Atmospheric Mercury and Carbonaceous Particles in Northern New York. *Environmental Science & Technology* 44(22): 8435-8440.
- Wang, Y. Q., A. F. Stein, et al. (2011). Global Sand and Dust Storms in 2008: Observation and HYSPLIT Model Verification. *Atmospheric Environment* 45(35): 6368-6381.
- Wen, D., J. C. Lin, F. Meng, P. K. Gbor, Z. He and J. J. Sloan (2011). Quantitative assessment of upstream source influences on total gaseous mercury observations in Ontario, Canada. *Atmospheric Chemistry and Physics* 11(4): 1405-1415.
- White, E. M., G. J. Keeler and M. S. Landis (2009). Spatial Variability of Mercury Wet Deposition in Eastern Ohio: Summertime Meteorological Case Study Analysis of Local Source Influences. *Environmental Science & Technology* 43(13): 4946-4953.
- Wilson, S., et al. (2010). Updating Historical Global Inventories of Anthropogenic Mercury Emissions to Air. AMAP Technical Report No. 3 (2010). Arctic Monitoring and Assessment Programme (AMAP), Oslo, Norway. (available as an electronic document from www.amap.no).
- Xu, X. H., X. S. Yang, D. R. Miller, J. J. Helble and R. J. Carley (2000a). A regional scale modeling study of atmospheric transport and transformation of mercury. I. Model development and evaluation. *Atmospheric Environment* 34(28): 4933-4944.
- Xu, X. H., X. S. Yang, D. R. Miller, J. J. Helble and R. J. Carley (2000). A regional scale modeling study of atmospheric transport and transformation of mercury. II. Simulation results for the northeast United States. *Atmospheric Environment* 34(28): 4945-4955.

- Xu, X. H., Y. S. Yang, D. R. Miller, J. J. Helble, H. Thomas and R. J. Carley (2000c). A sensitivity analysis on the atmospheric transformation and deposition of mercury in north-eastern USA. *Science of the Total Environment* 259(1-3): 169-181.
- Xu, X. and U. S. Akhtar (2010). Identification of potential regional sources of atmospheric total gaseous mercury in Windsor, Ontario, Canada using hybrid receptor modeling. *Atmospheric Chemistry and Physics* 10(15): 7073-7083.
- Yatavelli, R. L. N., J. K. Fahrni, M. Kim, K. C. Crist, C. D. Vickers, S. E. Winter and D. P. Connell (2006). Mercury, PM_{2.5} and gaseous co-pollutants in the Ohio River Valley region: Preliminary results from the Athens supersite. *Atmospheric Environment* 40(34): 6650-6665.
- Zeng, Y. and P. K. Hopke (1989). A Study of the Sources of Acid Precipitation in Ontario, Canada. *Atmospheric Environment* 23(7): 1499-1509.

8. Appendices

In the main body of the report, the geographical distribution of mercury deposition contributions to Lake Erie from direct anthropogenic sources and all sources are shown, both for a 2x2 degree global grid and a 1x1 degree grid over central North America.

In the following appendices, a full set of the maps are given, for each Great Lake and for each of the Great Lake's watersheds.

Appendix 1: Atmospheric deposition contribution maps for each Great Lake for direct anthropogenic mercury emissions displayed on a 2x2 degree global grid

Appendix 2: Atmospheric deposition contribution maps for each Great Lake's Watershed for direct anthropogenic mercury emissions displayed on a 2x2 degree global grid

Appendix 3: Atmospheric deposition contribution maps for each Great Lake for direct anthropogenic mercury emissions displayed on a 1x1 degree grid over a North American domain

Appendix 4: Atmospheric deposition contribution maps for each Great Lake's Watershed for direct anthropogenic mercury emissions displayed on a 1x1 degree over a North American domain

Appendix 5: Atmospheric deposition contribution maps for each Great Lake for total atmospheric mercury emissions displayed on a 2x2 degree global grid

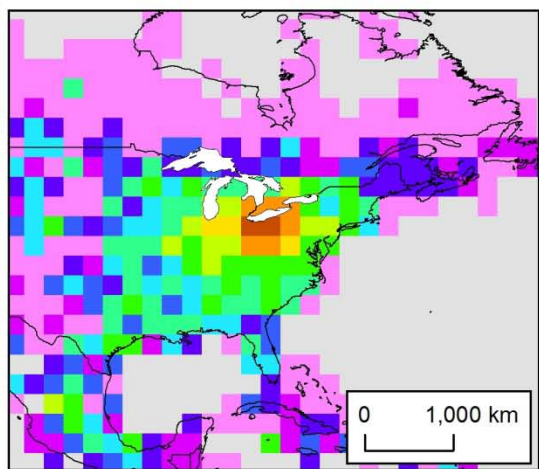
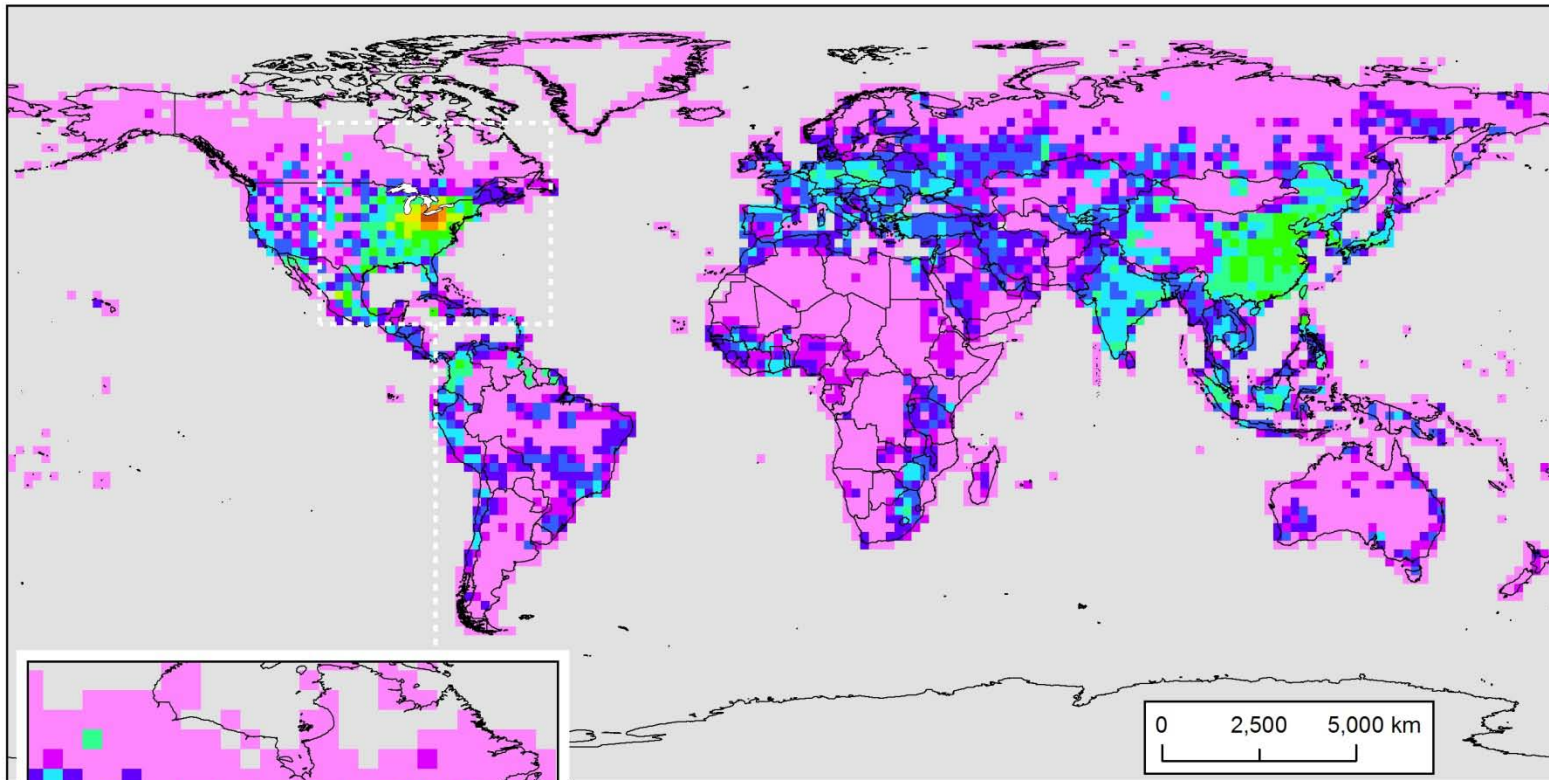
Appendix 6: Atmospheric deposition contribution maps for each Great Lake's Watershed for total atmospheric mercury emissions displayed on a 2x2 degree global grid

Appendix 7: Atmospheric deposition contribution maps for each Great Lake for total atmospheric mercury emissions displayed on a 1x1 degree grid over a North American domain

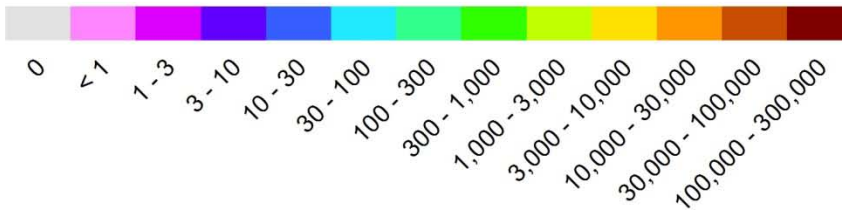
Appendix 8: Atmospheric deposition contribution maps for each Great Lake's Watershed for total atmospheric mercury emissions displayed on a 1x1 degree grid over a North American domain

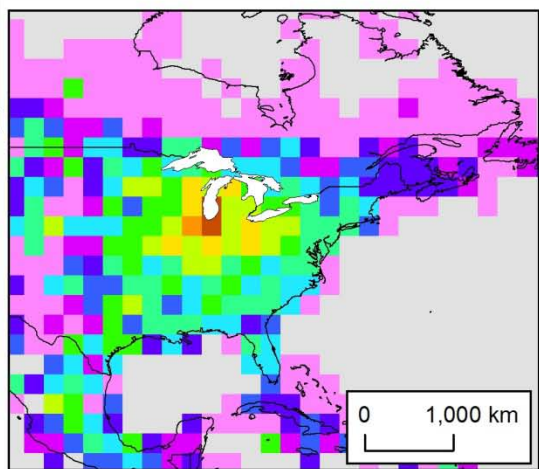
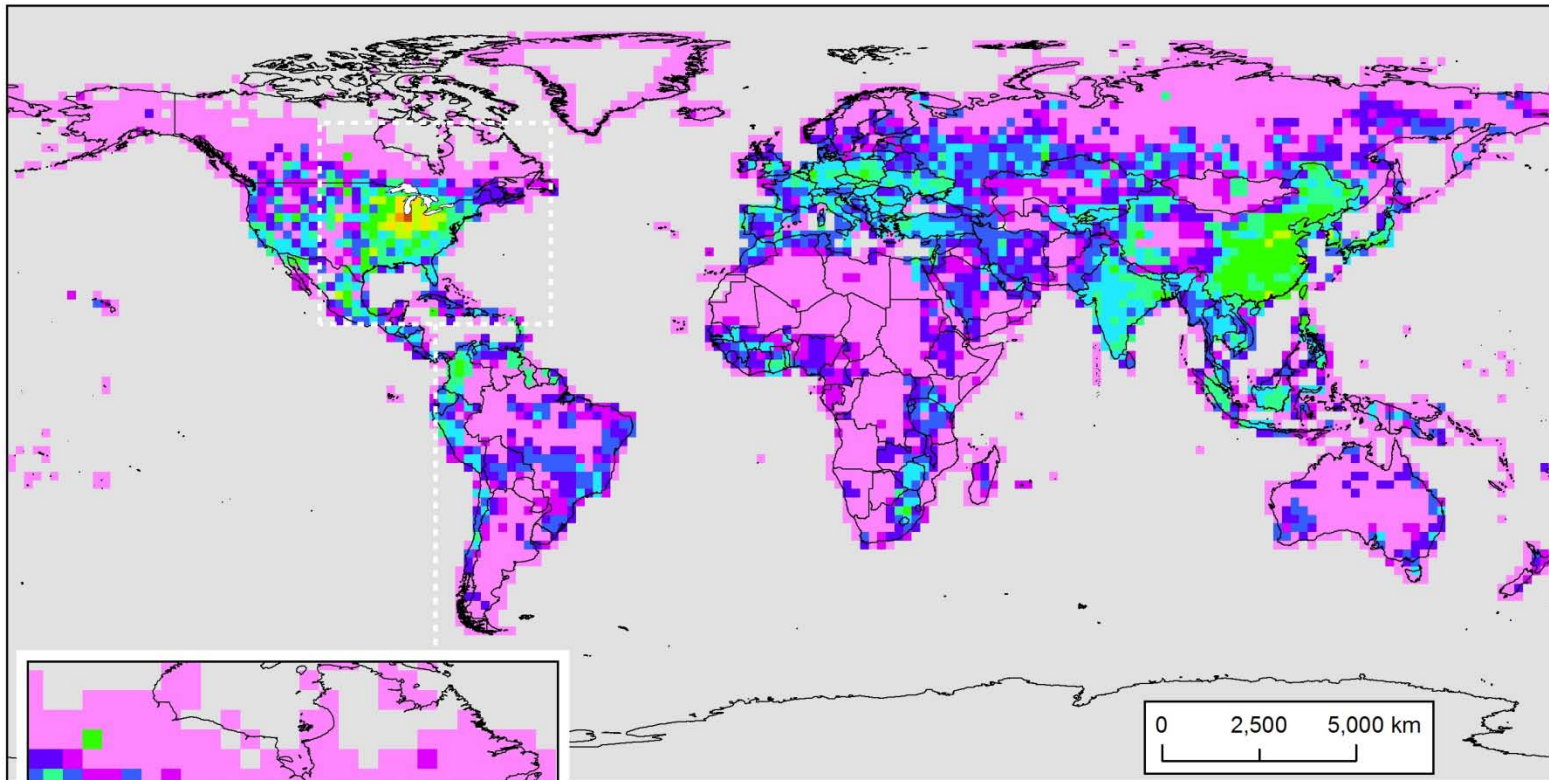
In addition, **Appendix 9** contains a set of graphs showing mercury emissions as a function of distance from each of the Great Lakes and their watersheds.

Appendix 1. Atmospheric deposition contribution maps for each Great Lake for direct anthropogenic mercury emissions displayed on a 2x2 degree global grid

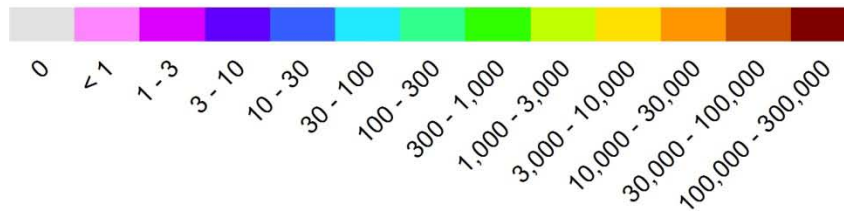


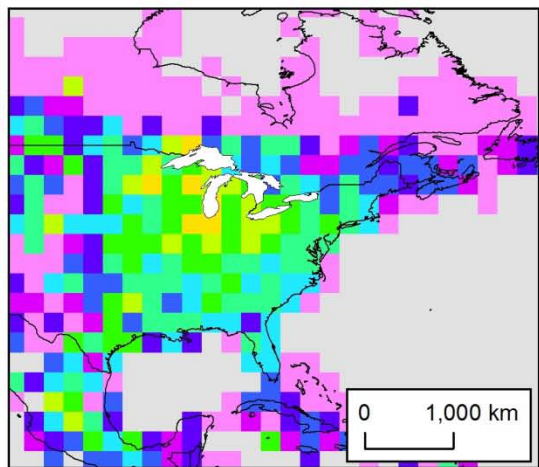
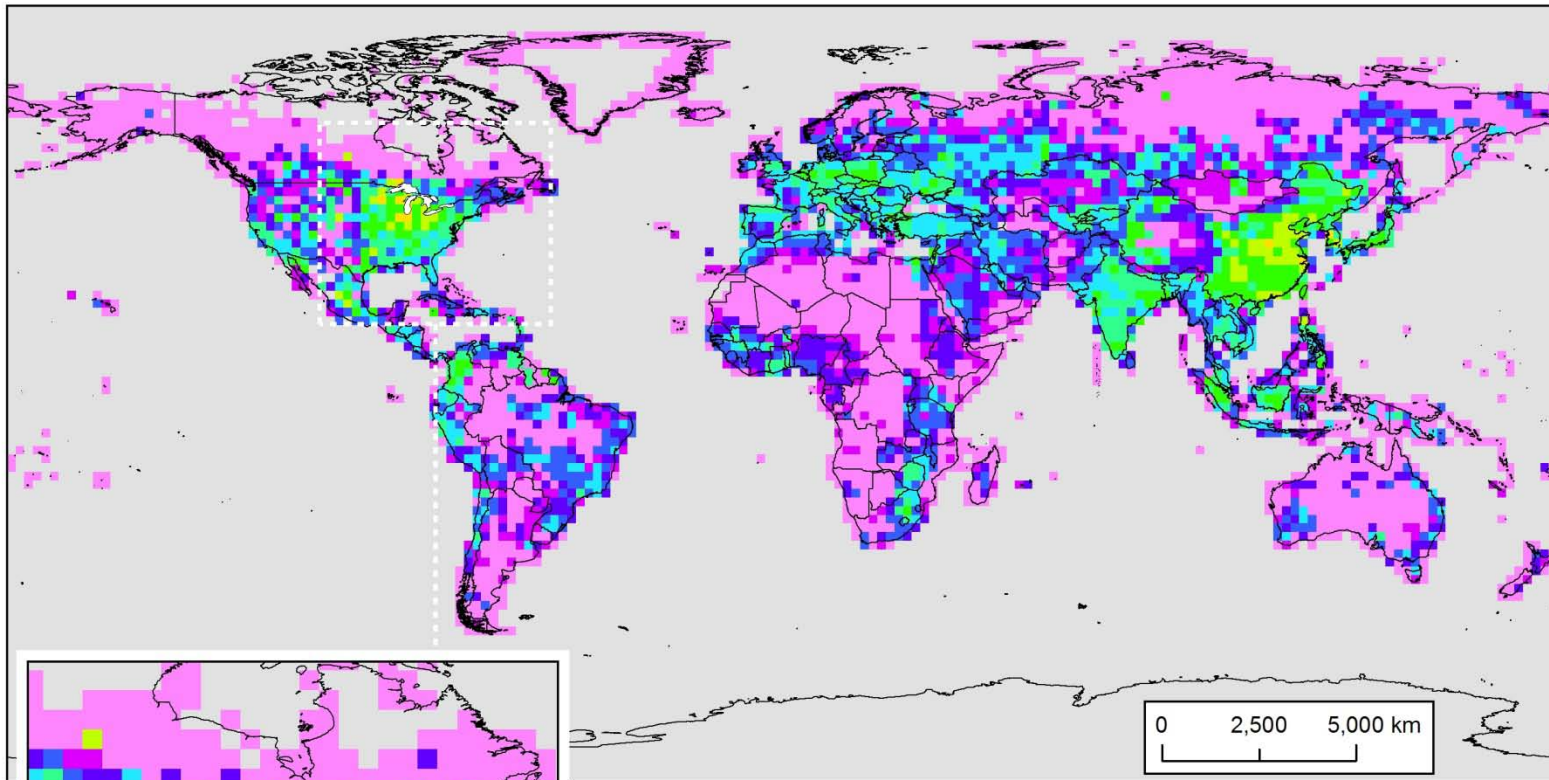
**Atmospheric mercury deposition contribution (g/yr)
to Lake Erie from direct anthropogenic emissions
in each 2x2 degree grid cell**



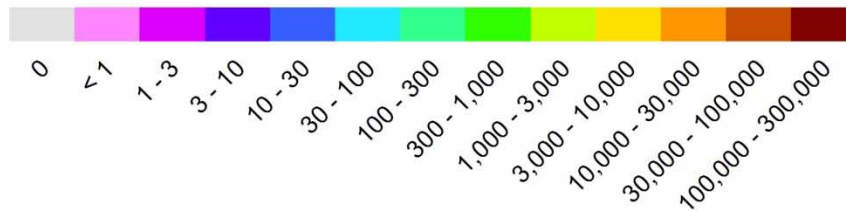


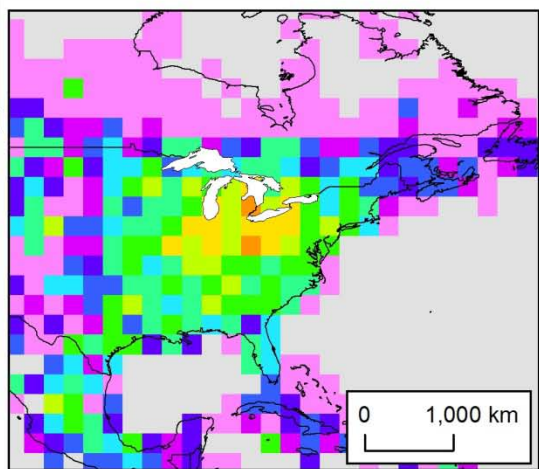
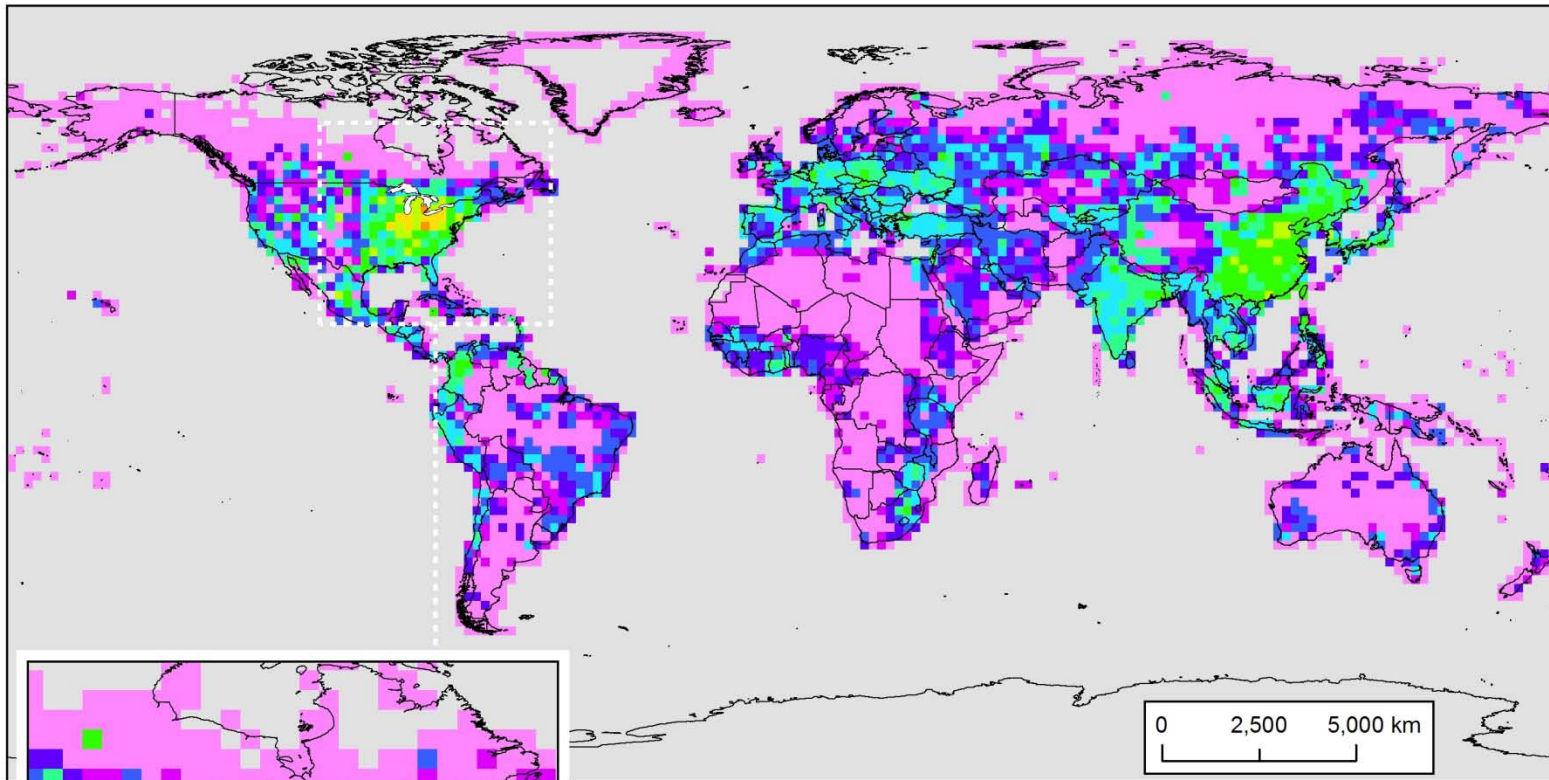
**Atmospheric mercury deposition contribution (g/yr)
to Lake Michigan from direct anthropogenic emissions
in each 2x2 degree grid cell**



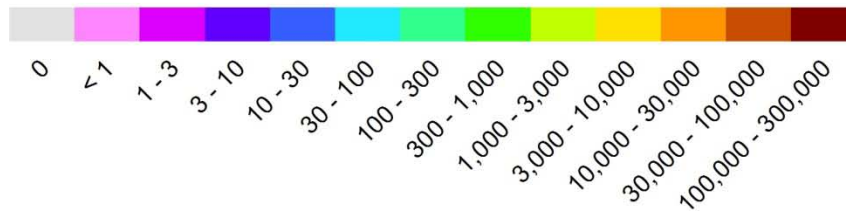


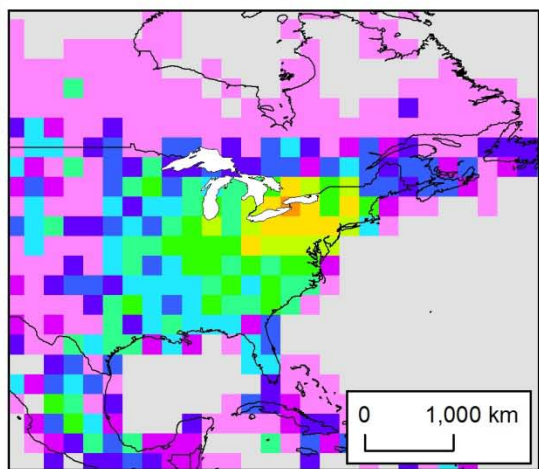
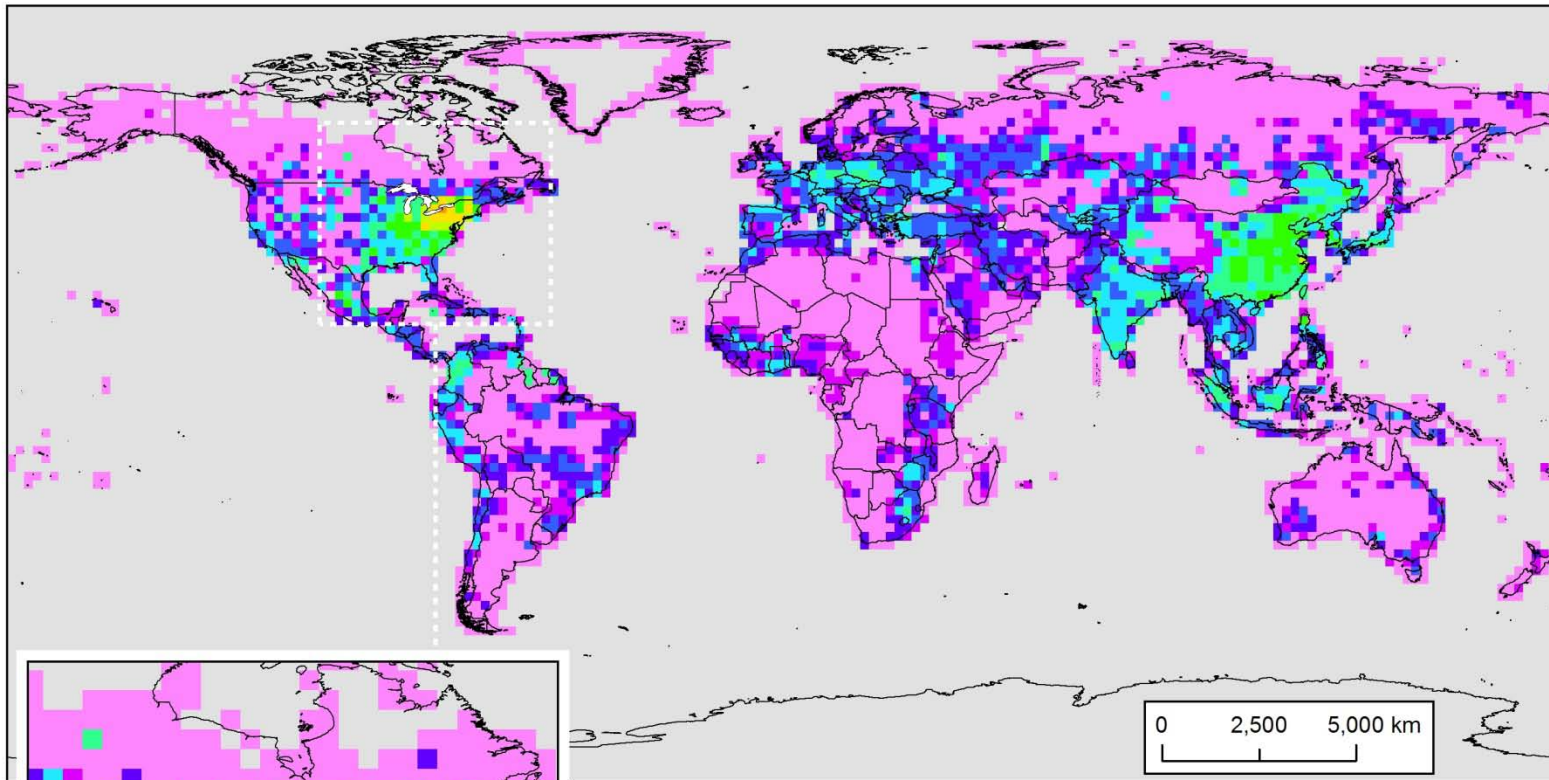
**Atmospheric mercury deposition contribution (g/yr)
to Lake Superior from direct anthropogenic emissions
in each 2x2 degree grid cell**



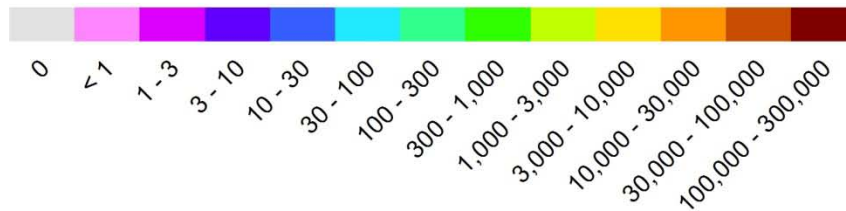


**Atmospheric mercury deposition contribution (g/yr)
to Lake Huron from direct anthropogenic emissions
in each 2x2 degree grid cell**

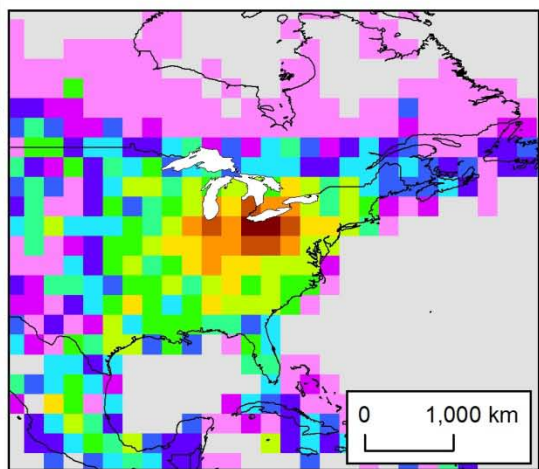
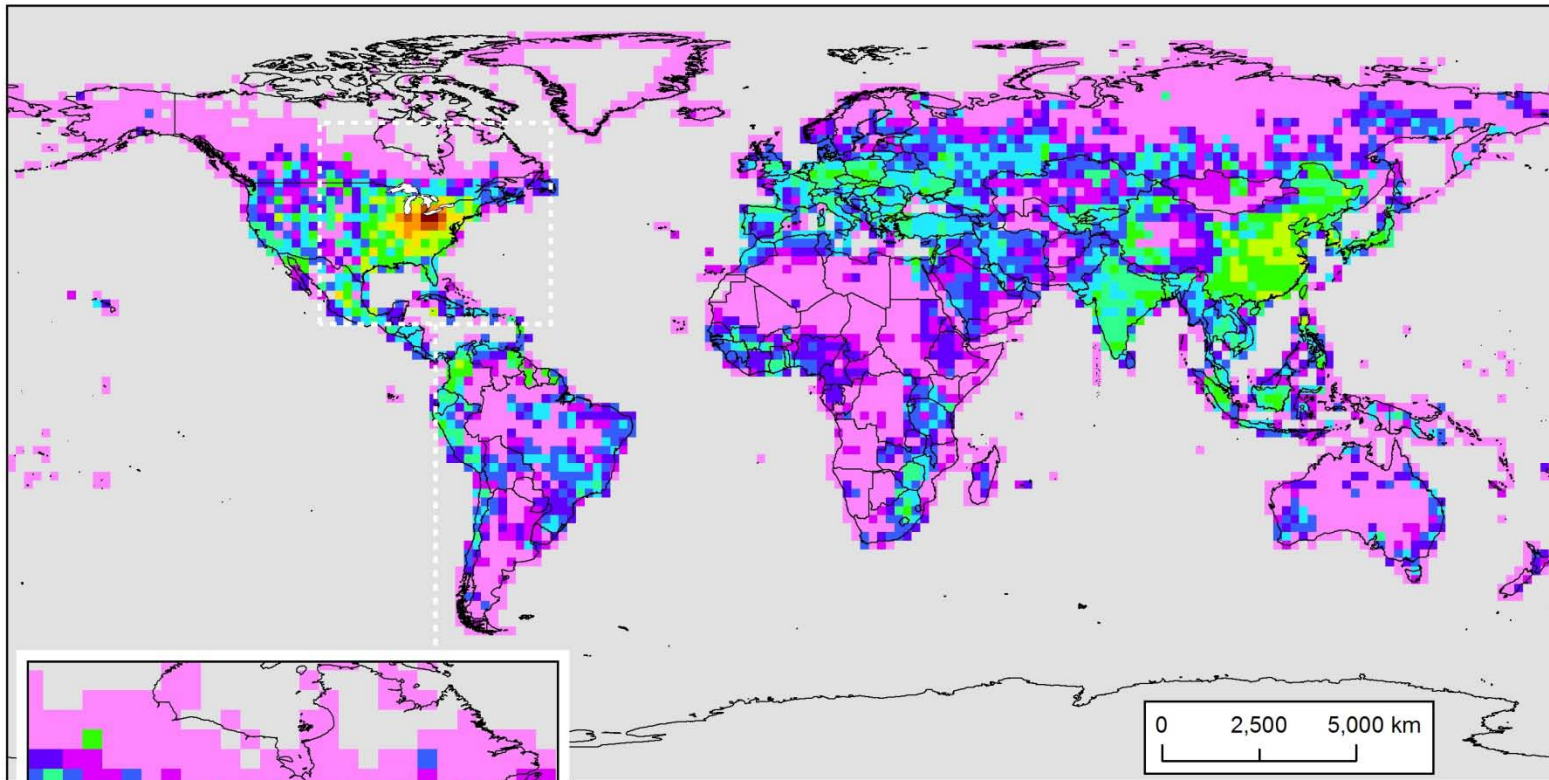




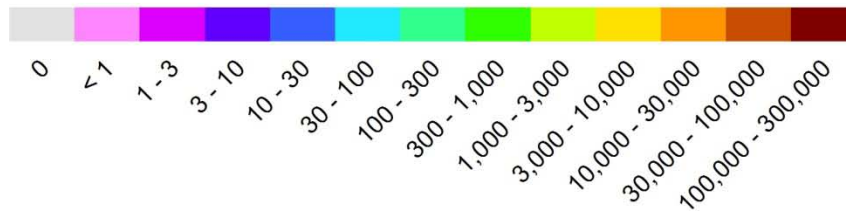
**Atmospheric mercury deposition contribution (g/yr)
to Lake Ontario from direct anthropogenic emissions
in each 2x2 degree grid cell**

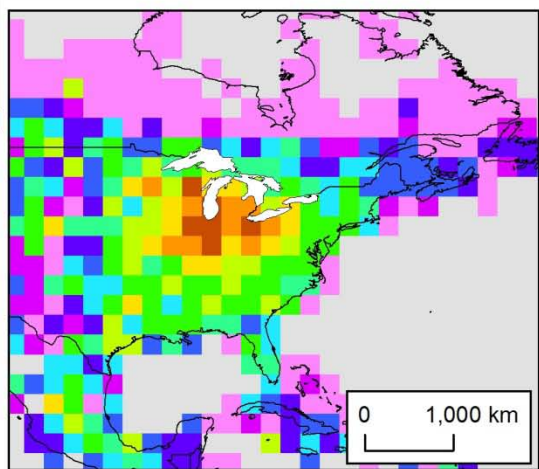
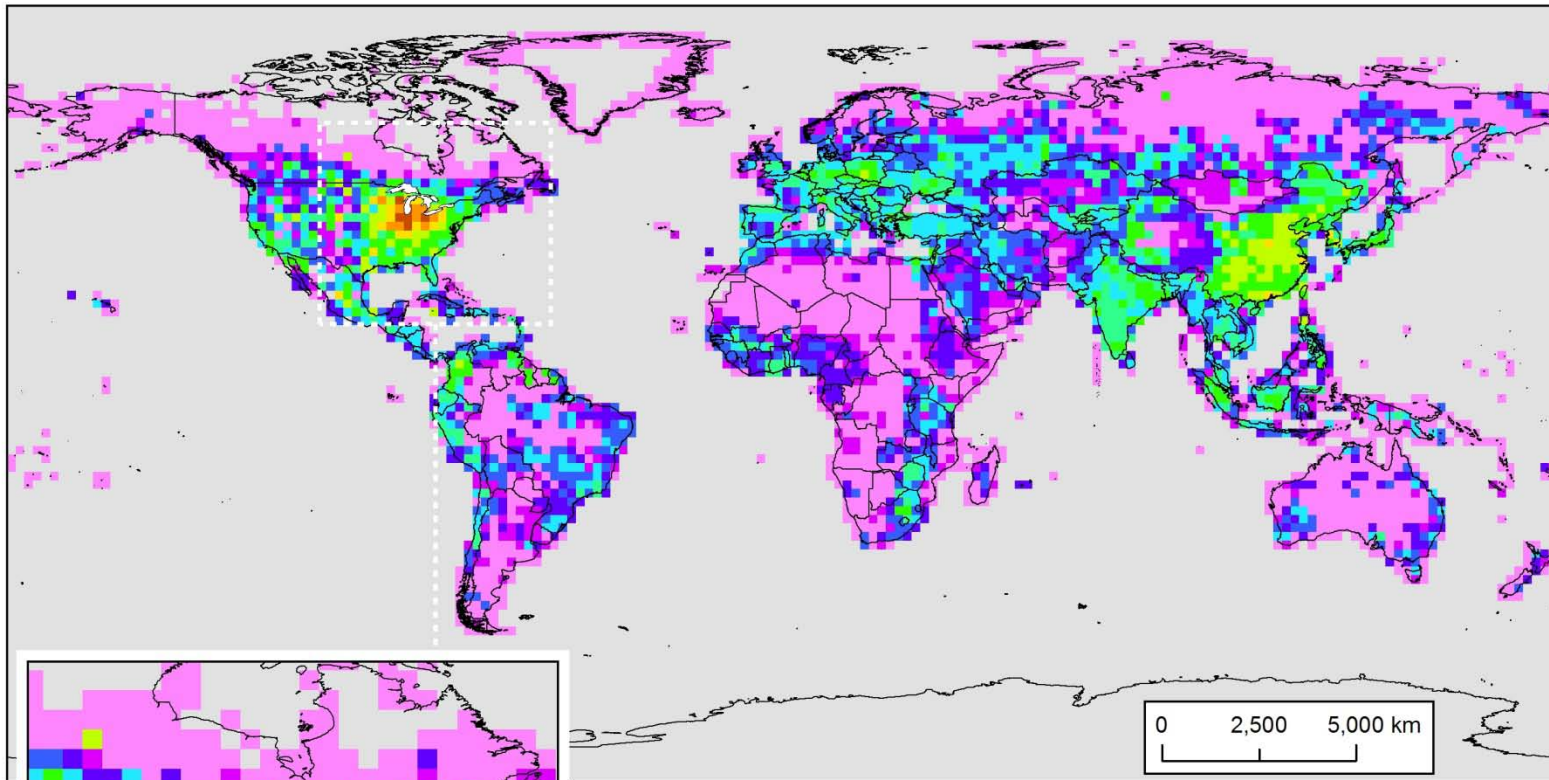


Appendix 2. Atmospheric deposition contribution maps for each Great Lake's Watershed for direct anthropogenic mercury emissions displayed on a 2x2 degree global grid

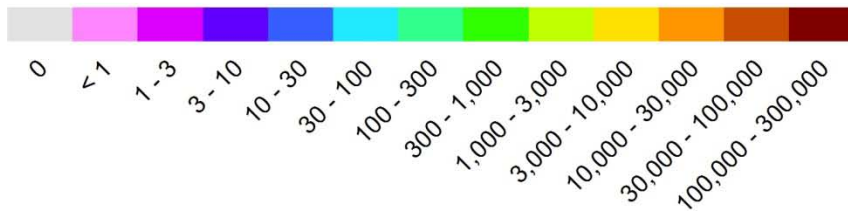


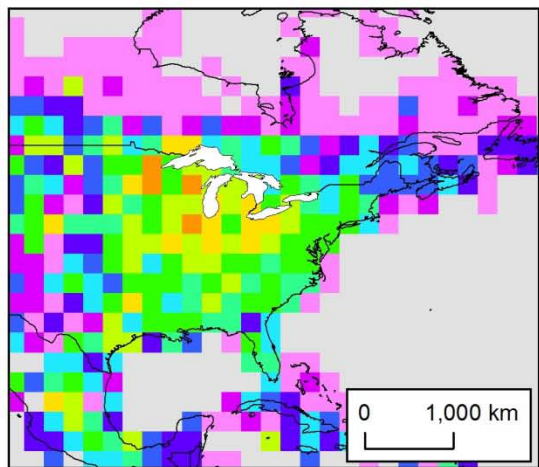
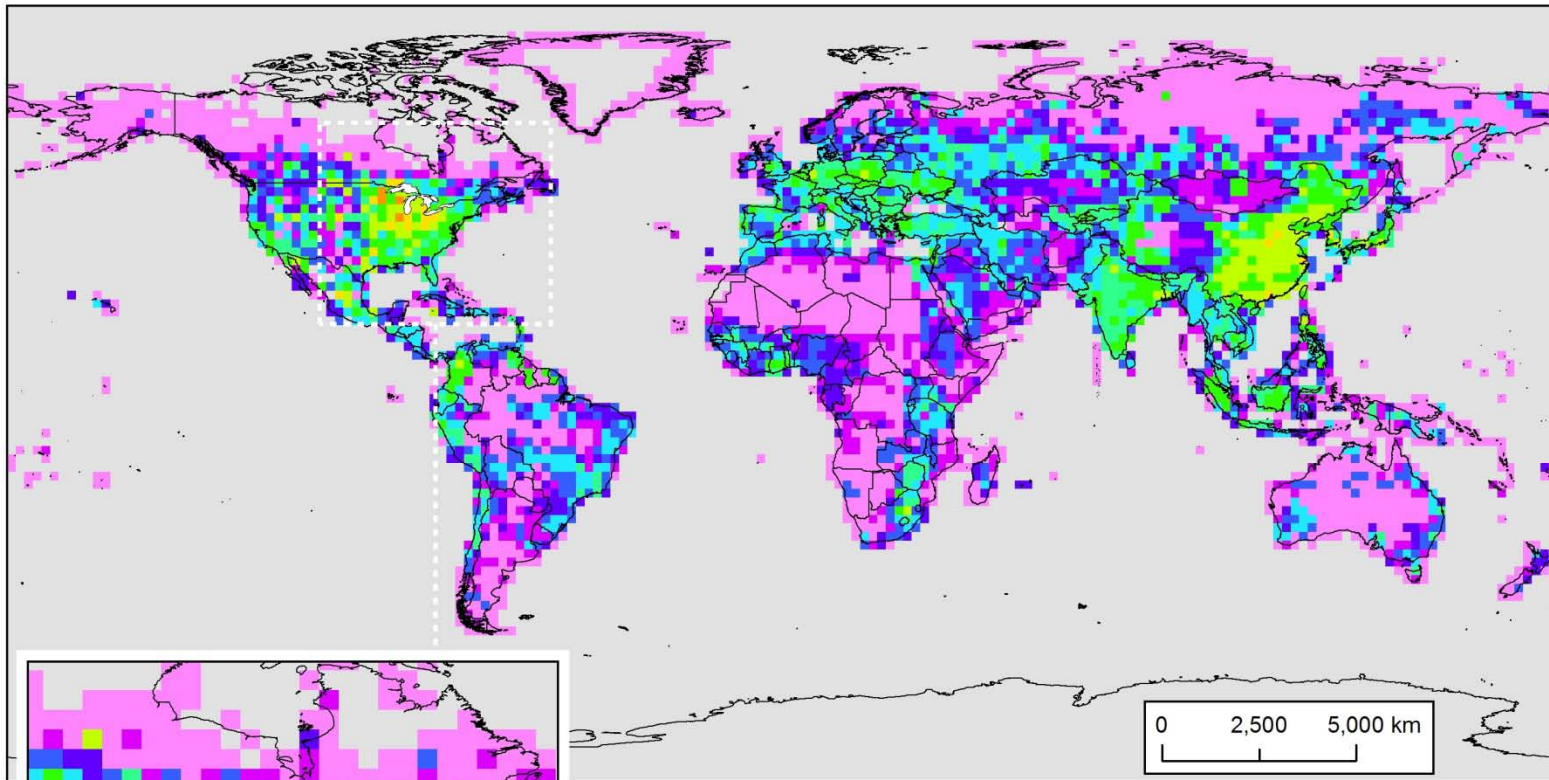
**Atmospheric mercury deposition contribution (g/yr)
to the Lake Erie Watershed from direct anthropogenic
emissions in each 2x2 degree grid cell**



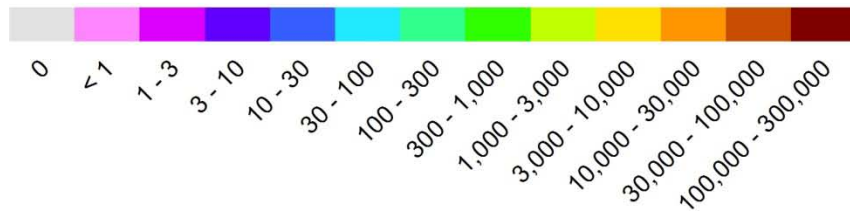


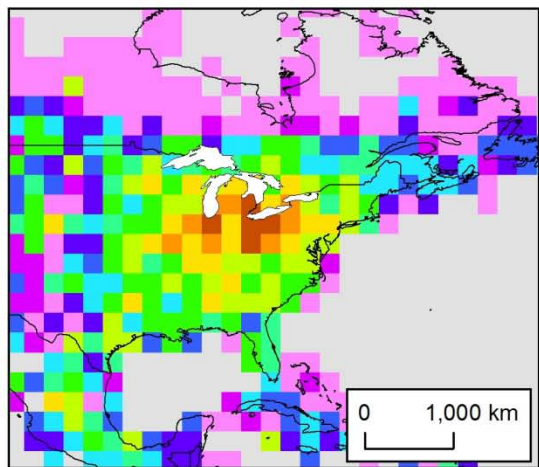
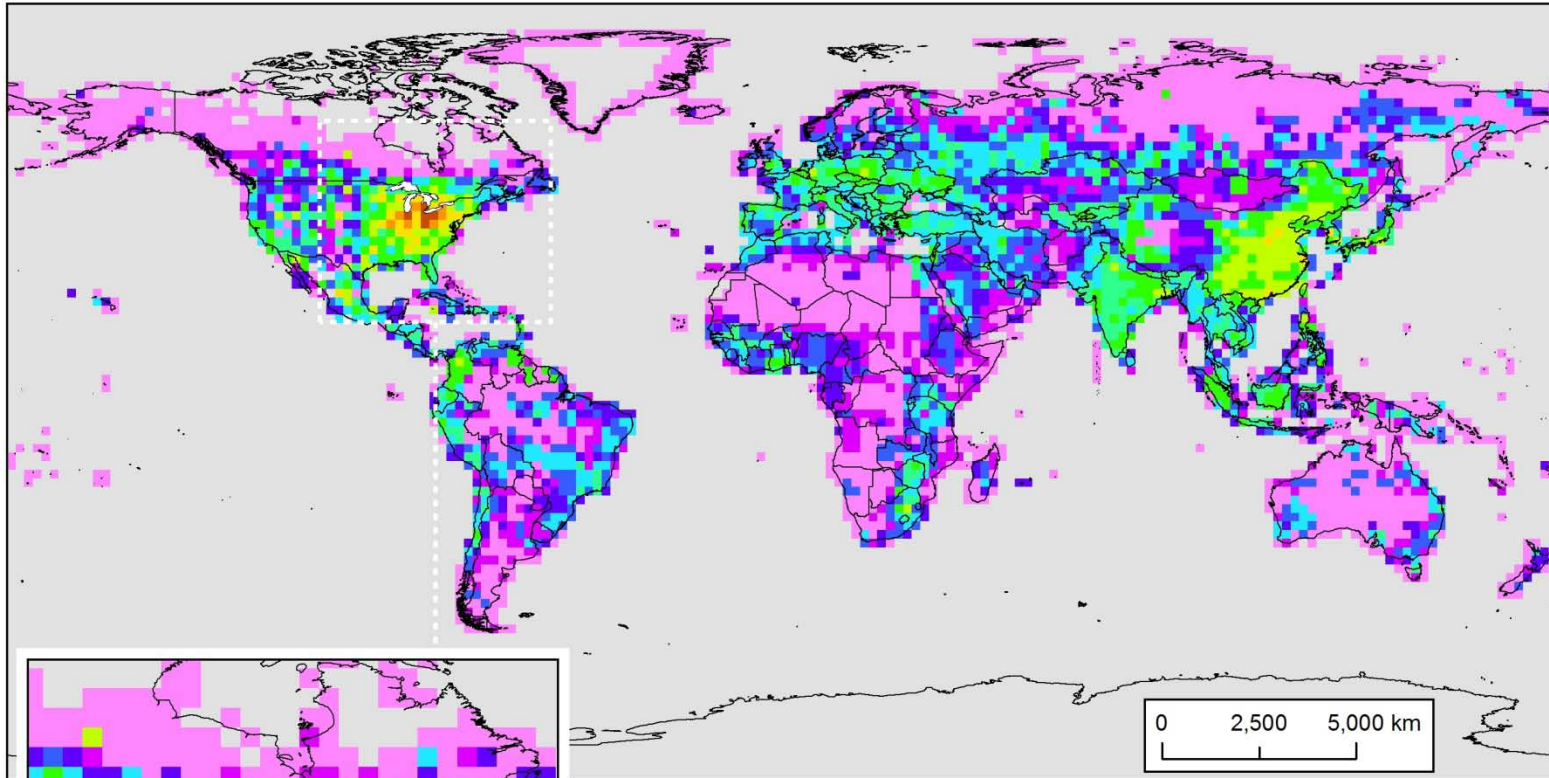
**Atmospheric mercury deposition contribution (g/yr)
to the Lake Michigan Watershed from direct anthropogenic
emissions in each 2x2 degree grid cell**



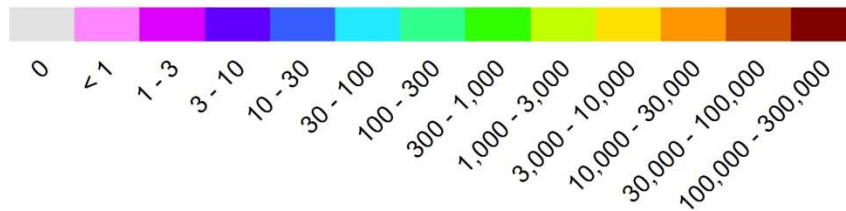


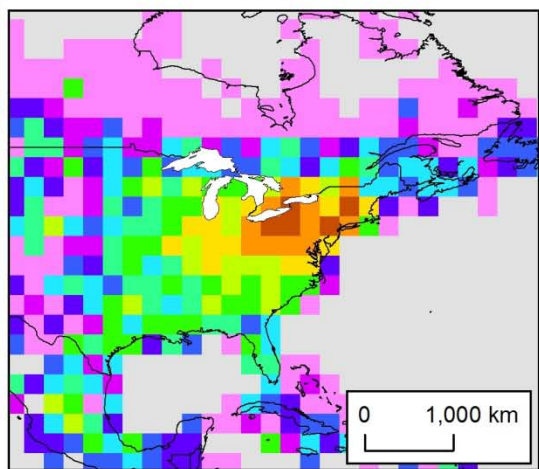
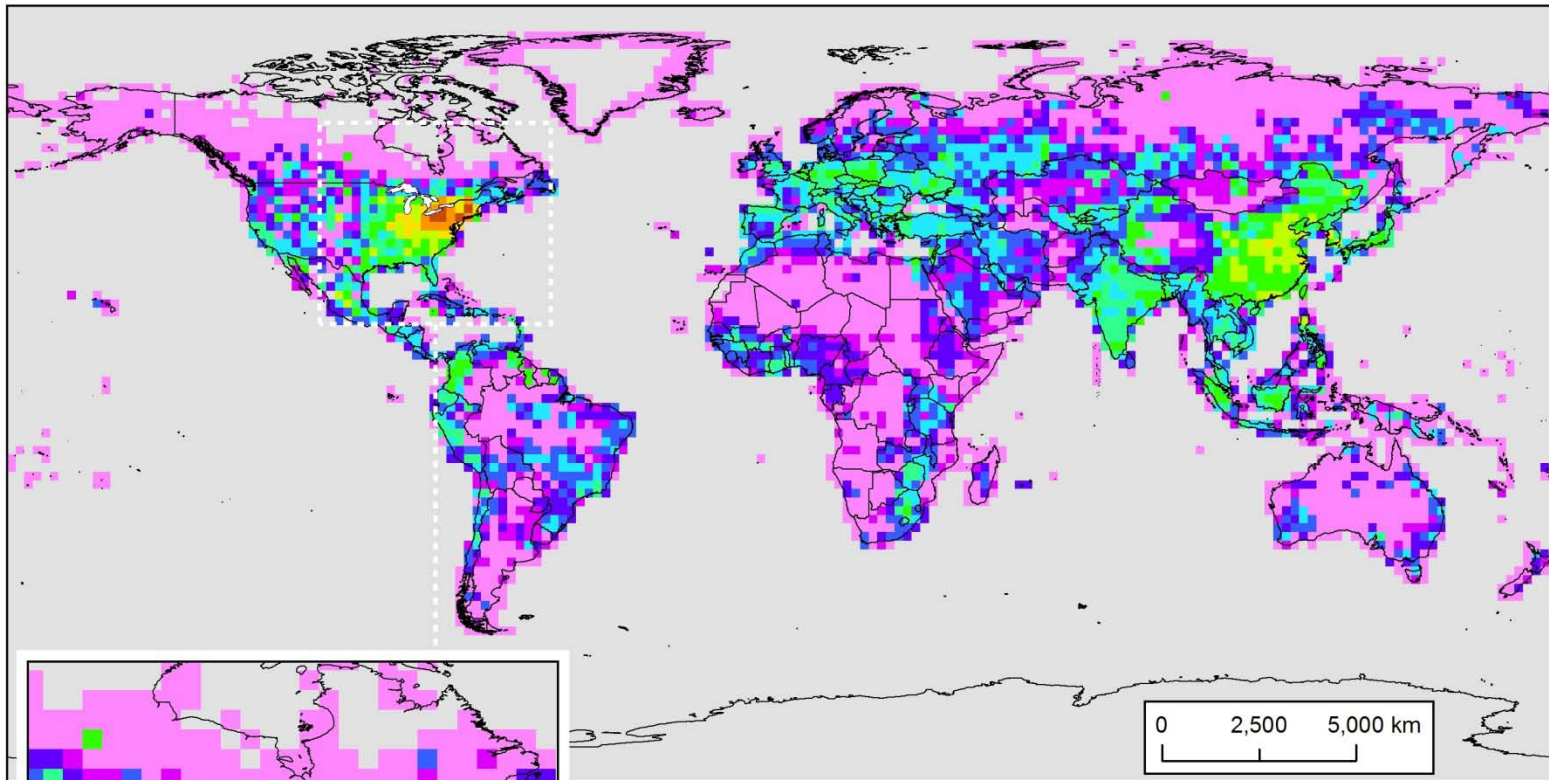
**Atmospheric mercury deposition contribution (g/yr)
to the Lake Superior Watershed from direct anthropogenic
emissions in each 2x2 degree grid cell**



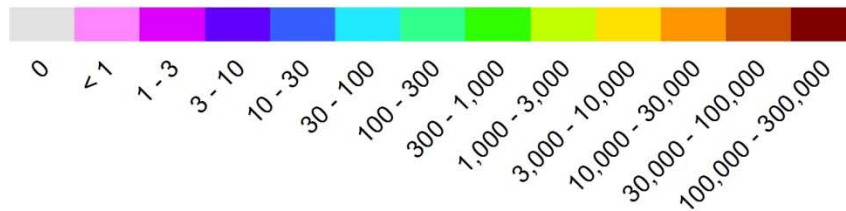


**Atmospheric mercury deposition contribution (g/yr)
to the Lake Huron Watershed from direct anthropogenic
emissions in each 2x2 degree grid cell**

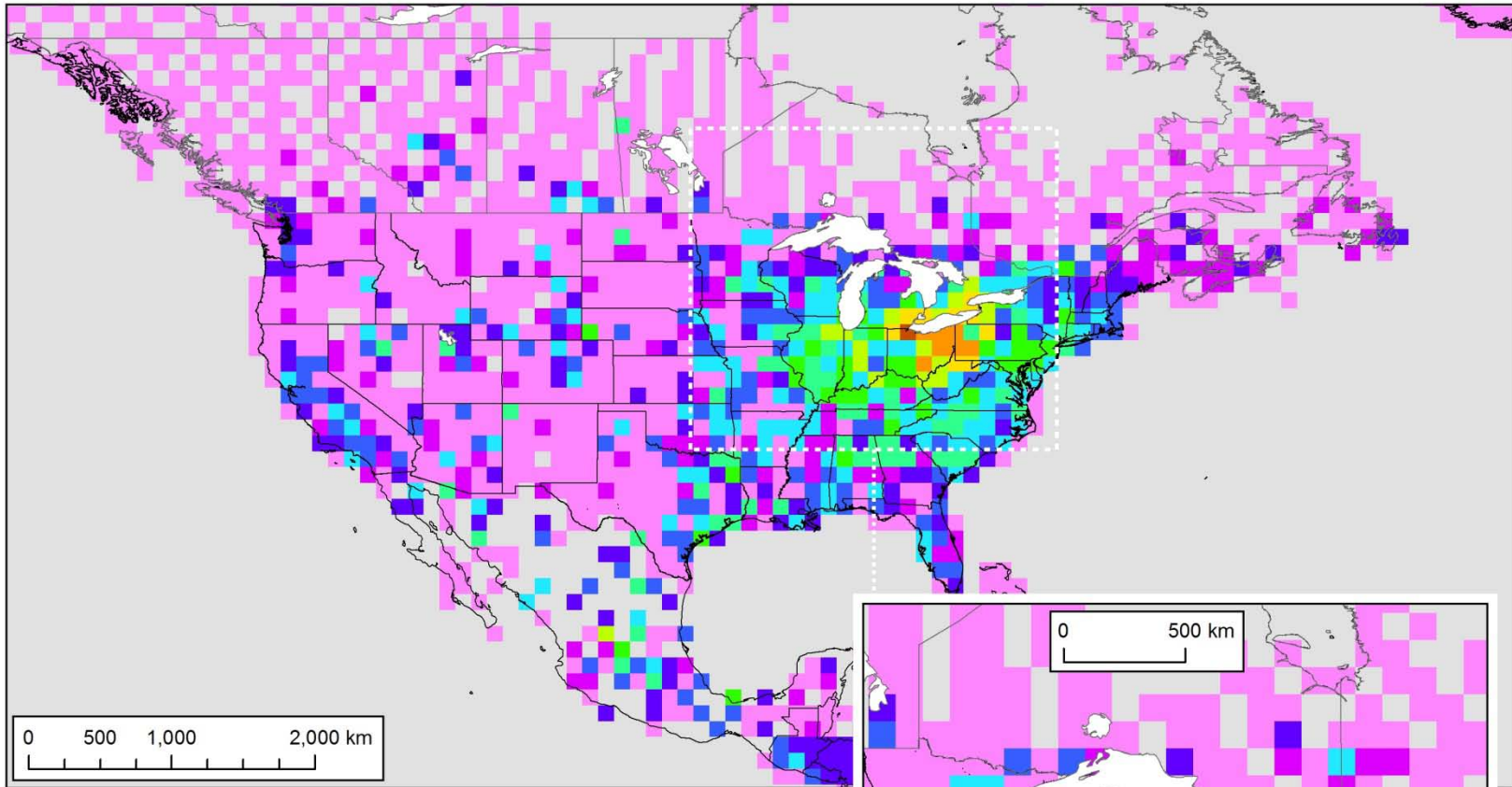




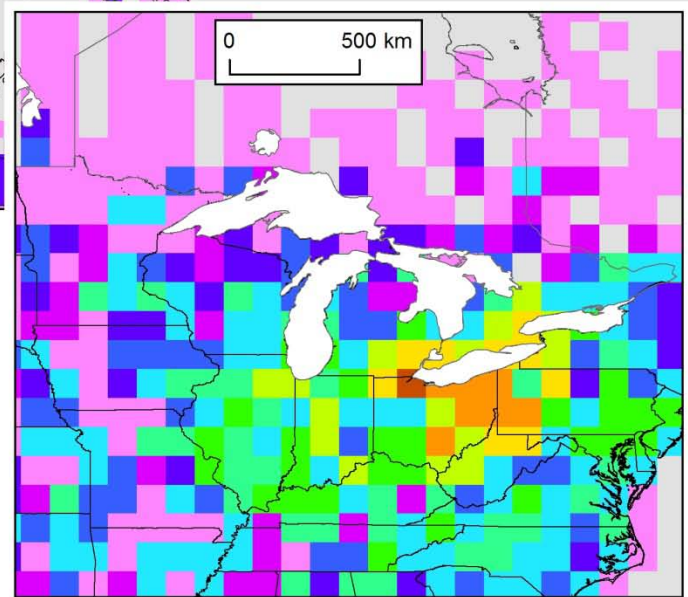
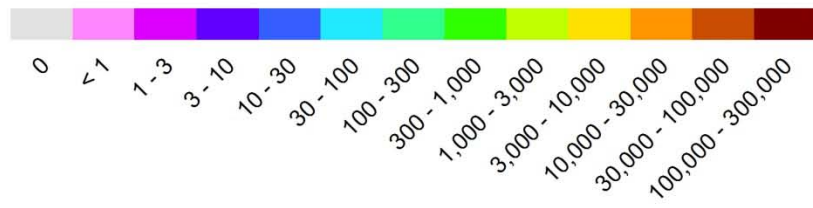
**Atmospheric mercury deposition contribution (g/yr)
to the Lake Ontario Watershed from direct anthropogenic
emissions in each 2x2 degree grid cell**

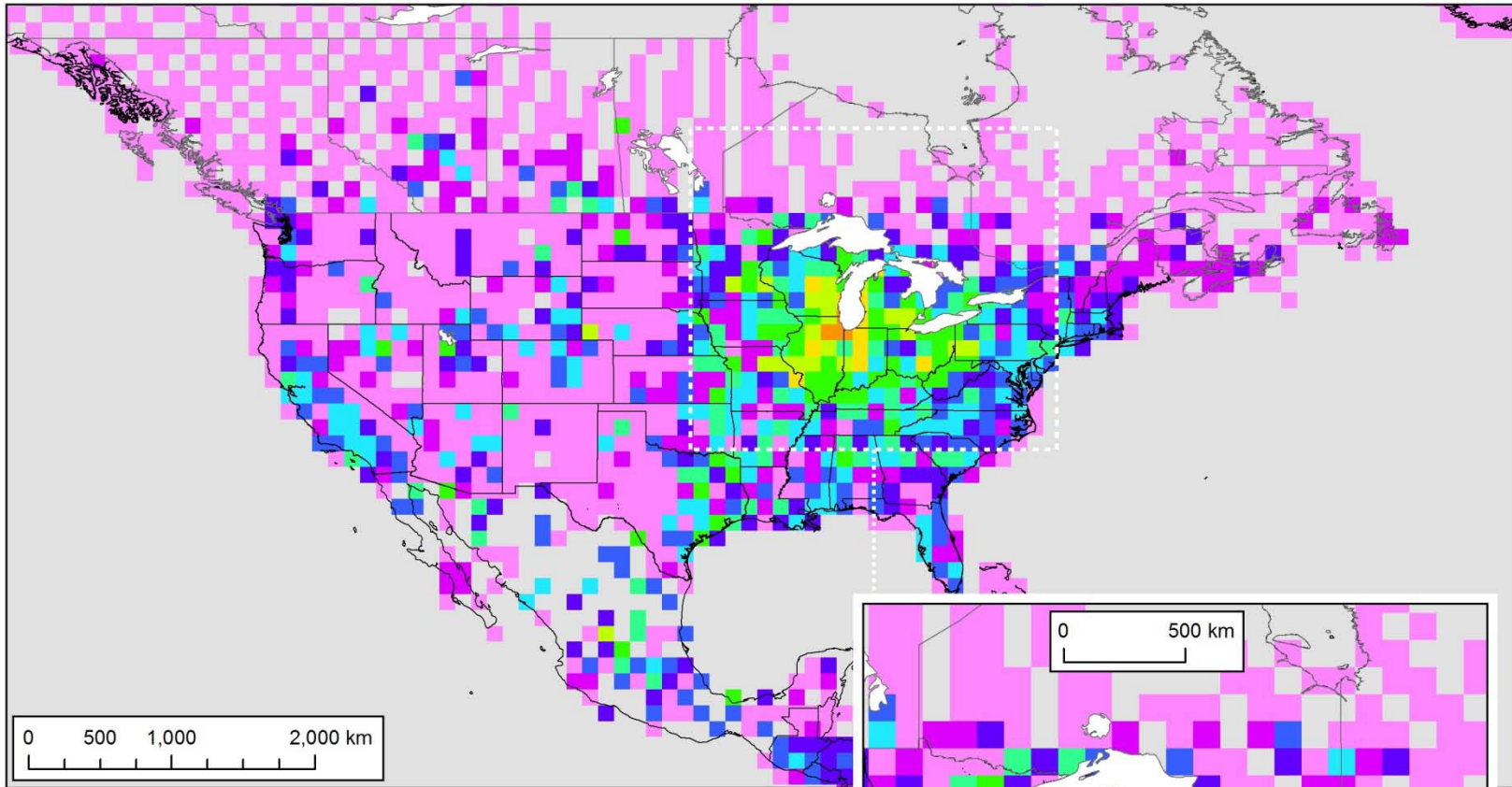


Appendix 3. Atmospheric deposition contribution maps for each Great Lake for direct anthropogenic mercury emissions displayed on a 1x1 degree grid over a North American domain

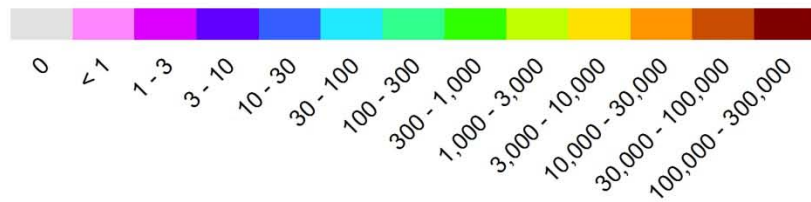


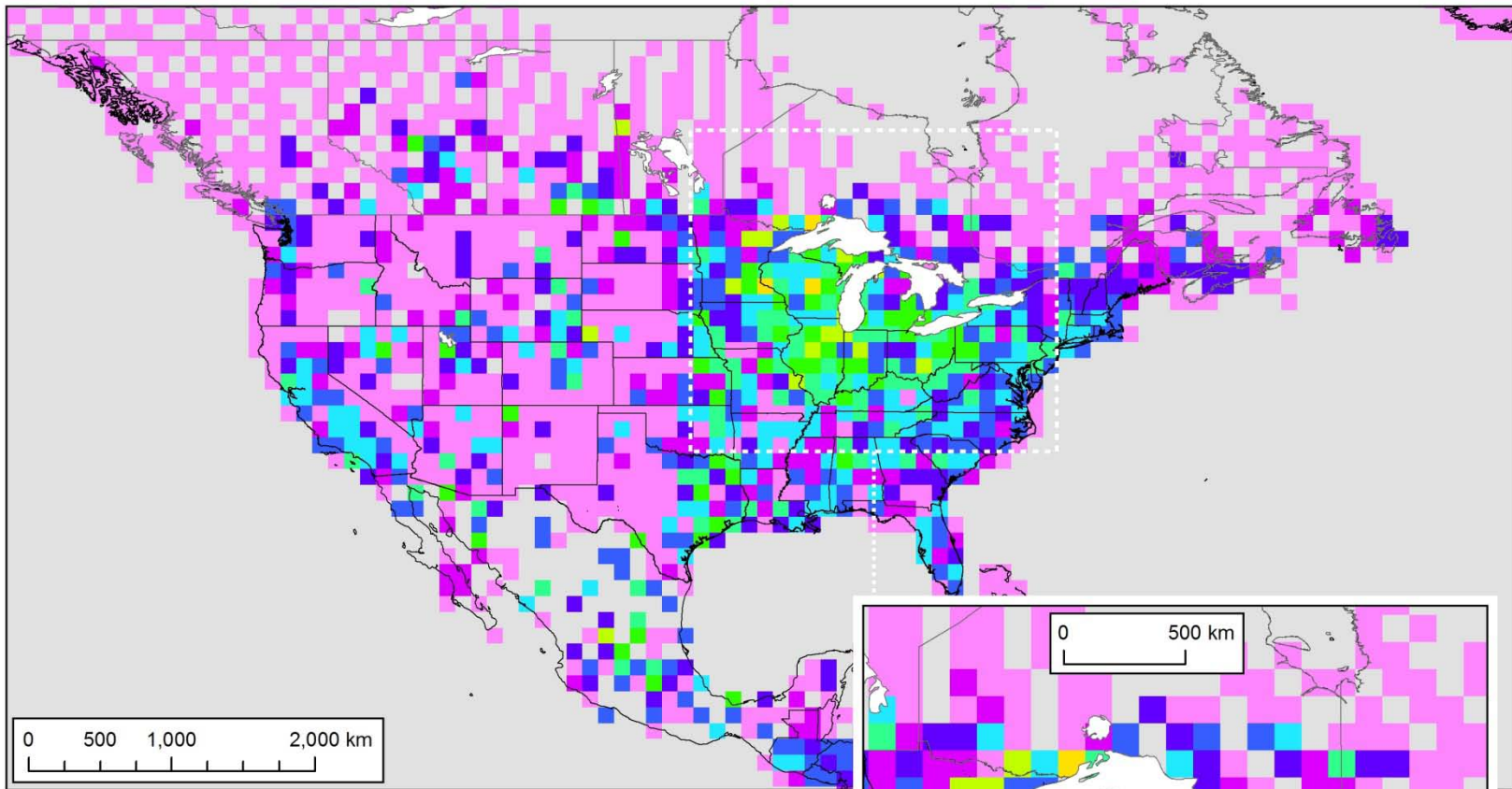
Atmospheric mercury deposition contribution (g/yr) to Lake Erie from direct anthropogenic emissions in each 1x1 degree grid cell



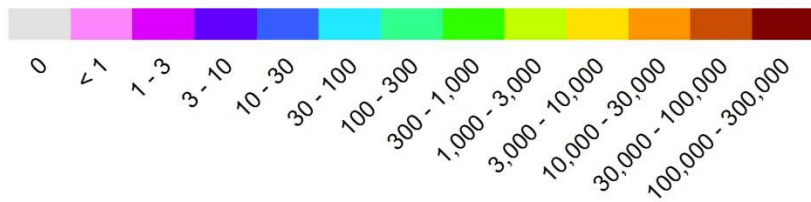


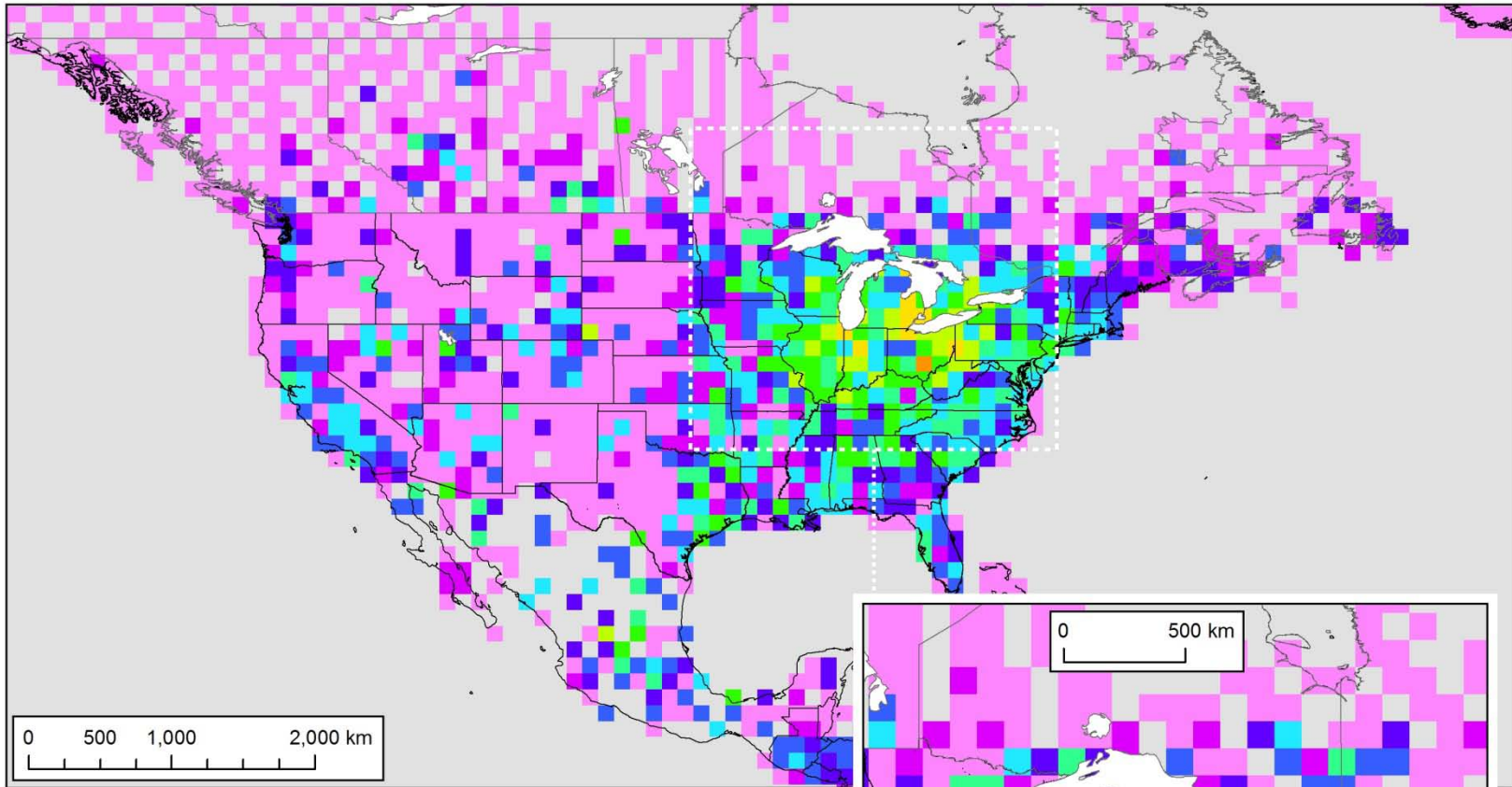
Atmospheric mercury deposition contribution (g/yr) to Lake Michigan from direct anthropogenic emissions in each 1x1 degree grid cell



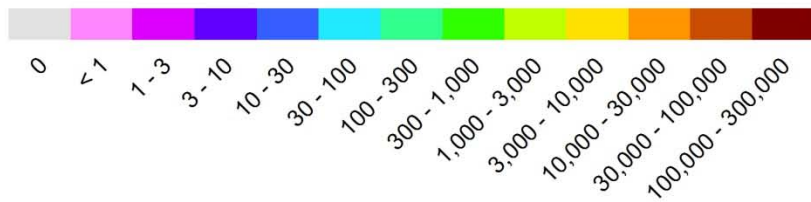


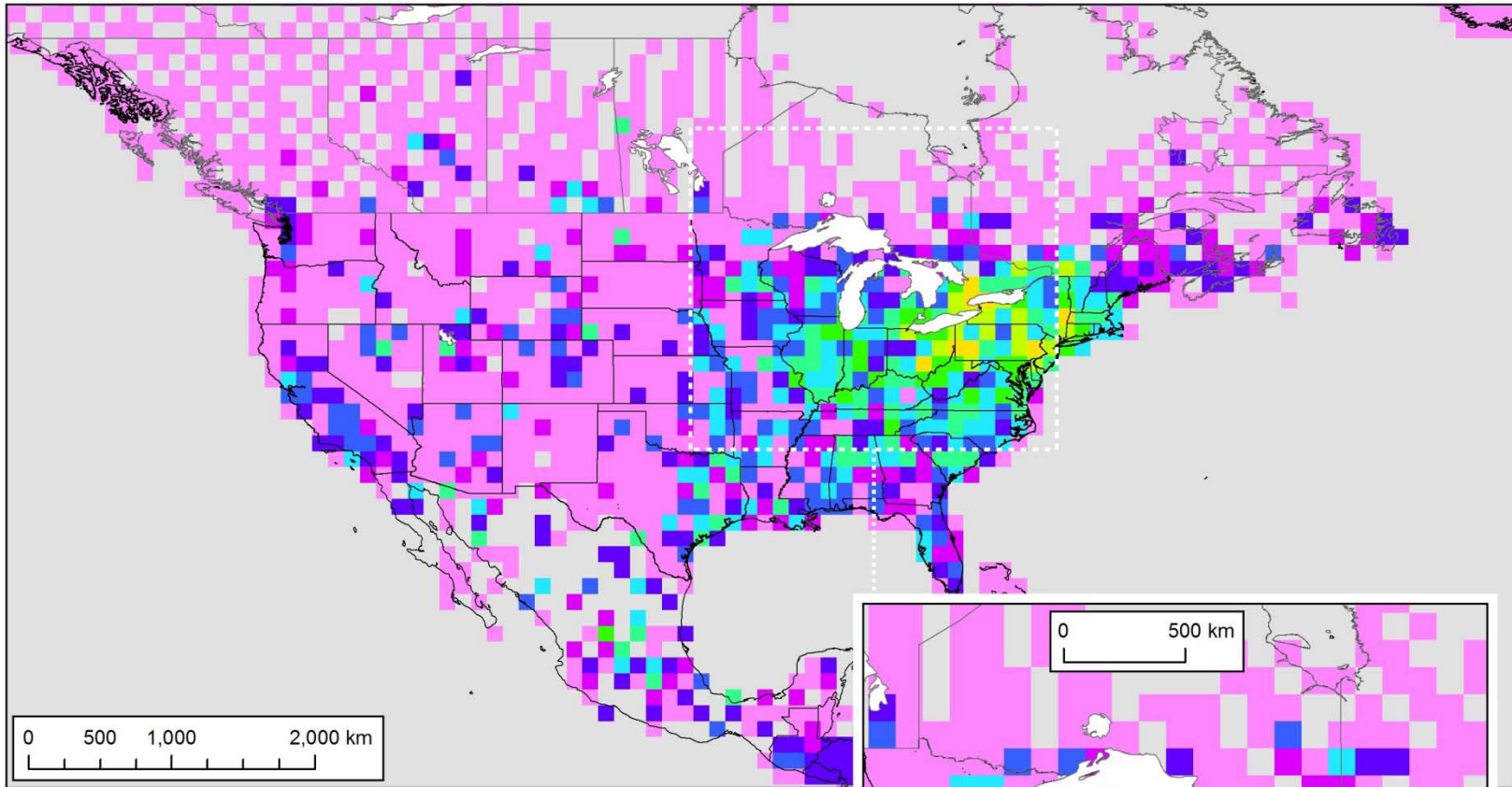
Atmospheric mercury deposition contribution (g/yr) to Lake Superior from direct anthropogenic emissions in each 1x1 degree grid cell



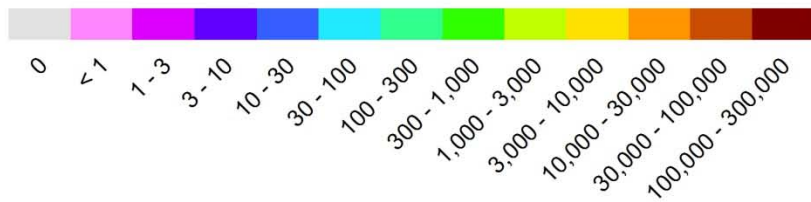


Atmospheric mercury deposition contribution (g/yr) to Lake Huron from direct anthropogenic emissions in each 1x1 degree grid cell

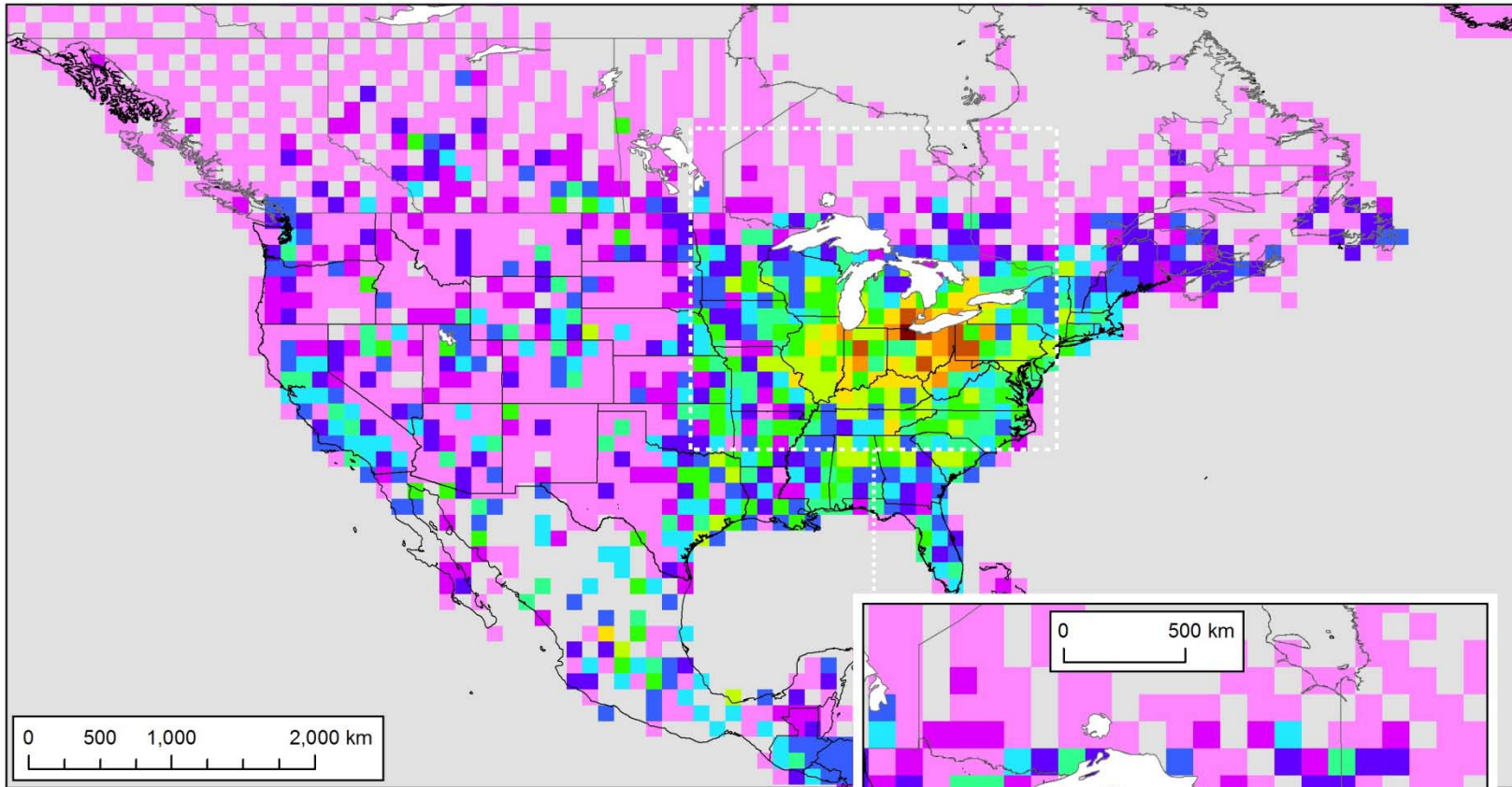




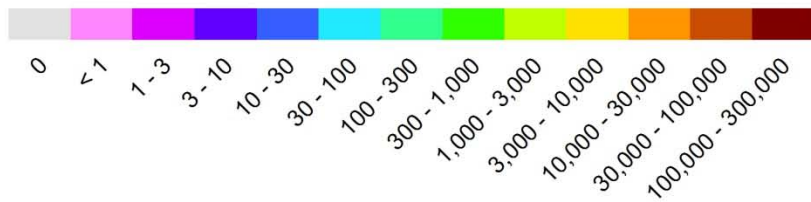
Atmospheric mercury deposition contribution (g/yr) to Lake Ontario from direct anthropogenic emissions in each 1x1 degree grid cell

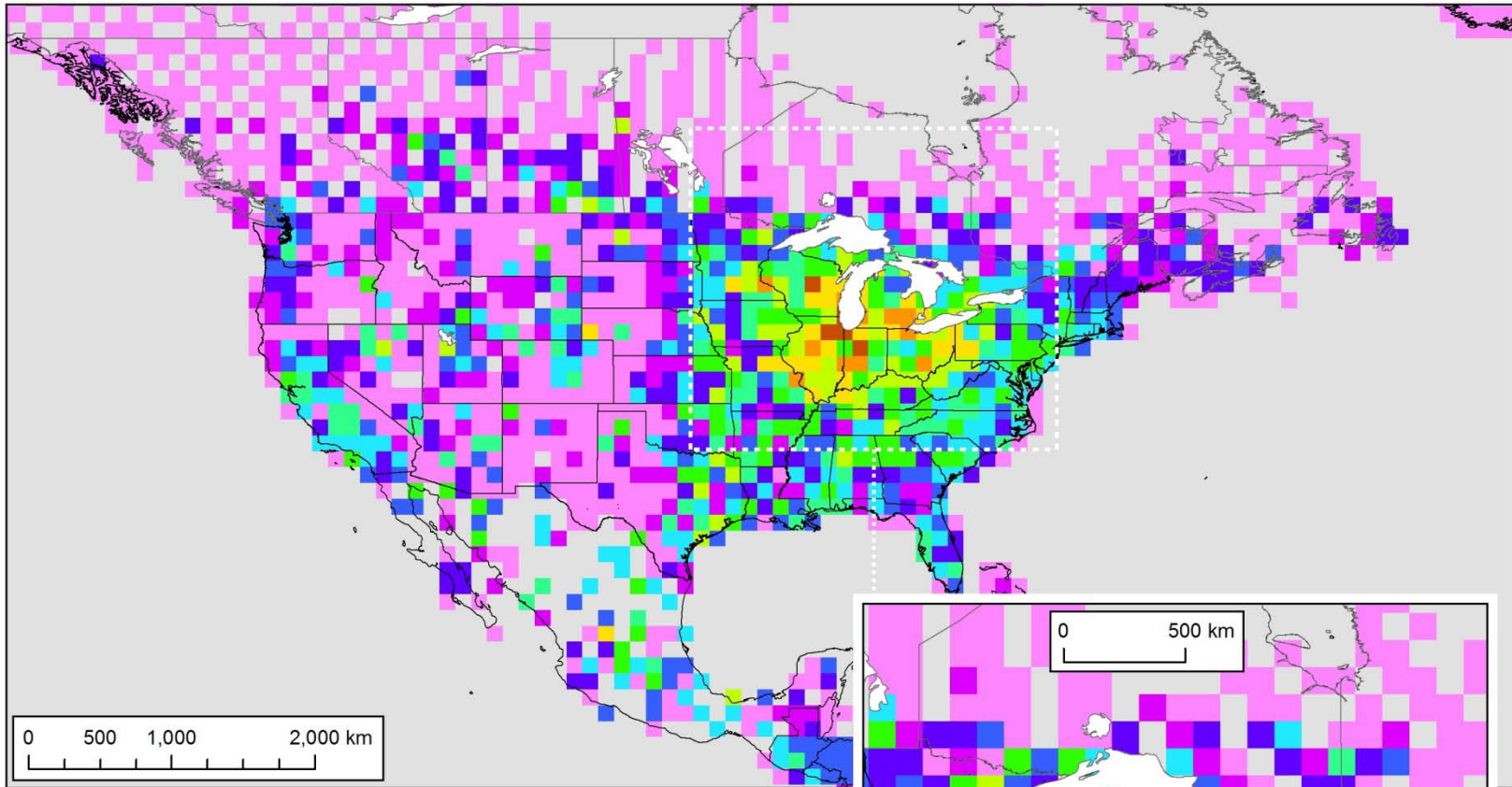


Appendix 4. Atmospheric deposition contribution maps for each Great Lake's Watershed for direct anthropogenic mercury emissions displayed on a 1x1 degree over a North American domain

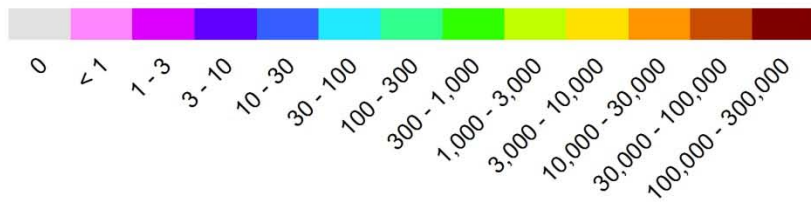


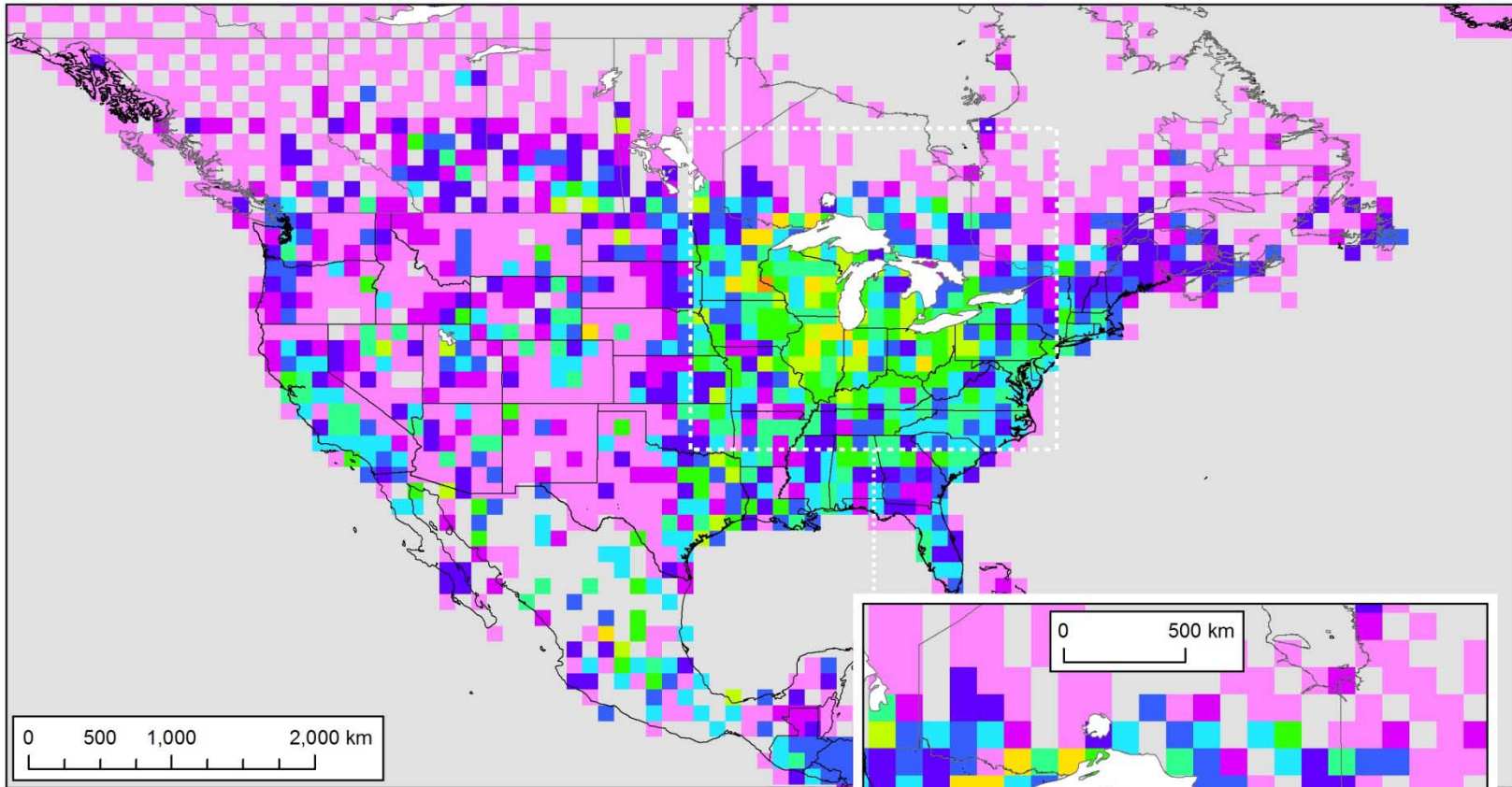
Atmospheric mercury deposition contribution (g/yr) to the Lake Erie Watershed from direct anthropogenic emissions in each 1x1 degree grid cell



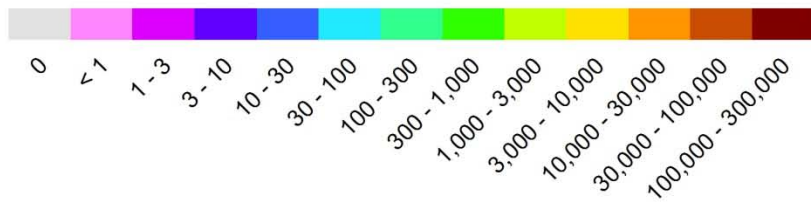


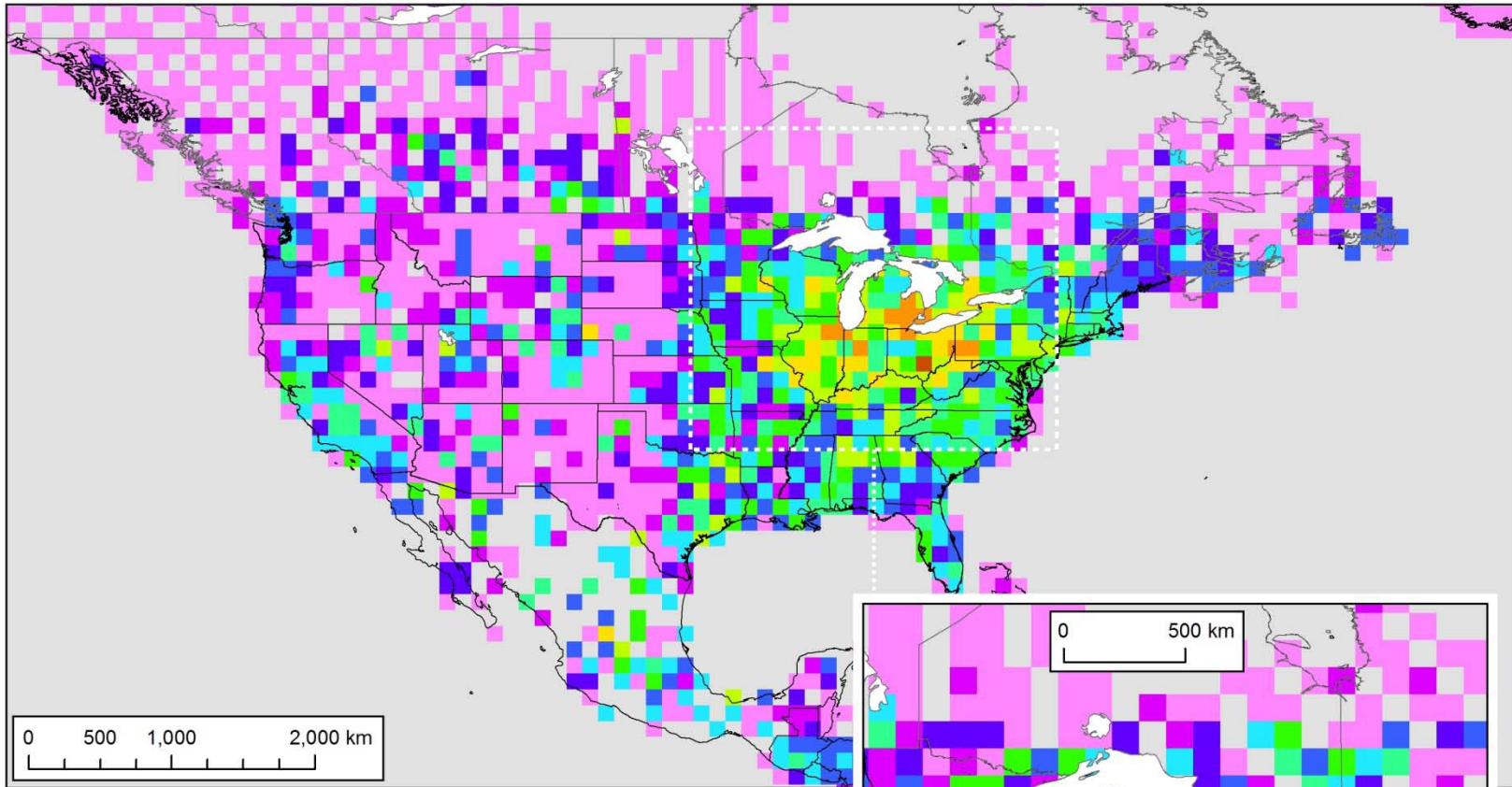
Atmospheric mercury deposition contribution (g/yr) to the Lake Michigan Watershed from direct anthropogenic emissions in each 1x1 degree grid cell



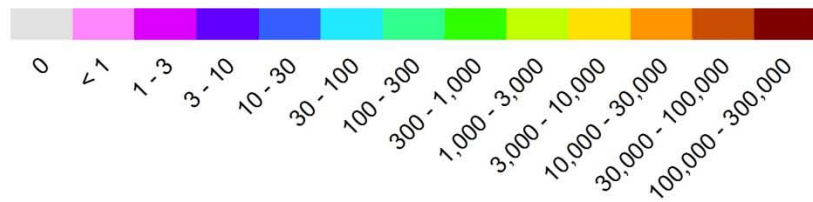


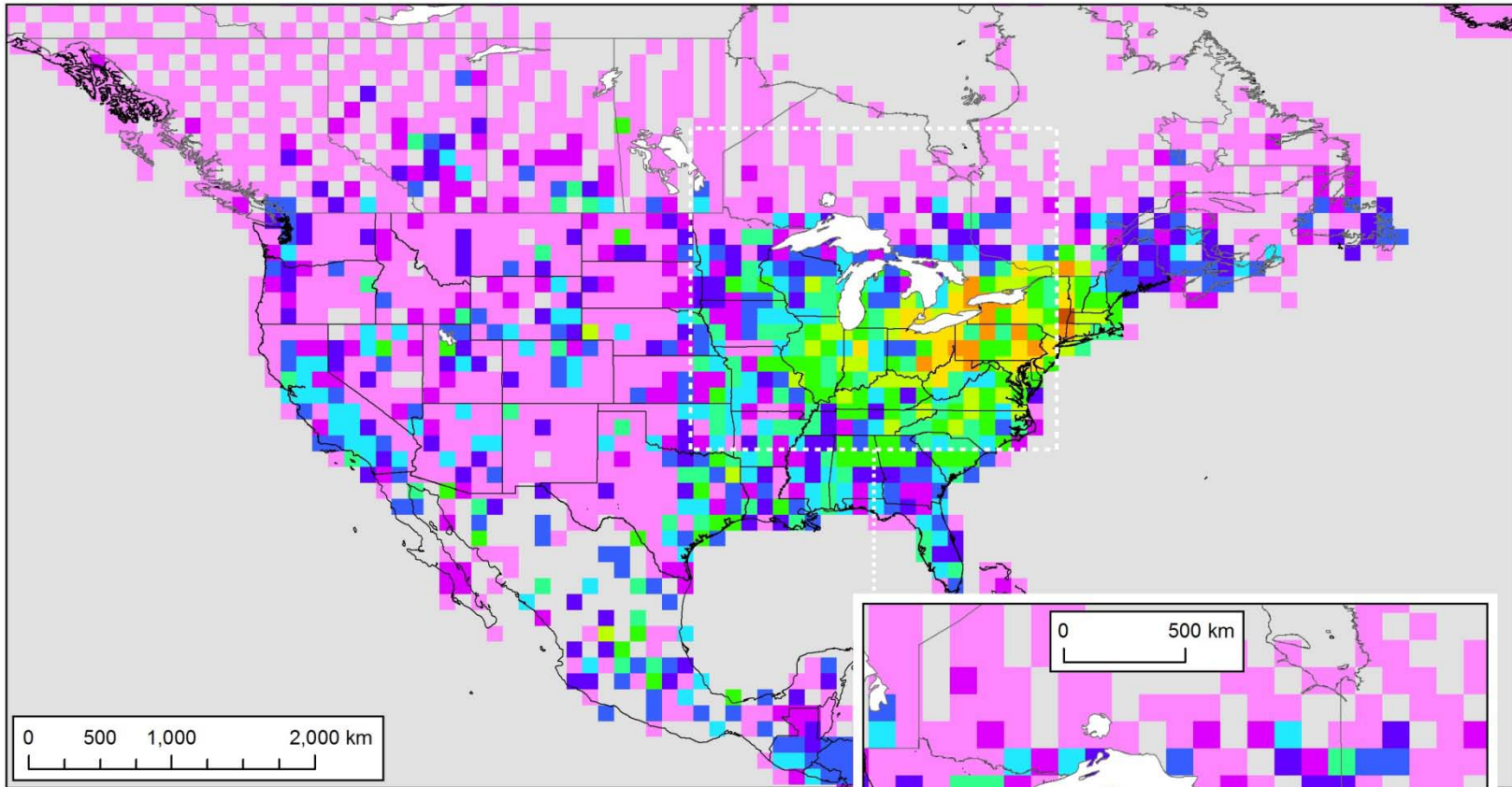
Atmospheric mercury deposition contribution (g/yr) to the Lake Superior Watershed from direct anthropogenic emissions in each 1x1 degree grid cell



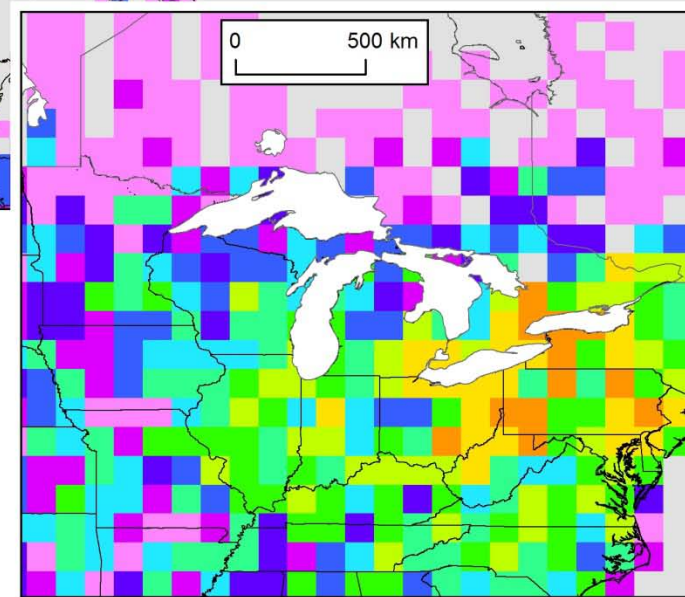
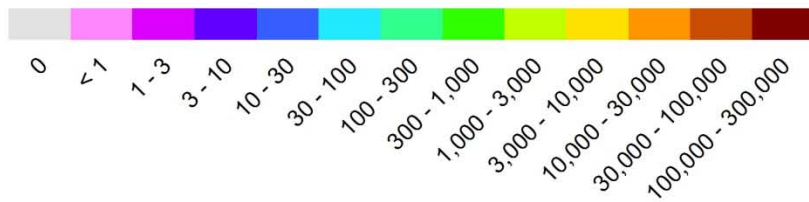


Atmospheric mercury deposition contribution (g/yr) to the Lake Huron Watershed from direct anthropogenic emissions in each 1x1 degree grid cell

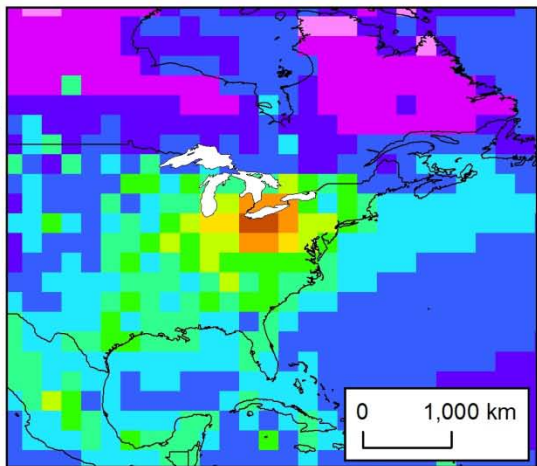
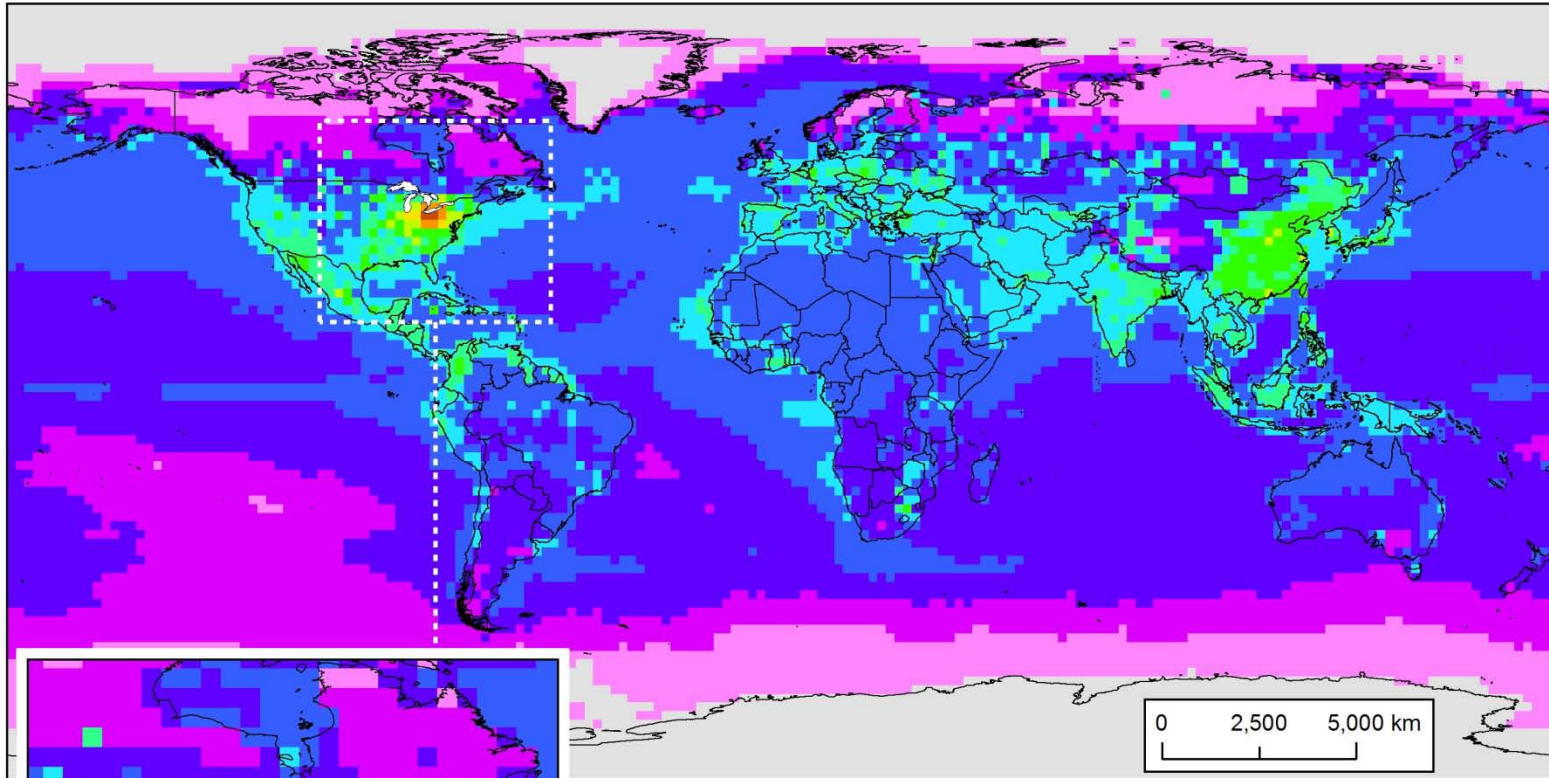




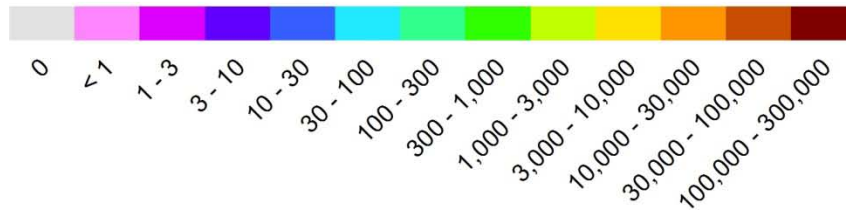
Atmospheric mercury deposition contribution (g/yr) to the Lake Ontario Watershed from direct anthropogenic emissions in each 1x1 degree grid cell

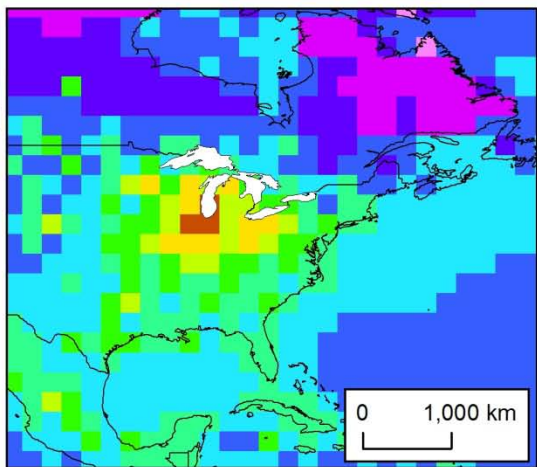
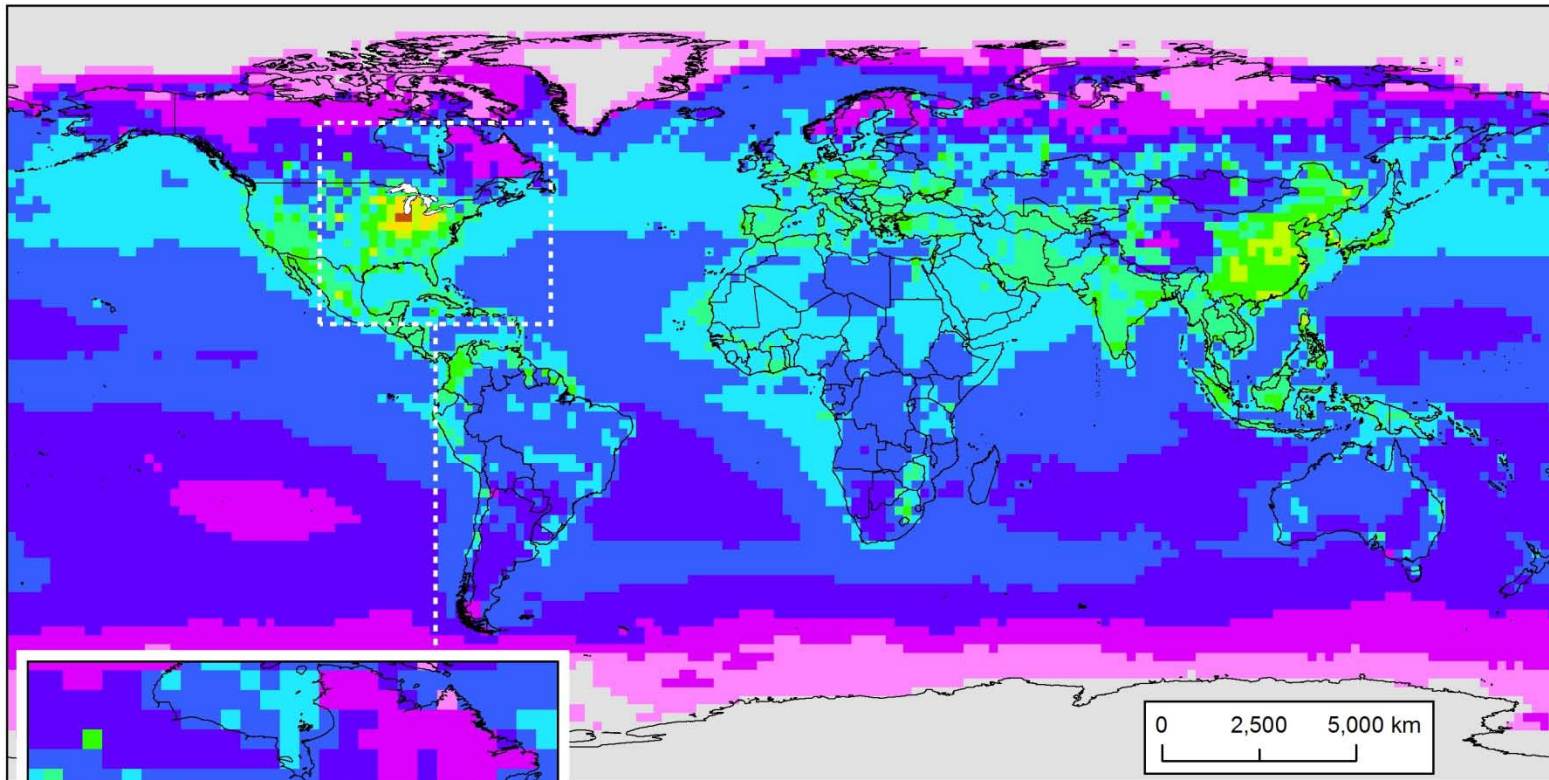


Appendix 5. Atmospheric deposition contribution maps for each Great Lake for total atmospheric mercury emissions displayed on a 2x2 degree global grid

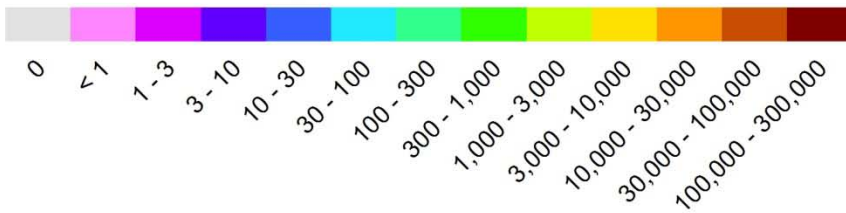


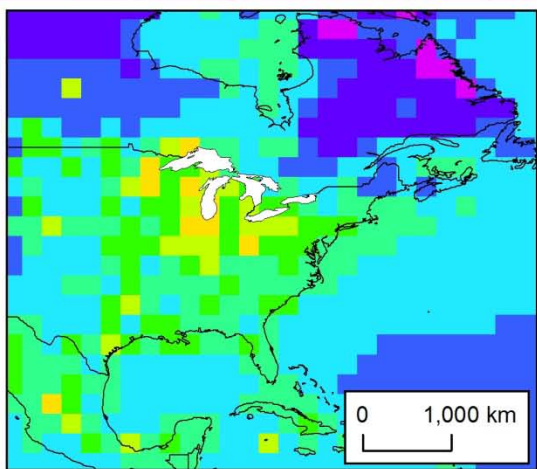
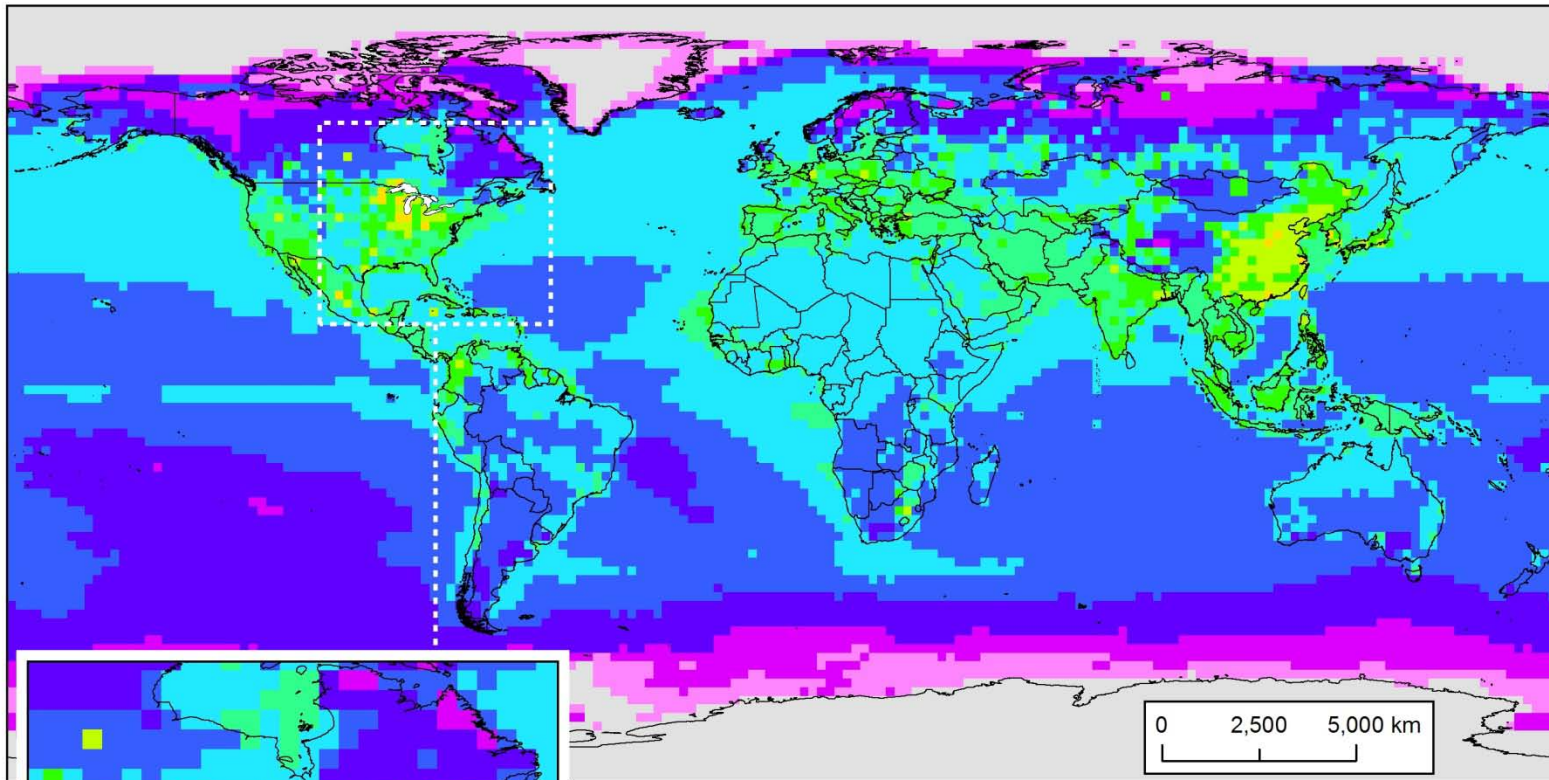
Atmospheric mercury deposition contribution (g/yr) to Lake Erie from all emissions sources in each 2x2 degree grid cell



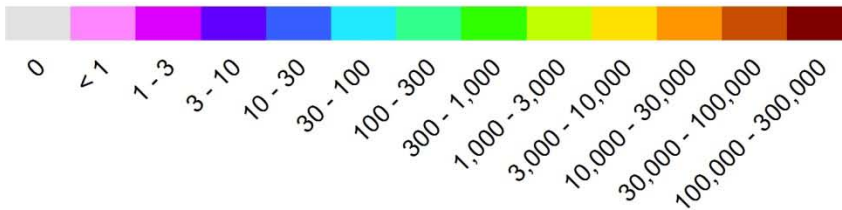


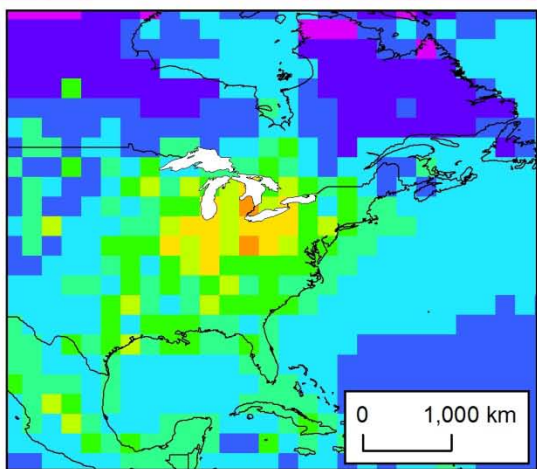
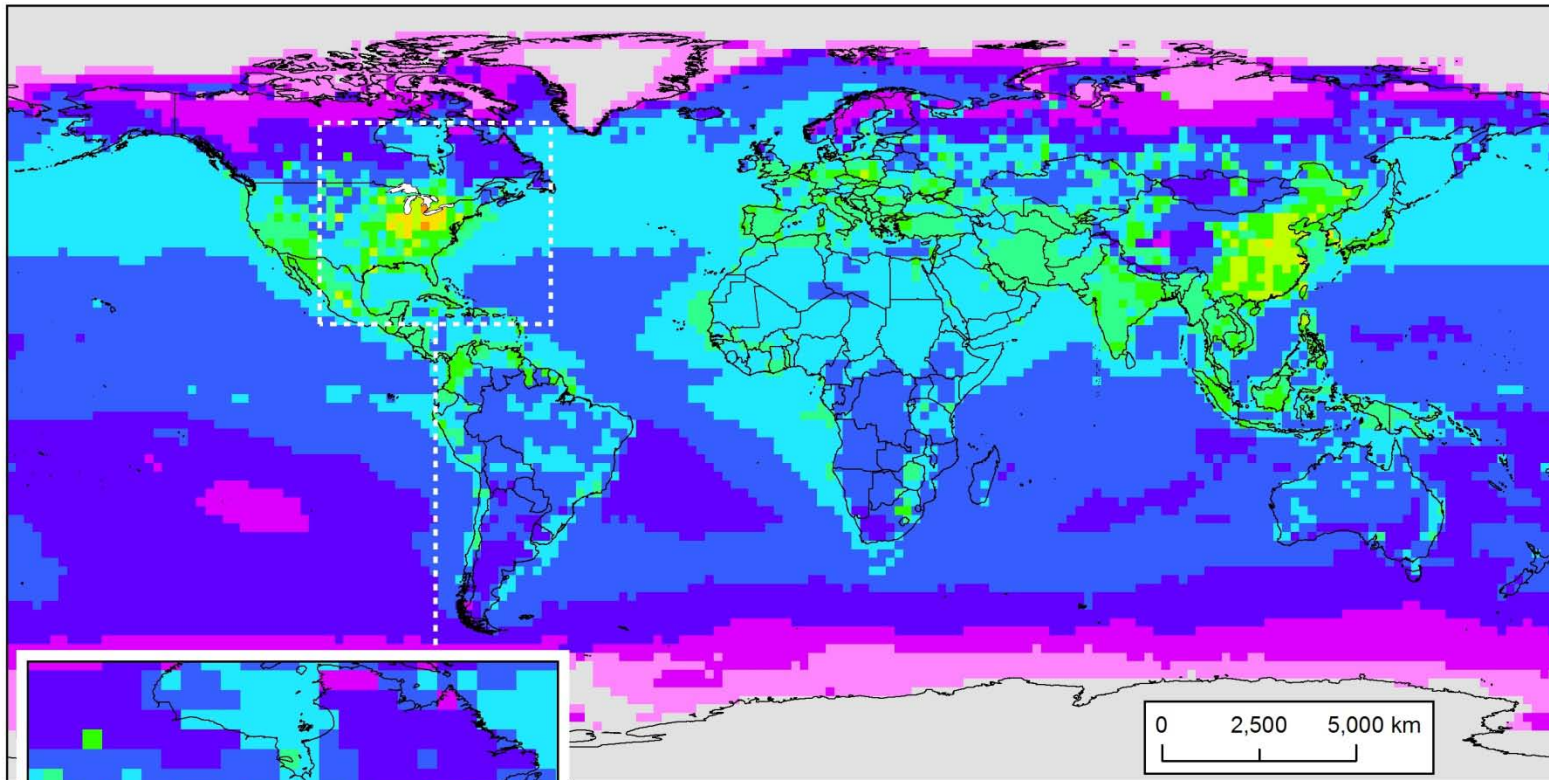
Atmospheric mercury deposition contribution (g/yr) to Lake Michigan from all emissions sources in each 2x2 degree grid cell



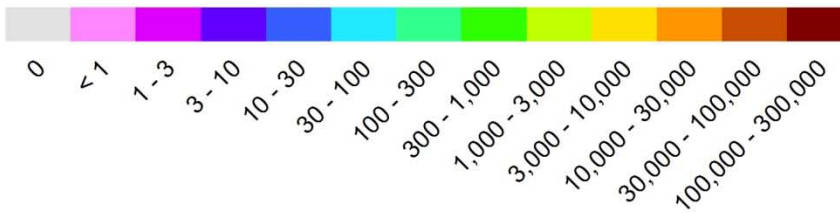


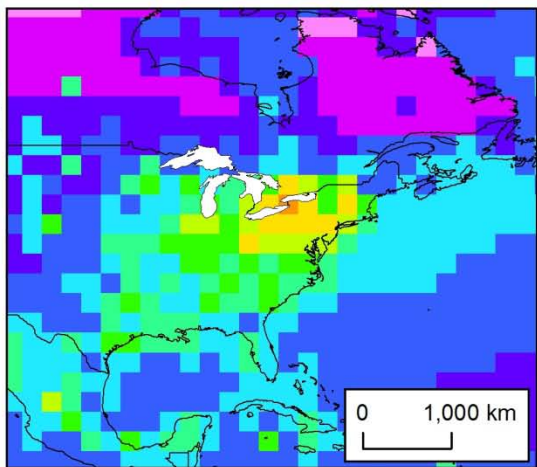
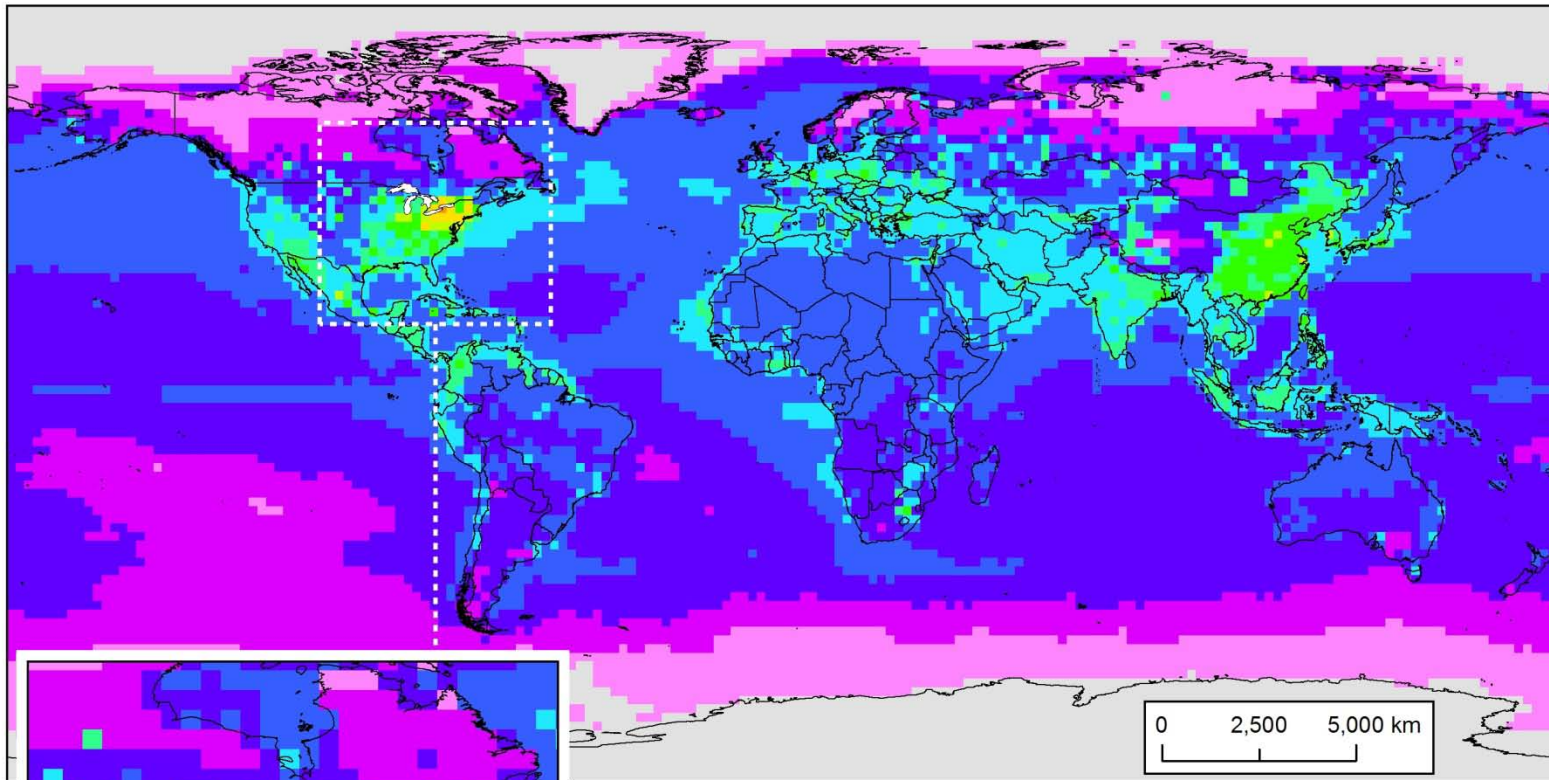
**Atmospheric mercury deposition contribution
(g/yr) to Lake Superior from all emissions sources
in each 2x2 degree grid cell**



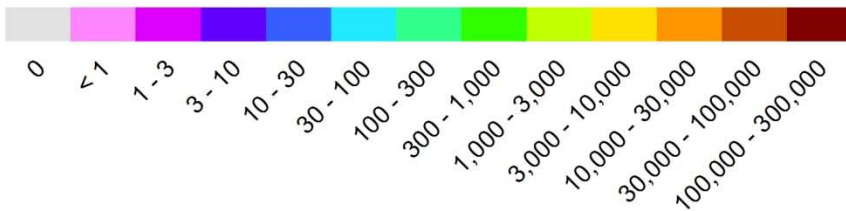


Atmospheric mercury deposition contribution (g/yr) to Lake Huron from all emissions sources in each 2x2 degree grid cell

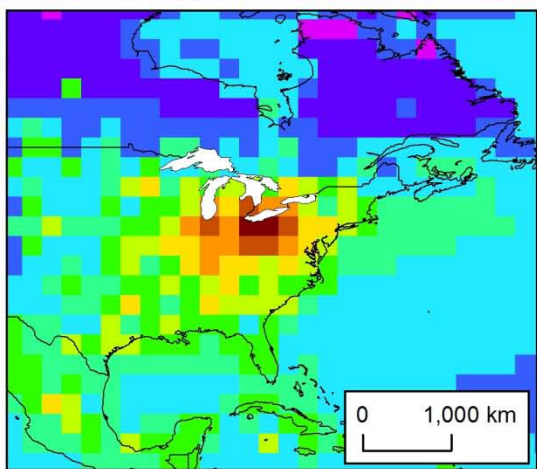
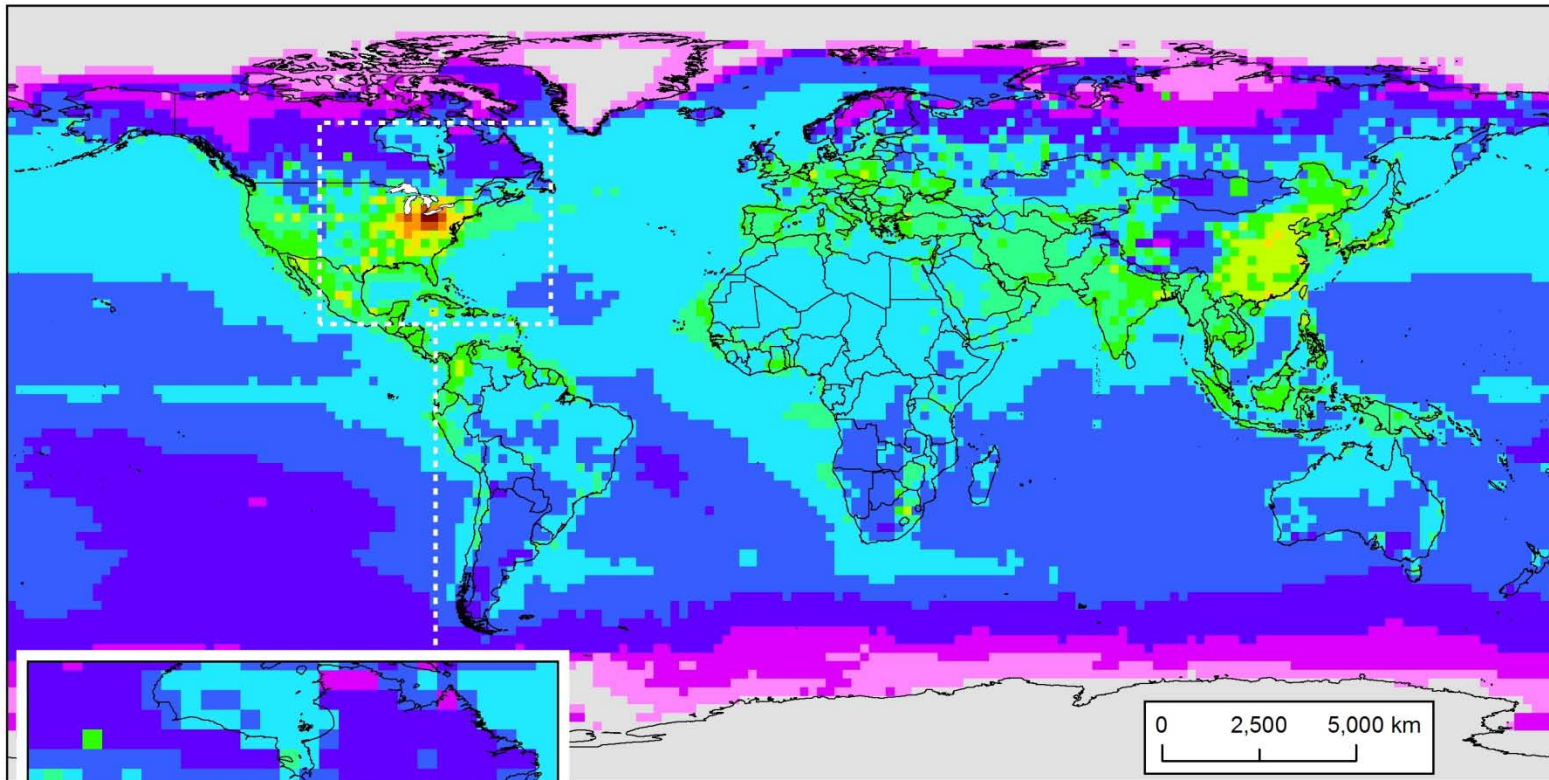




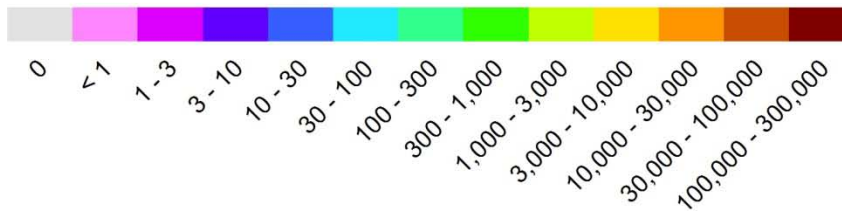
**Atmospheric mercury deposition contribution
(g/yr) to Lake Ontario from all emissions sources
in each 2x2 degree grid cell**

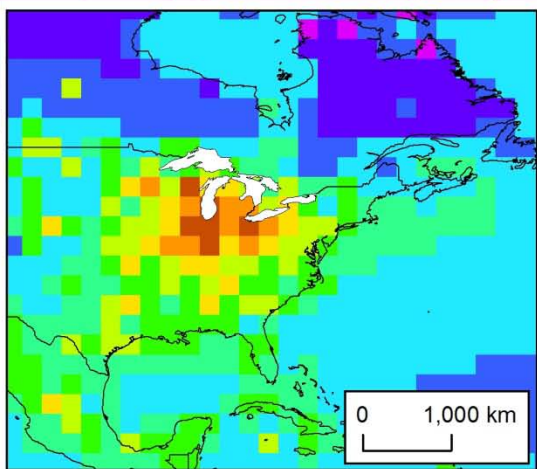
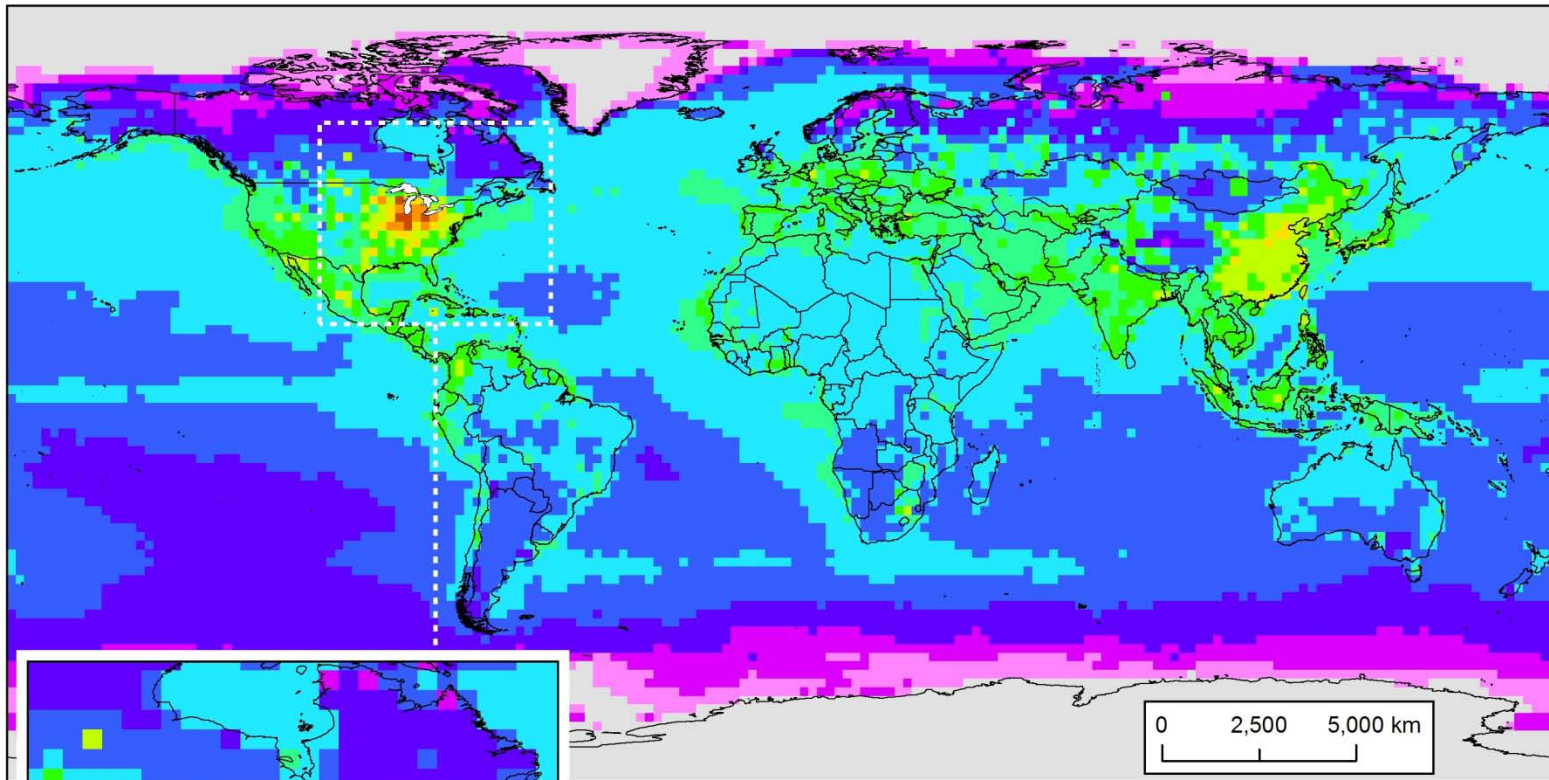


Appendix 6. Atmospheric deposition contribution maps for each Great Lake's Watershed for total atmospheric mercury emissions displayed on a 2x2 degree global grid

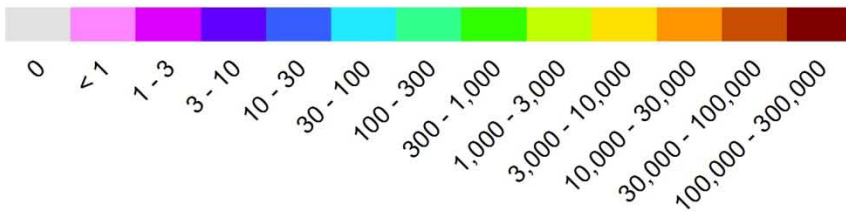


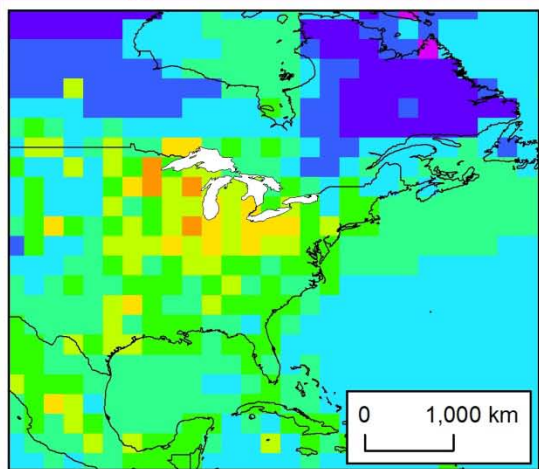
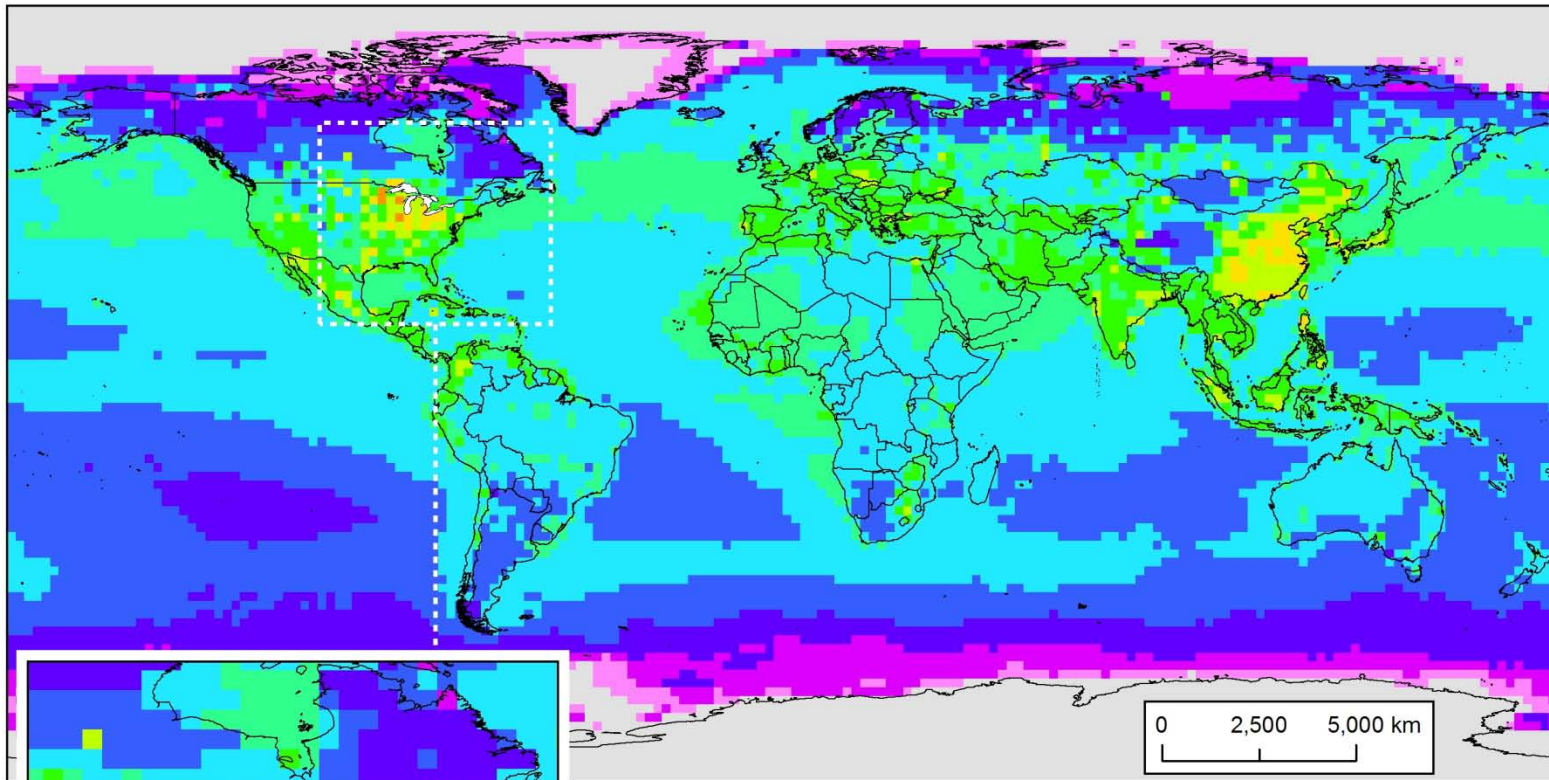
**Atmospheric mercury deposition contribution (g/yr)
to the Lake Erie Watershed from all emissions sources
in each 2x2 degree grid cell**



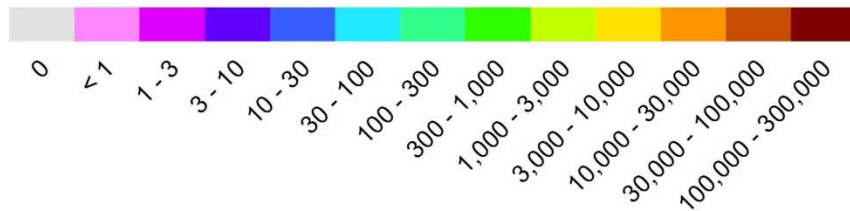


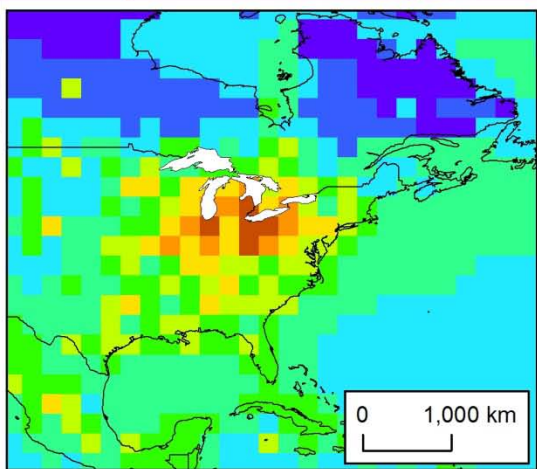
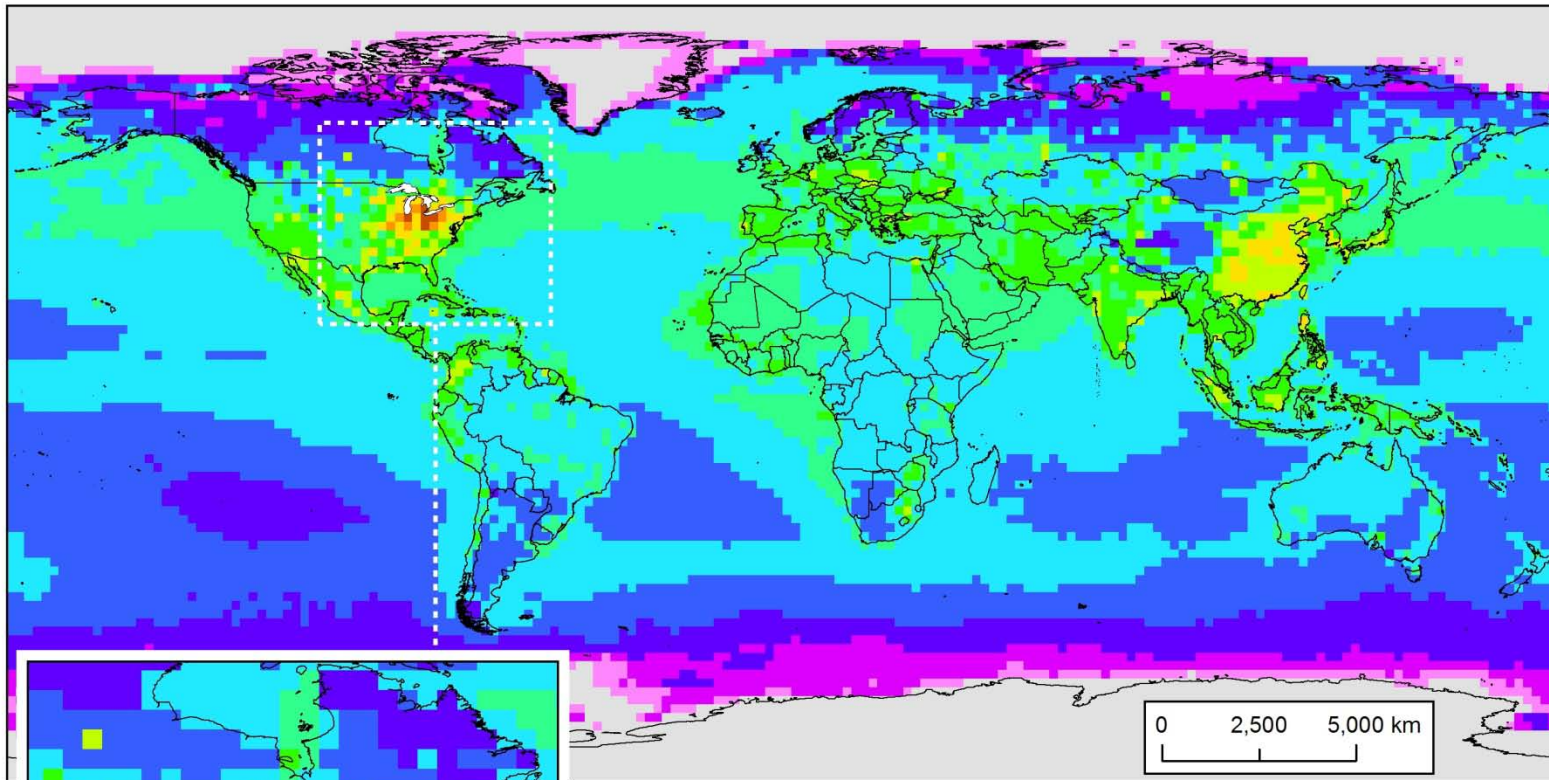
Atmospheric mercury deposition contribution (g/yr) to the Lake Michigan Watershed from all emissions sources in each 2x2 degree grid cell



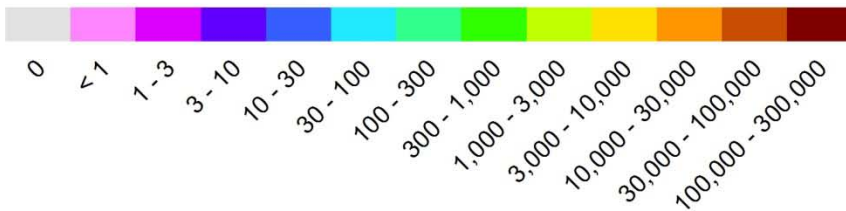


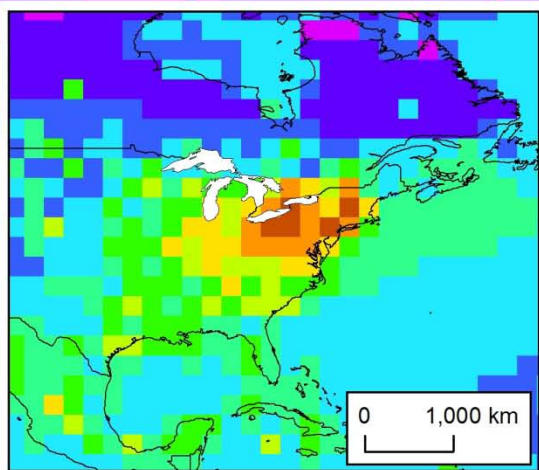
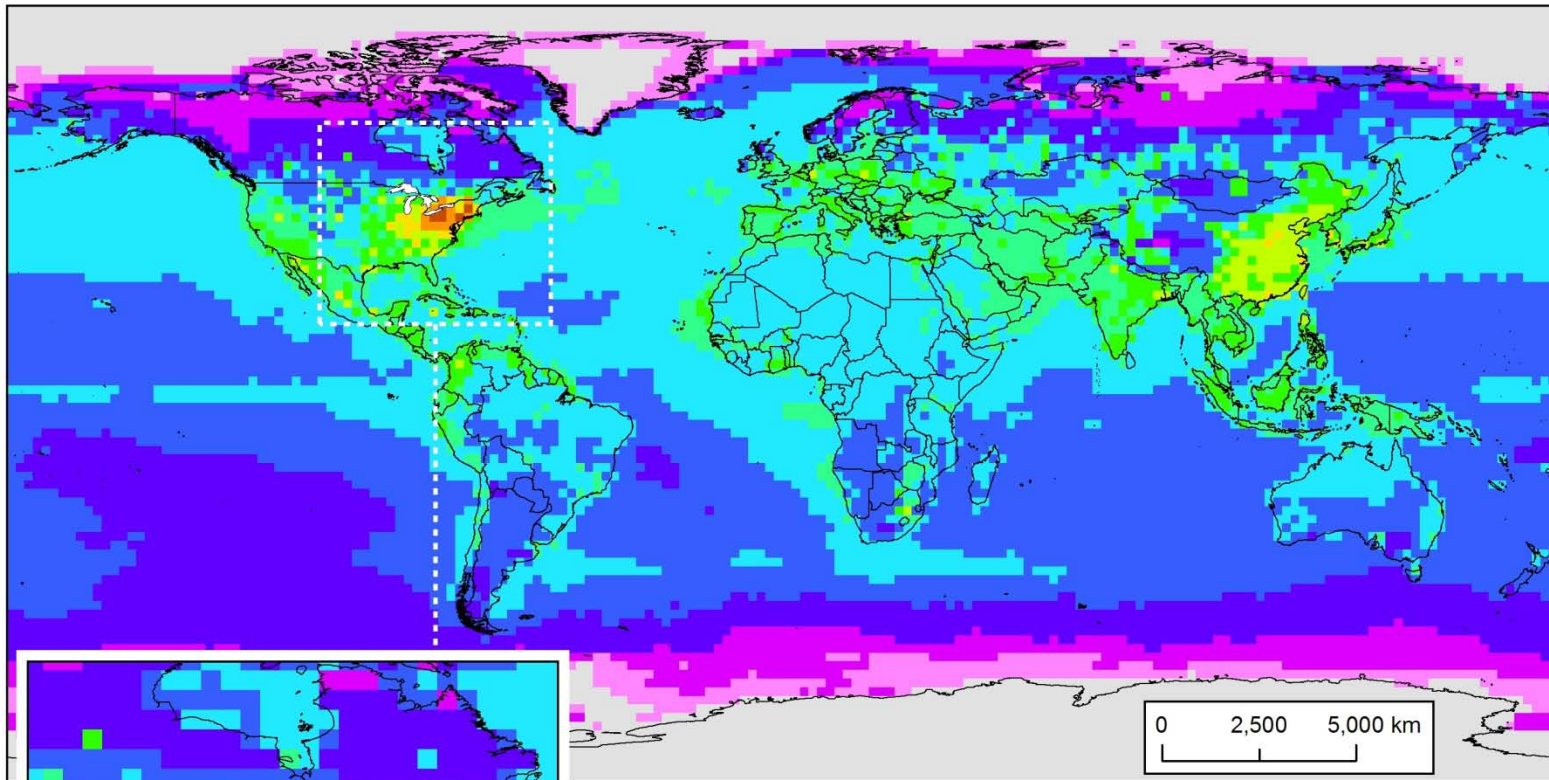
Atmospheric mercury deposition contribution (g/yr) to the Lake Superior Watershed from all emissions sources in each 2x2 degree grid cell



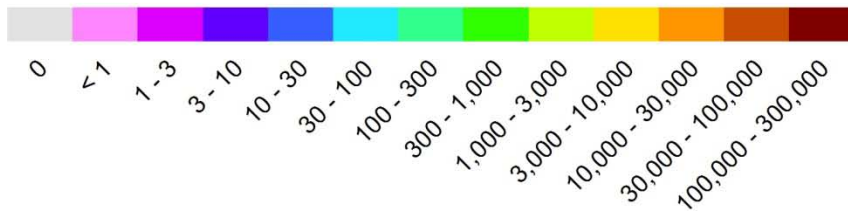


Atmospheric mercury deposition contribution (g/yr) to the Lake Huron Watershed from all emissions sources in each 2x2 degree grid cell

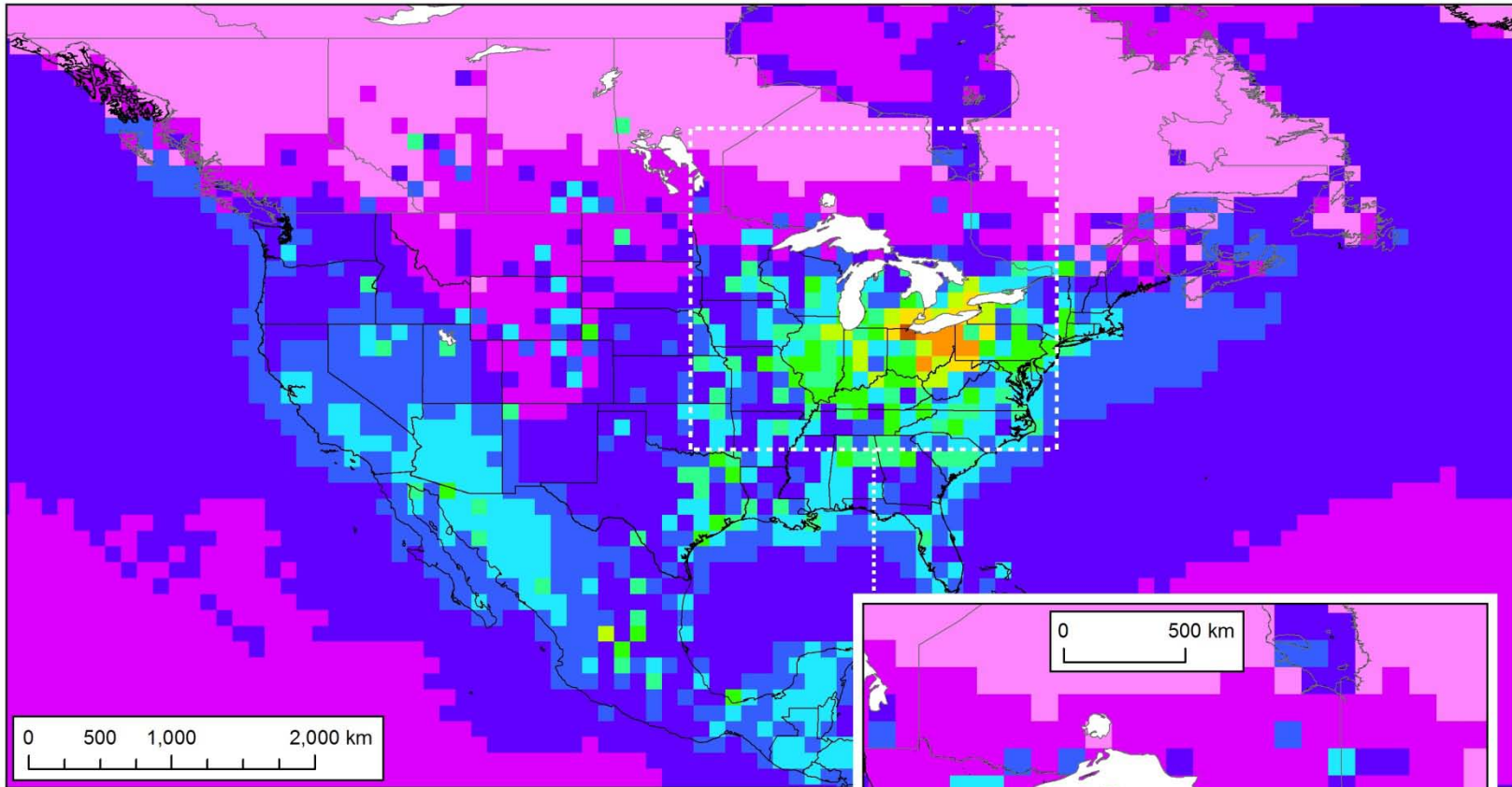




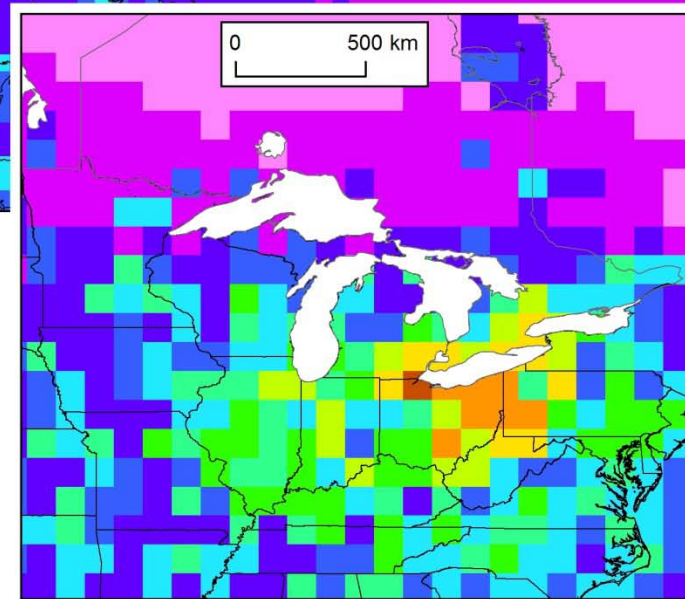
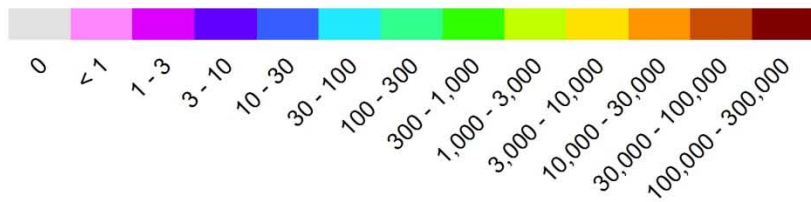
Atmospheric mercury deposition contribution (g/yr) to the Lake Ontario Watershed from all emissions sources in each 2x2 degree grid cell

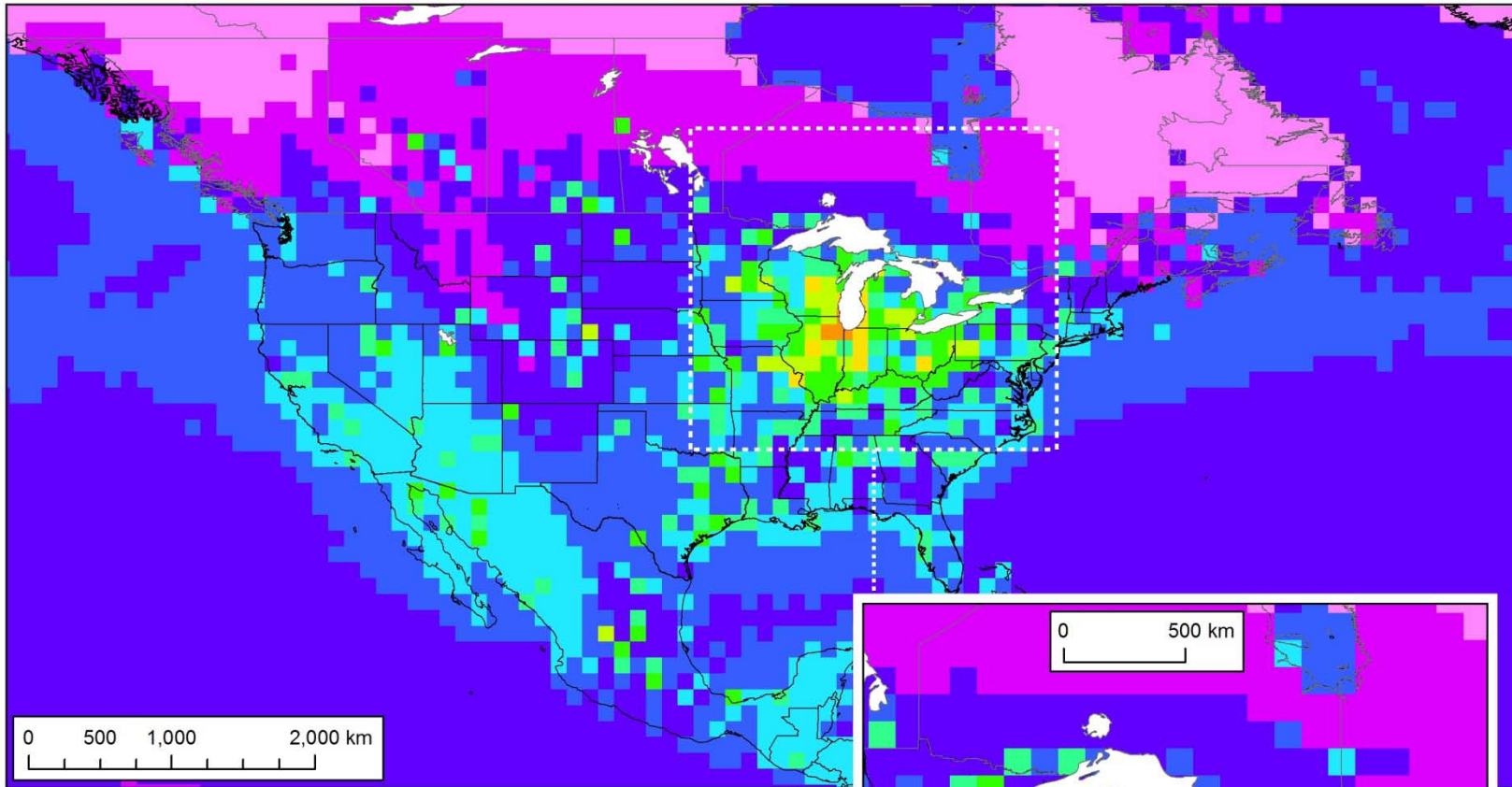


Appendix 7. Atmospheric deposition contribution maps for each Great Lake for total atmospheric mercury emissions displayed on a 1x1 degree grid over a North American domain

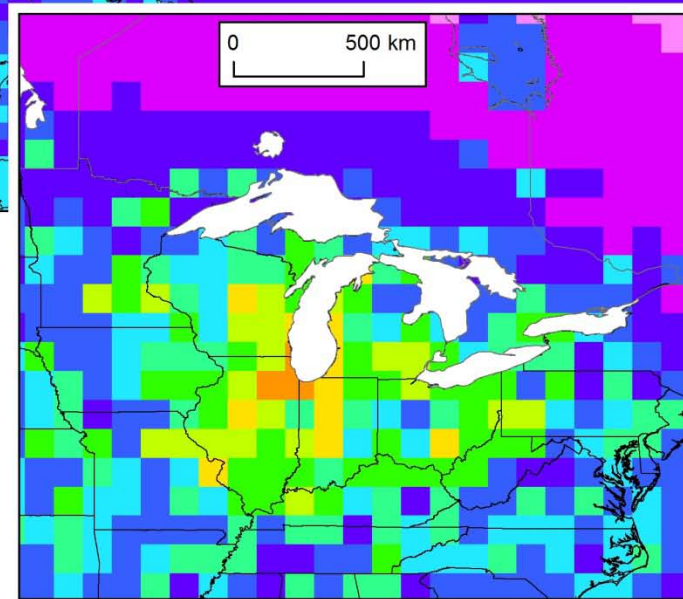
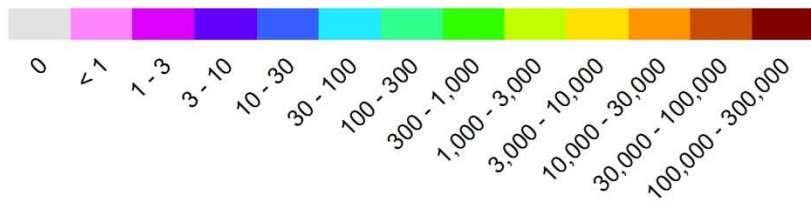


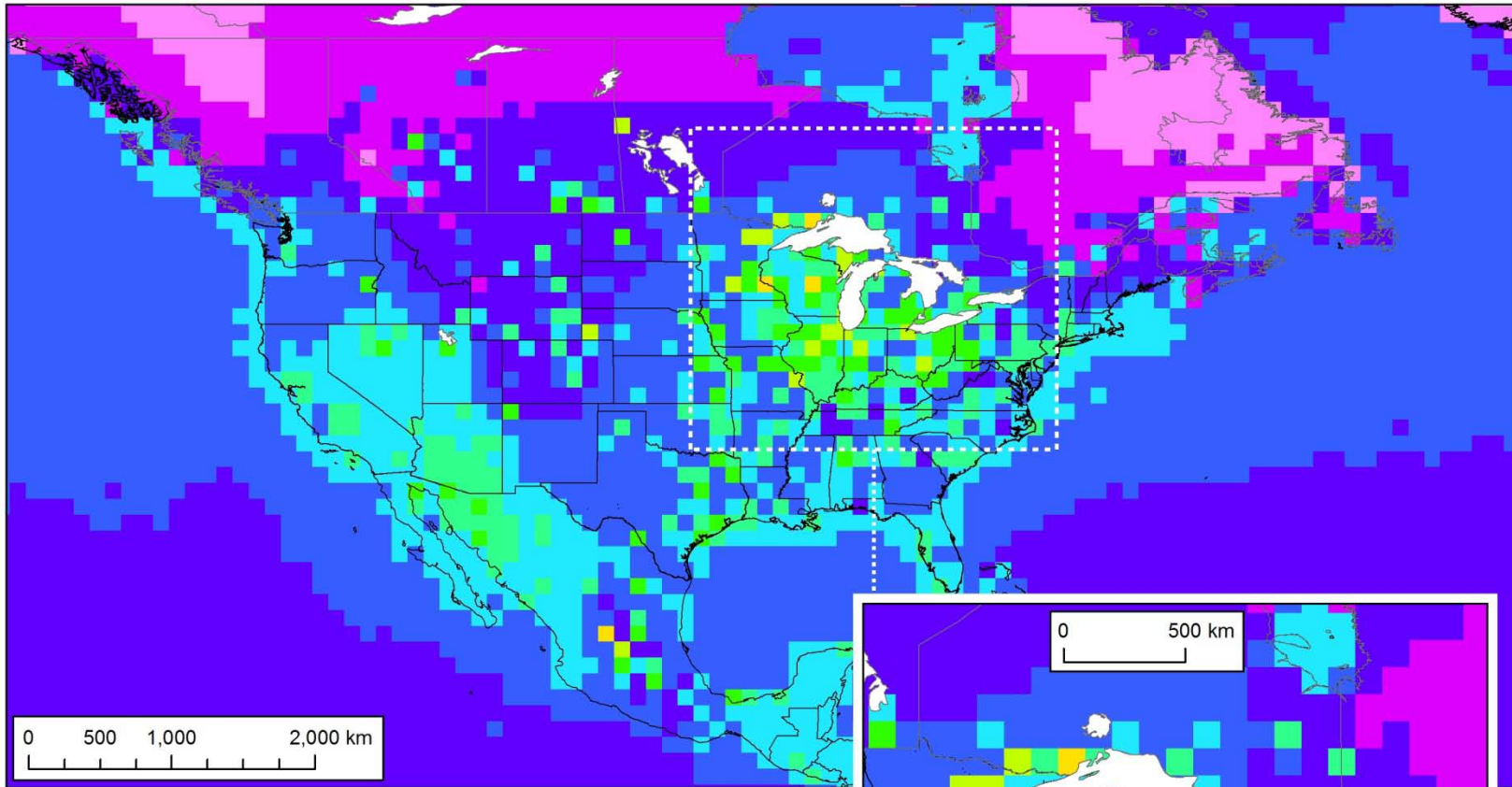
**Atmospheric mercury deposition contribution (g/yr)
to Lake Erie from all emissions sources in
each 1x1 degree grid cell**



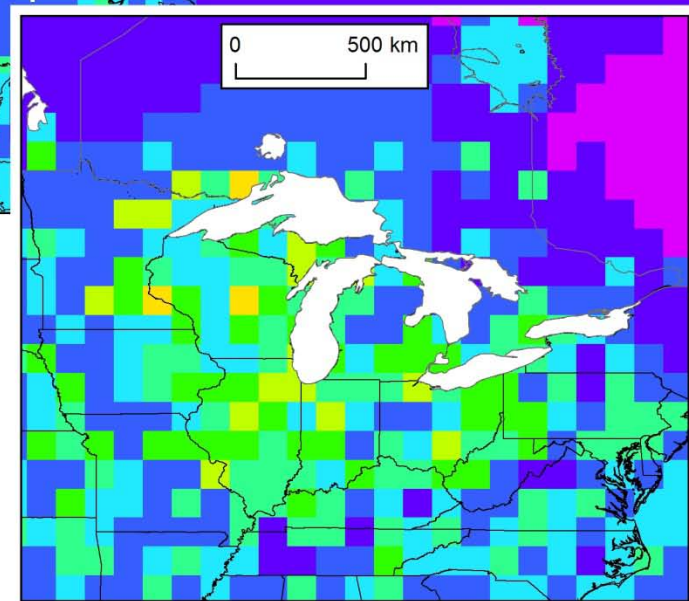
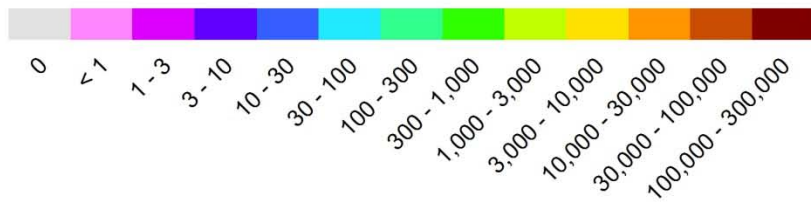


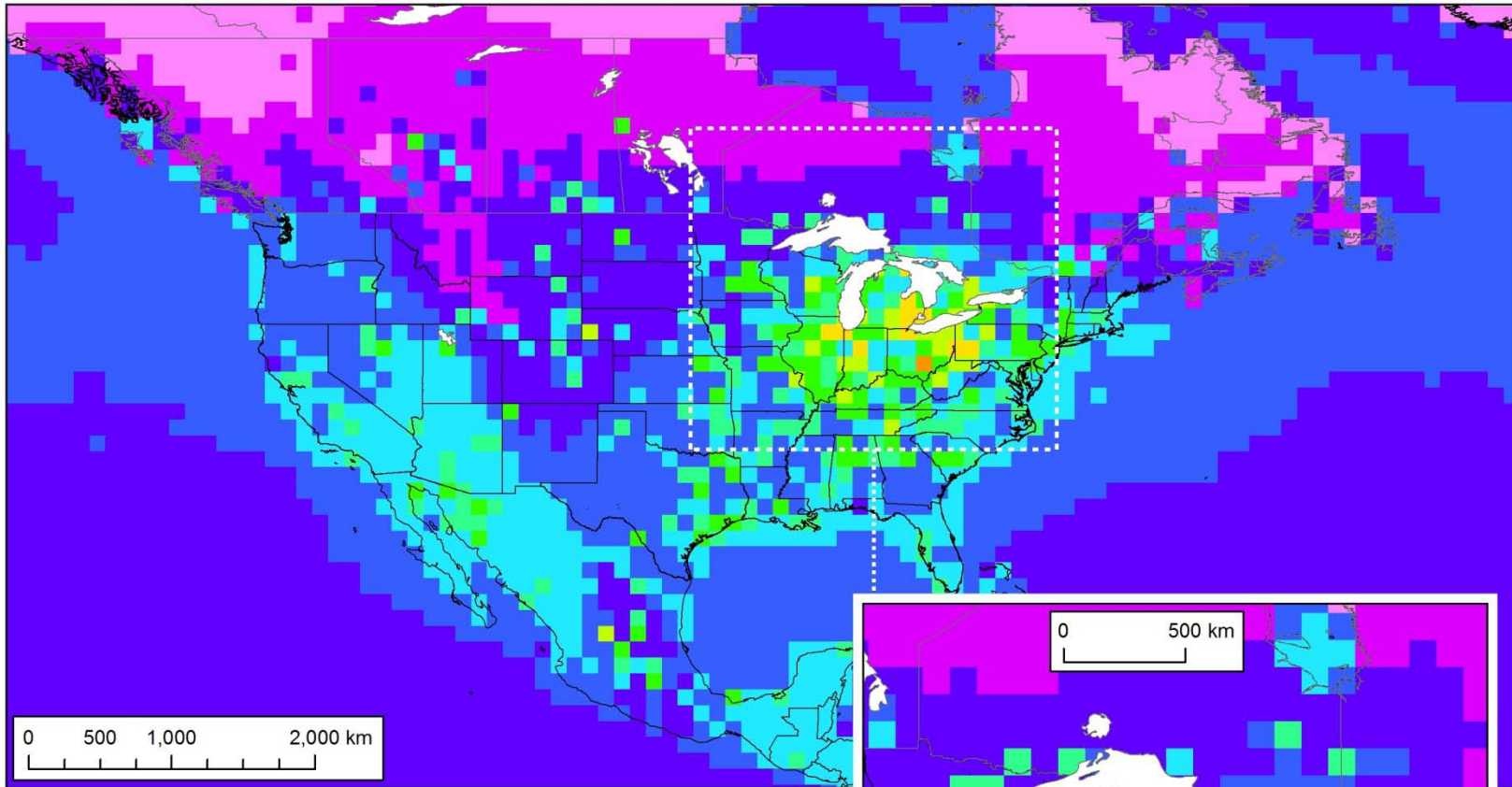
Atmospheric mercury deposition contribution (g/yr) to Lake Michigan from all emissions sources in each 1x1 degree grid cell



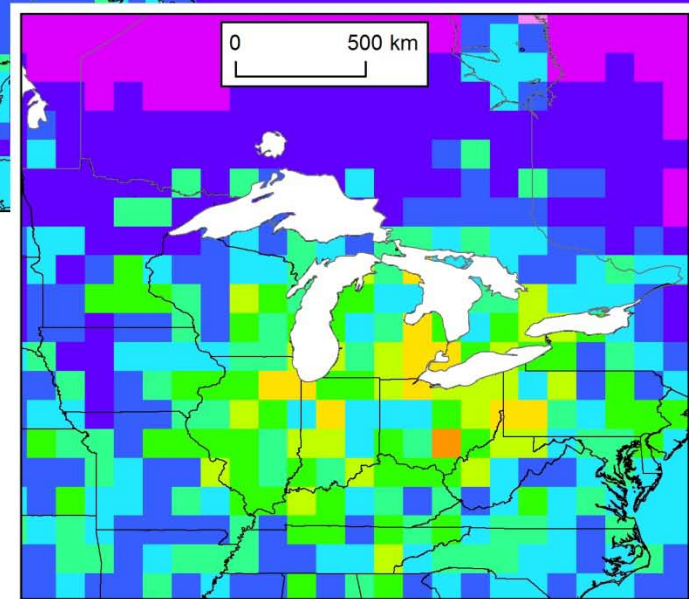
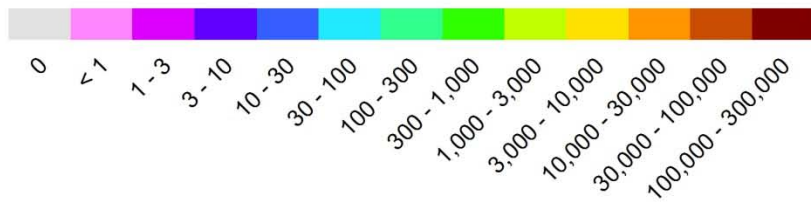


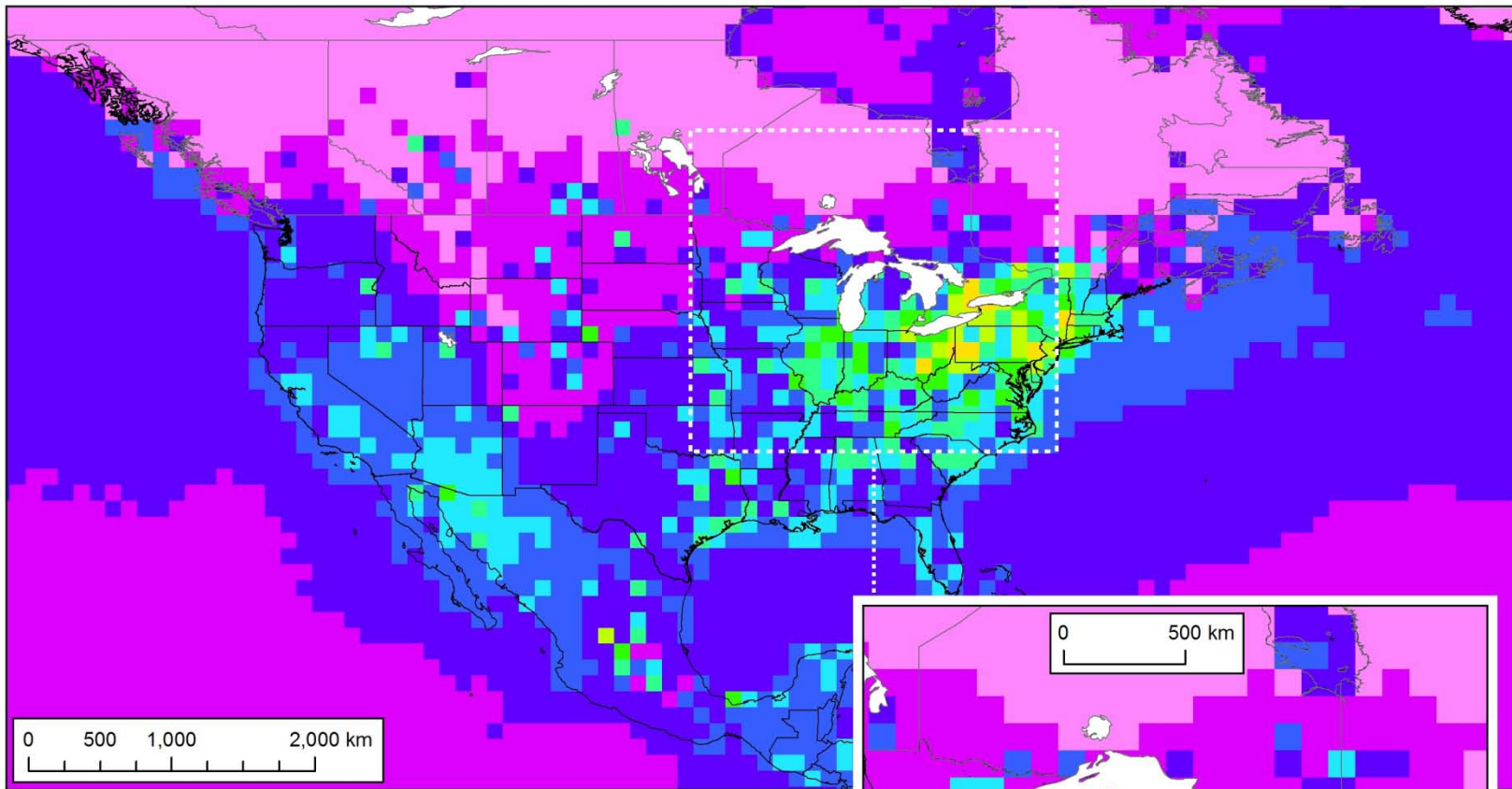
Atmospheric mercury deposition contribution (g/yr) to Lake Superior from all emissions sources in each 1x1 degree grid cell



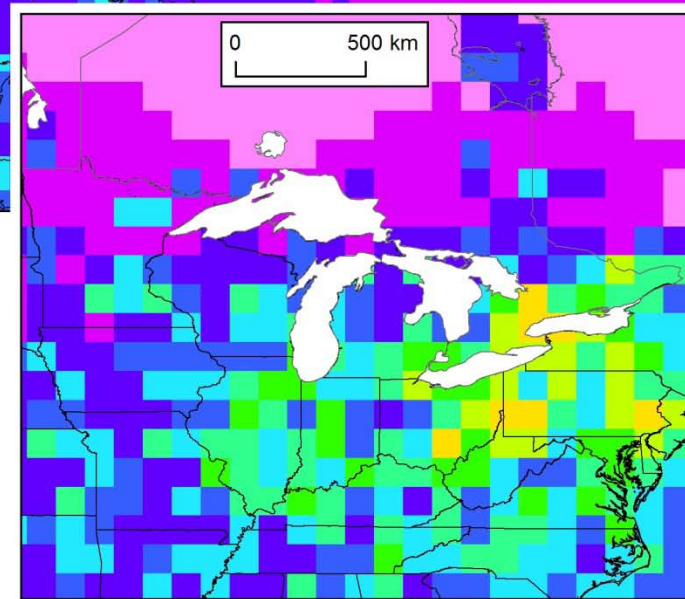
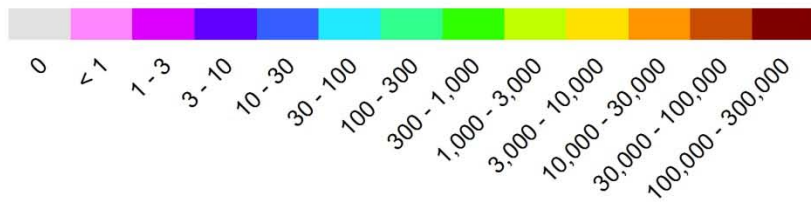


**Atmospheric mercury deposition contribution (g/yr)
to Lake Huron from all emissions sources in
each 1x1 degree grid cell**

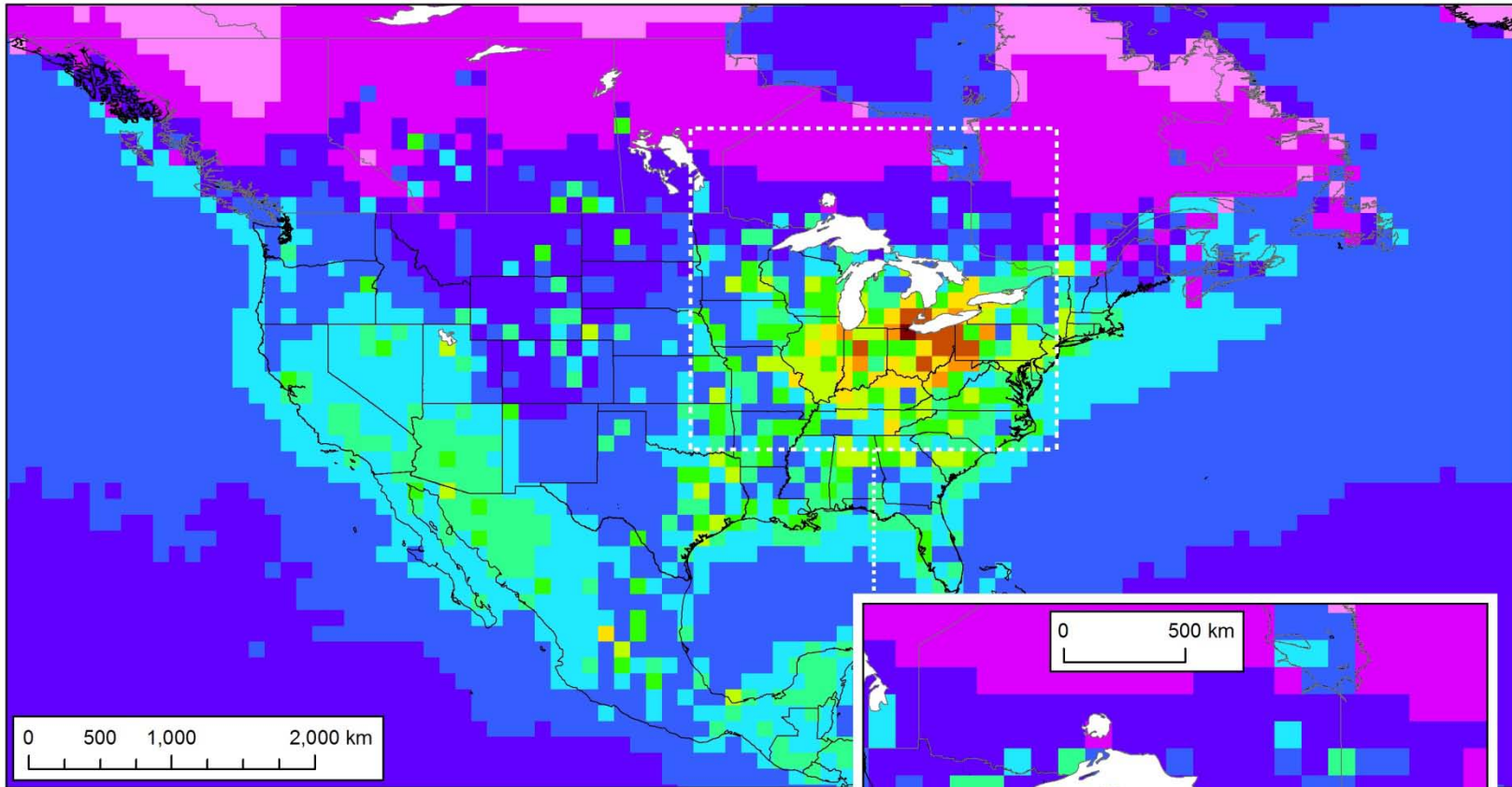




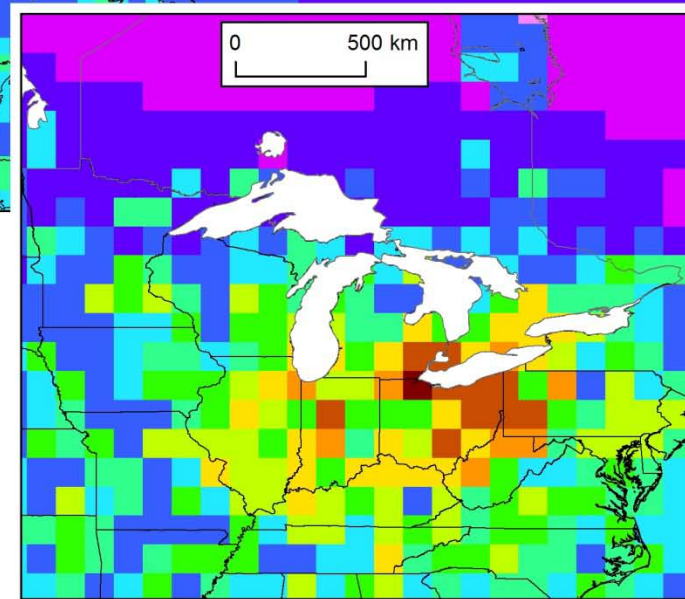
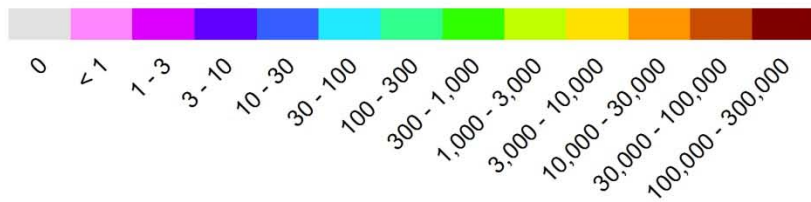
**Atmospheric mercury deposition contribution (g/yr)
to Lake Ontario from all emissions sources in
each 1x1 degree grid cell**

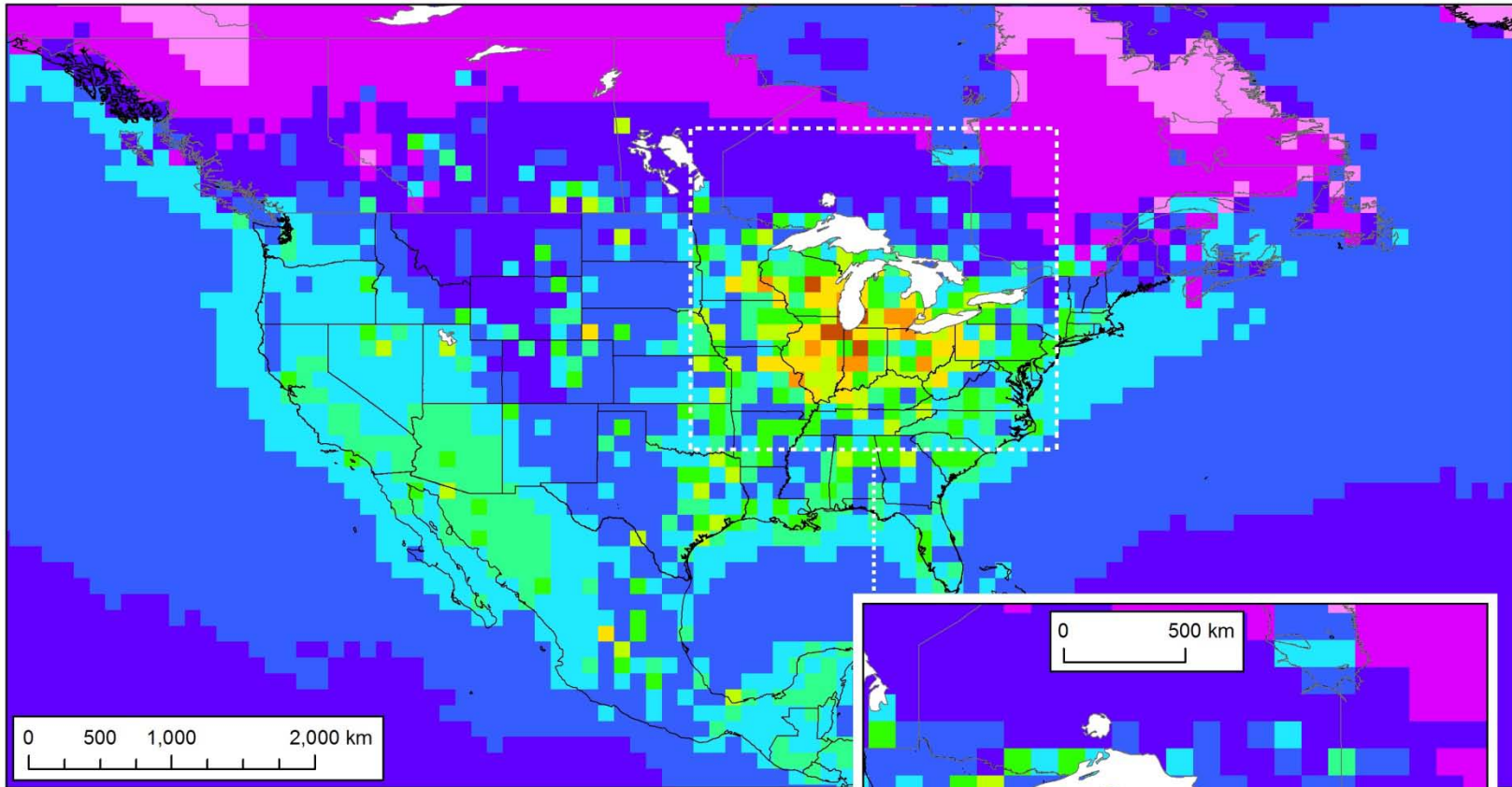


Appendix 8. Atmospheric deposition contribution maps for each Great Lake's Watershed for total atmospheric mercury emissions displayed on a 1x1 degree grid over a North American domain

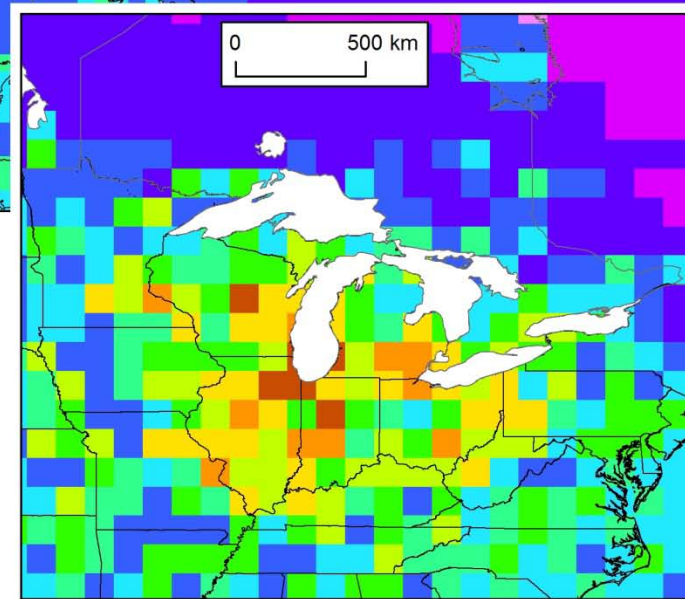
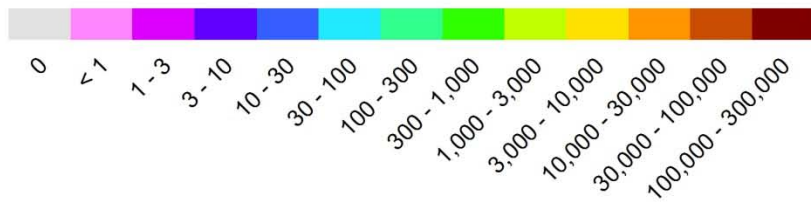


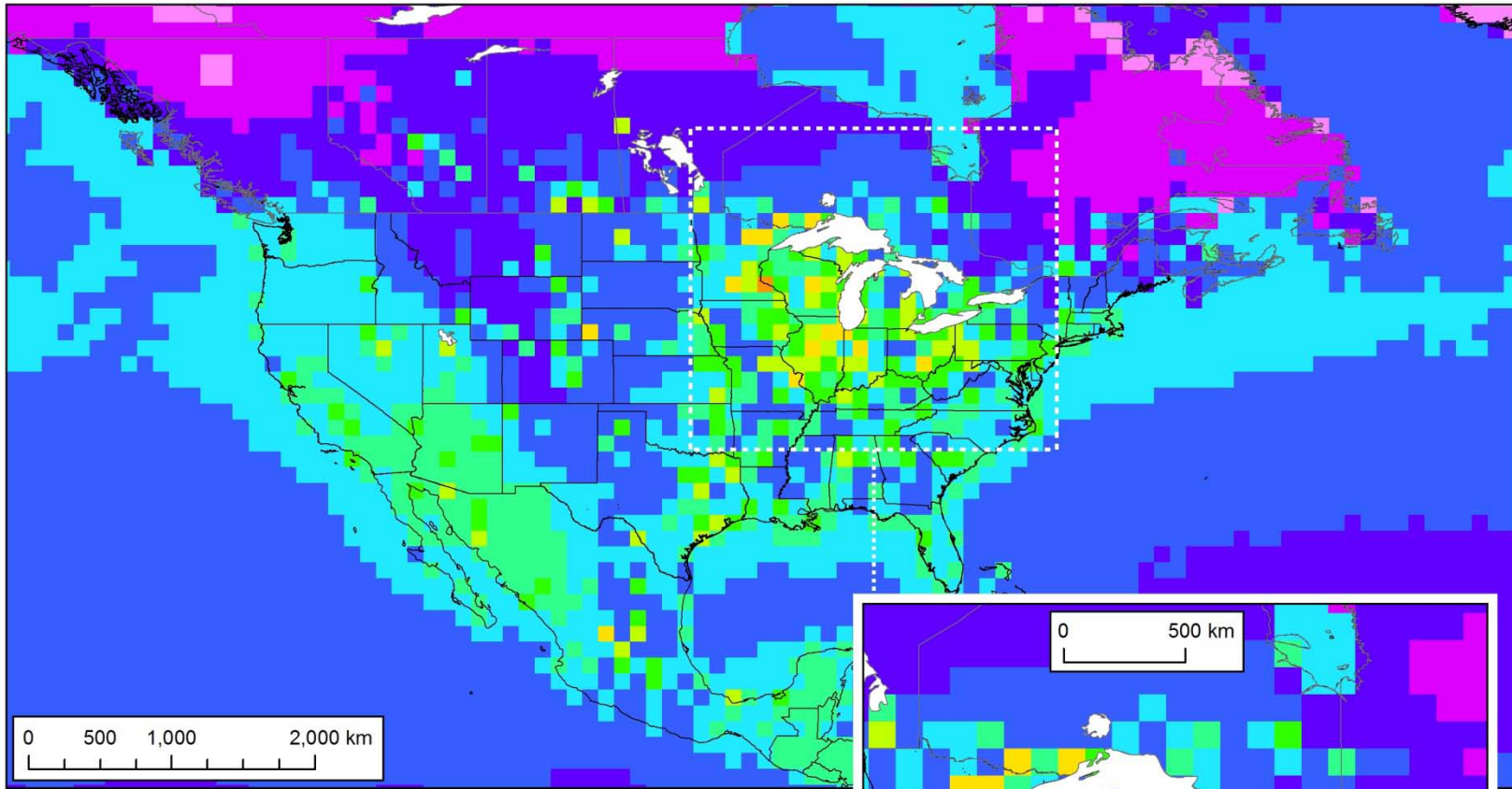
Atmospheric mercury deposition contribution (g/yr) to the Lake Erie Watershed from all emissions sources in each 1x1 degree grid cell



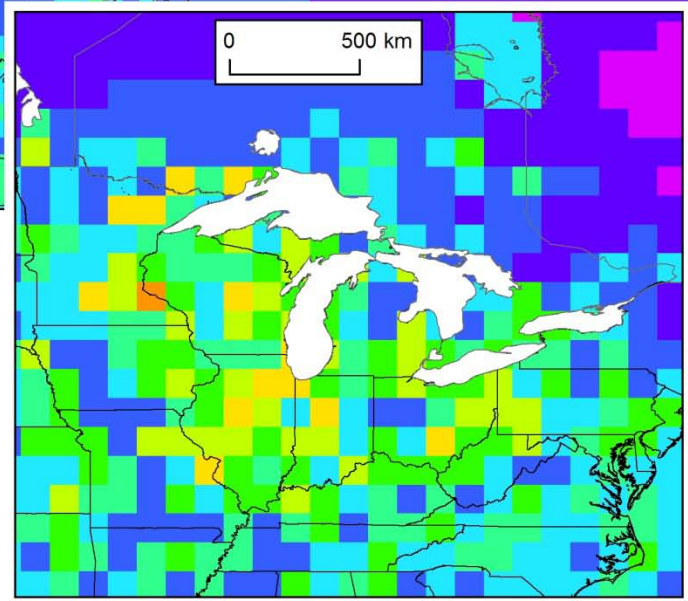
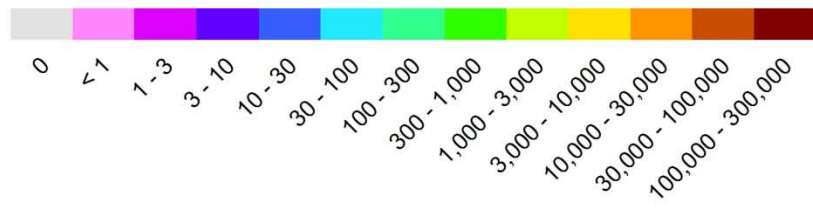


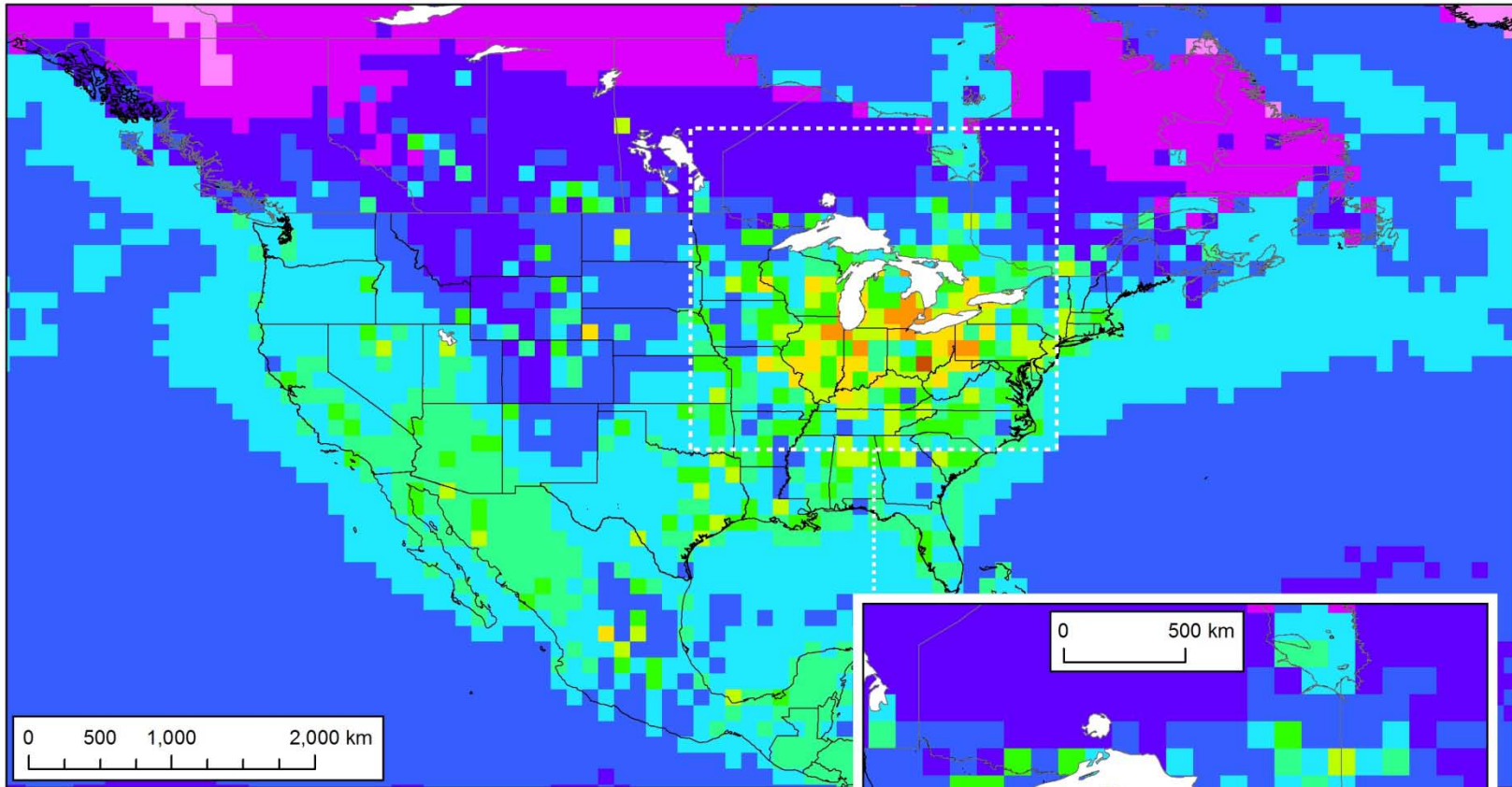
Atmospheric mercury deposition contribution (g/yr) to the Lake Michigan Watershed from all emissions sources in each 1x1 degree grid cell



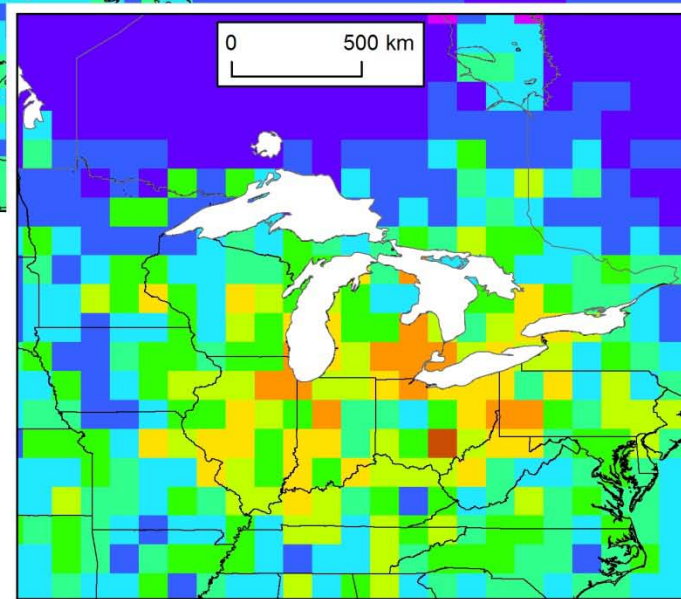
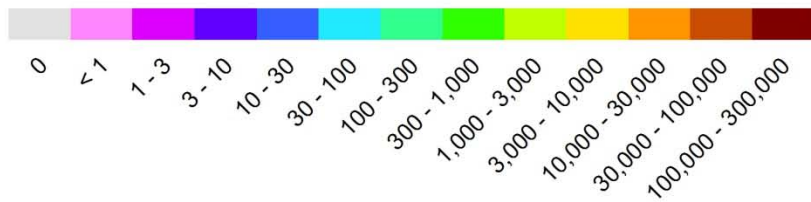


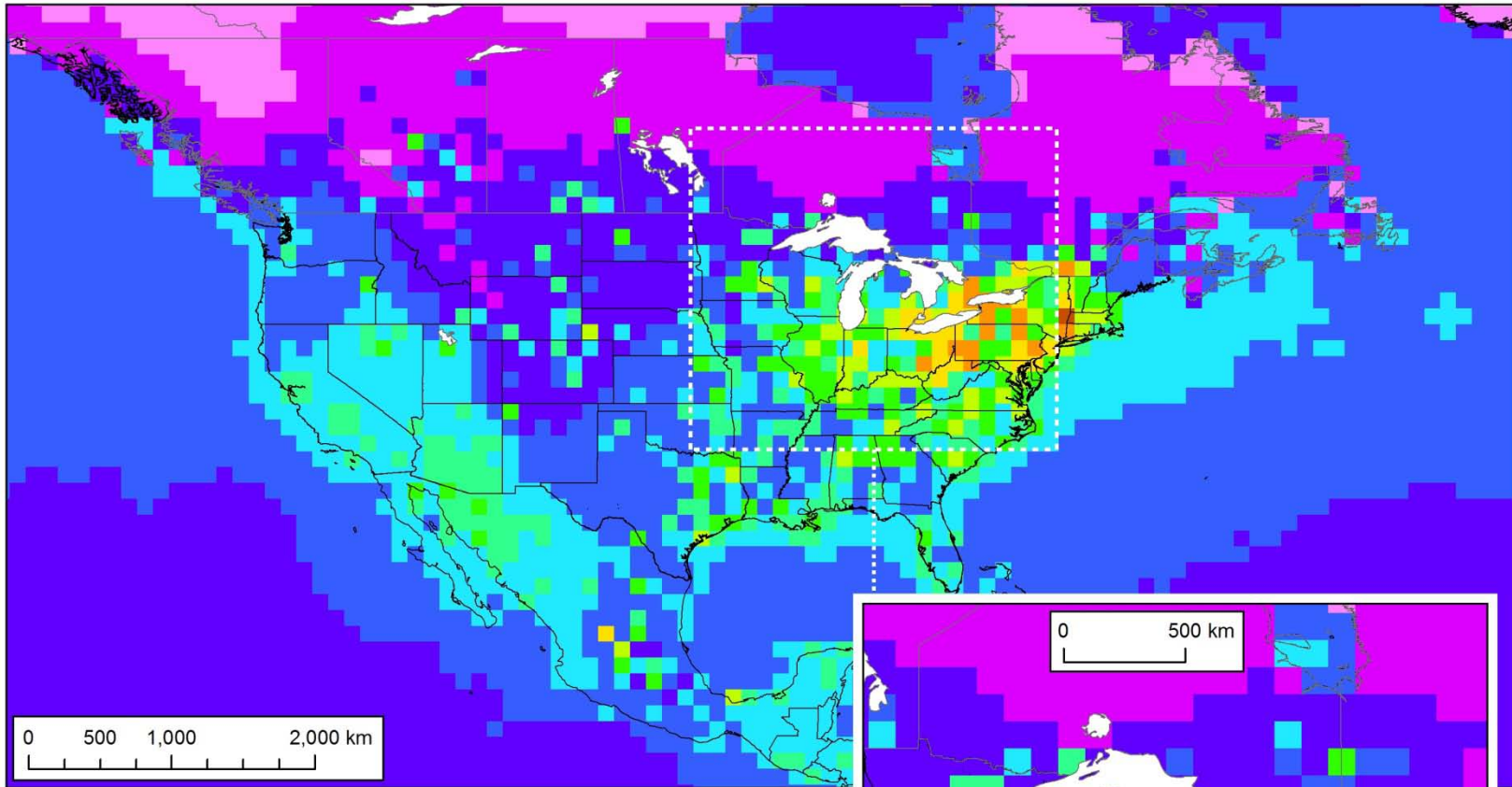
Atmospheric mercury deposition contribution (g/yr) to the Lake Superior Watershed from all emissions sources in each 1x1 degree grid cell



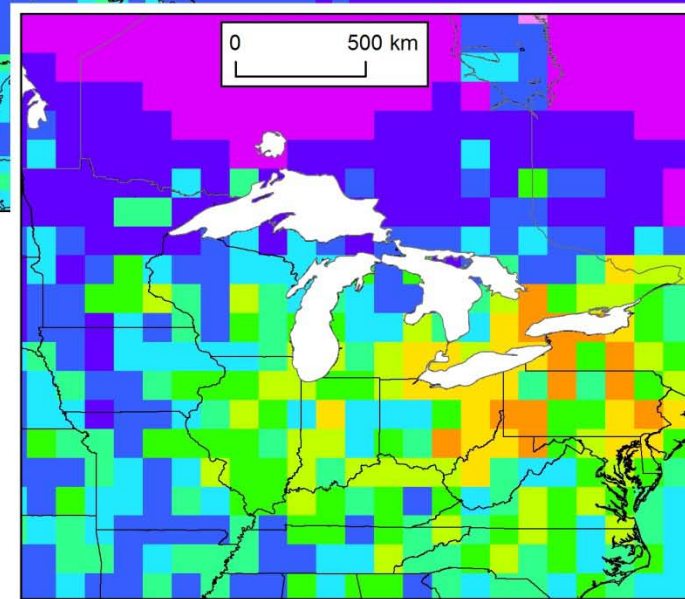
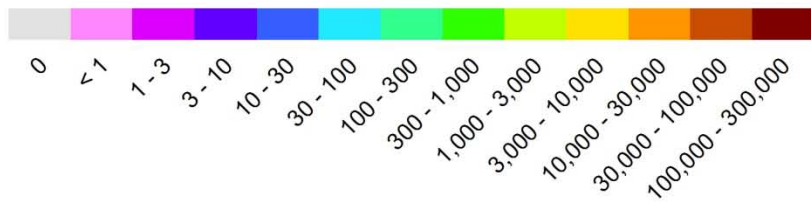


Atmospheric mercury deposition contribution (g/yr) to the Lake Huron Watershed from all emissions sources in each 1x1 degree grid cell





Atmospheric mercury deposition contribution (g/yr) to the Lake Ontario Watershed from all emissions sources in each 1x1 degree grid cell



Appendix 9. Atmospheric mercury emissions as a function of distance from each of the Great Lakes and their watersheds

